

11

THE DEVELOPMENT OF THE PIEZOELECTRIC^{AL}
CRYSTAL DETECTOR AND ITS APPLICATION
TO SOME ASPECTS OF ATMOSPHERIC POLLUTION

by

David C. Street, B.Sc. A.T.P.

December 1975

A thesis submitted for the degree of
Doctor of Philosophy of the University of London

Analytical Chemistry Department,
Imperial College,
London S.W.7.

Abstract

In this work the development of the piezoelectric crystal detector and its applications to some of the problems of the determination of atmospheric concentrations of sulphur dioxide and nitrogen dioxide are described.

The mode of operation of the piezoelectric crystal detector is described as being the absorption of the sample (pollutant) gas by a specially selected reagent which has been previously fixed to the surface of the vibrating quartz crystal. When sample gas is absorbed by the coating the crystal experiences the increase in the total mass of material on its surface and consequently decreases its resonant frequency; the extent of the frequency decrease being directly related to the mass of material absorbed onto the surface which is in turn a function of the concentration of the sample.

The development of techniques to secure solid absorbers, e.g. manganese dioxide and lead dioxide, onto the crystal surface is described. The use of these materials was instrumental in the discovery of frequency changes that were not predicted by the theory of piezoelectric crystal detectors in that frequency increases not decreased were obtained on the addition of mass to the crystal surface. The occurrence and probable causes of this effect are considered in some detail.

Two g.c. stationary phase materials were examined, one, triethanolamine, was found to be capable of determining sulphur dioxide in nitrogen in a flowing gas stream at a concentration of 0.025 ppm.

The solid reagents examined were not as sensitive as triethanolamine, more difficult to coat and the response of the crystal difficult to predict.

ACKNOWLEDGMENTS

I should like to thank Professor T. S. West for his guidance and supervision of this work and Barringer Research for a period of financial assistance. I must also thank Dr. P. Watts of C.D.E., Porton Down, for many interesting discussions - and the loan of a syringe pump!

Special thanks must be made to T. E., R.A. and S. E. for scientific and moral support during this study and also to F. E. for having the courage to tackle the mammoth task of typing this tome.

Contents

<u>Chapter</u>	<u>Section</u>	<u>Page</u>
1	<u>Introduction</u>	15
	1.1. <u>Air Pollution</u>	15
	1.1.1. History and Background	15
	1.1.2. Occurrence and Industrial Exposure	16
	(i) Sulphur Dioxide	16
	(ii) Nitrogen Dioxide	17
	1.1.3. Effects of Atmospheric Sulphur Dioxide and Nitrogen Dioxide	18
	1.1.3.1. Effects on Man	18
	(i) Sulphur Dioxide	18
	(ii) Nitrogen Dioxide	20
	1.1.3.2. Effects of Atmospheric Pollution on Man's Environment	21
	1.1.4. Analysis of Air Pollutants	24
	1.1.4.1. Sampling Techniques, General Considerations	24
	1.1.4.2. Collection Devices	27
	1.1.4.3. Analysis Techniques	28
	(i) Sulphur Dioxide	28
	(ii) Nitrogen Dioxide	30
	1.1.4.4. Summary of Techniques for Air Pollution Analysis	32

Chapter

<u>1</u>	<u>Section</u>	<u>Page</u>
	1.2. <u>Piezoelectricity</u>	34
	1.2.1. History and Development	34
	1.2.2. Theory of Piezoelectric Materials	34
	1.2.3.1. Development of High Frequency Shear Mode Crystals and their Properties	39
	1.2.3.2. The Effect of Added Mass on an AT Cut Crystal The Sauerbrey Equation	44
	1.2.3.3. Advantages Offered by the AT Cut	47
	1.2.4. Applications of the Quartz Crystal Micro Balance Technique	49
2	<u>Instrumentation</u>	56
	2.1. <u>Basic Requirements</u>	56
	2.1.1. Single Sided System	56
	2.1.2. Double Sided System	58
	2.2. <u>Equipment Details</u>	61
	2.2.1. Crystals	61
	2.2.2. Oscillators	61
	2.2.3. Power Pack	61
	2.2.4. R.f. Mixer	64
	2.2.5. Frequency Meter	64
	2.2.6. Cell Design	66
	2.2.7. Gas Handling Systems	68

Chapter

<u>2</u>	<u>Section</u>	<u>Page</u>
	2.3. <u>Experimental Investigation of Instrumental Parameters</u>	74
	2.3.1. Temperature Effect	75
	2.3.2. Coating Bleed	77
	2.4. <u>Comparison of Cell Performance and the Precision of the System</u>	80
<u>3</u>	<u>Coatings and Application Techniques</u>	88
	3.1.1. <u>Introduction</u>	88
	3.1.2. Required Characteristics of a Coating	88
	3.1.3. Reported Coating Techniques	89
	3.2. <u>Potential Coating Materials</u>	91
	3.2.1. Non Selective Coatings	91
	3.2.2. Selective Coatings	92
	3.3. <u>Development of Coating Techniques</u>	99
	3.3.1. Soluble Materials	99
	3.3.2. Insoluble Materials	102
	3.3.2.1. Nickel II Hydroxide	102
	3.3.2.2. Silver Oxide/Silver Metavanadate Mixture	106
	3.3.2.3. Manganese Dioxide	109
	3.3.2.4. Particle Fractionater	110
	3.3.2.5. Latex Bonded Coatings	120

Chapter

4	<u>Section</u>	<u>Page</u>
	<u>The Response of Solid Coating Materials</u>	126
4.1.	<u>Introduction</u>	126
4.2	<u>Sodium Tetrachloromercuriate</u>	126
4.3.	<u>Nickel II Hydroxide</u>	127
4.4.	<u>Silver Compounds</u>	131
4.5.	<u>Manganese Dioxide</u>	134
4.5.1.	Loosely Bound Coatings	134
4.5.2.	Firmly Bound Coatings	142
4.6.	<u>Lead Dioxide</u>	156
4.6.1.	Static Assessment, Critical Loading Percentage	158
4.6.2.	Dynamic Studies	163
5	<u>Investigation of High Frequency Effect</u>	170
5.1.	<u>Introduction</u>	170
5.2.	<u>Experimental Investigation</u>	171
5.2.1.	Collodion Deposits	171
5.2.2.	Apiezon Deposits	174
5.3.	<u>Anomalous Responses of Stationary Phase Coated Crystals</u>	184
5.4.	<u>Discussion of High Frequency Effect</u>	188
5.4.1.	Coupling of Vibrational Modes	191
5.4.2.	General Considerations of Electro- Mechanical Transducers	194

Chapter

<u>6</u>	<u>Section</u>	<u>Page</u>
	<u>The Response of Organic Coating</u>	200
	<u>Materials</u>	
6.1.	<u>Introduction</u>	200
6.2.	<u>Carbowax 20M</u>	200
6.2.1.	Static Studies	200
6.2.2.	Dynamic Studies	203
6.3	<u>Triethanolamine</u>	209
6.3.1.	Static Studies	211
6.3.2.	Dynamic Studies	213
7	<u>Conclusion</u>	235
7.1.	<u>Introduction</u>	235
7.2:	<u>Instrument Evaluation and Coating</u>	236
	<u>Techniques</u>	
7.3.	<u>High Frequency Effect</u>	237
	(i) Active Participation of Coating	237
	(ii) Alternative Frequency Changing Mechanism	238
	(iii) Changing Electrical and Mechanical Environment	239
7.4.	<u>Response of Various Coatings</u>	240
7.5.	<u>Suggestions for Further Work</u>	245
	<u>References</u>	247

List of Figures

<u>Figure Number</u>	<u>Title</u>	<u>Page</u>
1	Concentrations of Nitric Oxide, Nitrogen Dioxide and "Oxidant" During a Daytime Smog	19
2 a-c	Variation of Apparent Pollution Levels as a Function of Sampling Time	26
3	Charge Separation as a Result of Applied Longitudinal Strain	36
4	Coupling to External Circuit	36
5	Natural Quartz Crystal and Related Crystal Cuts	38
6	Charge Separation as a Result of Applied Shear Strain	40
7	Motion of Crystal Vibrating in Shear Mode	40
8	Temperature Coefficients of Orientated Y Cut Crystals	41
9	Frequency Constant of Orientated Y Cut Crystals	41
10	Variation of Temperature Coefficient as a Function of Temperature	43
11	Variation of Turnover with Angle of Rotation about X Axis for an AT Cut Crystal	43

<u>Figure Number</u>	<u>Title</u>	<u>Page</u>
12	Simultaneous Recordings of Thermal Conductivity and Squalane Sorption Detectors	52
13	Block Diagram of Single Sided System	57
14	Block Diagram of Double Sided System	59
15 a,b	Sketches of AT Cut Crystals from Different Manufacturers	62
16	Circuit Diagram of Oscillator	63
17	Circuit Diagram of Mixer/Amplifier System	63
18 a,b	Occurrence of Increasing and Decreasing Frequency Difference from Mixer Circuit	65
19	Glass Cell	67
20	Sectional Elevation, AA' and Sectional Plan, BB' of Impinger Cell	69
21	Spoiler Cell (Schematic)	69
22	Sectional Projection of Stainless Steel Cell Assembly	70
23	Gas Line	72
24 a	Gas Reservoir (1l and 100 ml)	72
24 b	Gas Reservoir (250 ml) Pressure Levelling Device	73

<u>Figure Number</u>	<u>Title</u>	<u>Page</u>
25 a,b	Variation of Frequency with Temperature	76
26 a,b	Coating Bleed and Correction Obtained with Double Sided System	79
27 a	Histogram of Frequency Measurement	85
27 b	"Clock" Representation of Count Period and Display Time	85
28	Particle Fractionater	111
29 a-c	Peak Shapes Representing Interaction between Manganese Dioxide Coated Crystals and Nitrogen Dioxide	137
29 d-f	Peak Shapes Representing Interaction between Manganese Dioxide Coated Crystals and Nitrogen Dioxide	138
30	Calibration Graphs of Crystals 1 and 2	145
31	Calibration Graphs of Crystals 4 and 6	146
32	Calibration Graphs of Crystals 8 and 12	147
33 a,b	Peak Profiles of NO ₂ on Crystal 4	149
34 a,b	Peak Profiles of NO ₂ on Crystal 6	150
35	Comparison of Peak Shapes for NO ₂ and SO ₂ injected onto Crystal 1	153

<u>Figure Number</u>	<u>Title</u>	<u>Page</u>
36	Frequency Change Combinations	155
37	Frequency Change due to 100 μl of SO_2 injected into Static Environment of Crystal 7	159
38	Frequency Change due to 10 μl of SO_2 injected into Static Environment of Crystal 7	159
39	Frequency Change due to first 20 μl of SO_2 injected into Static Environment of Crystal 9	160
40	Frequency Change due to second 20 μl of SO_2 injected into Static Environment of Crystal 9	160
41	Determination of Critical Percentage	164
42	Decrease in Response of Lead Dioxide Coated Crystals	166
43	Dependence of Frequency Change upon Loading	173
44	Deposit Profiles of Apiezon Deposits on Crystals 2 and 3	183
45	Chloroform Vapour Sampling Device	186
46	Response of Squalane Coated Crystal to Chloroform Vapour	186

<u>Figure Number</u>	<u>Title</u>	<u>Page</u>
47	High Frequency Shear and Flexure Resonances in an AT Cut Quartz Plate	192
48	Schematic Representation of an Electro- mechanical Transducer	195
49	Vector Impedance Locus	195
50	Absorption and Desorption of SO ₂ from a Carbowax Coated Crystal	202
51	Response of Carbowax Coated Crystal to SO ₂ in a Static Environment	203
52	Response of a Carbowax Coated Crystal to SO ₂ in a Dynamic Environment (Six flow rates)	206
53	Dependence of Response of a Carbowax Coated Crystal upon Carrier Gas Flow Rate	207
54	Decreased Recovery Time and Response as a Function of Flow Rate	208
55	Response of a Triethanolamine Coated Crystal to SO ₂ in a Static Environment	212
56	Peak Profiles Representing Dynamic Inter- action between Triethanolamine Coated Crystal and SO ₂	214

<u>Figure Number</u>	<u>Title</u>	<u>Page</u>
57	Calibration Graph of Triethanolamine Coated Crystal with Dilute SO ₂	216
58	Long Sample Presentation (SO ₂) to Triethanolamine Coated Crystal 4	219
59	Calibration Graph of Triethanolamine Coated Crystal 4	222
60	Response of Triethanolamine Coated Crystal 5 to 10 minute Samples of SO ₂ (low concentrations)	224
61	Calibration Graph of Triethanolamine Coated Crystal 5 (low concentrations)	225
62	Calibration Graph of Triethanolamine Coated Crystal 5 (high concentrations)	225
63	Response of Triethanolamine Coated Crystal 5 to 10 minute Samples of SO ₂ (high concentrations)	226
64	Calibration Graphs of Triethanolamine Coated Crystals 5-11	230
65	Dependence of Frequency Change upon Area of Coating	232
66	Frequency Change as a Function of Mass/Area of Absorbed Sample	233

1. Introduction

1.1. Air Pollution

1.1.1. History and Background

The recognition of pollution problems in Great Britain has a long history, but widespread action to abate this problem has only very recently been taken. During the reign of Edward I (1272-1307) a protest was recorded by the nobility, against the use of "sea" coal: in the succeeding reign of Edward II (1307-1327) a man was tortured ostensibly for filling the air with a "pestilential odour" through the use of coal. Further action, under the order of Richard III (1377-1399) saw the introduction of a tax to limit the use of coal: Henry V (1413-1422) established a commission to oversee the movement of coal into the City of London.

During the next 250 years there were various studies and attempts to control pollution, none having a great impact upon the problem. In 1661 a notable paper by John Evelyn, one of the founder members of the Royal Society, discussed the sources of atmospheric pollution, its effects and broader aspects relating to the control of pollution. This is one of the earliest reports in which the problem and its implications were realised by one of the scientific leaders of the period. After the appearance of Evelyn's paper there was, as could be expected, a flurry of activity but again, no appreciable results. Public concern however, in 1819 was sufficient to prompt various Parliamentary Select Committees to study and report upon smoke abatement. The very dramatic end to "mere Parliamentary studies" occurred with the death of 4,000 people in a few days in the notorious London smog of December, 1952.

The term "smog" is in fact a contraction of "smoke-fog" and thus the origin of this noxious gas mixture becomes obvious, i.e. the

effluent gases from combustion processes. The range of constituents in effluent gases - especially from coal combustion are numerous, but readily group as follows:-

1. Particulate material: i) less than 100 μ diameter
 ii) greater than 100 μ diameter
2. Sulphur compounds
3. Nitrogen compounds
4. Non organic carbon compounds
5. Organic compounds.
6. Halogen compounds

This arbitrary grouping is one which has emerged through common usage: however as a general list it is probably as inclusive as any other.

As the main topic of this study is the analysis of gas streams for very low levels (ppm and ppb) of sulphur dioxide and nitrogen dioxide the occurrence, effect of these compounds on man and his environment and also their analysis by current methods will be outlined in a little more detail.

1.1.2. Occurrence and Industrial Exposure

(i) Sulphur dioxide

Interest in the sulphur dioxide content of the atmosphere has been prolonged and intense especially since its suspected role in the London smog of 1952 when an average concentration of sulphur dioxide during a two day period was 1.34 ppm (1).

The formation of sulphur dioxide occurs whenever sulphur containing compounds are burnt in air, also as a by-product of the smelting of sulphide ores, in paper manufacture and in the action of sulphuric acid on reducing agents. The uses of sulphur dioxide in industrial processes are as numerous as the number of processes that generate

sulphur dioxide as a waste product. A large and important use of sulphur dioxide gas is as an intermediate in the manufacture of sulphuric acid. Large quantities are also used in bleaching and preservation, even some bacon is cured using sulphur dioxide to avoid contamination of the foodstuff with sodium nitrite.

Workers in some magnesium foundries are subjected to highly variable concentrations of sulphur dioxide. The concentrations may range from fractional parts per million to over 10 ppm as an average concentration with occasional peak concentrations of short duration in excess of 50 ppm. This exposure is due to addition of powdered sulphur or sulphur dioxide gas, as an antioxidant to the molten magnesium during the casting process. Also atmospheres of up to 0.5% sulphur dioxide are used in heat treatment ovens for magnesium components.

(ii) Nitrogen Dioxide

As with sulphur dioxide concern about pollution attributable to nitrogen dioxide has been prolonged. An early investigation of five American cities revealed maximum concentrations of 0.8 ppm (2). It has however, been reported that during the winter of 1960-1961 a maximum concentration of 3 ppm was measured in Los Angeles County (3).

Nitrogen dioxide is a by-product in the manufacture of many chemicals including explosives, dyes, lacquers and celluloid. It is formed whenever nitric acid acts upon metals as in bright dipping, pickling and etching. Significant quantities also arise from electric arc furnaces, electric and gas welding, from internal combustion engines and from operations incidental to the manufacture or recovery of nitric acid.

Fatal concentrations of NO_2 have been reported in farm silos shortly after filling (4).

It is pertinent to describe here the chemical relationship of nitrogen dioxide to other oxides of nitrogen.

At normal environmental temperatures nitrogen dioxide, NO_2 , and its dimer nitrogen tetroxide, N_2O_4 , are always found together. At temperatures greater than 135°C the gas is almost entirely the dioxide and dark chocolate brown in colour. Below -9.3°C the oxides are a colourless solid composed completely of the dimer. At 35.5° , the temperature of the body and therefore, the temperature at which the gases react upon the human lung the ratio of $\text{NO}_2 : \text{N}_2\text{O}_4$ is 30 : 70 (5).

Calculations and conversion factors for the gas mixture are almost always made on the basis that the mixture is composed entirely of NO_2 .

The other oxide of nitrogen that presents a health hazard is nitric oxide, NO , however as nitric oxide is 4 or 5 times less toxic than NO_2 (6) and is also oxidised under atmospheric conditions to NO_2 its toxicity is not of much importance.

The interrelationship of NO , NO_2 and "oxidants" in the atmosphere have been studied during a period of smog in Cincinnati, Ohio (7). The results are shown graphically in figure 1.

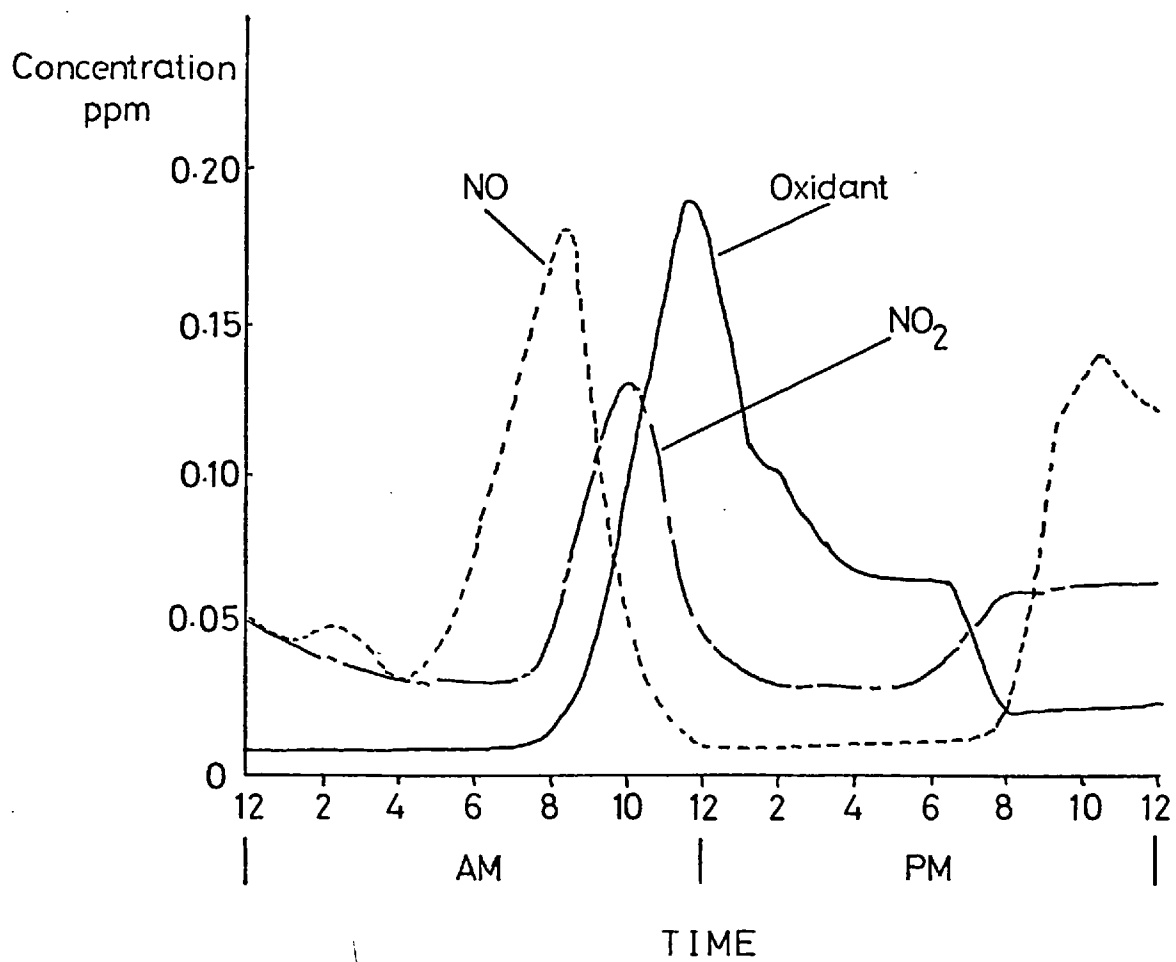
1.1.3. Effects of Atmospheric Sulphur Dioxide and Nitrogen Dioxide

1.1.3.1. Effects on Man

(i) Sulphur Dioxide

Sulphur dioxide is an irritant gas, 6-12 ppm causing immediate irritation to nose and throat. The average person can detect between 0.3 - 1 ppm probably by taste rather than odour, whilst 3 ppm has an easily noticeable odour. As sulphur dioxide is a readily soluble gas its inhalation chiefly affects the upper respiratory tract, although it can cause respiratory paralysis (8).

A period of human exposure of over two years to variable concentrations of the order of 30 ppm with occasional peaks of up to 100 ppm



Concentrations of Nitric Oxide, Nitrogen Dioxide
and "Oxidant" During a Daytime Smog

Figure 1

were found to have produced a significantly higher than normal incidence of nasopharyngitis (9), an alteration of the senses of smell and taste, and increased fatigue. There was also an extension of the duration of colds but not a significant change in their incidence.

The accepted permissible limit for prolonged exposure is 5 ppm, however, the irritating effects of this concentration are insufficient to provide ample organoleptic warning.

(ii) Nitrogen Dioxide

The odour of nitrogen dioxide is distinct in concentrations as low as 5 ppm. In concentrations of 10 - 20 ppm the gas is mildly irritant to the eyes, nose and upper respiratory mucosa. There is very little difference in intensity of odour and irritation however, between concentrations of 20 and 100 ppm. Concentrations that are considered dangerous for short exposures for man are between 50 and 150 ppm, the lower level being moderately irritating to the eyes and the upper level causing an acid taste but not painfully irritating. There is a similarity with sulphur dioxide in that the irritant property of the gas is not, under any circumstance, sufficient to give an adequate warning. In its mode of action nitrogen dioxide is quite different from sulphur dioxide. This is so as the hydrolysis of nitrogen dioxide to form nitrous and nitric acids in humid air proceeds only slowly and as a consequence relatively dry inhaled air containing nitrogen dioxide reacts little with the slightly moist surfaces of the respiratory tract. The lungs, however, offer a large surface area of moist tissue, humid air and sufficient time for almost complete hydrolysis in intimate contact with lung tissue (10).

This results in collection of fluid in the lungs. A person who has been exposed to a lethal concentration of nitrogen dioxide may

feel no discomfort up to eight hours after exposure, but death will result in most cases within 48 hours. The American Industrial Hygiene Association standard for maximum atmospheric concentration with an eight hour exposure is 5 ppm.

1.1.3.2. Effect of Atmospheric Pollution on Man's Environment

When considering the effects of atmospheric pollution on the materials found in the service of mankind it is not sufficient to consider the concentration of the pollutant in isolation. There are many other factors to be considered of which the more important are moisture, temperature, sunlight and air movement.

A summary of air pollution damage is given in table 1.

A large amount of work has been carried out investigating the rates of corrosion of metals in polluted atmospheres and many studies of the role played by other environmental factors have been undertaken. Examples of this work is the establishment of the concept of a "critical humidity". (11-13).

Below values of the critical humidity the corrosion rate of metals such as aluminium, mild steel, nickel, copper, zinc and magnesium is relatively low but above this value the corrosion rate is much faster. Each metal has its own specific value of the critical humidity.

The effects of atmospheric pollution upon buildings and building materials is well known: the blackening of once light-coloured buildings by soot to an extent where the observer may be excused the erroneous thought that the buildings were made from "black stone"; the reaction of sulphur dioxide in the presence of moisture with limestone and marble forming water soluble calcium sulphate, the product of this reaction being promptly washed away in the next rainstorm. Perhaps the most well documented occurrence of this latter effect is the frieze on the Parthenon in Athens. A plaster cast made in 1802 shows relatively minor damage that occurred during the

TABLE I

1a

AIR POLLUTION DAMAGE TO VARIOUS MATERIALS

Materials	Typical manifestation	Measurement	Principal air pollutant	Other environmental factors
Metals	Spoilage of surface, loss of metal, tarnishing	Weight gain of corrosion products, weight loss after removal of corrosion products, reduced physical strength, changed reflectivity or conductivity.	SO ₂ , acid gases	Moisture, temperature
Building materials	Discoloration, leaching	Not usually measured quantitatively	SO ₂ , acid gases, sticky particulates	Moisture, freezing
Paint	Discoloration, softened finish	Not usually measured quantitatively	SO ₂ , H ₂ S, sticky particulates	Moisture, fungus
Leather	Powdered surface, weakening	Observation, loss of tensile strength	SO ₂ , acid gases	Physical wear

TABLE I

1b

AIR POLLUTION DAMAGE TO VARIOUS MATERIALS

Materials	Typical manifestation	Measurement	Principal air pollutant	Other environmental factors
Paper	Embrittlement	Decreased folding resistance	SO ₂ , acid gases	Sunlight
Textiles	Reduced tensile strength, spotting	Reduced tensile strength, altered fluidity	SO ₂ , acid gases	Moisture, sunlight, fungus
Dyes	Fading	Fading by reflectance measurements	NO ₂ , oxidants, SO ₂	Sunlight, moisture
Rubber	Cracking, weakening	Loss in elasticity, increase in depth of cracks when under tension	Oxidants, O ₂	Sunlight
Ceramics	Changed surface appearance	Changed reflectance measurements	Acid gases	Moisture

first 2240 years, but a photograph of the same marble taken in 1938 is almost unrecognisable because of the rapid deterioration during the intervening 136 years of the industrial age (14).

The effects of pollutants upon plant life and vegetation are well documented, but they are not as obvious as the blackening and erosion of buildings. There is difficulty in identifying the effects of pollution upon plants since there are many naturally occurring bacterial and fungal blights that produce similar markings on the plants.

A general effect of sulphur dioxide upon leaves is cellular injury combined with chlorosis - i.e. the destruction of chlorophyll. This results in a leaf with a blotchy or stippled effect. Acute injury is not generally experienced at levels below 0.25 - 0.30 ppm but chronic injury may occur between 0.10 and 0.30 ppm with sensitive plants. Present estimates would suggest that sensitive plants such as wheat, barley and apple can endure 0.05 ppm for an indefinite time period. The effects of nitrogen dioxide are very similar to sulphur dioxide with retardation of growth occurring at 0.5 ppm. Sensitive plants are tomato, tobacco and bean plants.

Generally the study of the effect of pollutants upon vegetation in situ is very complex as there are so many variables and unknown quantities involved.

1.1.4. Analysis of Air Pollutants

1.1.4.1. Sampling Techniques, General Considerations

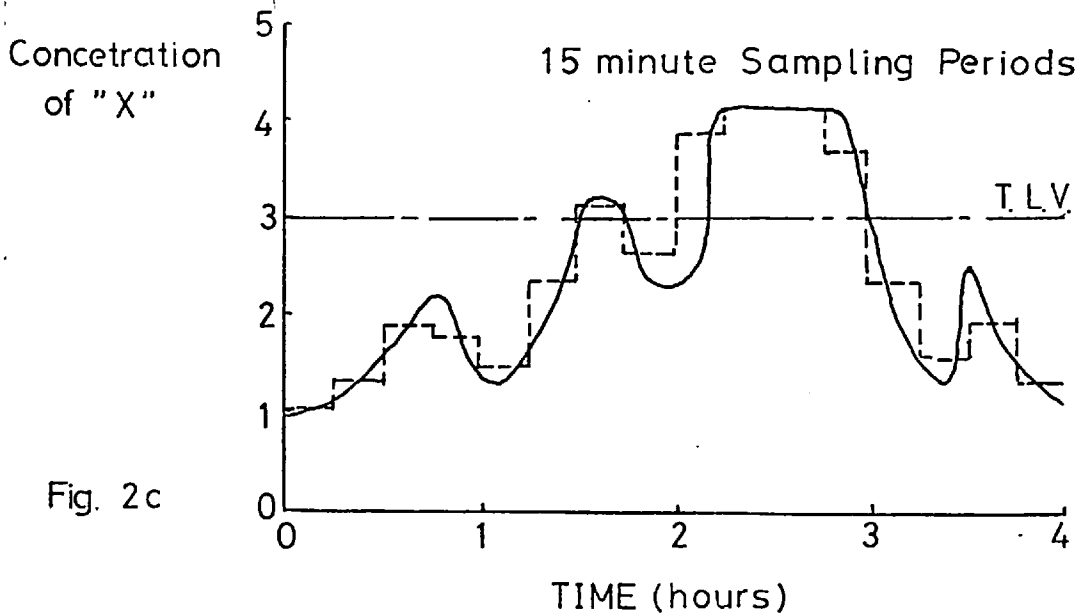
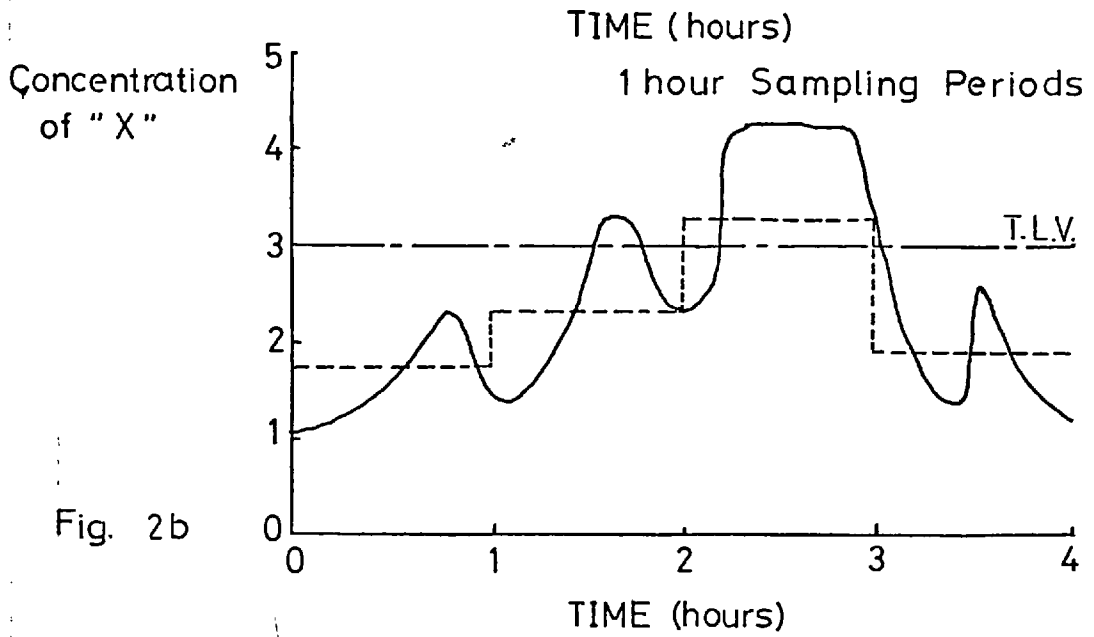
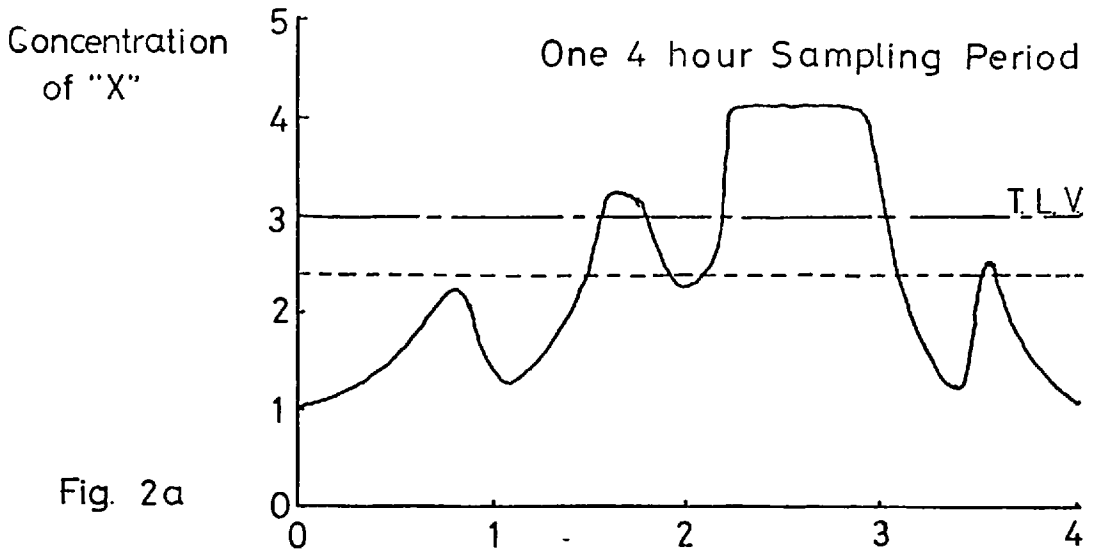
The analysis of the atmosphere for pollutants is readily divided into three distinct operations. These include: the collection of the sample at the site of interest, removal of the sample to the laboratory for analysis; the calculation of the results.

The validity of the final result of any analysis is dependant upon

the ability of the sampling technique to accurately represent the bulk of the material from which the sample was taken; this is especially applicable to atmospheric analysis. Thus the process of atmospheric sampling will be considered more closely.

The parameters of sampling are controlled by three factors, the most important being the type of information required from the analysis. This can be understood by consideration of figures 2a-c. In figure 2a the solid line represents the actual variation of concentration of pollutant "x" with time. The broken line is the concentration of pollutant "x" as determined using a four hour sampling period, note that this determined value is below the threshold limit value (T.L.V.) whereas the actual concentration does at times exceed the T.L.V. By decreasing the sampling time and increasing the number of analyses the concentration profile obtained by analysis becomes a much more accurate representation of concentration variations. This is shown in figures 2b and 2c. Thus if only general information regarding average concentration is required then a long sampling time may be used; however shorter successive sampling periods must be used if more detailed information is required. It is also worth while to note that an average concentration of pollutant can be calculated from detailed information but more detailed information cannot be obtained from a long term average value.

Other factors that control the sampling parameters, i.e. size of sample and rate of sampling, are the lower detection limit of the analytical technique and the efficiency of the collecting device. Care must be exercised when attempting to increase the size of the sample, to improve measurement, by increasing the rate of sampling, as the efficiency of the various collecting devices will change with flow rate passing through the collector.



Variation of Apparent Pollution Levels as a Function of Sampling Time

Figure 2 a-c

1.1.4.2. Collection Devices

The phenomenon of adsorption has been used, but not extensively, in the sampling of air pollutants. The adsorption bed is packed with a highly porous solid through which the sample gas is passed. The nature of the adsorbent may afford some degree of selectivity. Commonly used adsorbents used are charcoal, silica gel, alumina, lithium chloride and bauxite.

Once a pollutant gas is adsorbed onto the solid it must then be removed for analysis. This may be achieved by heating and passing a stream of nitrogen through the column and collecting the gas of interest in an absorption tube or by stripping the adsorbate off the adsorbant with a solvent. Vacuum removal has also been used.

One of the most frequently used techniques for gas collection is that of absorption or the dissolution of the pollutant gas in a liquid. The dissolution may or may not be followed by a chemical reaction, indeed this technique can be tailored to individual needs resulting in quite selective absorption. This is typified by the use of a solution of sodium tetrachloromercuriate (0.1M) as the absorbent in sulphur dioxide analysis, the absorbent reacts with the dissolved sulphur dioxide to form a stable non volatile dichlorosulphitomercurate ion (15).

A number of devices have been developed to achieve a high efficiency of absorption. These include sintered glass scrubbers, impingers, packed columns, counter current scrubbers and atomizing scrubbers. There are many factors that contribute to the operating efficiency of these devices but when working under optimum conditions the sintered glass scrubber and the impingers have collection efficiency in excess of 90% although some workers have reported that generally the impinger efficiency is lower than that of the glass frit scrubber (16). It is generally accepted that the efficiency of a

collection technique need not be 100% but an efficiency below about 75% is not suitable for air pollution sampling (17).

The packed column and countercurrent scrubbers are very similar in principle to a fractionating column, the first using a column packed with glass beads to break up the bubbles of sample gas and the second consisting of a column packed with concentric helicies, the absorbing reagent flows down the column in a thin layer and is brought into intimate contact with the turbulent air coming in the opposite direction.

As an alternative technique to drawing large volumes of air through a scrubber of some description it is possible to use the grab sampling technique. In its most common form this technique employs an evacuated flask containing some reactive solution, which after preparation is taken to the point of sampling - the vacuum released and the air so drawn into the flask is shaken with the reactive solution contained in the flask. The efficiency of absorption of this technique approaches 100%. The major disadvantage of this procedure is the small amount of sample that can be collected; sample sizes vary from 200 ml. to 2 l. The successful use of stainless steel containers has permitted a larger sample to be taken. There are also many variations upon this theme using large plastic bags and inflating these at the chosen sampling site with a hand pump (18). The collected sample is then returned to the laboratory for analysis.

1.1.4.3. Analysis Techniques

(i) Sulphur Dioxide

There are many methods available for the analysis of sulphur dioxide in ambient air. These include colourimetric, titrimetric, conductometric and turbidimetric techniques.

Relative to other colourimetric techniques the West and Gaeke

method (15) has been the mainstay of sulphur dioxide analysis. This method involves the absorption of sulphur dioxide in a solution of sodium tetrachloromercuriate and then subsequent analysis by the addition of acid bleached pararosaniline and formaldehyde to the sulphur dioxide containing solution. The resultant red-purple pararosaniline methylsulphonic acid is determined spectrophotometrically.

There have been numerous reports regarding the effect of inter-ferants, notably nitrogen dioxide, and various modifications suggested to increase the reliability of the method (19-22).

A comprehensive study of the technique was made (23) which incorporated all of the modifications suggested to that date. This work gave a high degree of reliability to the method but it emerged cumbersome and time consuming.

The titrimetric, conductometric and turbidimetric techniques are all based upon the absorption of sulphur dioxide in acidified (pH5) hydrogen peroxide solution.

The titrimetric method requires determination of the sulphuric acid formed on absorption by titration with standard sodium hydroxide solution (24,25). The conductometric method measures the conductance of the absorbing solution before and after absorption (26,27) and the turbidimetric method determines the sulphuric acid formed by precipitation of barium sulphate (28-29). This is formed by the addition of barium chloride and subsequent turbidimetric measurement of the glycerol/alcohol stabilized suspension.

The disadvantage of using acidified hydrogen peroxide as the absorbing reagent and the subsequent determination of sulphuric acid is the vulnerability of these techniques to interference. The absorption of any other strongly acidic gas will give erroneously high results for both titrimetric and conductometric techniques.

Similarly alkaline gas absorption such as ammonia, will give a low result with both techniques.

The turbidimetric method is prone to error from soluble particulate sulphate absorption, hydrogen sulphide and sulphuric acid mist. It is possible however, to circumnavigate the problem of particulate sulphate and sulphuric acid mist interference by the inclusion of a filter or aerosol collector before the sulphur dioxide absorption device.

A cumulative method for measuring the sulphur dioxide content of the atmosphere has been devised (30,31) which involves the exposure of lead dioxide (PbO_2) to the contaminated atmosphere and subsequent measurement of any sulphate formed. The lead dioxide is mixed with a solution of gum tragacanth to form a paste which is then applied to a type of former - usually a porcelain cylinder. This cylinder is placed in a shelter - to avoid direct wetting of the surface by rainfall, and sulphation of the lead dioxide by atmospheric sulphur dioxide occurs. The rate of sulphation has been found to be proportional to the sulphur dioxide content of the atmosphere at least up to 15% conversion of the reactive material (32). Much work has been done (33) to correlate the effects of particle size, the use of different binders in the preparation of the cylinder, exposure times and the behaviour of the system in the region of the critical loading percentages. A definite relationship was found to exist between allowable exposure times and atmospheric concentrations of sulphur dioxide with particle size as a major parameter.

(ii) Nitrogen Dioxide

As with sulphur dioxide the most sensitive and commonly used technique for the determination of atmospheric nitrogen dioxide is a colourimetric technique. This is based upon the

Griess-Ilosvay reaction in which a pink complex is formed between sulphanilic acid, nitrite ion and α naphthylamine in an acid medium. Various modifications have been proposed but the one most widely used is that introduced by Saltzman (34).

This modification utilizes an absorbing reagent of a mixture of sulphanilic acid and N-(1-naphthyl)-ethylenediamine dihydrochloride in a solution of acetic acid. The complex is formed in the absorber and no further addition of any reagent is necessary. A more complex absorbing reagent has been proposed (35) in which the addition of R-salt (2-naphthol-3,6-disulphonic acid, disodium salt) promotes the colour development and the concentration of the diazotizing and coupling agents are optimised. Under identical conditions of absorption the efficiency of the improved reagent was found to be in excess of 90%, whereas the Saltzman reagent has an efficiency of absorption of approximately 72%.

This technique may also be used for the analysis of nitric oxide after it is oxidized to an equivalent amount of nitrogen dioxide by passage through a potassium permanganate solution (36).

A variant of this technique has also been used for measurement of nitrogen dioxide in the field (37).

Interference by other pollutant gases with the Saltzman technique is not very marked. A 10 fold ratio of sulphur dioxide produces no effect and a 30 fold ratio produces some slow bleaching of the colour, however if the spectrophotometric analysis is performed within 45 minutes no appreciable interference results. Alternatively addition of 1% by volume of acetone to the reagent retards fading by the formation of an addition product with sulphur dioxide. This permits the analysis of the solution to be delayed by 4-5 hours.

The concentration ranges for which the above described techniques

are applicable are as follows:-

Method	Range	Sampling time
For Sulphur Dioxide		
Colourimetric (West and Gaeke)	0.005 - 5 ppm	few minutes to 24 hours
Titrimetric	0.01 - 10.0 ppm	30 minutes
Conductometric	0.01 - 2 ppm	30 minutes
For Nitrogen Dioxide		
Colourimetric (Saltzman)	0.005 - 5 ppm	10 minutes

Table 2

1.1.4.4. Summary of Techniques for Air Pollution Analysis

In the methods of analysis just described it will be noticed that the general pattern is similar in all cases, that is the collection of, or preconcentration of, the sample at the sampling site, and then removal for analysis. If detailed information regarding concentration of pollutant and time is required these techniques, though analytically good, would require a large outlay in terms of manpower, especially for sample collection.

There are commercially available pieces of equipment that will operate automatically in the laboratory and also equipment that will operate on site, but these require complicated and expensive instrumentation.

It is hoped in the following pages to show how the piezoelectric monitoring device can contribute to the solution of the problems found in atmospheric analysis. The chief attractions are that it is intrinsically sensitive - responding to mass changes of the order of

10^{-12} g; it is instrumentally very simple and robust and in its mode of operation it combines the act of sampling and analysis.

These features combine to give a device which has the potential of operating remotely without the need for pre-treatment of the sample gas, and the simplicity, and therefore price, of the device make it possible economically to undertake pollution monitoring on a large scale.

1.2. Piezoelectricity

1.2.1. History and Development

The piezoelectric property of quartz, Rochelle salt and other materials was first discovered by Pierre and Jacques Curie in 1880. This property however, remained a scientific curiosity for more than 30 years until the advent of World War I when applications of the phenomenon were made to devices of war. The first development was the design and construction of a depth sounding device for use in submarines. These systems transmitted and received compressional waves. The first quartz crystal controlled oscillator circuits appeared in 1921 as a result of the work of Cady (38). He pointed out the superior frequency stability of these circuits over conventional oscillators.

The development of quartz crystals particularly in finding crystals with a low or zero temperature coefficient was very rapid. By 1940 most of the crystal types in use to-day had been developed. The second world war saw a massive increase in the actual use of quartz crystals. This was made necessary by the need for extensive interference free radio communication.

To-day quartz crystals find application in many fields besides communications. These include the use of crystals as control elements in time standards where a high degree of stability is essential and also as filter elements in electronic circuits where a very narrow band width is required.

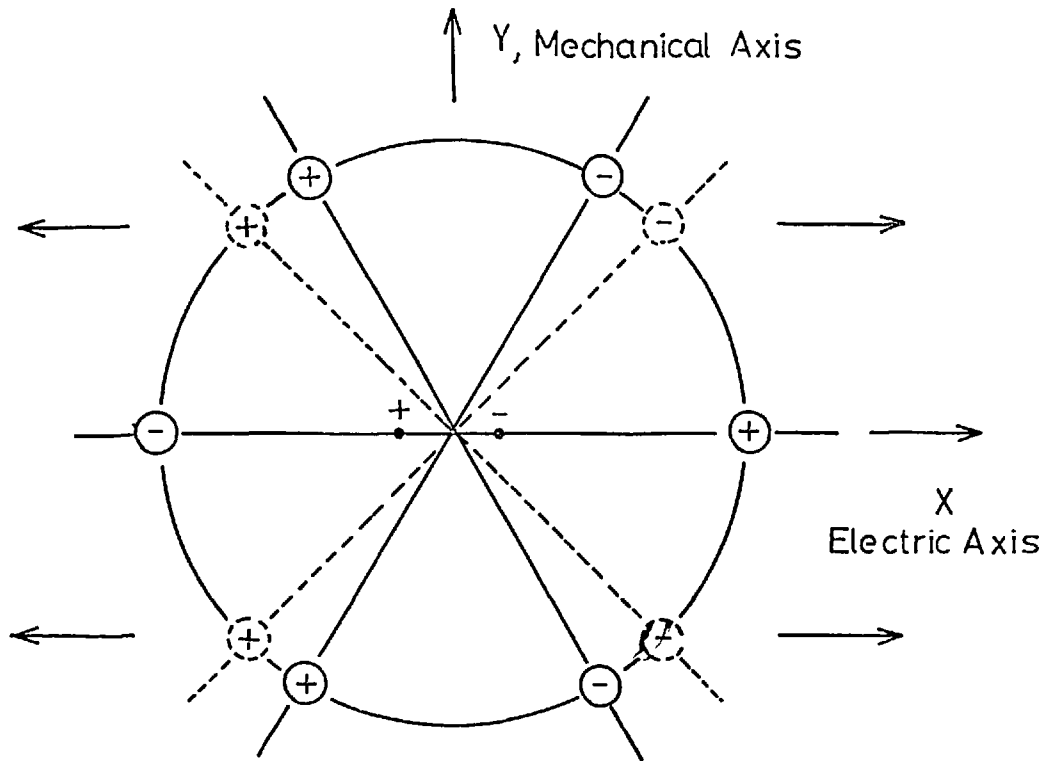
1.2.2. Theory of Piezoelectric Materials

The widespread application of piezoelectric crystals in frequency dependant equipment has arisen because they possess three important properties.

These are:-

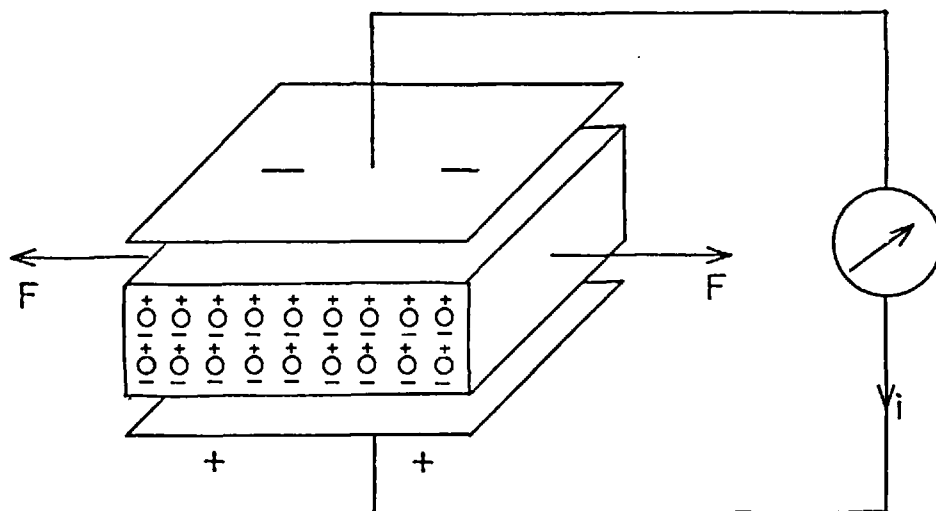
- i) the piezoelectric effect provides a coupling between the electrical circuit and the mechanical properties of the crystal:
- ii) the internal dissipation of most crystals and particularly quartz crystals is very low and the density and elastic constants of the crystals are very uniform so that a crystal cut at a given orientation always has the same frequency constant:
- iii) at specified orientations crystals can be cut which have advantageous mechanical properties such as a small change in frequency with a change in temperature or a freedom from secondary modes of motion.

In order to understand the nature of the piezoelectric effect and the coupling between mechanical and electrical systems consider figure 3. This is a representation of the approximate arrangement of silicon and oxygen atoms in the quartz structure. The silicon atoms are represented by + and the oxygen atoms by - . If a compressional force is applied along the Y or mechanical axis a deformation of the crystal lattice occurs (dotted lines on diagram) which causes a separation of the centres of gravity of the positive and negative charges, thus generating a dipole moment along the X or electric axis. If metal electrodes are placed normal to the direction of charge separation then coupling to an external electrical circuit can take place. This is shown in figure 4. If a resistance is placed in the connecting wire in place of the current indicating device and a sinusoidal stress is applied to the crystal, an alternating current will flow through the load and consequently



Charge Separation as a Result of Applied
Longitudinal Strain

Figure 3



Coupling to External Circuit

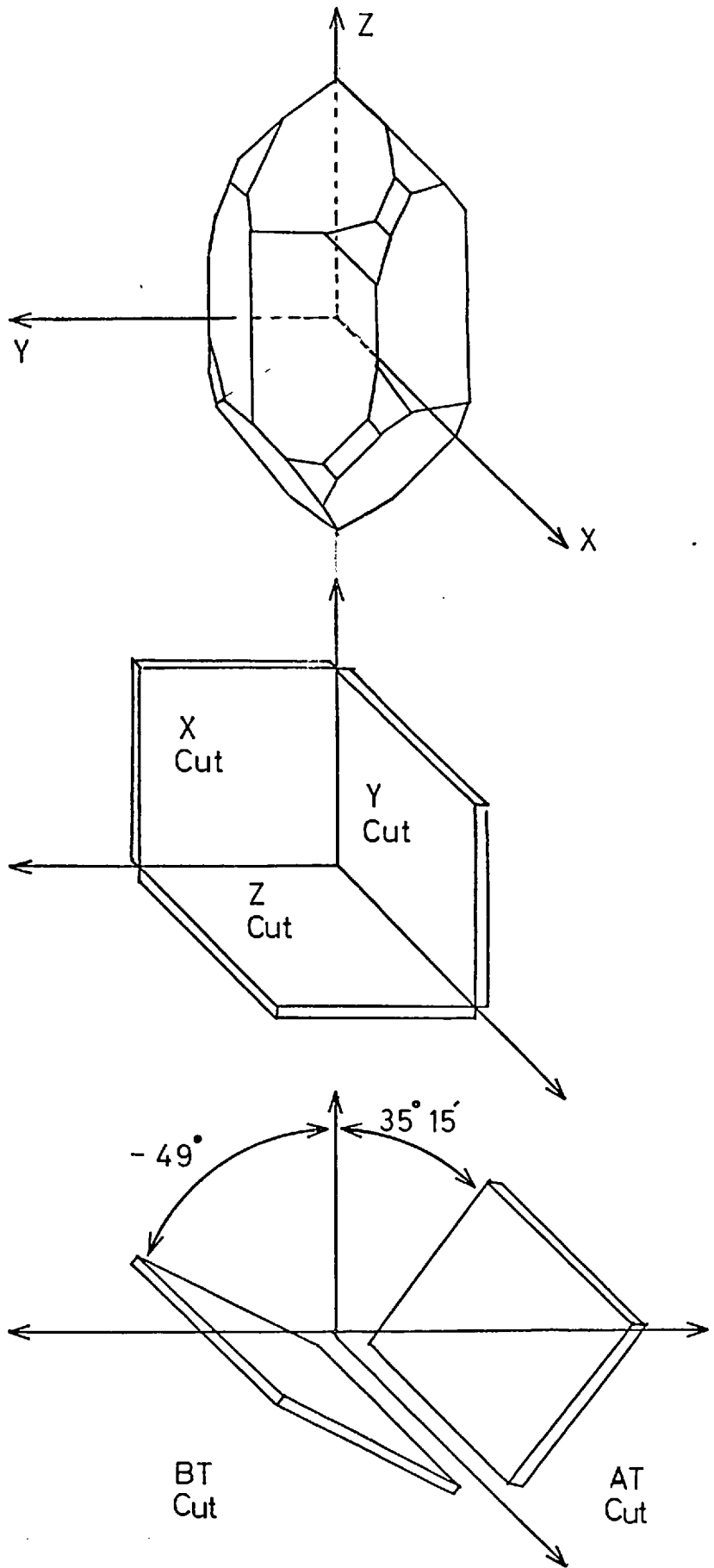
Figure 4

mechanical power will be changed into electrical power. The converse effect also occurs in that a source of alternating voltage in the circuit will produce an alternating stress in the crystal and if this is working against a mechanical load the electrical energy will be changed into mechanical energy.

The coupling ability of a piezoelectric crystal is well demonstrated with a large piece of Rochelle salt cut in a specific orientation. If tinfoil electrodes connected to a neon lamp are placed normal to the X axis of the crystal and the crystal then compressed by hitting it with a hammer a charge is generated on the surface and a voltage applied to the lamp in excess of the breakdown voltage thus the neon will be seen to flicker. A voltage as high as 5,000 volts can be generated by striking the crystal hard.

At this point it is necessary to introduce the notation used to describe different types or cuts of quartz crystal used in piezoelectric devices. These cuts are small pieces, either rods or slices of quartz cut with a specific orientation from a natural quartz crystal. The relationship of a few of these cuts to the natural quartz is shown in figure 5.

The first oscillators to employ crystals for frequency control employed a crystal cut in the Y Z plane with ^{the} exciting electrical field applied along the X axis. This resulted in a longitudinal vibration along the Y axis. However, it was not possible to obtain high frequency crystals, where the length was the principle frequency determining dimension, as lengths were required that were too small to be practical. The obvious development from this problem was to make the thickness the frequency determining dimension, but with this particular orientation of cut interference from overtones and harmonics made the required frequency difficult to pick out, this



Natural Quartz Crystal and Related Crystal Cuts

Figure 5

led to the development of Y cut crystals vibrating in shear mode (39).

1.2.3.1. Development of High Frequency Shear Mode Crystals
and their Properties

The mode of action of a crystal vibrating in shear mode is readily understood by consideration of figure 6. The arrangement is identical to that of figure 3 but in this case the compressional force is applied at 45° to the X and Y axes. This results in a charge separation along the Y or mechanical axis.

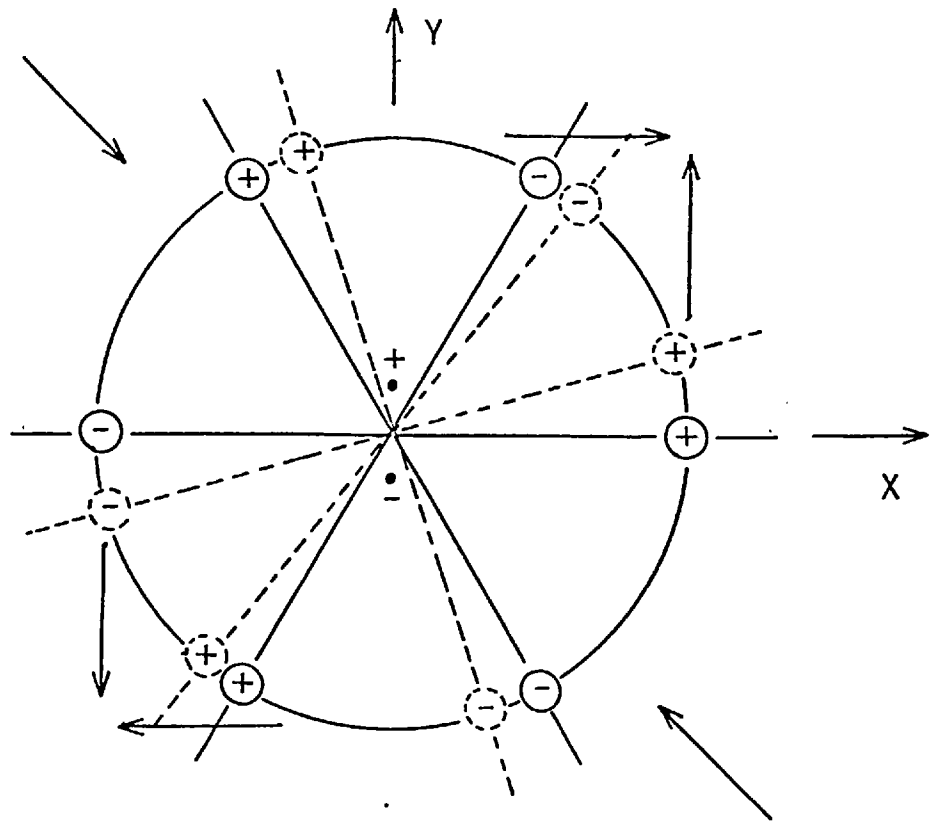
If the piece of quartz cut in this orientation has a large length and width compared with thickness then the resultant motion that occurs is shown in figure 7. The exciting voltage is applied to gold electrodes that are vacuum deposited on either side of the crystal.

These crystals gave good results with few interfering modes of vibration, unfortunately the Y cut crystal vibrating in shear mode was quite sensitive to external temperature variations with a temperature coefficient of $86 \text{ ppm}/^\circ\text{C}$ i.e. if the crystal had a fundamental frequency of 100 KHz then the frequency change would be $8.6 \text{ Hz}/^\circ\text{C}$.

As a direct result of this high temperature coefficient studies were carried out (40) to investigate the variation of temperature coefficient and also the frequency constant with the angle of rotation of a Y cut crystal about the X axis (see figure 5).

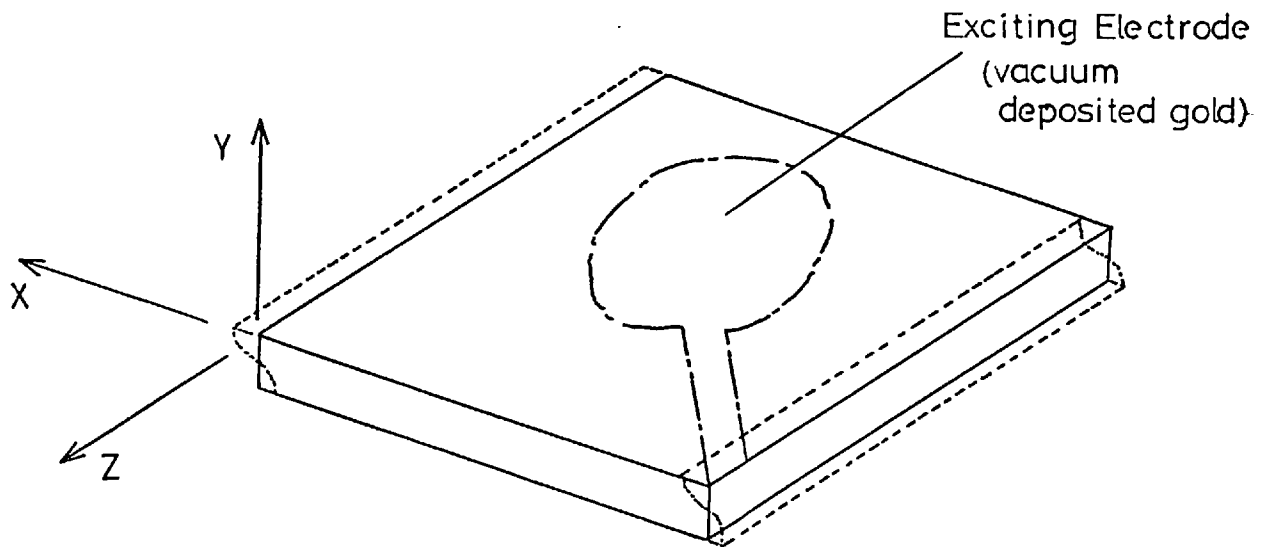
The variation of temperature coefficient with angle of rotation about the X axis is shown in figure 8. There are two angles of cut which have a zero temperature coefficient i.e. $+35^\circ 19'$ and -49° these are designated the AT and BT cuts respectively.

If the value of frequency constant is also plotted as a function of rotation about the X axis the resulting graph has a maximum and minimum point (figure 9). These points are significant in that a high frequency shear mode crystal cut at these angles has zero



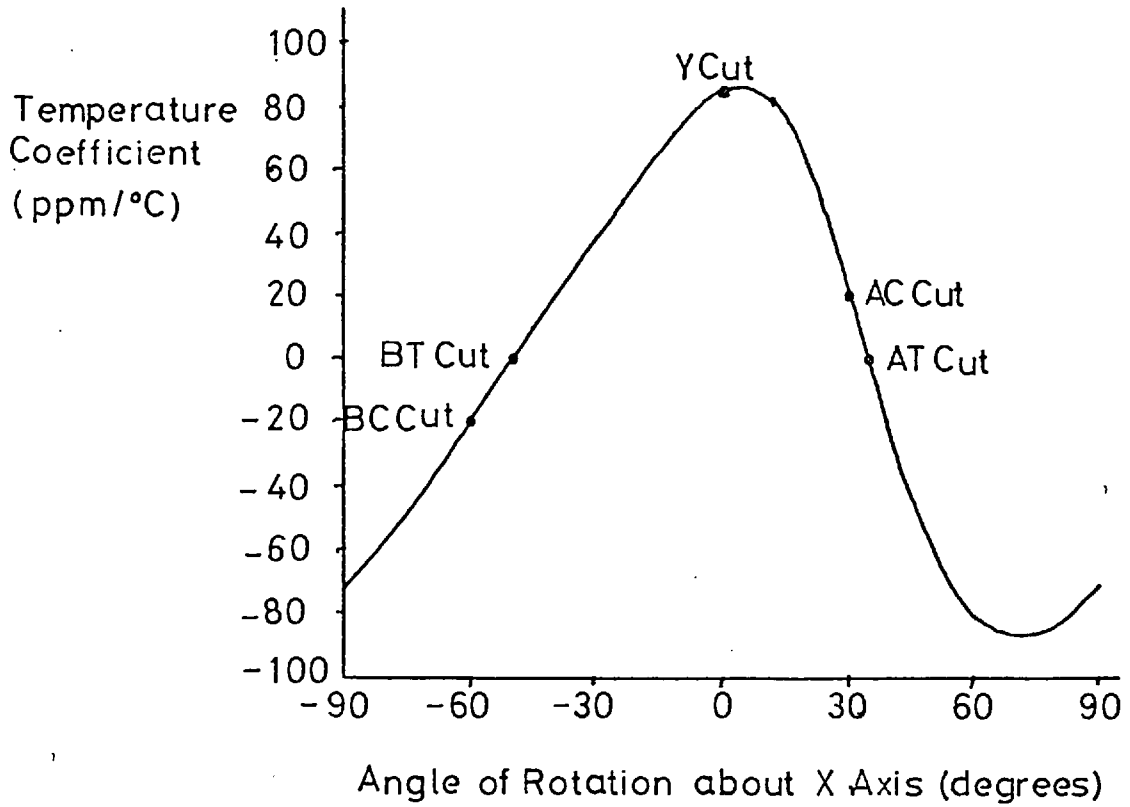
Charge Separation as a Result of Applied
Shear Strain

Figure 6



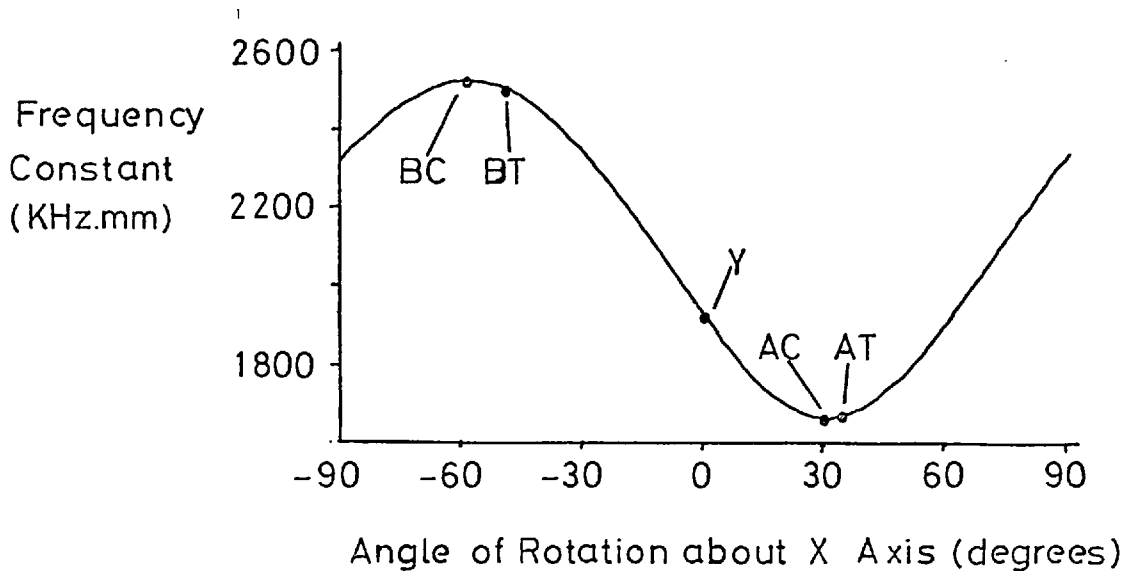
Motion of Crystal Vibrating in Shear Mode

Figure 7



Temperature Coefficients of Orientated Y Cut Crystals

Figure 8



Frequency Constant of Orientated Y Cut Crystals

Figure 9

coupling with the low frequency shear mode system of vibrations, thus these crystals have a much cleaner frequency spectrum than Y cut crystals. It is important to note also that the two cuts with zero temperature coefficient, AT and BT, are very close to the point of zero coupling and therefore they will also have a relatively clean frequency spectrum.

If the graph plotting effect of temperature upon the resonant frequency of AT and BT cut crystals is studied (figure 10) it will be noticed that at only one point does each crystal have a temperature coefficient of zero. It will be observed however, that for an AT cut crystal between 10 and 30°C the temperature coefficient is of the order of 4 ppm/°C.

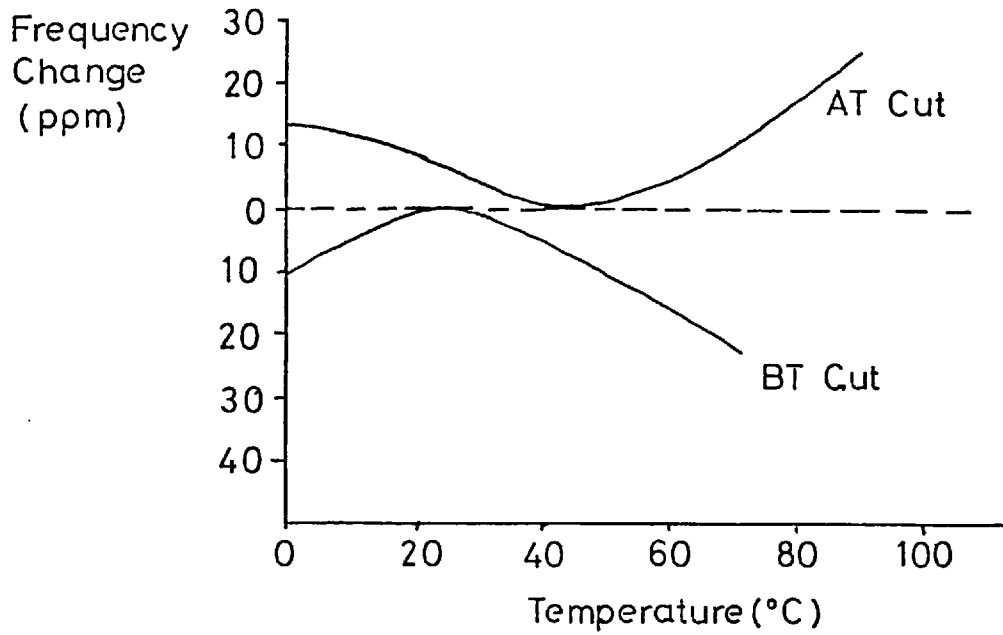
The temperature at which the zero coefficient occurs is known as the turnover temperature. A study of the variation of turnover with angle of rotation about the X axis for an AT cut crystal was made (41). In this graph (figure 11) two points are evident;

- i) the temperature at which turnover is required can be selected by choosing a suitable angle to cut the crystal
- ii) the actual position of the turnover point is very sensitive to slight variations in the angle of cut. A change of 1.5 minutes in cut angle changes the turnover point by 30°.

The effects of gas pressure upon the vibrational frequency of AT cut quartz crystal has also been studied (42). The effect was found to be relatively small and attributable to three functions. These can be summarised as follows:

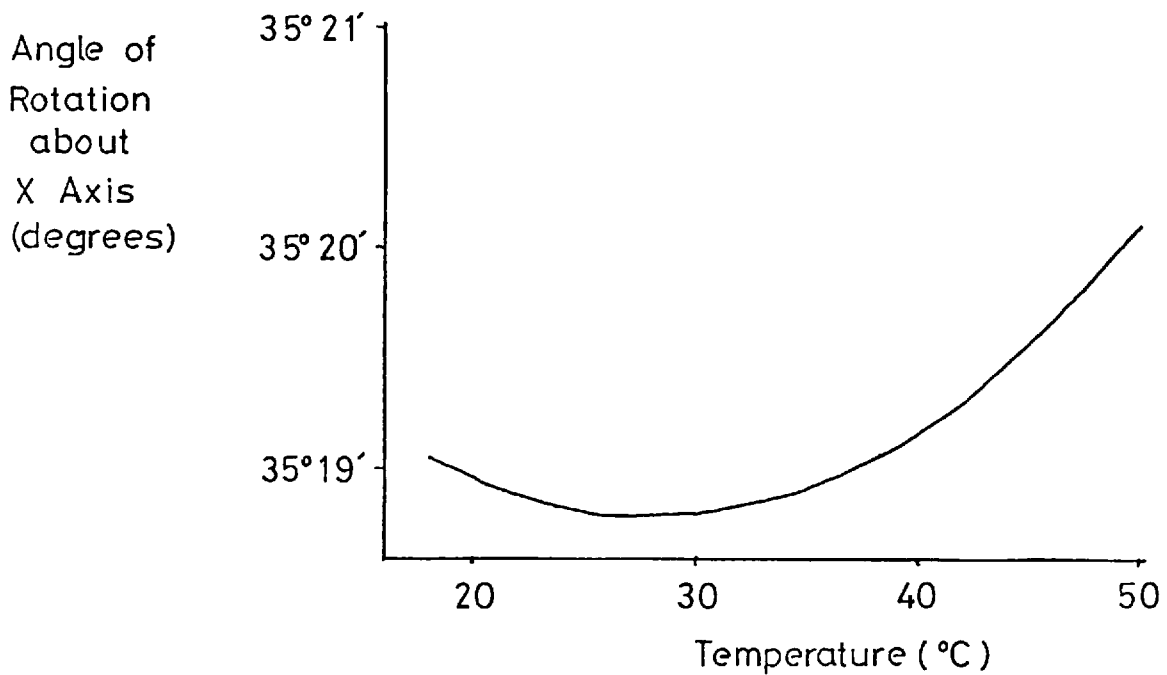
- i) $\Delta f_p \propto p$

the change in frequency as a direct result of changing the gas pressure. This is due to an increased stiffness of the crystal.



Variation of Temperature Coefficient as a Function of Temperature

Figure 10



Variation of Turnover with Angle of Rotation about X Axis for an AT Cut Crystal

Figure 11

$$\text{ii) } \Delta f_x \propto \sqrt{\pi F \rho \eta}$$

the change in frequency as a result of the complex shear impedance of the gas.

$$\text{iii) } \Delta f_m \propto Q_p$$

the change in frequency due to adsorption of the gas.

The sum effect of these factors was found to be a decrease in frequency of 100 Hz for a 5 MHz fundamental AT cut crystal with an increase in pressure of 1 atmosphere.

1.2.3.2. The Effect of Added Mass on an AT Cut Crystal

The Sauerbrey Equation

The fact that mass added on to the electrodes of an AT cut crystal will decrease its resonant frequency has been known, qualitatively, for a long time. Early crystal manufactures used this knowledge to finely adjust the frequency of a crystal by drawing pencil lines on the quartz. Present day manufacturers adjust the final crystal frequency by vacuum depositing the electrodes, usually gold or silver onto the crystal until the required frequency is obtained.

The original idea that this effect could be used as the basis for a sensitive micro balance was put forward by Sauerbrey (43) and later a mathematical expression relating frequency changes and added mass was developed by him (44). A quantitative explanation of the effect is as follows. For an AT cut crystal the vibrational mode is almost entirely face shear mode. There is very little contribution to the vibration by flexural or extensional modes therefore the statement that parallel layers shear against each other without causing deformation of these layers is justified: thus on the surface of the quartz there is an oscillating centre and the layers of quartz that are near to the surface influence the fundamental frequency only by their mass not by their elastic properties. Consequently a coating

which is thin enough influences the fundamental frequency of the plate in the same way as a layer of the plate of equal mass.

The motion that occurs in an AT cut plate is shown in figure 7. For this plate the motion is perpendicular to the thickness which is the direction of transmission of the wave, and hence a shear wave is sometimes called a transverse wave.

The frequency of such a high frequency shear vibration is given by (45).

$$f = \frac{1}{2} \sqrt{\frac{C_{jj}}{\rho}} \cdot \sqrt{\frac{m^2}{t^2} + k \frac{n^2}{l^2} + k_1 \frac{(p-1)^2}{w^2}} \quad (1)$$

where C_{jj} = shear modulus in plane of motion

ρ = density

l, w, t = length, width and thickness

m, n, p = overtones along the three dimensions

k, k_1 = correction constants

For crystals where the length and width are large compared to the thickness the following simplification can be made

$$f = \frac{m}{2t} \sqrt{\frac{C_{jj}}{\rho}} \quad \text{Hz} \quad (2)$$

For the fundamental vibrational mode $m = 1$

$$\therefore f = \frac{1}{2t} \cdot v_{tr} = \frac{N}{t} \quad \text{Hz} \quad (3)$$

where $v_{tr} = \frac{C_{jj}}{\rho} =$ (velocity of the transverse wave)

and $N = \frac{v_{tr}}{2} = \text{frequency constant}$

If equation (3) is differentiated and the differential form is divided by equation (3) the result is

$$\frac{\Delta f}{f} = - \frac{\Delta t}{t} \quad (4)$$

If the change in thickness of the quartz crystal is then expressed in terms of a change in mass, area and density of the added mass then

$$\Delta t = \frac{\Delta m}{A \cdot \rho} \quad \text{cm} \quad (5)$$

Substitute (5) into (4)

$$\Delta f = - \frac{\Delta m}{A} \cdot \frac{f}{t\rho} \quad \text{Hz} \quad (6)$$

where Δf = change in frequency resulting from the
addition of mass

f = fundamental frequency of the crystal

Δm = mass of additional layer of quartz

A = area of the quartz plate

t = thickness of the quartz plate

ρ = density of the quartz plate

When this relationship is used in practice Δm is taken as being the mass of an arbitrary, homogeneously spread coating on the plate. The significance of A , the area of the plate also changes in practice. It has been calculated (46) and shown experimentally (47)

that the oscillations are negligible outside the area of the exciting electrodes and any deposit made in that region contribute only 1% to frequency shifts of the crystal (44), therefore it is sufficient to consider A as being the area of the electrode or of the deposit placed on the crystal.

In equation (6) it is considered that f and t are constant, in fact they are not but the error involved is very small. Only a 1% error is introduced by considering the resonant frequency of a 10MHz crystal as still being 10MHz after an actual decrease in frequency of 50KHz (48).

Other workers have also derived expressions for the dependance of frequency change with added mass of vibrating quartz crystal. Lostis (49), at the same time as Sauerbrey, arrived, via a different mathematical route, at an equation very similar to one which can be derived from Sauerbrey's original equation.

A later and more sophisticated treatment was carried out by Stockbridge (50) using a Rayleigh perturbation analysis, which gives more accurate results for very low added masses. In his final equation, which is almost identical to that of Sauerbrey, a constant occurs which contains integrals and constants that are not calculable. The form of this equation was:

$$\Delta f = \Delta m \cdot \frac{f}{A \cdot \rho \cdot t} \cdot \frac{1}{k} \quad \text{Hz}$$

where $k = 0.98 \pm 0.01$

1.2.3.3. Advantages Offered by the AT Cut

A.T. cut quartz crystals offer several advantages when used as a sensing element in micro weighing:

- (i) The change in resonant frequency of a high frequency

shear crystal is simply related to additional mass. This is not so for crystals vibrating in extensional mode (51).

- (ii) They can be designed to have a simple resonance involving only quartz and the electrode material. The resonance is free of coupling to other modes of vibration and is also quite isolated from the edge of the plate and its support structure (50).
- (iii) The temperature coefficient of the AT and BT cut crystals is very small thus offering a higher precision of measurement.
- (iv) The piezoelectric constant of an AT cut crystal is higher than that of a BT cut crystal therefore, the shear mode of vibration is driven more strongly in the AT cut crystal. This will result in a greater ability of the crystal to vibrate with loads on the surface of the crystal.
- (v) The frequency constant for an AT cut crystal is lower than that of a BT cut (see figure 9). The significance of this can be demonstrated as follows:

From equ 6

$$\Delta f = \frac{-\Delta m}{A} \cdot \frac{f}{\rho} \cdot \frac{1}{t}$$

The frequency constant $N = f \cdot t$

$$\text{or } \frac{1}{t} = \frac{f}{N} \tag{7}$$

substitute (7) into (6)

$$\Delta f = \frac{-\Delta m}{A} \cdot \frac{f^2}{\rho N} \tag{8}$$

Thus an AT cut crystal will be more sensitive to added mass.

By consideration of equation 6 it would appear that the sensitivity of the technique could be infinitely extended by using crystals with a very high vibrational frequency. However, Sauerbrey has pointed out (44) that because of the high mechanical sensitivity of high frequency quartz crystals and subsequent loss in accuracy there is no special advantage in using crystals with a fundamental frequency higher than 10MHz.

Detailed consideration as to which frequency is best suited for accurate and precise micro weighing by using a quartz crystal is given in a study by Warner and Stockbridge (41). They consider the effects of the degree of control of temperature, variation of oscillation amplitude, and variation of the Q or quality of the crystal. The use of a crystal vibrating in overtone mode is also considered. In a later paper (52) the theoretical limit of detection of the quartz micro balance $\sim 10^{-12}$ g is approached; however the instrumentation involved is very complex.

1.2.4. Applications of the Quartz Crystal Micro Balance Technique

Since Sauerbrey's work, in which vacuum deposited metal films were used to establish and test the equation, the application of the quartz crystal microbalance technique to the monitoring of vacuum deposited metals has been extensive. Considerable attention has been paid to the calibration of the device; some techniques used were indirect (53) others direct (54). General agreement with the Sauerbrey equation has been found. Various crystal holders have been designed to facilitate the use of the device in ultra high vacuum (10^{-9} torr) (55) and at high temperatures (56). The measurement of thin film density of metals has also been facilitated by this

technique. The measurement of mass of the film was carried out with the crystal microbalance and the film thickness was measured by multiple beam interferometry (57,58).

The information supplied by the crystal microbalance has been used not only to monitor thin film deposition but also to control automatically the rate of deposition of 2 metals to form an alloy film (48,59,60).

Several workers have made use of the high sensitivity of the crystal microbalance to study the adsorption of gases onto quartz and various electrode materials (61-63).

Other applications, of a chemical nature, have also been made with this sensitive weight sensing device. Of the more straightforward ideas electrogravimetric analysis (64) and corrosion studies (65) have been carried out. The electrogravimetric analysis involved the electrodeposition of metals from a dilute solution onto the electrodes of a quartz crystal and subsequent measurement of the frequency change of the crystal. The analysis was essentially non destructive as the deposition occurred only over a short period of time. Minimum solution concentration for the determination of cadmium was reported as 5.0×10^{-8} M.

A more subtle use of the device is to deposit on the surface of the crystal a metal or material of interest and then permit this material to react with a gaseous reactant. The reaction that occurs can then be followed by monitoring the changing mass on the surface of the crystal.

The study of the kinetics of chemisorption of oxygen on aluminium (66) and rates of sulphuration on silver (67) are examples of this work. The application of material, other than a metal, to the surface of a quartz crystal was carried out (68). This study was

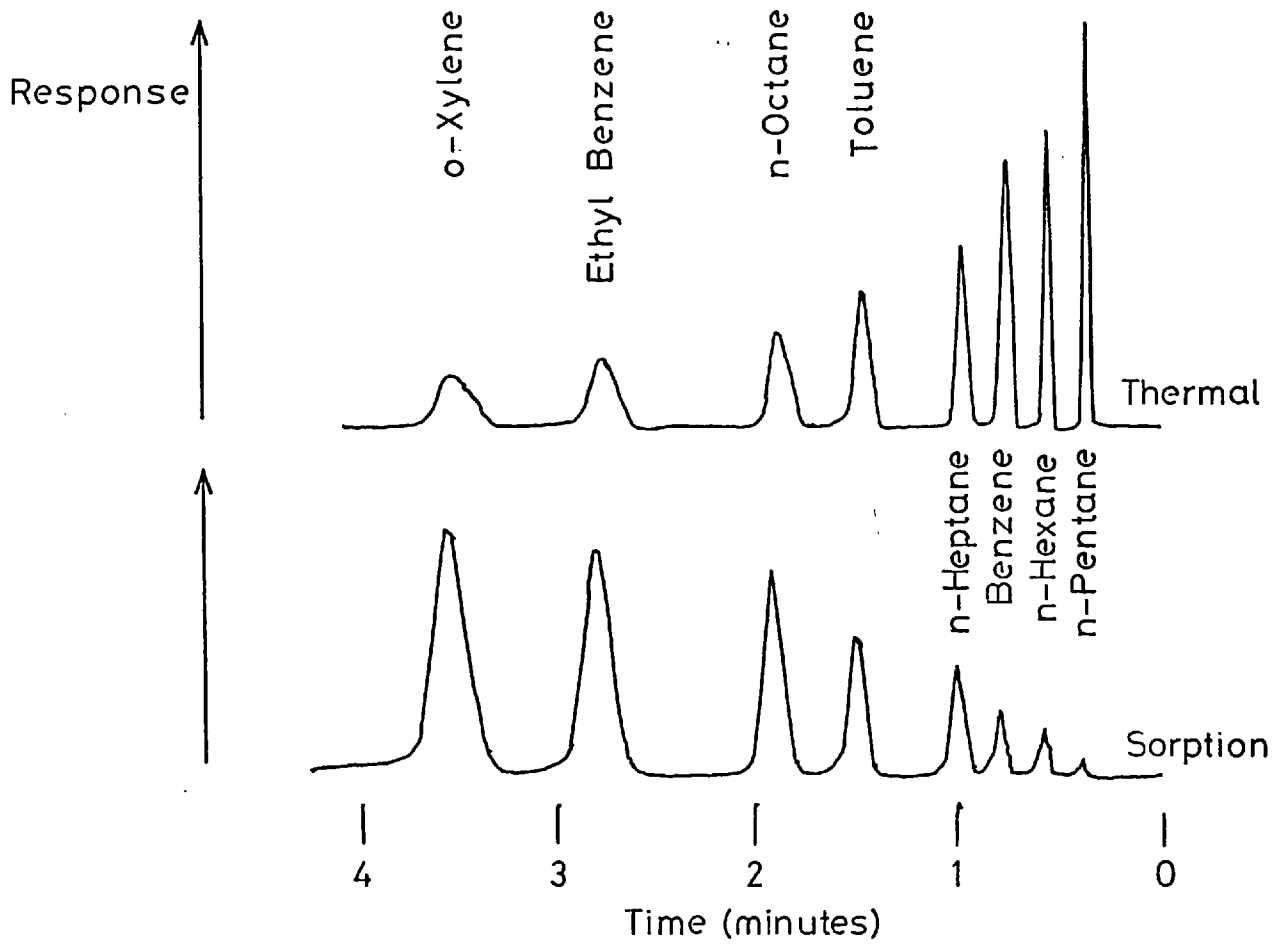
concerned with the oxidation stability of elastomers, the elastomer being deposited, from solution, on the electrode of the crystal.

The weight changes that occurred by changing the environment of the elastomer were recorded.

The idea that a crystal, coated with a suitable compound, could be used as a gas detector was first put forward by King (69). He proposed and demonstrated that a vibrating quartz crystal when coated with various gas chromatographic stationary phases would act as a sensitive detector when placed in the effluent of a gas chromatographic column. He compared the response of this detector to a thermal conductivity detector under identical operating conditions (figure 12). It is clear, in figure 12, that the crystal detector is a mass detector, having a higher response to higher molecular weight compounds. A study of the basic parameters of the partition detector has been made (70). The effect of temperature, flow rate of carrier gas, position of the coating on the crystal and precision of the system were included in the work. Other workers (71-72) have developed the partition detector for use in a portable gas chromatograph.

A crystal coated with a gas chromatographic stationary phase relies upon the partitioning of the sample gas between the carrier gas and the stationary phase on the crystal. Thus it is possible to mathematically predict the response of such a detector if the parameters of the partition system are known. Detailed work concerning the predictability of the response of the partition detector has been carried out with very good agreement between mathematical prediction and experimental results (73).

The major disadvantage of using a partition detector for pollution studies is its lack of selectivity. The ability to differentiate between different compounds in figure 12 is as a result



Simultaneous Recordings of Thermal Conductivity
and Squalane Sorption Detectors

Figure 12

of the chromatographic separation of a discrete sample prior to detection. However, in the envisaged application of this device the sample gas (polluted air) would pass continuously over the detecting crystal without separation prior to detection. Thus any material in the polluted air that would dissolve in the stationary phase on the crystal would cause a change in frequency of the crystal.

In an attempt to obtain selectivity of response the possibility of utilizing the different values of partition coefficients of organic vapours for various coatings has been examined. By passing the sample gas simultaneously over several crystals, each coated with a different stationary phase it is possible to perform selective, multicomponent gas analysis. The applicability and constraints of this technique are pointed out in reference 73.

A system that appears to offer selectivity for the analysis of organic vapours has been studied (74). This work involved the use of cholesteryl esters as the coatings on the crystal. These compounds are known as liquid crystals which within a defined temperature range are liquid in mobility and crystalline in optical properties. The selectivity of these compounds is attributable to a molecular structure in which there are long channels; the organic vapours passing over the detector then dissolve in the coating according to the ease with which they fit into the crystal lattice of the coating. It was reported that the cholesteryl esters used had the ability to separate the structural isomers of substituted benzene.

A considerable amount of work has been carried out by King concerning the development of a coating suitable for the selective, sensitive determination of atmospheric moisture. He tried several coatings (75,76) with an eventual choice of lithium chloride (77).

This was later modified to incorporate a heater in the sample cell which was operated at intervals to avoid saturation of the lithium chloride coating by moisture (78).

Several workers have attempted to develop a sensitive selective coating for the analysis of atmospheric sulphur dioxide. One study (79) involved the screening of a large number of amines for use as a coating, however the rate of loss of the coating due to evaporation was in many cases unacceptable. A coating with sufficient sensitivity for atmospheric sulphur dioxide was not found. In order to obtain sufficient sensitivity one group of workers placed their coated crystal in a static environment (80) i.e. the sample gas was not flowing past the crystal but stationary. This permitted an integrating mode of action of the detector. The coating employed was a 1:1 copolymer of styrene and dimethylaminopropyl maleimide (81), however substantial interference from nitrogen dioxide and moisture was noted.

A similar technique was also used (82) to evaluate a number of gas chromatography stationary phases for their suitability for sulphur dioxide analysis.

It was concluded that a deposit of sodium tetrachloromercuriate (as used in the West and Gaeke method (15)) was the best coating of those tested. The other coatings, in order of sensitivity, were Silicone QF-1, Versamid 900, Apiezon N, Carbowax 20M and Silicone SE30. The tetrachloromercuriate complex was found to be more sensitive than Silicone QF-1 by an order of magnitude, with 4.01 μg of sulphur dioxide adsorbed in 15 minutes as opposed to 0.40 μg . However in a later paper (83) the same authors described the use of Carbowax 20M as being most suitable for the determination of sulphur

dioxide in a flowing system. In this paper the detection device was preceded by a gas chromatograph operating at room temperature.

The use of the crystal detector for the determination of very low levels of organophosphorous compounds has also received attention. Preliminary work using Diisopropylmethyl phosphonate (D.I.M.P.) as a model compound indicated chemisorbtion was occurring on crystals coated with transition metal halides (84). Subsequent work (85) selected iron (III) chloride as a coating, but alone it was insufficiently sensitive: complexed with D.I.M.P. much greater sensitivity was achieved. The same approach was tried with a real pesticide, paroxon, (O,O-diethyl-o-p-nitrophenyl phosphate); however, a poor detection limit (10 ppm) was obtained.

Recently (86) work has been done in an attempt to find a suitable coating for the determination of atmospheric nitrogen dioxide and ammonia. The coatings that were used were Ucon fluids which are polyalkylene glycols used as stationary phases in gas chromatography. The reported minimum detectable concentration of both nitrogen dioxide and ammonia were of the order of 1-10 ppb.

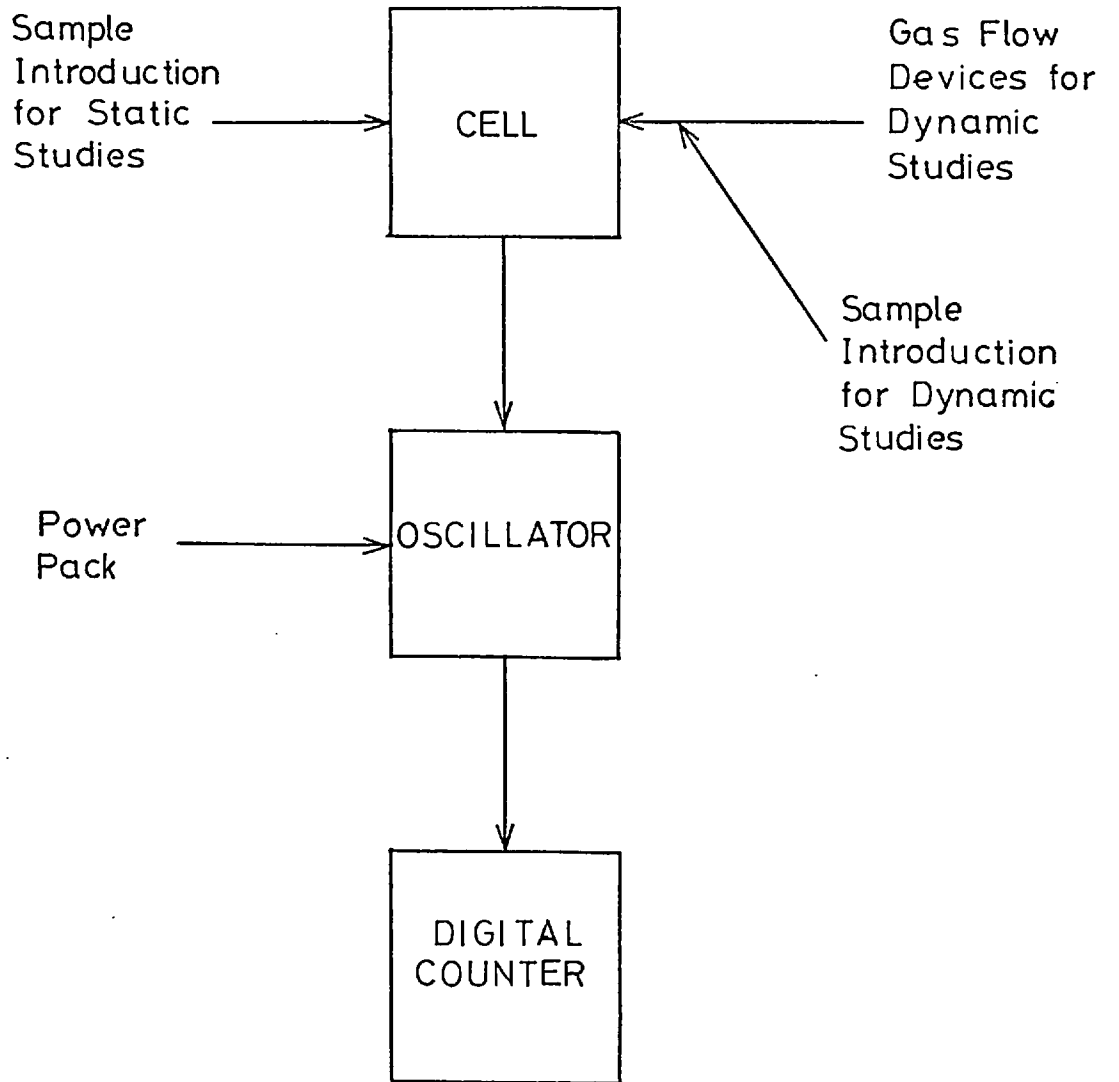
The ucon fluid coating however suffered from bad interference by water vapour and also if the coating was left exposed to the atmosphere for a period of one hour the activity of the coating disappeared.

2. Instrumentation
- 2.1. Basic Requirements
- 2.1.1. Single Sided System

The instrumentation associated with the quartz crystal micro balance is basically very simple, the main requirements being an electronic oscillator to vibrate the crystal at its natural mechanical resonant frequency and a means of monitoring this frequency. The crystal itself is housed in a cell suitable for the introduction of sample gas into a static atmosphere and also having facility to pass the sample through the cell in a flowing gas stream. A block diagram of the equipment used for a single sided system is shown in figure 13.

There are a number of disadvantages associated with the single sided system. These disadvantages are the alternative methods by which the crystal may change its frequency other than the interaction of coating and sample gas. The main source of error is attributable to the effect of temperature. As stated previously the A.T. cut crystal has a small but significant temperature coefficient which will result in frequency changes due to temperature fluctuations of the cell and crystal^{if they} are not thermostated.

The second major source of error is associated with the actual coating on the crystal. If the coating is of the gas chromatography stationary phase type then it will have, dependant upon the exact nature of the material, a small but appreciable vapour pressure at room temperature. This will result in a slow evaporation of the coating from the crystal surface with a subsequent increase in the frequency of the crystal. If the crystal is in a static environment then an equilibrium may be reached between the coating on the crystal and the environment and a stable frequency obtained. The problem of bleed of coating is, however, exacerbated when the coated crystal is



Block Diagram of Single Sided System

Figure 13

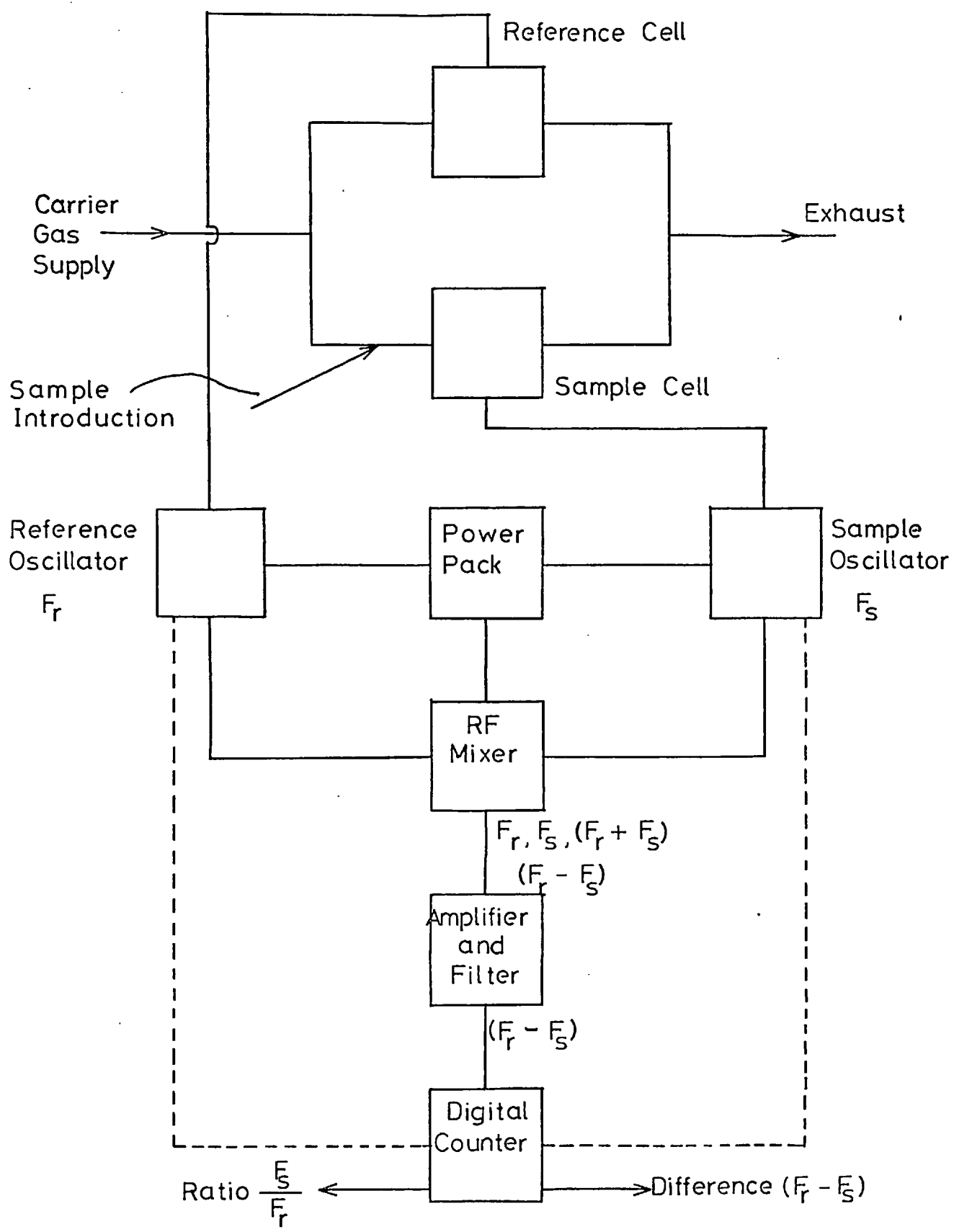
used in a dynamic system.

Drift due to bleed is not experienced when solid coatings such as manganese dioxide and lead dioxide are used. A third source of error is observed with both solid and liquid coatings. This error is the frequency decrease due to the non-selective pickup of material from the environment. This material may be moisture, dust particles or gases inadvertently introduced into the system in addition to the sample gas.

2.1.2. Double Sided System

It is possible to obtain a good degree of correction for these various effects instrumentally as opposed to trying to prevent each error separately. This can be achieved by employing a double sided system, involving the use of an additional crystal and cell with its own oscillator to act as a reference (figure 14).

The frequency of both the reference and sample crystals, are compared in such a manner that only the frequency change due to the interaction between sample gas and the coating on the sample crystal will be displayed in the processed result. The signal comparison is achieved by monitoring the difference between the sample frequency, f_s and the reference frequency, f_r . The difference frequency is obtained by feeding the two frequencies f_s and f_r into an r.f. mixer. From the mixer the original frequencies f_s and f_r , the sum $f_s + f_r$ and the difference $f_s - f_r$ are obtained. As the frequencies of f_s and f_r are of the order of 9MHz the sum will be of the order of 18MHz whereas the difference frequency $f_s - f_r$ will only be a few kilohertz. It is thus simple to electronically filter out and amplify the desired difference frequency and monitor this frequency with a frequency meter or digital counter. If the reference and sample crystals are in identical environments then any effect leading to the change of



Block Diagram of Double Sided System

Figure 14

frequency of the sample crystal (with the exception of sample introduction) will also cause an identical change in frequency of the reference crystal.

If the form of instrumentation just described is used the difference between the two frequencies will remain constant thus effectively correcting for the sources of error previously described. If the reference and sample systems are identical then only the introduction of sample into the sample cell will give a change in the frequency difference of the two crystals.

It is possible to compare the frequencies of the sample and reference crystals without using an r.f. mixer with associated filter and amplifier. This technique uses the frequency ratio facility of the frequency meter and involves only the direct feeding of f_s and f_r into the frequency meter with no additional electronic circuitry. The figure displayed by the counter is the ratio $\frac{f_s}{f_r}$. This ratio is obtained by substituting the internal frequency standard of the frequency meter by the reference oscillator. A single sided system i.e. direct monitoring of f_s can be obtained simply by switching the internal frequency standard of the frequency meter back into the control circuit of the instrument. With the ratio measuring technique it is easier to obtain separate information about the reference and sample crystal frequencies. This is so as the displayed ratio $R = \frac{f_s}{f_r}$

$$\therefore f_r = \frac{f_s}{R}$$

As the value of f_s can be found simply by operating a switch then f_r can easily be calculated with an electronic calculator.

This facility is occasionally useful.

2.2. Equipment Details

2.2.1. Crystals

The crystals used in these studies were supplied by two manufacturers, The Piezoelectric Crystal Co., Carlisle, Pennsylvania and the Quartz Crystal Company, New Malden, Surrey. The crystals were of a similar specification and are illustrated in figure 15a and b. The crystals were AT cut, 9MHz ($\pm 50\text{KHz}$) fundamental frequency with vacuum evaporated gold electrodes. The holder was type HC6U and the crystal was not sealed into the holder.

The cans or outer covers with which the crystals were supplied, were not sealed to the crystal holders.

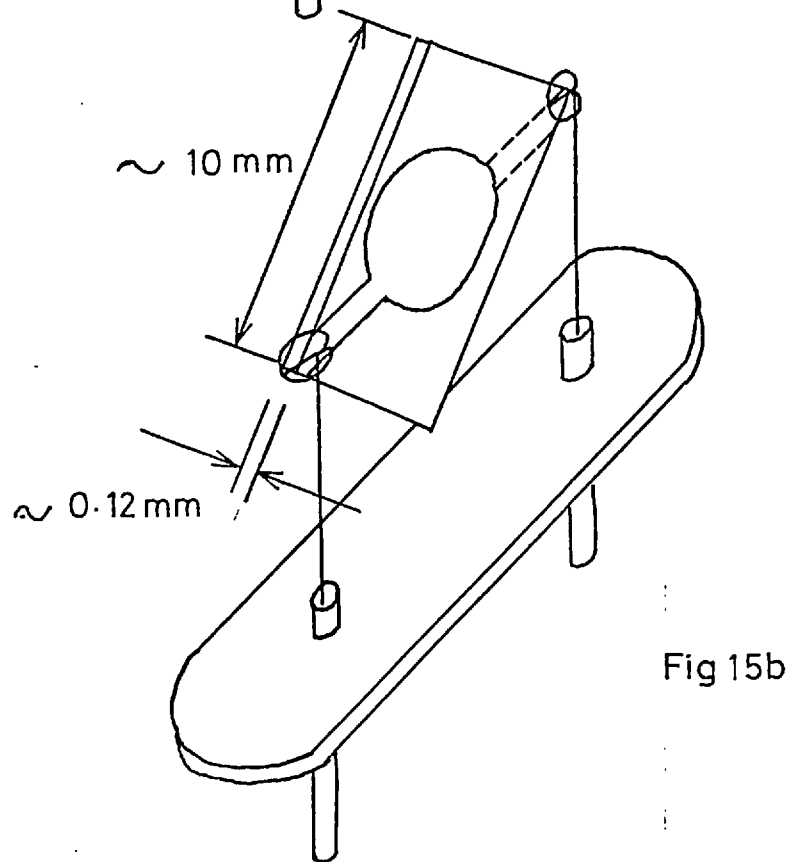
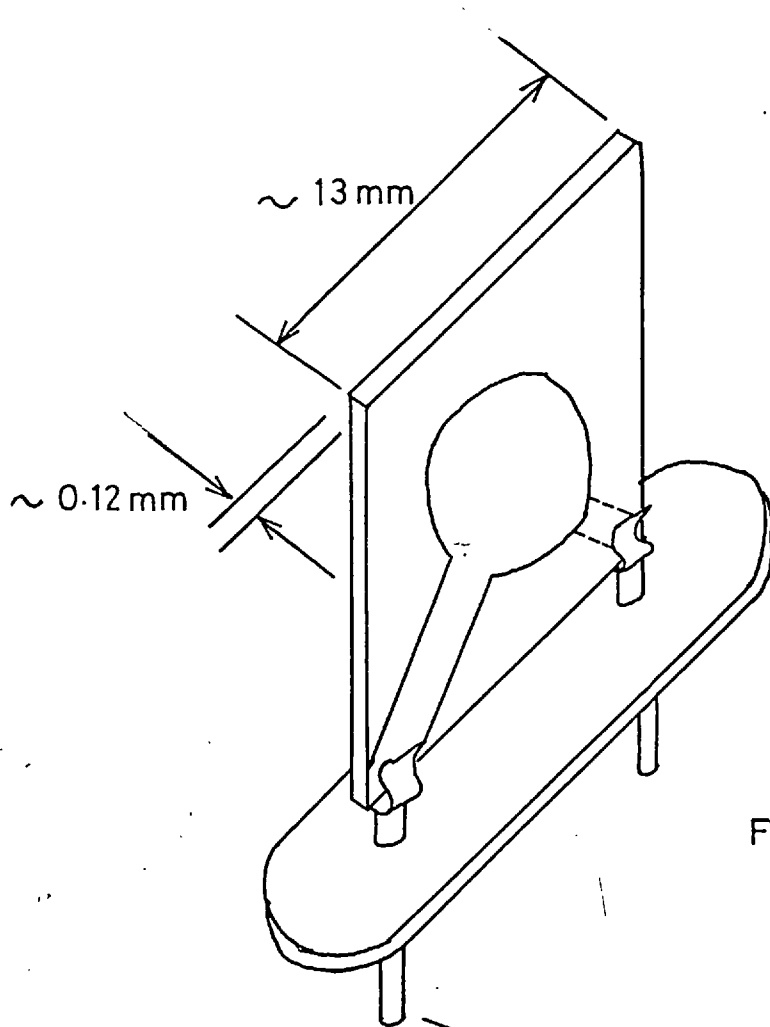
2.2.2. Oscillators

The oscillators used to drive the crystals were constructed from kits of parts supplied by International Crystal, Oklahoma. A circuit diagram of the oscillators used is given in figure 16. The frequency range of the oscillators was 6-10MHz.

2.2.3. Power Pack

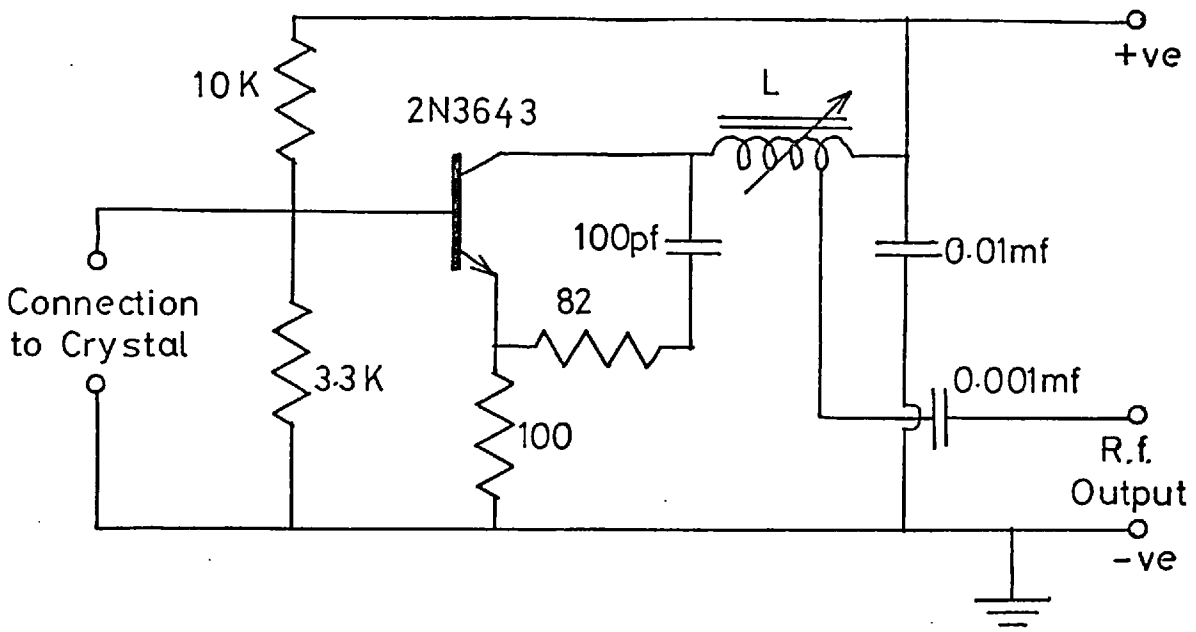
The power pack used was a solid state stabilized device (manufactured by Coutant Electronics, Ltd., Type LM50/30) with a stability of $\pm 0.01\%$ of the output voltage. It has been reported (81) that a 9MHz AT cut crystal driven with the oscillator described was sensitive to the voltage used to power the oscillator. The magnitude of this effect was 0.5Hz/mV . Thus with the oscillator driven at 8 volts d.c. by the stabilized power pack the voltage variation would not exceed $\pm 0.8\text{mV}$ with a resultant frequency variation of $\pm 0.4\text{Hz}$.

As this variation was less than the error associated with the counter when used with a one second counting time ($\pm 1\text{ Hz}$) the use of this power pack was considered satisfactory.



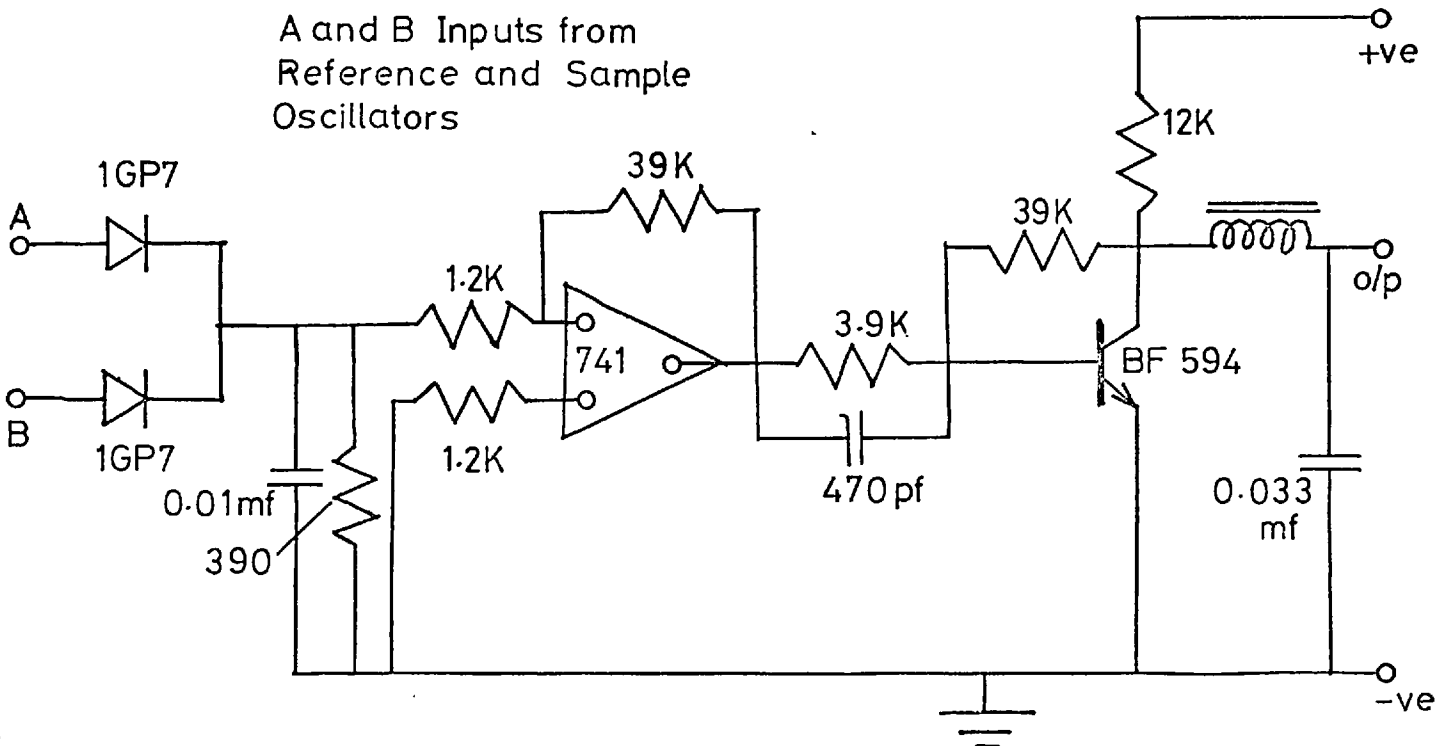
Sketches of AT Cut Crystals from Different
Manufacturers

Figure 15 a,b



Circuit Diagram of Oscillator

Figure 16



Circuit Diagram of Mixer/Amplifier System

Figure 17

2.2.4. R.f. Mixer

The mixer used with some double sided studies was a diode mixer. The filter and amplifier following the mixer were combined in one operational amplifier. The external components associated with the amplifier were chosen to give a high frequency cut off point at 40KHz. A circuit diagram of this system is given in figure 17.

With this mixing circuit it was found that when sample interacted with a coating on the sample crystal the frequency difference between the sample and reference crystals could increase and for a different crystal similarly coated the interaction between sample and coating could cause a decrease in the frequency difference. This can be explained by consideration of figure 18a and b.

In 18a the frequency of the coated reference crystal is higher than the coated sample crystal. This is due to differences in the two coatings. On addition of sample to the sample crystal its frequency decreases and the frequency difference increases.

In 18b the frequency of the sample crystal is higher than that of the reference crystal thus on addition of sample to the sample crystal f_s decreases and so does the frequency difference.

2.2.5. Frequency Meter

The frequency meter or digital counter that was used was an A.M.F./Venner Digital Counter Model 7737 with a seven digit display on numerical neon indicator tubes. The frequency range of the counter when operating with a sinusoidal input was from 10Hz to 50MHz. The gating time, the period during which the instrument counts the number of incoming pulses, was variable in decade steps from 0.1 μ s to 10s.

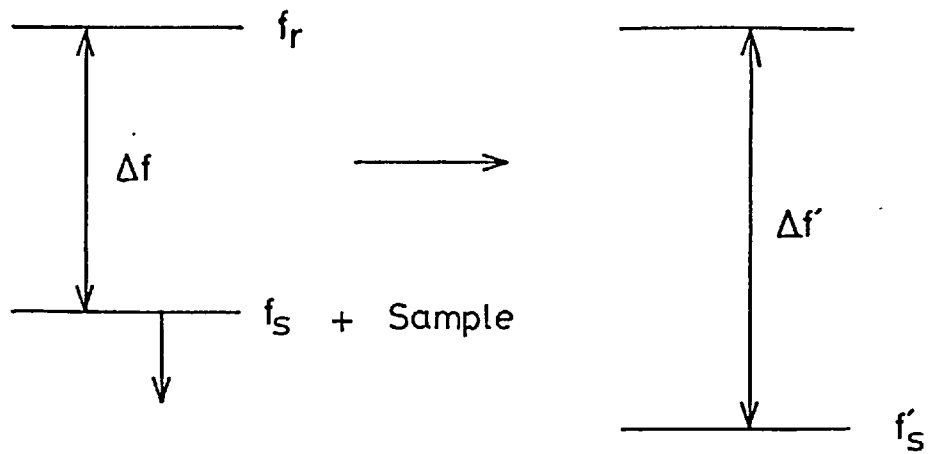


Figure 18a

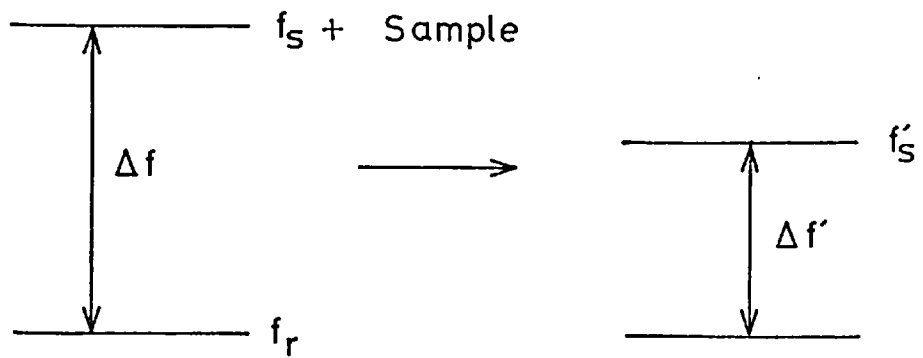


Figure 18b

Occurrence of Increasing and Decreasing
Frequency Difference from Mixer Circuit

Figure 18 a,b

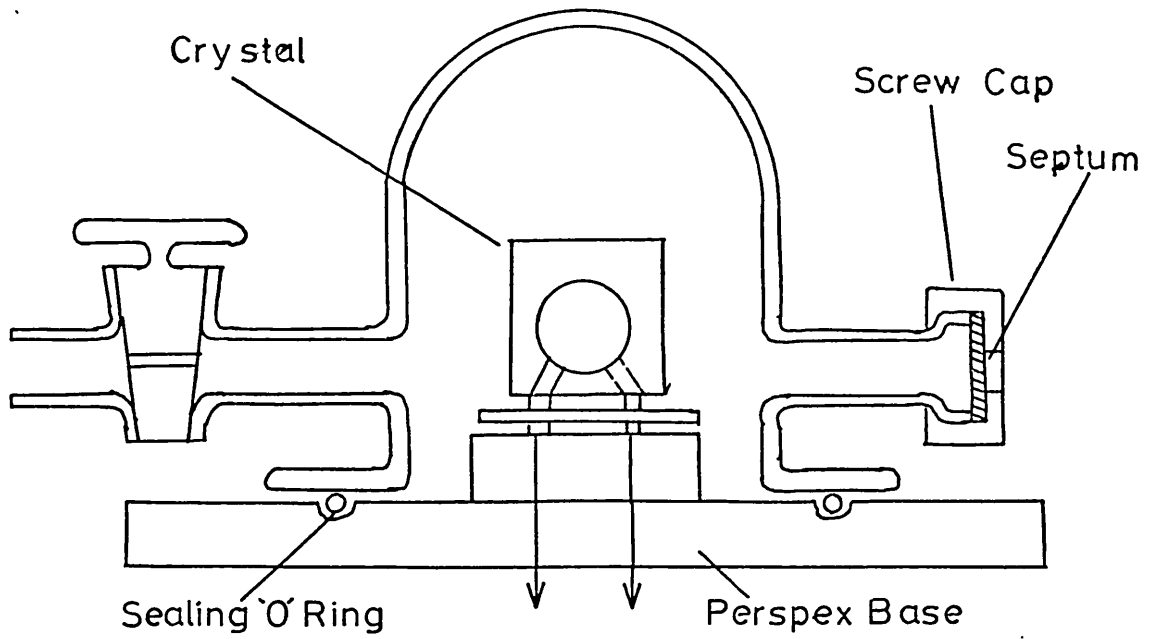
The actual gating time was derived from the standard frequency reference source of the meter, a 10MHz crystal controlled oscillator, and a frequency dividing chain. The accuracy of a measured frequency was ± 1 count. The significance of the gating time and accuracy of measurement can be readily demonstrated by consideration of the following example: suppose a sinusoidal signal with a frequency of exactly 9MHz were to be measured and the gating time was 1 μ s, then the displayed result on the frequency meter would be 9 with an accuracy of ± 1 . The units of this measurement would be MHz. If the same signal was measured with a 1 s gating time the displayed result would be 9,000,000 with an accuracy of ± 1 . The units of this measurement would be Hz. Similarly if a 10s gating time was used then a result of (9)000000.0 \pm 0.1 Hz would be displayed. (The first digit -9 would not be seen as it would be carried off scale).

Most of the frequency measurements were made using a 1s gating time.

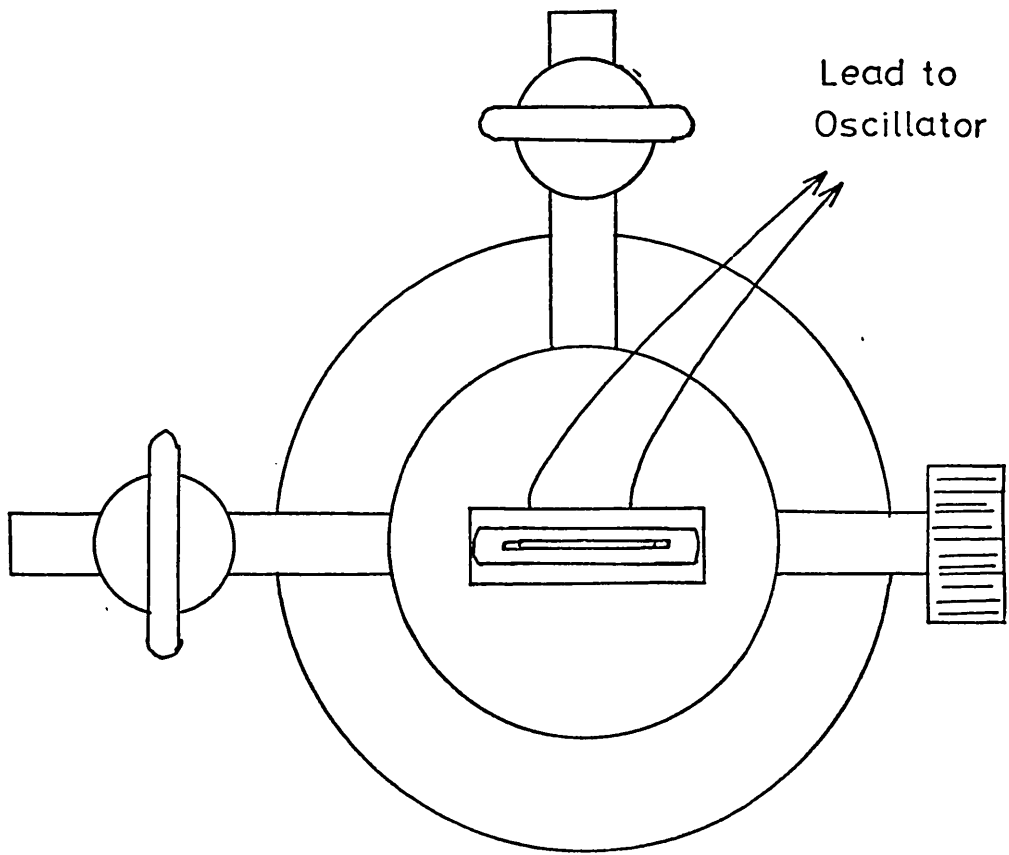
2.2.6. Cell Design

Three cell systems were designed for use with the quartz crystal microbalance. A glass cell was constructed which was used throughout the work for studying static systems, i.e. the interaction of sample gas and coated crystal in a non-flowing environment. This cell was also used in earlier dynamic studies and is illustrated in figure 19.

The cell was mounted on a perspex base fitted with quick release phosphor-bronze clips. Connection from the crystal to the oscillator was made with coaxial cable. For static studies sample was introduced into the cell via the silicone rubber septum with a gas tight micro-syringe. The cell could be flushed with nitrogen when required and then isolated from the gas stream. The volume of the



SECTIONAL ELEVATION



PLAN

GLASS CELL

Figure 19

cell was 27 ml. As the dead volume of this cell was large and the geometry of gas inlet and exit ports did not give adequate flushing of the cell, when used in a flowing system, two smaller flow cells were designed. These cells were all metal in construction with a volume of 2 ml. and are depicted schematically in figures 20 and 21.

The design shown in figure 20 directed the nitrogen carrier gas and sample through small holes (0.61 mm., No.70 drill) in the outer casing onto the centre of the crystal. The type shown in figure 21 flowed the gas stream in a laminar fashion over both faces of the crystal. The gas entrance and exit ports were placed diagonally opposite each other so that the gas stream was made to flow over the centre of the crystal and good flushing was obtained.

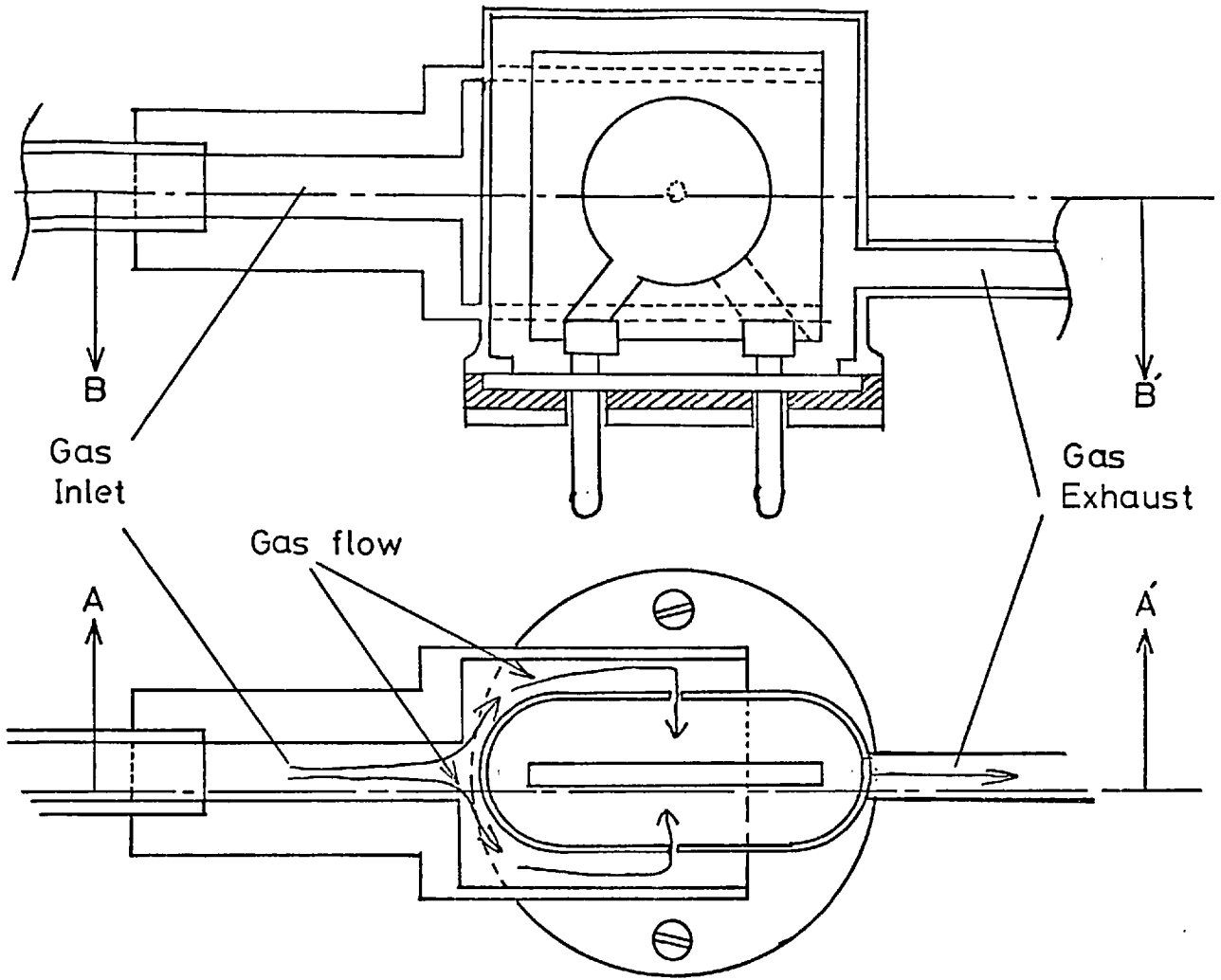
Two cells of this design were constructed in such a manner that both completed cells were in the same block of stainless steel (figure 22). Provision was also made for the total exclusion of water from the cells thus permitting easy operation in a water bath if desired.

The two cells, one for the reference crystal and one for the sample crystal, were well isolated from small, rapid temperature changes of the environment because of the large thermal capacity of the cell block.

The reference and sample cells were connected in parallel with respect to the carrier gas supply. Connected in this manner the reference and sample crystals experienced identical environments. If the cells were connected in series this would not be the case.

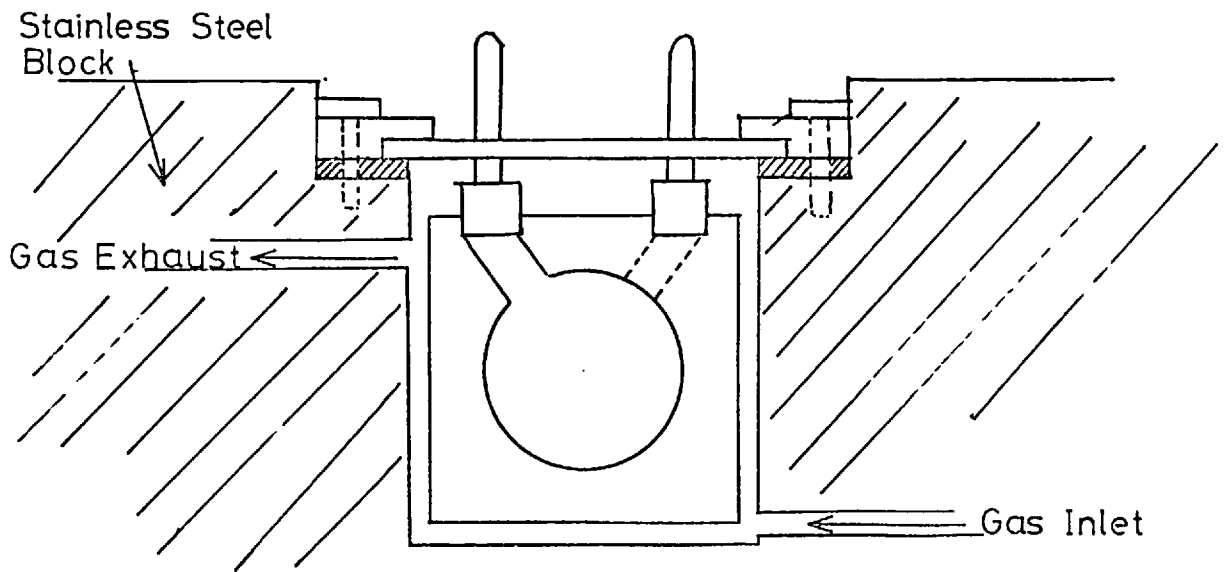
2.2.7. Gas Handling Systems

The carrier gas supply line used in dynamic studies and for flushing the static cell when required consisted of a cylinder of oxygen free nitrogen with a coarse regulating valve, a fine regulating



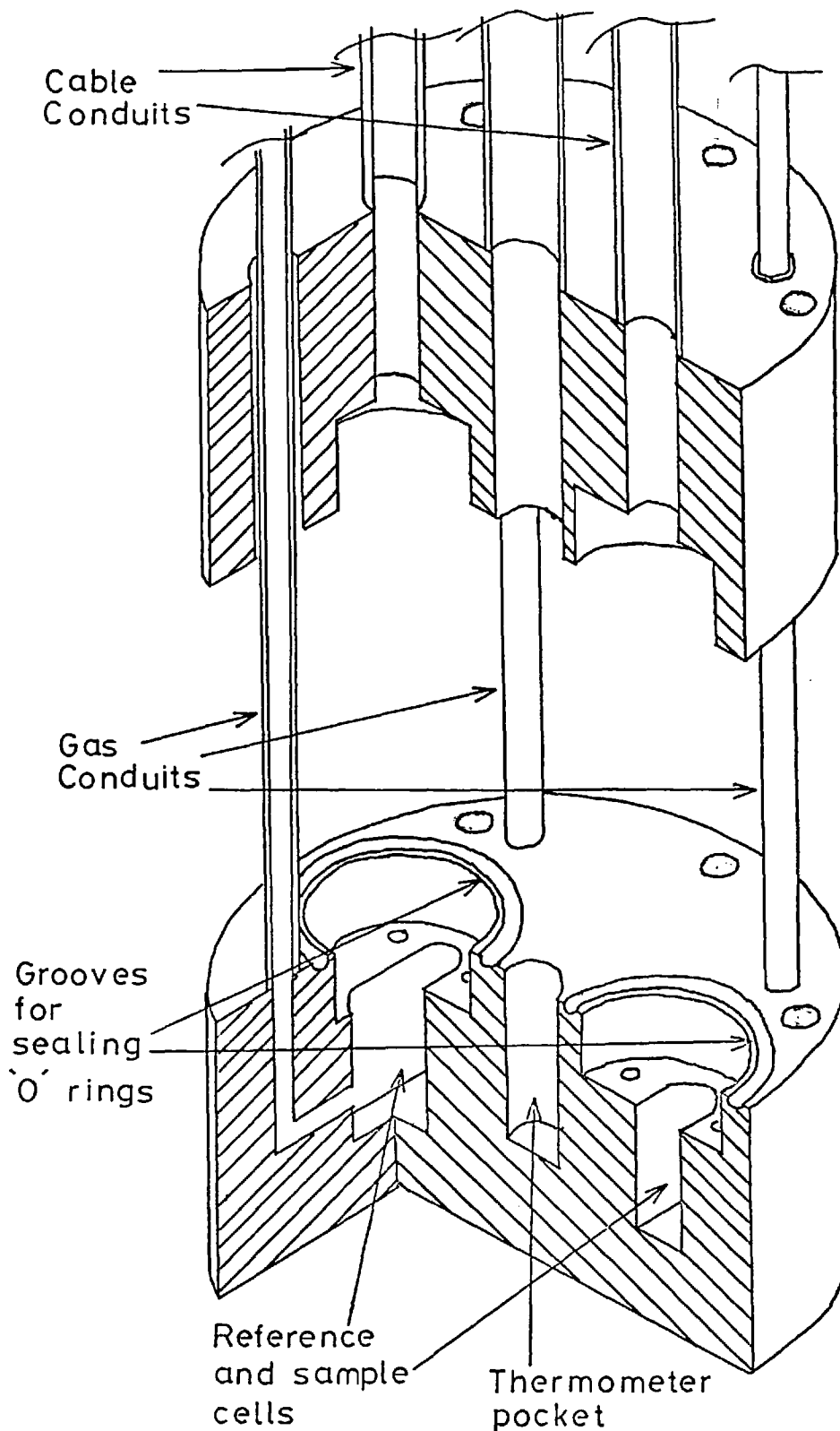
SECTIONAL ELEVATION, AÁ and SECTIONAL PLAN, BB\' of IMPINGER CELL

Figure 20



Spoiler Cell (Schematic)

Figure 21



Crystals and electrical connectors not shown

Sectional Projection of Stainless Steel Cell Assembly

Figure 22

valve with a p.t.f.e. diaphragm and a calibrated tapered tube and float flow meter (range 20-500 ml/min.). The interconnecting tube was 1/4" o.d. nylon tube. No special measures were taken to dry the gas. Facility for injecting quantities of sample gas into the gas stream prior to the sample cell was also provided. The gas line is shown schematically in figure 23.

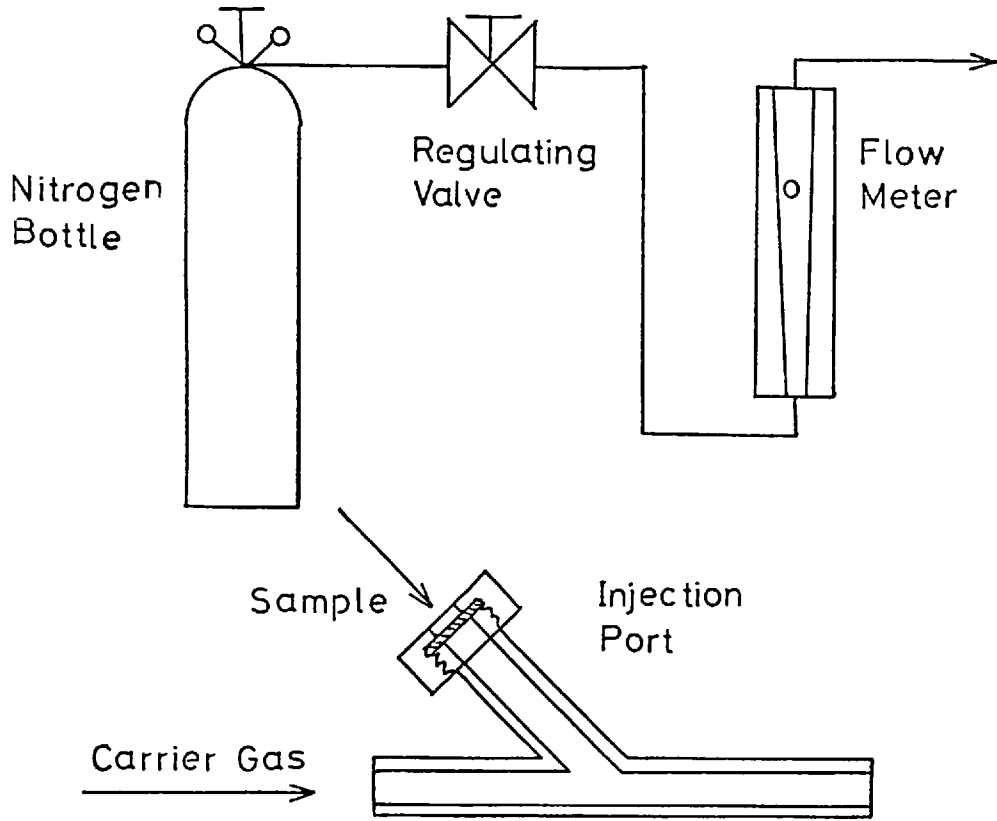
The sample gases used in this work were sulphur dioxide and nitrogen dioxide. These were obtained in liquified form in small lecture cylinders from B.D.H. Ltd.

The sample gas was allowed to expand from the lecture cylinder into an evacuated glass reservoir. The reservoir was filled to a pressure of approximately 10 mm above atmospheric pressure. Aliquots of the sample gas were withdrawn by syringe and introduced into the cell system, whether static or dynamic.

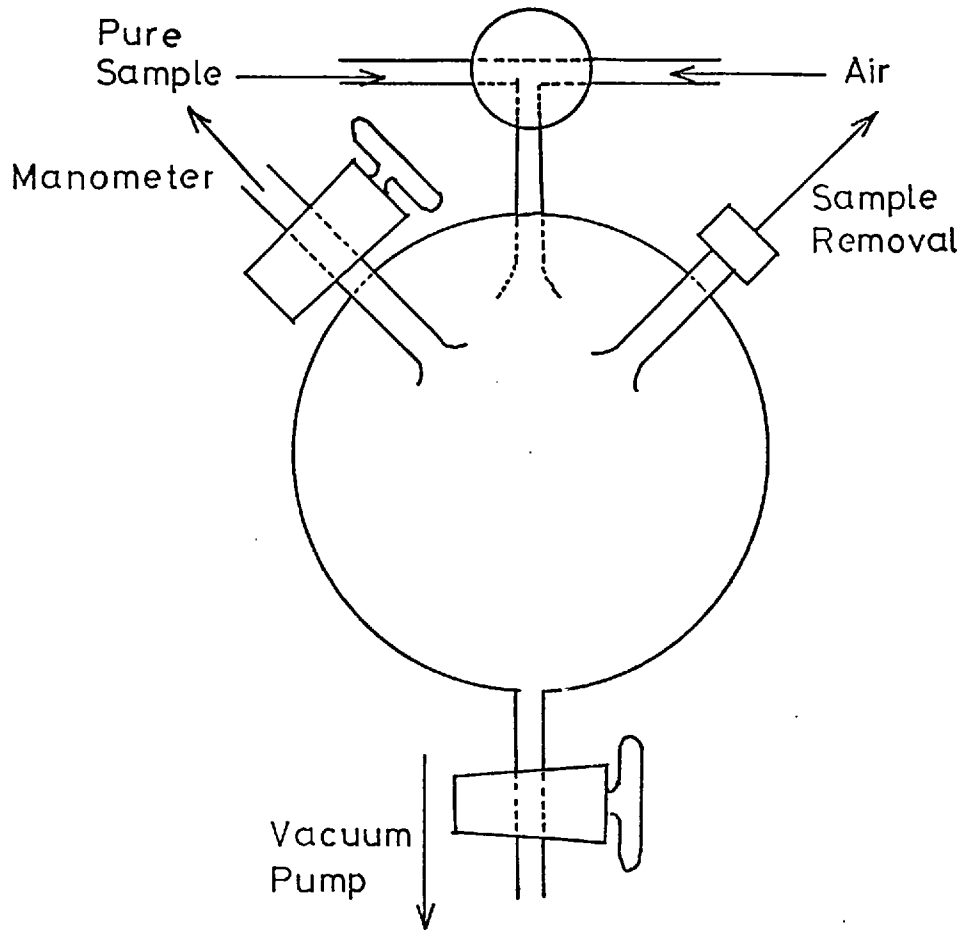
Three sizes of reservoir were constructed, 1 litre, 250 ml. and 100 ml. The design of this 1 l and 100 ml. reservoirs were similar and is depicted in figure 24a. These vessels were used for handling pure sample gas and dilute solutions down to 1000 ppm. For the preparation of dilute solution (100 - 1 ppm) a reservoir with teflon taps was constructed as considerable contamination of samples was experienced when attempting to prepare dilute solutions in the 1 l and 100 ml. vessels.

The source of the contamination was established as being due to the stopcock grease.

The new reservoir also incorporated a mercury pressure levelling device. After the withdrawal of 5 ml. of sample and before removal of the syringe the pressure in the vessel could be returned to atmospheric pressure to prevent contamination by air as the syringe needle was withdrawn.

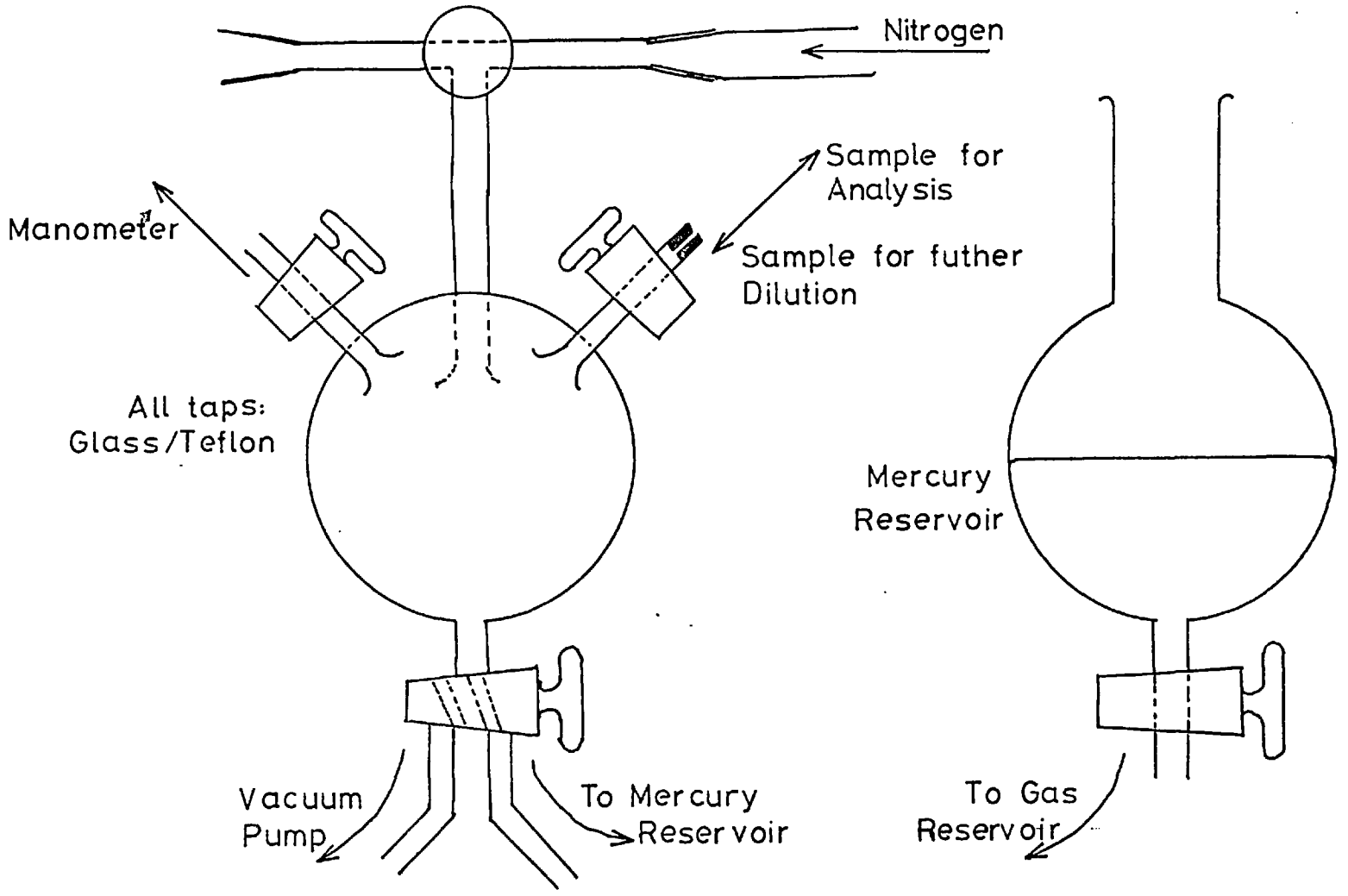


Gas Line
Figure 23



Gas Reservoir (1l and 100 ml)

Figure 24a



Gas Reservoir (250 ml) Pressure Levelling

Device

Figure 24b

The dilute gas solutions were made up with nitrogen. The modified vessel is shown in figure 24b.

The microsyringes used in this work were manufactured by Scientific Glass Engineering of Australia. A liquid syringe of 10 μ l capacity, subdivided into 1 and 0.2 μ l was used for the application of some coatings to the crystals.

Gas tight syringes of capacities 250 μ l, subdivided into 50 and 10 μ l; and 100 μ l, subdivided into 10 and 2 μ l were used to inject aliquots of sample gas.

In later work it was necessary to provide not small aliquots of short duration of sample gas in the carrier stream but a longer (10-15 minutes) presentation of a very dilute solution of sample. To fulfil this requirement a syringe pump (Sage Instruments, syringe pump model 355) and a ground glass syringe (5 ml.) fitted with a 15 cm. flexible teflon needle was used.

The syringe was filled with dilute sample gas which was then expelled at a pre-selected rate by the syringe pump. This dilute gas was introduced into the carrier gas flow via the injection port where the sample gas was further diluted. As the flow rate of the carrier gas and sample gas was known the dilution factor, and hence the final concentration of the sample in the carrier gas, could be calculated.

2.3. Experimental Investigation of Instrumental Parameters

Earlier in this chapter considerable emphasis has been given to the advantages offered by a double sided system i.e. the use of a coated reference crystal to correct for unwanted frequency changes of the sample crystal. Experiments were carried out to establish the effect of temperature change, bleed of coating on a single sided system and show the degree of correction for these effects when a

double sided system was used.

2.3.1. Temperature Effect

For the investigation of temperature effects upon a single crystal two glass cells, as illustrated in figure 19, were assembled with a clean uncoated crystal in each. Nitrogen carrier gas was passed through each cell at a rate of 120 ml./min. The signals from the two oscillators were fed into the mixer the frequency meter thus displayed the difference frequency.

A small electrical heater was constructed by winding approximately 65 cm. of nichrome wire ($18.67\Omega/m$) around the outside of one of the glass cells. Previously the cell was wrapped with asbestos paper, and the heater was completed by a final cover of asbestos paper. The cell and heater were insulated in a small box of expanded polystyrene. The power applied to the heater was 6.8Vd.c. at 0.5A i.e. 3.4 watts. The temperature of the heated cell was measured by a Chromel/Alumel thermocouple arrangement with one junction immersed in an ice/water bath, the other in the cell. The potential difference of the thermocouple arrangement was measured with a calibrated potentiometric chart recorder.

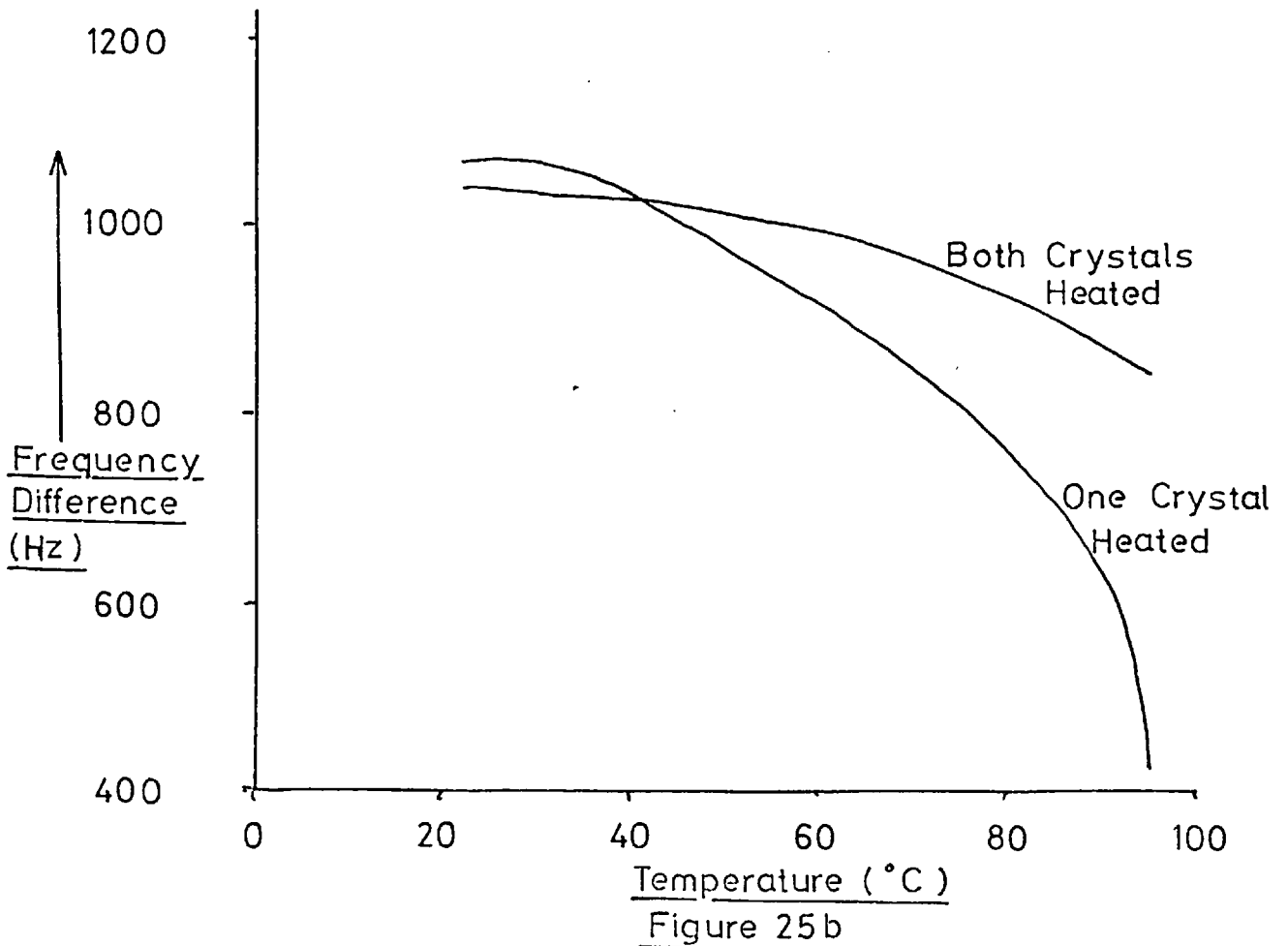
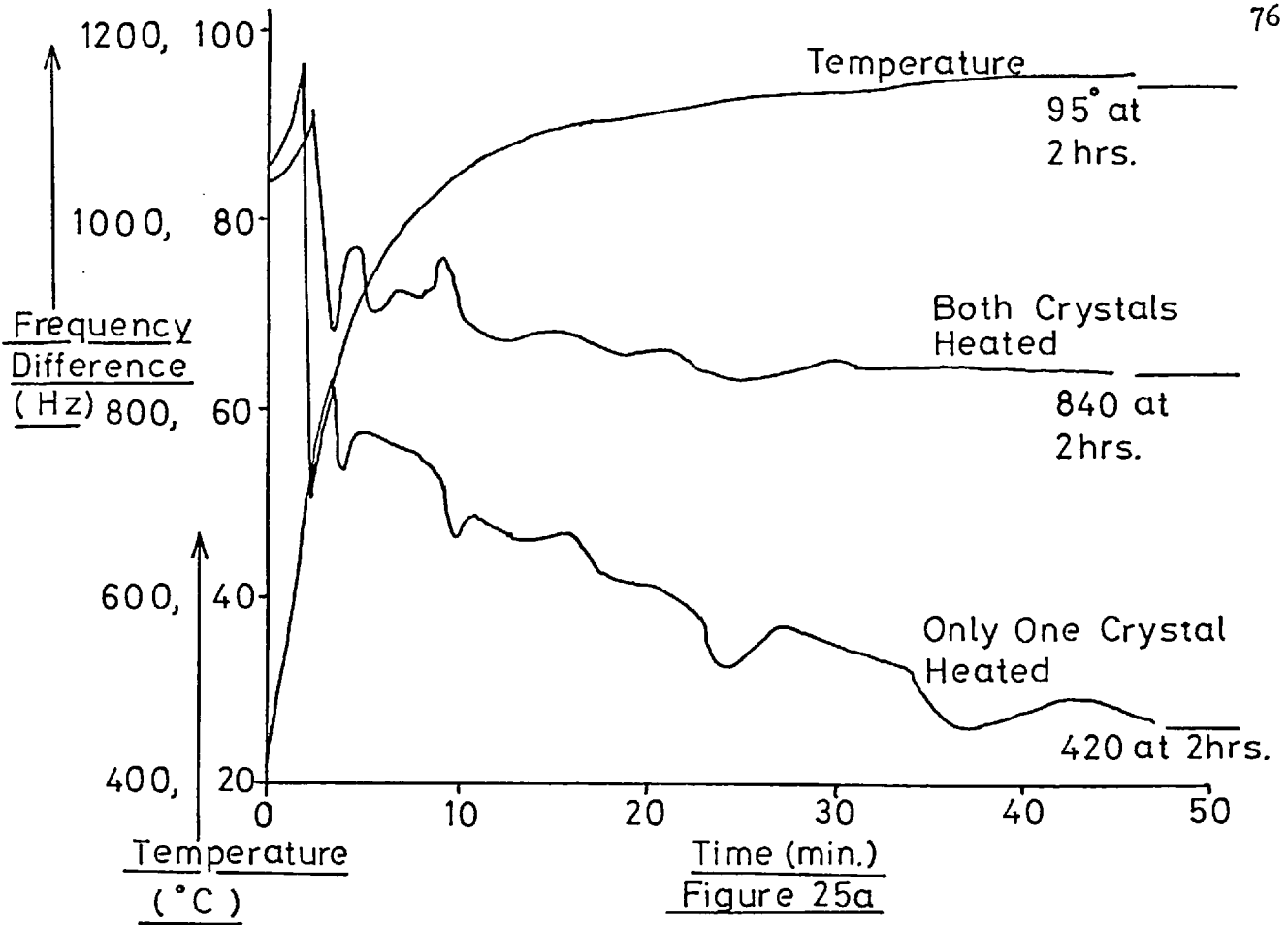
The frequency difference of the system was monitored prior to the application of power to the heater to establish a stable baseline.

The power was applied to the heater and the frequency difference, temperature and time were recorded.

To check the effect of temperature when reference and sample crystals were heated together only one cell was used with both crystals placed in the heated cell with the aid of a modified base plate. Other experimental conditions were as in the first experiment.

Again the frequency difference, temperature and time were recorded.

The results of this study are shown in figure 25 (a and b).



Variation of Frequency with Temperature

Figure 25 a,b

From this graph several points become clear:

- i) the crystal is a more sensitive temperature sensor than the thermocouple - hence the irregular frequency curves:
- ii) when only one crystal is heated the temperature coefficient between 25° and 95° is approximately $10\text{Hz}/^{\circ}\text{C}$ which ^{is} in reasonable agreement with published data:
- iii) there is a fair degree of correction when both crystals are heated. The temperature coefficient of this particular system being $3\text{ Hz}/^{\circ}\text{C}$.

Further experiments have shown that it is difficult to get a better degree of temperature correction than that shown in figure 25. Crystals have to be chosen so that they are matched i.e. they have their turnover point at the same place.

The sensitive nature of the turnover point with respect to the angle of cut of the crystal was discussed previously and illustrated in figure 11. Thus it will be appreciated that crystals cut in different manufacturing batches are difficult to match and a close match may only be obtained from close neighbours in the same batch.

2.3.2. Coating Bleed

In this study the stainless steel cell (figure 22) and the frequency ratio method of correction were employed. The crystals used were coated with triethanolamine on one electrode only. Care was taken to ensure that the coatings on the crystals were as similar as possible. (The techniques and problems associated with coating crystals will be described in the next chapter).

The details of the crystal coatings are shown below:-

Crystal number	Frequency change due to coating	Mass of coating	Diameter of coating
1	16,738Hz	48.3 μg	6.86 mm
2	14,342Hz	51.0 μg	7.04 mm

Table 3

Immediately after the preparation of the coatings the crystals were located in the cells. The flow rate of the carrier gas was regulated to 12 ml./min. through each cell, the frequency ratio and frequency of crystal number 1 were recorded at various intervals of time. From the results the frequencies of crystal number 2 were calculated. The frequencies of crystals 1 and 2 and the frequency ratio were plotted as a function of time. (Figure 26a).

A similar experiment was carried out with two crystals that had dissimilar coatings. The coating was triethanolamine on both crystals, the diameter of the coatings was very similar but the masses of the coatings were not equal. Details are shown below:-

Crystal number	Frequency change due to coating	Mass of coating	Diameter of coating
3	11,679Hz	53.9 μg	6.98 mm
4	6,837Hz	28.2 μg	7.02 mm

Table 4

The bleed of triethanolamine from these crystals was recorded as in the previous experiment and is shown in figure 26b.

By comparison of figures 26a and b it is clear that if a good degree of correction is required then this can only be obtained when the coatings are as closely matched as possible. The rate of drift

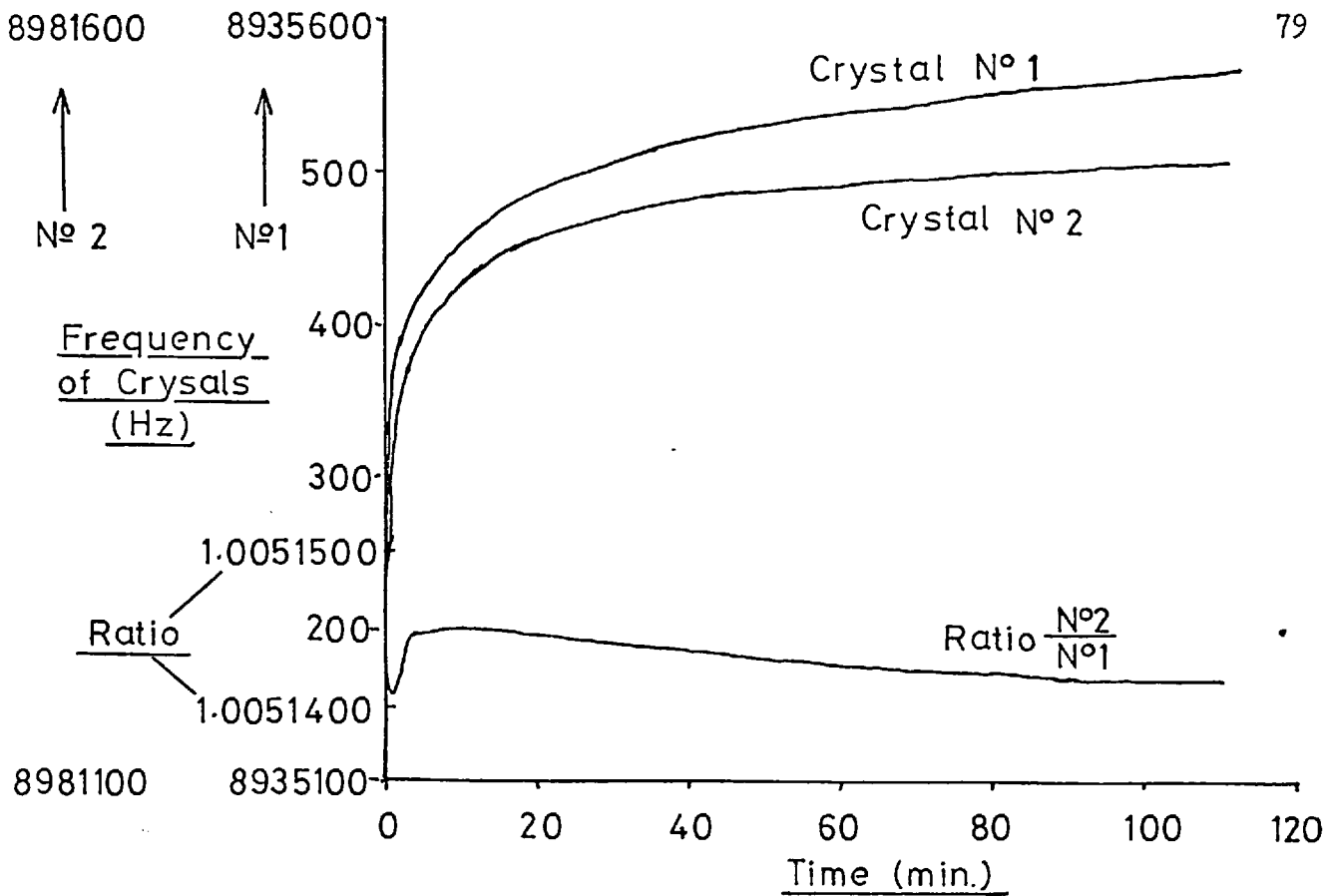


Figure 26a

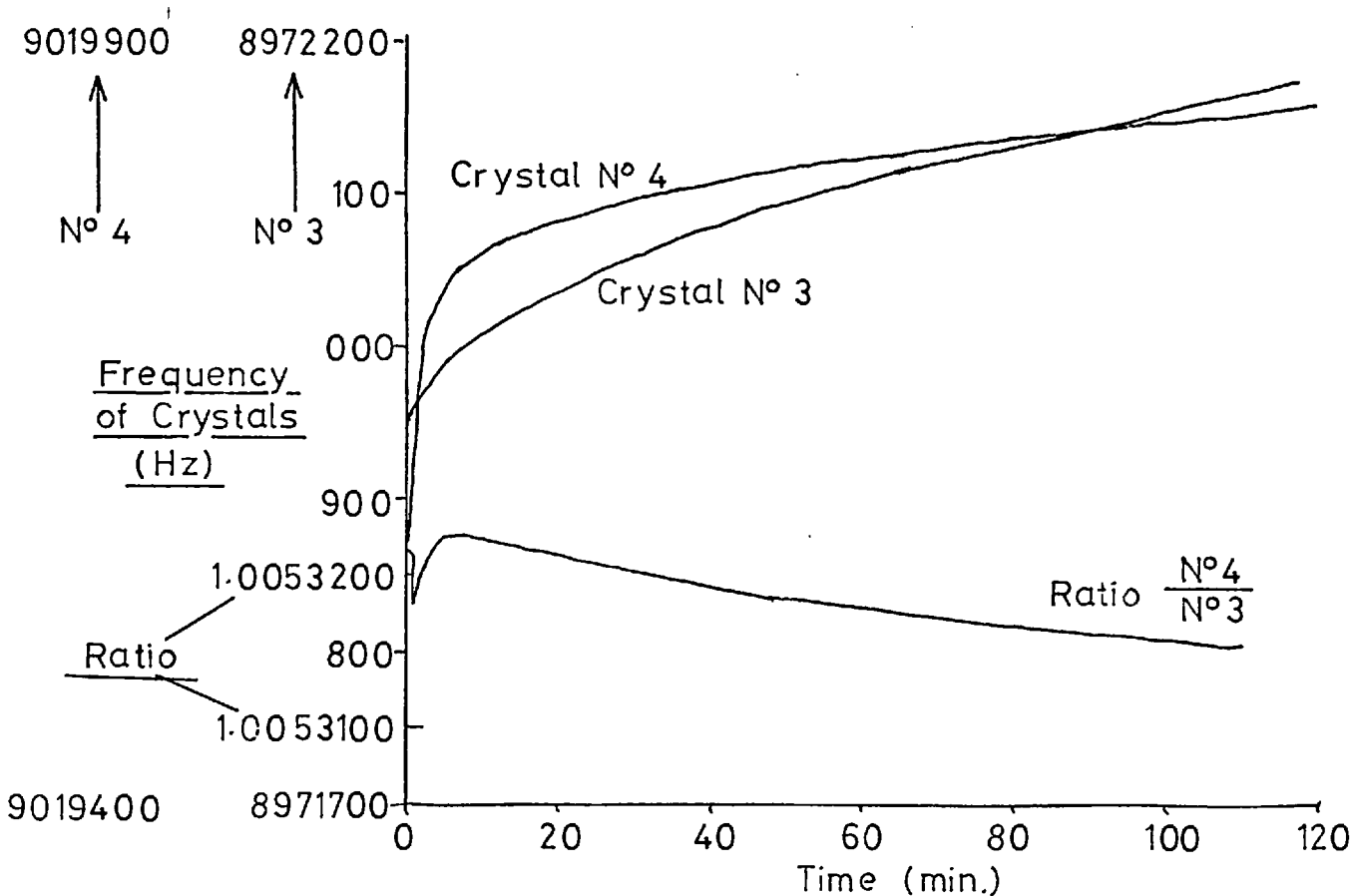


Figure 26b

Coating Bleed and Correction Obtained with
Double Sided System

Figure 26 a,b

for the ratio-ed frequencies of crystals 3 and 4 is however, much lower at 28 units/hour than the individual rates of drift for these crystals; crystal 3:- 72 Hz/hour and crystal 4:- 44 Hz/hour. The drift rates of crystals 1 and 2 are 31 Hz/hour and 18 Hz/hour respectively with the drift of the ratio-ed frequencies at 11 units/hour.

2.4. Comparison of Cell Performance and the Precision of the System

When the impinger cell shown in figure 20 was designed it was hoped that, as a result of the geometry of the gas inlet holes, the response of a coated crystal in this cell would be greater than the response of a similarly coated crystal in the cell shown in figure 21.

In order to compare the two cell designs two crystals were similarly coated with Carbowax 20M (a polyethylene glycol stationary phase used in gas chromatography). The material was deposited onto both electrodes of each crystal from a solution of carbowax in chloroform ($15\mu\text{g}/\mu\text{l}$). A microsyringe was used to place $1\mu\text{l}$ of this solution over the entire electrode area and the solvent was allowed to evaporate. A total of $30\mu\text{g}$ of material was deposited on each crystal with resulting frequency changes of 39,599 Hz for crystal 1 and 42,009 for crystal 2. Crystal 1 was placed in the impinger cell (figure 20) and crystal 2 in the stainless steel cell. The response for each cell was determined separately, the conditions being the same for both. The conditions were a carrier gas flow rate of 70ml./min. and aliquots of undiluted sulphur dioxide injected into the carrier gas stream with a $250\mu\text{l}$ microsyringe before the stream entered the cell. The distance of the injection part to the point of entry of the gas into the cell was 10 cm.

A single sided measurement system was used as a comparison of bleed rates was required. The carbowax/sulphur dioxide system is reversible i.e. sulphur dioxide is not chemisorbed by carbowax. The measurement taken to indicate the degree of interaction between sample and coating was the difference in frequency between the base line frequency and the lowest frequency achieved after sample introduction, and before desorption of sample occurred, i.e. a peak height measurement. The experiments were conducted over several days during which time the carrier gas was constantly passing over the coated crystal. The results are tabulated below, each mean value and relative standard deviation being calculated from 16 results. The results are also grouped according to the day that they were obtained.

The rate of bleed of coating from the crystals in the stainless steel and impinger cells was determined as being 19 and 50 Hz/hour respectively.

Day	Impinger cell		Stainless steel cell	
	Volume of SO ₂ injected	Response (Hz) ± % r.s.d.	Volume of SO ₂ injected	Response (Hz) ± % r.s.d.
1	250 μl	162 ± 9%		
	125 μl	85 ± 11%		
2	100 μl	64 ± 9%	100 μl	93 ± 9%
3			100 μl	73 ± 22%
			100 μl	94 ± 17%
4			100 μl	90 ± 20%
			100 μl	101 ± 8%
			20 μl	23 ± 14%

Table 5

If a comparison of these results is made, ignoring for the moment the results whose % relative standard deviations are greater than 17%, it will be seen that the precision of both cell designs is similar at about 8-9%. The mean value of response is significantly higher for the stainless steel cell than for the impinger cell, with an average response of 97Hz and 64Hz respectively for an injection of 100 μ l of sulphur dioxide.

Both cells gave linear calibration graphs with sensitivities of 8.6 and 6.5 Hz 10 μ l of injected sulphur dioxide for the stainless steel and impinger cells respectively.

The lower precision obtained for 125 μ l injections in the impinger cell (11%) and for the 20 μ l injections in the stainless steel cell (14%) are due to error in syringe manipulation: there is no graduation mark for a volume of 125 μ l, the volume being estimated, and the small volume of 20 μ l being measured with the sub-divisions of a relatively large 250 μ l syringe.

The highest errors associated with the system i.e. 17, 20 and 22% are attributable to a quite different cause: in these measurements a permanent feature of the measuring technique was exaggerated and the reduced precision observed. To explain these results it is necessary to describe the exact method by which the frequency meter measures the frequency of an incoming signal. As described previously the frequency meter has its own internal time standard from which the count period or gating time is derived. In most cases in this work a gating time of 1 second was used. During this period of 1 second the meter counts the incoming pulses, and at the end of the count period the result of this count is immediately displayed. Whilst this count total is displayed the next count is being performed and

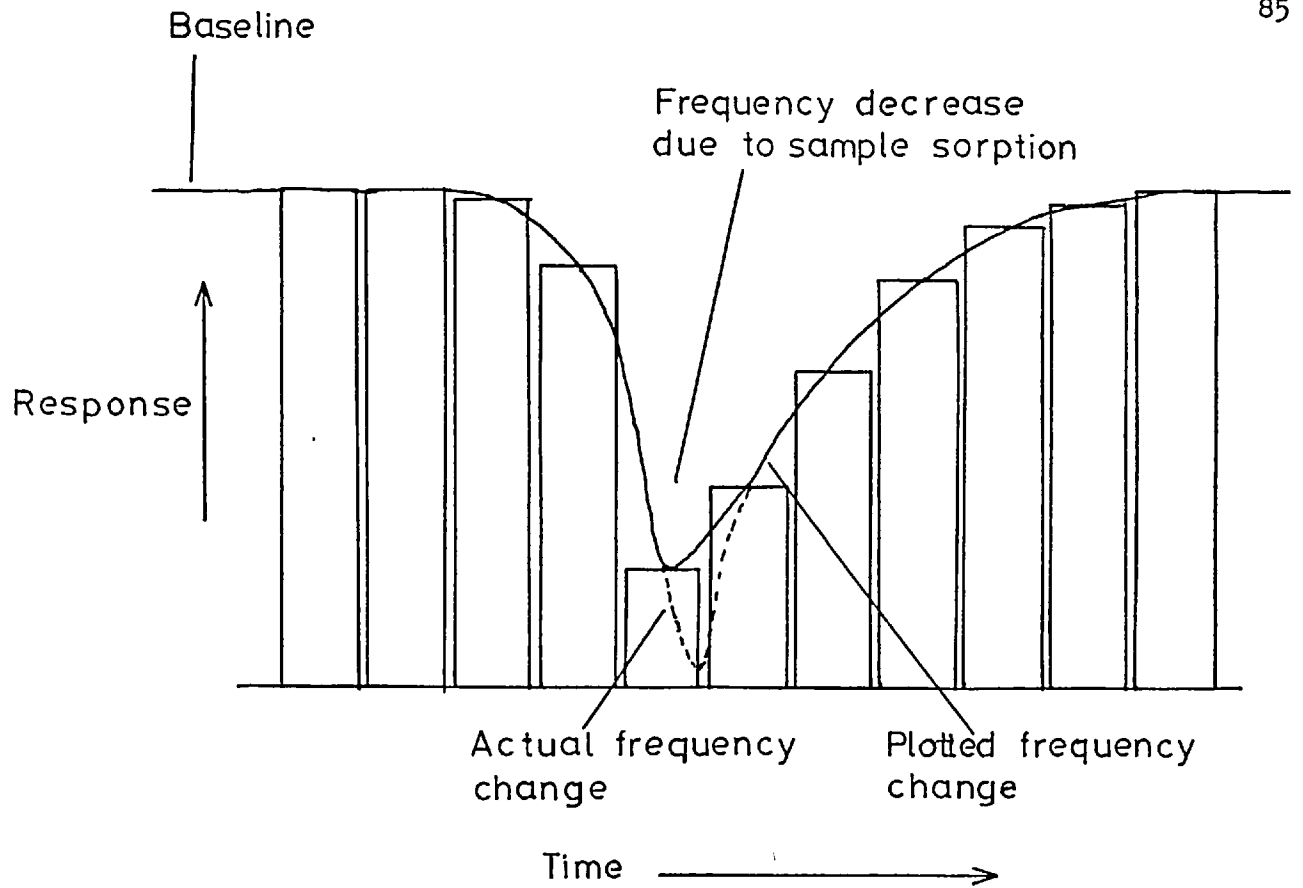
the new result is displayed immediately the count is complete. There is a slight pause between the completion of one count and the commencement of the next count. Thus when the frequency variation of a coated crystal is plotted as a function of time the graph should strictly speaking be a histogram with small gaps between each sample count.

When the signal from the detector is of short duration, i.e. the same order of time as the sampling period then the peak minimum or part thereof will occur in the same place in time as the slight pause between each counting period. This is illustrated in figure 27a. It was possible to vary the length of time between each count period with the frequency meter used in this work. This time, referred to as display time, could be varied from a minimum of 0.1s to 5 seconds. See figure 27b. For most frequency measuring work the display time was set at its minimum value of 0.1s, however this time was increased to approximately 0.5s for the measurements made on the third and fourth day of the cell comparison experiments. The result being that the percentage relative standard deviation of the system became worse from a value of 9% to 22%.

In order to improve the precision of the measuring system to better than 8-9% a peak area type of measurement was devised and investigated. With this technique a gating time of 10 seconds and minimum display time of 0.1s were used.

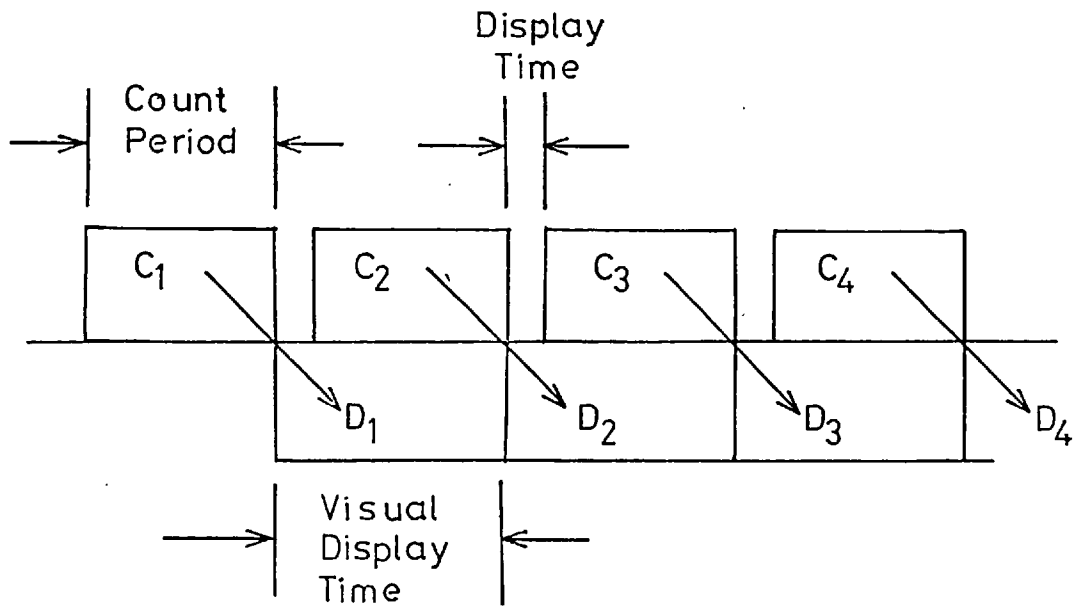
A base line count was established and noted prior to the sample injection after which the sampling of the counter was stopped.

The sample was prepared i.e. syringe flushed and filled, and injected into the system. At the same time as injection occurred the sampling of the counter was started. The results of the subsequent 10 second counts were noted until the count had returned to the same value as the base line count established before sample injection.



Histogram of Frequency Measurement

Figure 27a



"Clock" Representation of Count Period and Display Time

Figure 27b

For the system being investigated i.e. the stainless steel cell and the same experimental conditions as used on the previous experiment, it was established that for an injection of 100 μl of sulphur dioxide five consecutive 10 second sampling periods were required before the base line count was re-established. The peak area was then obtained by calculating the difference between the base line count and each of the five sample counts and summing the five differences.

The logic of this technique can be seen by comparing this description with figure 27a.

Using this technique and identical experimental conditions the percentage relative standard deviation of 100 μl injections of sample injected into the stainless steel cell was $\pm 5\%$.

These experiments establish that:

- i) the response of the stainless steel cell is significantly greater than that of the impinger cell under similar conditions:
- ii) the rate of drift due to coating bleed was higher for the impinger cell:
- iii) the precision of both cell designs using a peak height measurement was at the 8-9% level:
- iv) the precision of the stainless steel cell can be improved by peak area measurement to the 5% level.

As a result of (i) and (ii) it was decided to use the stainless steel cell in subsequent experiments. The large thermal capacity of stainless steel cell also favoured its use.

With regard to the increase in precision obtained by using peak area measurements, it was decided that this increase did not

compensate for the lack of information about the peak shape resulting from sample/coating interaction. The large majority of results were obtained by plotting the frequency of the sample crystal (or a function thereof) against time, the shape of the peak being more important than a 3% increase in precision.

3. Coatings and Application Techniques

3.1.1. Introduction

The essential difference between the quartz crystal microbalance and the quartz crystal detector is that the former is a general detector of mass whilst the latter is a specific mass detector. The specificity of the latter is obtained by placing on the surface of the quartz crystal some material which by nature of its chemical or physical properties will specifically interact with the component of interest in a static atmosphere or in a gas stream flowing past the crystal: thus to a large extent the success or failure of the quartz crystal detector as a pollution monitor depends upon the nature of the coating used to detect a specific pollutant.

In this chapter the basic requirements of a coating will be discussed and the problems encountered when different materials are applied to quartz crystals will be examined.

3.1.2. Required Characteristics of a Coating

Any compound considered for use as a coating should fulfil the following basic requirements;

- i) it should be easy to apply to the crystal in a reproducible manner;
- ii) the crystal should be capable of oscillating once coated;
- iii) the coating should have a high affinity for the analyte, preferably reversible;
- iv) the coating should be selective;
- v) the coating should preferably operate at room temperature.

In King's original paper (69) he advocated the use of gas chromatographic stationary phases as coating materials. At room temperature these compounds vary, in physical state, from very viscous liquids to greases and waxy solids. They are generally easy to apply

to the crystal giving good, uniform and easily reproducible coatings. The performance is mathematically predictable, calculations giving good agreement with experimental results (87). The selectivity and specificity of these coatings is not very great as these materials are designed for partition on chromatographic columns. A high degree of specificity is not part of the nature of the coating material itself.

Other workers have suggested, and used with varying degrees of success, specific reagents, as coatings on crystals as opposed to a relatively non-specific g.c. stationary phase. Shackelford and Guilbault have used the cobalt complex of isonitrilobenzoylacetone as the coating for the detection of organophosphorous pesticides (88). The use of mercury II bromide as a coating for organophosphorous compounds has also been investigated by the same author (83).

King has suggested the use of specific reagents e.g. lead acetate for the detection of hydrogen sulphide but he has not demonstrated the use of such materials. He has however, devoted much effort to the development of a moisture detector using lithium chloride as the coating on the crystal. The selectivity of these and other systems previously described are reported as being generally good.

3.1.3. Reported Coating Techniques

The techniques that have been used for the deposition of the specific reagents are in general outline very similar to those methods used for the deposition of gas chromatographic stationary phases. This technique involves the dissolution of the material in a solvent, usually a volatile organic solvent, and the application of an aliquot of this solution to the crystal surface. The solvent is then allowed to evaporate leaving on the crystal the desired reagent.

The actual application of the solution to the crystal has been carried out in several different ways: these include the use of a

micro-syringe for the application of small volumes of solution, spraying the crystal, through a mask, with the reagent solution or simple dipping of the crystal into the reagent solution. The "dip" technique was used for the application of sodium tetrachloromercuriate from aqueous solution (82) but the resultant coatings were unsatisfactory due to a lack of smoothness of the coating and very poor reproducibility. The "spray" method did, however, give good results with the aqueous solution. The "dip" method was used satisfactorily for the application of mercury II bromide from ether solution (83). Hartigan (79) carried out a detailed study of the "spray" technique and did develop a method of coating amines onto his crystals. He did note that for a heavier deposit of coating it was necessary to use a more concentrated solution when spraying rather than trying to apply a second layer of coating over a layer already applied. To attempt to "overlay" more coating resulted in the disturbance of the first coat with a subsequent loss of coating precision on the coated crystal.

The use of a micro-syringe to apply the reagent solution has been well documented. The method is simple and controllable in that it is easy to obtain deposits of varying areas and masses. This technique can be applied, with certain limitations, equally well to organic materials in an organic solvent and inorganic materials in aqueous solution, the resultant coatings being quite uniform and reproducible.

A "non solution" technique for crystal coating has been used by King (77). This method involved the vacuum evaporation of lithium chloride, and other deliquescent salts, onto the crystal. Masks were employed to define the area of deposition. The frequency change that occurred during deposition was used to monitor the mass of the deposit.

Other "non solution" techniques were suggested by King (69) which included; metal oxide coatings prepared by the oxidation of a metal which had been electrodeposited onto the crystal electrodes; the

deposition of insoluble materials from suspensions or the use of a glue or cement to secure powders onto the crystal surface. In another publication (89) however, King does state that it is difficult to coat crystals with materials that are insoluble and also that "non uniform films result in crystals which are difficult to maintain in a stable oscillation condition".

3.2. Potential Coating Materials

3.2.1. Non Selective Coatings

After consideration of the information in the literature it was obvious that a detector for atmospheric sulphur dioxide would have to incorporate a specific reagent, very likely a solid compound, as opposed to a g.c. stationary phase; however the initial work with a coated crystal, employed Carbowax 20M as a coating.

This material was chosen as previous workers (82,83) had used this compound as a coating for sulphur dioxide detection in both static and dynamic systems. No unexpected problems were reported with these systems, and a moderate sensitivity was obtained. Consequently this coating material was considered, by the author, as being an ideal starting point for the investigation of piezoelectric crystal detectors. During the course of this investigation only one other organic stationary phase type of material was used, this was triethanolamine.

The work published by Hartigan (79) was concerned with the application of piezoelectric crystals to study the interaction between amines coated on the crystal and sulphur dioxide.

He reviewed evidence for the formation of 1:1 amine-sulphur dioxide complexes and, in the light of this evidence correlated the results he obtained in terms of the basicity and structure of the amines. Triethanolamine was one of the numerous amines studied. It was reported that a

triethanolamine coated crystal gave a high response to a standard sample of sulphur dioxide, however, approximately 90% of the sample that was sorbed onto the crystal was retained on the crystal. This contrasted with phenyldiethanolamine which gave a somewhat lower response to a standard sample of sulphur dioxide but did not retain more than 10% of the sorbed sample on the crystal. As this study made no attempt to detect low concentrations of sulphur dioxide, (the standard samples used were several millilitres of undiluted sample gas injected into the system), the application of triethanolamine to the detection of low concentrations of sulphur dioxide was investigated.

The bleed rate of triethanolamine was reported as being less than phenyldiethanolamine, which lost 30% of the coating in 12 hours, and less than diethanolamine which had a higher response than triethanolamine to a standard sample of sulphur dioxide.

Thus triethanolamine was considered more suitable for low concentration determination.

3.2.2. Selective Coatings

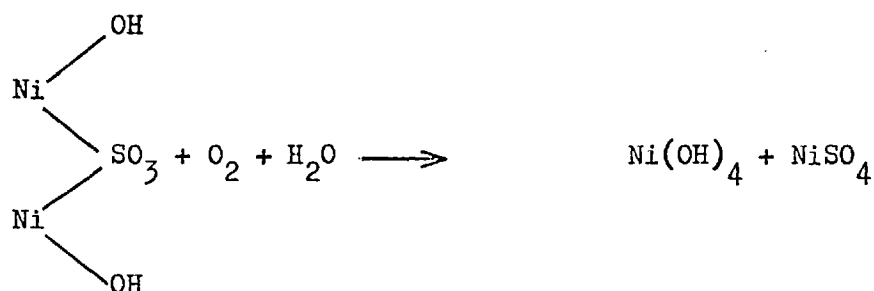
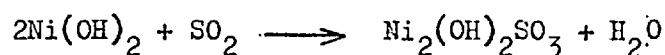
The first attempts to use a selective solid reagent as a coating on a crystal were directed towards the use of sodium tetrachloromercuriate and nickel II hydroxide.

The use of an aqueous solution of sodium tetrachloromercuriate as a trapping agent for atmospheric sulphur dioxide (15) has been described in an earlier chapter. Similarly the application of the solid material to a quartz crystal has been described (82). As a sensitivity better than that obtained for carbowax 20M and sulphur dioxide was reported, sodium tetrachloromercuriate was chosen as the first solid reagent to be investigated.

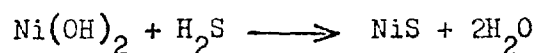
The use of nickel II hydroxide as a possible coating material was

inspired by the fact that sulphur dioxide induces the oxidation of green nickel II hydroxide to black nickel IV hydroxide.

This fact was used by Feigl (90) in the development of a spot test for sulphites. He noted that this oxidation is strange in that normally it is only accomplished by strong oxidizing agents. Hydrogen peroxide has no effect. The postulated stoichiometric equations for this reaction are;



The methodology of the test involved soaking a strip of filter paper in an ammoniacal solution of nickel sulphate and drying this treated strip at 110° . The dry strip was then dipped into a solution containing sodium hydroxide and sodium carbonate. The strips, now impregnated with nickel II hydroxide were washed and again dried at 110° . The treated filter paper could be stored indefinitely in a stoppered container. When test strips prepared in this manner were exposed to sulphur dioxide in a dry condition, the green nickel II hydroxide rapidly darkened to a grey/black colour. The test described is susceptible to interference from hydrogen sulphide; black nickel sulphide being formed:



This reaction would also interfere with a sulphur dioxide crystal detector as, at the end of the reaction there is a net increase in weight on the crystal surface.

Despite the possibility of interference by hydrogen sulphide, nickel II hydroxide was attractive as a coating material as the reaction with sulphur dioxide occurred in the dry state.

Several potential coating materials are to be found in the literature pertaining to organic elemental microanalysis. The technique of organic microanalysis requires the complete combustion of an organic compound in a stream of oxygen and subsequent determination of the carbon dioxide and water formed by the combustion process. The percentage composition of carbon and hydrogen in the sample can then be calculated.

The technique used to determine the formed water and carbon dioxide involves the selective absorption of these compounds from the oxygen stream by Anhydrone, a commercial desiccant, and soda asbestos respectively. The absorption materials are contained in separate tubes which are connected in series after the combustion tube. The absorption tubes may be independently sealed and readily removed from the combustion apparatus so that they can be weighed before and after the combustion process. The gain in weight of the tubes is a direct measure of the quantity of water or carbon dioxide absorbed.

If, however the sample contains elements other than carbon, hydrogen and oxygen, say nitrogen and sulphur, then upon combustion, the oxides of these elements would be formed and subsequently absorbed in the absorption tubes giving an erroneous result. It is thus necessary to selectively remove these oxides from the oxygen stream which also contains the carbon dioxide and water formed by combustion of the sample.

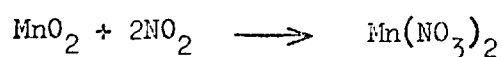
In the microanalytical technique developed by Pregl (91) hot silver wire was used to remove oxides of sulphur and the halogens and hot lead dioxide to remove the oxidation products of nitrogen from the gas stream.

There are however, a number of problems associated with lead dioxide.

These are; its ability to temporarily absorb moisture, and the absorption of carbon dioxide when quite dry and subsequent release of it when again coming in contact with moisture.

These disadvantages, and others, were instrumental in the use of various substitute reagents which were also operated at an elevated temperature in the combustion tube. Work was also directed towards the establishment of an external absorber of nitrogen oxides which would therefore, operate at room temperature. Most of the reagents recommended for external absorbers were either solutions or moist materials. None of these materials were considered suitable for a coating material. Granular manganese dioxide has been recommended as being a very efficient external absorbent of nitrogen dioxide (92). This material was compared with other potential external absorbers for nitrogen dioxide (93). This survey concluded that, of the dry absorbers examined, the only materials of sufficient activity to absorb nitrogen dioxide at room temperature were, manganese dioxide, a mole ratio mixture of silver metavanadate and silver oxide, and a mole ratio mixture of silver metavanadate and lead dioxide.

Efficiency trials showed that manganese dioxide was superior to the silver compounds and mixtures. In a later review article (94) the performance of manganese dioxide as an external absorber for nitrogen dioxide was compared with lead dioxide. The author concluded that the use of manganese dioxide prepared by the method of Clemser (95) i.e. the oxidation of an acidic solution of manganese II sulphate with ammonium persulphate, was preferable to lead dioxide. It was also stated that only black manganese dioxide should be used for nitrogen dioxide absorption and preparations that were brown in colour were not suitable. The probable reaction that occurs upon absorption was stated as being:



As manganese dioxide is a dry, solid, readily prepared reagent suitable for the absorption of nitrogen dioxide at room temperature it was considered as a potential coating material for a nitrogen dioxide detector.

The removal of oxides of sulphur in the Pregl combustion method was accomplished by using hot silver wire as the absorbent. Many variations upon this theme have been reported (96-99) using metallic silver in different forms, not only for the removal of oxides of sulphur, but also for the determination of the sulphur content of the sample. The disadvantage of these techniques, when considering their suitability for use as a coating for the crystal detector, is that the silver adsorber must be operated at a high temperature (400-450°). High temperature operation of the crystal detector is not desirable and thus a low temperature adsorber is required. A survey of solid reagents that would absorb sulphur dioxide but not carbon dioxide, at room temperature, has been reported (100). The survey concluded that of those materials tested only two were suitable, manganese dioxide on pumice, and silver permanganate. Manganese dioxide was recommended as being preferable to silver permanganate although silver permanganate was at least as efficient as manganese dioxide: manganese dioxide is more conveniently prepared. In this survey the absorption characteristics of cold silver orthovanadate were investigated. (This material had previously been used at 650° for the absorption of sulphur dioxide and halogens (101)). The survey reported that several separate preparations of silver orthovanadate were made, but only one batch would absorb sulphur dioxide whilst cold. Attempts were made to repeat this result but without success. This led to the hypothesis "..... that a number of different silver salts of the hypothetical vanadic acids may be obtained under similar conditions. Only very exact conditions can

guarantee the production of one particular type".

This hypothesis is partially vindicated by a detailed physico-chemical study of the silver salts of vanadic acid (102-103). In this work the authors established that three compounds exist i.e. the ortho, pyro and meta silver vanadates. They preferred a ratio type of nomenclature for these compounds i.e. $(\text{Ag}_2\text{O})_x : \text{V}_2\text{O}_5$, the ortho compound being 3 : 1, the pyro 2 : 1 and the meta compound 1 : 1. The different compounds could be obtained simply by changing the ratio of the initial reactants. Using this work as a basis, further studies were carried out to establish the exact nature of the silver/vanadic acid salt that would absorb sulphur dioxide whilst cold and dry (104). It was established that none of the compounds prepared according to the methods described in reference 102 and 103 would absorb whilst cold and dry, however a 1 : 1 mole ratio mixture of silver metavanadate and silver oxide would absorb sulphur dioxide and carbon dioxide under these conditions. If this mixture was heated at 150° for several hours, then the ability to absorb sulphur dioxide was maintained, but carbon dioxide was no longer absorbed. It was also observed that after heating, the colour of the material had become green, which changed to brown when exhausted after absorption of sulphur dioxide. Analysis of the mixture after heating showed that the empirical formula of the new compound was identical with the empirical formula of silver orthovanadate

i.e.		empirical formula
orthovanadate	$(\text{Ag}_2\text{O})_3 : \text{V}_2\text{O}_5$	$\text{Ag}_3 \text{VO}_4$
metavanadate	$(\text{Ag}_2\text{O}) : \text{V}_2\text{O}_5$	$\text{Ag} \text{VO}_3$
mixture	$\text{AgVO}_3 : \text{Ag}_2\text{O}$	$\text{Ag}_3 \text{VO}_4$

It was suspected that the heated mixture of silver metavanadate and

silver oxide might have formed a polymer as the sulphur dioxide absorbing properties of the orthovanadate and the mixture were quite different. A large number of polyvanadates are known to exist (105).

The thermal decomposition product of silver permanganate, prepared simply by heating silver permanganate in a test tube (106), has been reported as being suitable for the absorption of sulphur dioxide at room temperatures (107). This material was originally developed as an oxidation catalyst, to ensure complete combustion of organic materials when being analysed for carbon and hydrogen content by the combustion technique. The precise nature of the material was not known but the composition ratio of the elements silver, manganese and oxygen was determined as being 1 : 1 : 2.6 respectively. Because this decomposition product was a "..... very active absorption material for sulphur dioxide", it was used as the basis for a method to determine the sulphur content of organic compounds (108). The sulphur containing compound was oxidised in the normal manner, with the subsequently formed sulphur dioxide being absorbed by the thermally decomposed silver permanganate. Upon absorption silver sulphate and manganese sulphate were formed, which were then determined to give the sulphur content of the sample.

Thus on the evidence available the heated mixture of silver metavanadate and silver oxide, and the thermal decomposition product of silver permanganate appear to be suitable for use with the crystal detector and sulphur dioxide analysis.

In the first chapter the use of the lead dioxide candle for the long term estimation of atmospheric sulphur dioxide was described. Simply, this technique involves the exposure of a suitably treated sample of lead dioxide to the polluted atmosphere; sulphur dioxide present in the atmosphere reacts with the lead dioxide to form lead sulphate which is determined by a standard gravimetric procedure. It is known that the

absorption of sulphur dioxide by lead dioxide is linearly related to concentration until about 15% of the lead dioxide has reacted (32); the wetness of the surface increases absorption, and temperature and humidity have negligible effects, for practical purposes (109). The effect of particle size of the lead dioxide is also known (33). From this information it was decided to investigate the use of lead dioxide as a potential coating material.

The solid materials that were considered and investigated as potential coating materials for use in the analysis of atmospheric sulphur dioxide and nitrogen dioxide were:

- i) Sodium tetrachloromercuriate
- ii) nickel II hydroxide
- iii) manganese dioxide
- iv) silver metavanadate/silver oxide mixture
- v) thermal decomposition product of silver permanganate
- vi) lead dioxide.

Coatings iii - vi inclusive were checked for their reactivity towards both sulphur dioxide and nitrogen dioxide, whilst i and ii were only checked with sulphur dioxide.

3.3. Development of Coating Techniques

In this section only the techniques used to coat crystals with various materials will be described. The responses of the coated crystals to sulphur dioxide and nitrogen dioxide will be described in subsequent chapters.

3.3.1. Soluble Materials

As described earlier in this chapter the application of a coating material to a crystal from solution should be relatively straight forward. The experience of the author generally agreed with this.

Carbowax 20M was applied to the crystals in chloroform solution with a microsyringe. Various volumes (1-10 μl) of standard solutions (3-15 $\mu\text{g}/\mu\text{l}$) of carbowax in chloroform were used. It was noticed that a large (10 μl) volume of 3 $\mu\text{g}/\mu\text{l}$ solution did not give a good coating as the steady continuous addition of the solution to the crystal surface washed away material deposited at the beginning of the coating procedure. This resulted in a ring of carbowax being deposited. This is similar to the results obtained by Hartigan (79) i.e. disturbance of coating by further addition of material. When small volumes (1-2 μl) of 15 $\mu\text{g}/\mu\text{l}$ solution were used good deposits were obtained. The area of the deposit was controlled by either applying the required solution directly onto the crystal as a droplet and then spreading the drop with the syringe needle or by very slow ejection of the solution from the syringe such that the solvent evaporation rate and solution delivery rate did not permit the formation of a large diameter deposit. This technique worked well with low volumes of solution and only a small diameter (1 - 2 mm) deposit. If the delivery rate of the solution from the syringe was too slow it was observed that the solution tended to creep up the outside of the needle: consequently the coating on the crystal was not as heavy as expected.

Sodium tetrachloromercuriate, prepared according to the method of West and Gaeke (15) was applied to the crystals from aqueous solution with a microsyringe.

The method of preparation required the addition of sodium chloride (0.01 moles; 0.58g) to a hot solution of mercury II chloride (0.005 moles; 1.35g in 45 ml of water). The solution was allowed to cool and then made up to 50 ml with distilled water. This solution was then 0.1M with respect to sodium tetrachloromercuriate i.e. 38.6 $\mu\text{g}/\mu\text{l}$.

It was observed that when a heavy loading of sodium tetrachlor-mercuriate ($77 \mu\text{g}/\text{side}$) was placed on the crystal it would not oscillate in the cell oscillator but would oscillate in a single test oscillator. The cause of this apparent conflict was established as being an excessive length of coaxial cable between the crystal holder and the driving oscillator. The length of cable (30 cm.) was placing a small, but significant, capacitive loading in parallel with the crystal sufficient to prevent oscillations from occurring when the crystal was heavily coated. In this section of work this problem was overcome by shortening the cable (15 cm.) and avoiding high coating masses on the crystal.

The only drawback observed when depositing materials from aqueous solution was that if a large (6 - 7 mm diameter) deposit was required then it was found necessary to add ethanol (1 - 2%) to an aliquot of the stock solution in order to lower the surface tension and thus permit spreading of the solution on the crystal face. It was found desirable to avoid using large volumes ($> 2 \mu\text{l}$) of a more dilute solution to obtain a large diameter deposit as this gave an irregular deposit.

The masses of the sodium tetrachlormercuriate and carbowax deposits were deduced from a knowledge of the solution concentration and the volume of solution used to form the deposit.

The technique used to deposit triethanolamine upon a crystal did not involve making a standard solution of the material. As triethanolamine is a very viscous liquid at room temperature it was established that with a very small drop, approximately $0.5 \mu\text{l}$, of undiluted material placed on the crystal surface and then spread with a piece of tissue paper, a uniform film of the required dimensions could readily be obtained. With this method the weight of the deposit was determined by weighing the crystal on a quartz fibre torsion microbalance before and after the

deposition was completed. With the balance used (Oertling, deci-micro balance model Q01) once calibrated it was possible to weigh with an accuracy of 0.1 μg with a reported standard deviation of better than 0.08 μg (110).

The complete coating technique involved:

- i) noticing the frequency of the clean uncoated crystal:
- ii) removal of the crystal from its mounting clips and weighing it:
- iii) replacement of crystal in its mounting clips:
- iv) application of small quantity of coating material:
- v) manipulation of coating until the required area and frequency change are obtained:
- vi) reweigh the crystal and note the final frequency.

If a crystal was required that was coated on both sides then the above procedure was repeated for the remaining side.

This technique offered the advantage that it was easier to tailor the coating to a required specification simply by spreading or removing the coating with tissue paper held with fine forceps. Any irregularity in the surface could readily be removed by placing the coated crystal in a warm environment e.g. on top of a laboratory oven.

This coating technique was only possible as the material, triethanolamine, was a viscous liquid. Attempts to modify in a similar manner, a coating of carbowax resulted in an uneven deposit, the irregularities of which required extensive heating (1 hour at 120^o) to remove them.

The average time required to coat a crystal on both sides with triethanolamine by the described method was approximately 20 minutes. No difficulty in obtaining reproducible surfaces was experienced.

3.3.2. Insoluble Materials

3.3.2.1. Nickel Hydroxide

According to the method of Feigl (90) the nickel hydroxide

test paper strips should be prepared by first soaking the strips in an ammoniacal solution of nickel sulphate, drying them and then soaking them in sodium hydroxide solution.

A similar in situ method of preparation was considered for coating a crystal with nickel hydroxide.

It was realized that there were a number of disadvantages to this method, these being the removal of unwanted reaction products from the required nickel hydroxide, and the fact that when nickel hydroxide is precipitated in aqueous solution, the precipitate is gelatinous. It was suspected that this material would not dry to form an even film on the crystal surface.

Attempts were made to precipitate nickel hydroxide using nickel ammonium sulphate and nickel sulphate as the nickel containing reagents. Sodium hydroxide solution was used as the precipitating agent. Aqueous solutions of these reagents were prepared such that, the application of 5 μl of a nickel containing reagent and 5 μl of sodium hydroxide solution to the crystal would result in a coating of 30 μg of nickel hydroxide. The solution concentrations were 16.5 $\mu\text{g}/\mu\text{l}$, 16.9 $\mu\text{g}/\mu\text{l}$ and 5.2 $\mu\text{g}/\mu\text{l}$ for nickel ammonium sulphate (weighed as $\text{Ni}(\text{NH}_3)_6\text{SO}_4$), nickel sulphate (weighed as $\text{NiSO}_4 \cdot 6\text{H}_2\text{O}$) and sodium hydroxide respectively.

A 5 μl aliquot of the nickel containing reagent, either nickel ammonium sulphate or nickel sulphate, was applied to a clean crystal and the water allowed to evaporate.

An aliquot (5 μl) of sodium hydroxide solution was added to this dry deposit.

The solution was left on the surface of the crystal, covering the previous deposit, for five minutes. The solution was then either allowed to dry, thus keeping the by-products of the reaction on the crystal

surface, or the solution was very carefully washed off the surface of the crystal with distilled water; the crystal and wet nickel hydroxide then being dried.

The deposits prepared in this manner were not successful in that the crystals would not vibrate in the test oscillator when coated. The deposits, in appearance, were thick and irregular. There was no difference in the final deposit as a result of using different nickel reagents and very little difference between coatings that still contained by-products of the reaction and those that did not. A difference was noticed between deposits that had been allowed to dry at room temperature and those dried at a higher temperature. Those that dried more slowly were much more regular - although the crystal still would not oscillate. This series of experiments was repeated with the concentration of the three reagents reduced by a factor of 10; as experienced previously none of the deposits so formed would permit the crystal to oscillate. It was suspected that deposits of nickel hydroxide formed in this way were not sufficiently regular and smooth due to the gelatinous nature of the freshly formed precipitate and the nature of this material when dry.

In order to circumnavigate this problem attempts were made to deposit nickel hydroxide from an aqueous suspension. Nickel hydroxide was prepared by the addition of a solution of sodium hydroxide to a solution of nickel sulphate. The resultant precipitate was filtered and washed with distilled water until the wash water was neutral to general pH indicator paper. The nickel hydroxide was dried at 110° . When the product was dry it was finely ground in an agate pestle and mortar and finally sieved through a 300 mesh sieve. A suspension of this nickel hydroxide was prepared with a nickel hydroxide content of 0.3g in 10 ml. of water. The suspension was well shaken and an aliquot taken with a very fine glass

dropping pipette. One drop, approximately 5 μl of the suspension was placed on the surface of a clean crystal and the deposit allowed to dry. The deposit was regular but the crystal would not oscillate. It was also found that a larger area deposit could not be made as the suspension could not be spread across the crystal surface. A fresh suspension was prepared with a solid content of 0.03g/10 ml of liquid: the liquid was 95% distilled water and 5% ethanol.

When 5 μl aliquots of this suspension were placed on crystals, fine, regular coatings were produced; approximately 20% of these coatings permitted the crystal to vibrate when coated. It was noticed that if the suspension was allowed to settle for one minute, an aliquot removed from the clearer part of the liquid and then deposited onto the crystal a very light, smooth but patchy deposit was formed. The crystals when coated on one side only vibrated; when a second similar deposit was placed on the opposite side of the crystal the crystal ceased to vibrate.

When these experiments were conducted it was not possible to weigh the crystals to determine the exact mass of the deposit, and as the coating material was in suspension, not solution, it was only possible to say that the deposit mass was not greater than 15 μg per side (i.e. 5 μl of "3 $\mu\text{g}/\mu\text{l}$ " suspension).

The Saurbrey equation could not be used with a high degree of accuracy to estimate the deposit mass as the deposit was not complete, but patchy. By comparing the deposition data available, i.e. the diameter of the deposits (about 4 mm) and the frequency decrease on coating (4,200Hz) with other data obtained from coated crystals, the mass of nickel hydroxide deposited was probably of the order of 6 - 8 μg . Thus, with both sides of the crystal coated the total loading of the crystal was 12 - 16 μg , with this loading the crystal would not oscillate when placed in the test

oscillator. This does not compare very well with the quantities of carbowax and triethanolamine that were coated upon the crystals without the cessation of vibrations occurring. Total loads of 60 μg of carbowax and 120 μg of triethanolamine were regularly used.

As the techniques for applying nickel hydroxide as a solid to a crystal were not successful, in that an even regular deposit which would permit the crystal to oscillate could not be regularly obtained, a solution method was tried. This involved dissolving nickel hydroxide in concentrated ammonia solution and applying this solution to the crystal. A solution of nickel hydroxide in ammonia (4.4 $\mu\text{g}/\mu\text{l}$) was prepared. With this solution, as with other solution techniques, very good deposits were formed. It was also established that cut off, the point where the crystal no longer vibrated, occurred between 17.6 and 20.4 μg , total load. The solution method was much simpler and more reliable than the other techniques, although the total quantity of nickel hydroxide that could be deposited before cut off occurred was still relatively low.

3.3.2.2. Silver Oxide/Silver Metavanadate Mixture

As described earlier in this chapter the silver metavanadate required to prepare an active sulphur dioxide absorbing mixture must be prepared under carefully controlled conditions. This factor and the experience gained with the deposition of nickel hydroxide preclude any attempt at an in situ preparation.

Similarly a solution technique should be avoided.

It was therefore, necessary to develop a reliable technique to apply solid materials to crystals.

The silver metavanadate was prepared according to the method of Britton and Robinson (102,103).

Sodium hydroxide (1g) was dissolved in distilled water (50 ml) and

the solution boiled. During the heating of the solution and subsequent reagent addition carbon dioxide free air was bubbled through the solution. To the boiling solution ammonium metavanadate (2.9g) was gradually added. The heat source was removed and the solution was allowed to cool to room temperature. To the cool solution, a solution of silver nitrate was added (4.25 g in 50 ml distilled water) with stirring.

The resultant orange/yellow precipitate was filtered, washed and dried at 120°. When the material was dry it was finely ground and sieved through a 300 mesh sieve.

A portion of the silver metavanadate prepared in this manner was weighed out (0.100g) and well mixed with a weighed portion of sieved silver oxide (0.112g). The mole ratio of the resultant mixture was 1:1. One half of the prepared mixture was slurried with a little distilled water. The slurried and dry mixtures were then heated at 150° for 24 hours. After heating, the material which had been slurried with water was again ground and sieved.

The first attempts at depositing the silver reagent onto a crystal involved the placing of a small drop of water (~ 1 µl) on the crystal surface and spreading this to a required diameter. The coating material was then sieved onto the crystal until the water drop was completely covered. The crystal was then placed in an oven at 120° for ten minutes. After removal from the oven, the material which had not come into contact with the water on the crystal surface was blown away, leaving a uniform deposit in the centre of the crystal. The deposit was easily removed by brushing, but stayed in place when placed in a fast flowing gas stream and when the crystal was handled. Unfortunately, no coating prepared in this manner would permit the crystal to oscillate in the test circuit. Various quantities of water spread over different areas were tried, but

none were successful.

It was suspected, that the reason a crystal, coated in such a manner, would not oscillate, was because the energy required to vibrate the crystal was dissipated in the loosely bound coating. In order to bind the coating more firmly to the crystal surface the use of an adhesive was considered. Collodion dissolved in acetone was thought to be suitable as it was firm when dry and also easily removed from a crystal when dry.

A dilute solution of collodion in acetone (approximately $4 \mu\text{g}/\mu\text{l}$) was prepared. A $1 \mu\text{l}$ aliquot of the solution was placed on the crystal surface and the reagent sieved onto the crystal as previously described. Deposits prepared in this manner were not very uniform, as the collodion dried too quickly, leaving a very patchy deposit, however the crystals would oscillate. Solutions of collodion in ethanol were tried in an attempt to reduce the rate of evaporation of the solvent but the surface tension of these solutions was too low, thus making it very difficult to control the size of the deposit. A mixture of acetone/chloroform (2 : 3 parts by volume) containing $16 \mu\text{g}/\mu\text{l}$ of collodion was found to give good results, in that the evaporation rate of the solvent was not too high, and the surface tension of the solution high enough to contain the deposit. The appearance of the final coating i.e. the silver reagent firmly fixed to the crystal surface with collodion, was acceptable, with a fine deposit of material covering approximately 75% of the collodion surface.

With this coating technique a totally unexpected result was obtained; of four coatings prepared in an apparently identical manner, one crystal failed to oscillate, one crystal oscillated with a decrease in frequency of approximately 23 KHz but two crystals oscillated with an increase in frequency. One crystal after coating was oscillating at a frequency 26.8KHz higher than the clean uncoated frequency, the other crystal was

oscillating 27.3KHz higher than its clean uncoated frequency.

These crystals were quite stable oscillating in this high state which is in direct opposition to the response predicted by the Sauerbrey equation. He predicted, and all the reported experimental evidence has confirmed, that when mass is added to the surface of a vibrating A.T. cut quartz crystal the frequency of vibration should decrease.

At the time of these coating experiments the possible causes of crystals behaving in this unpredicted manner were considered as being:-

- i) the coatings were not smooth enough to comply with the condition imposed by the Sauerbrey equation, i.e. a perfectly smooth coating:
- ii) some overload region was being entered into:
- iii) as the coating material was a binary mixture the mechanical properties of this mixture could effect the resonance system of the crystal:
- iv) perhaps some overtone mode of operation of the crystal was being induced.

In order to elucidate the cause of this unpredicted effect it was decided to investigate the coating of a chemically simpler compound, manganese dioxide, in place of the two component mixture

3.3.2.3. Manganese Dioxide

Earlier in this chapter the use of manganese dioxide as an absorber of nitrogen dioxide and sulphur dioxide was described. The most suitable type of manganese dioxide applicable to this work was reported as being prepared by the method of Clemser (95), consequently a sample of manganese dioxide was prepared by this method which is described below.

Manganese II sulphate (1g) was dissolved in distilled water (40ml).

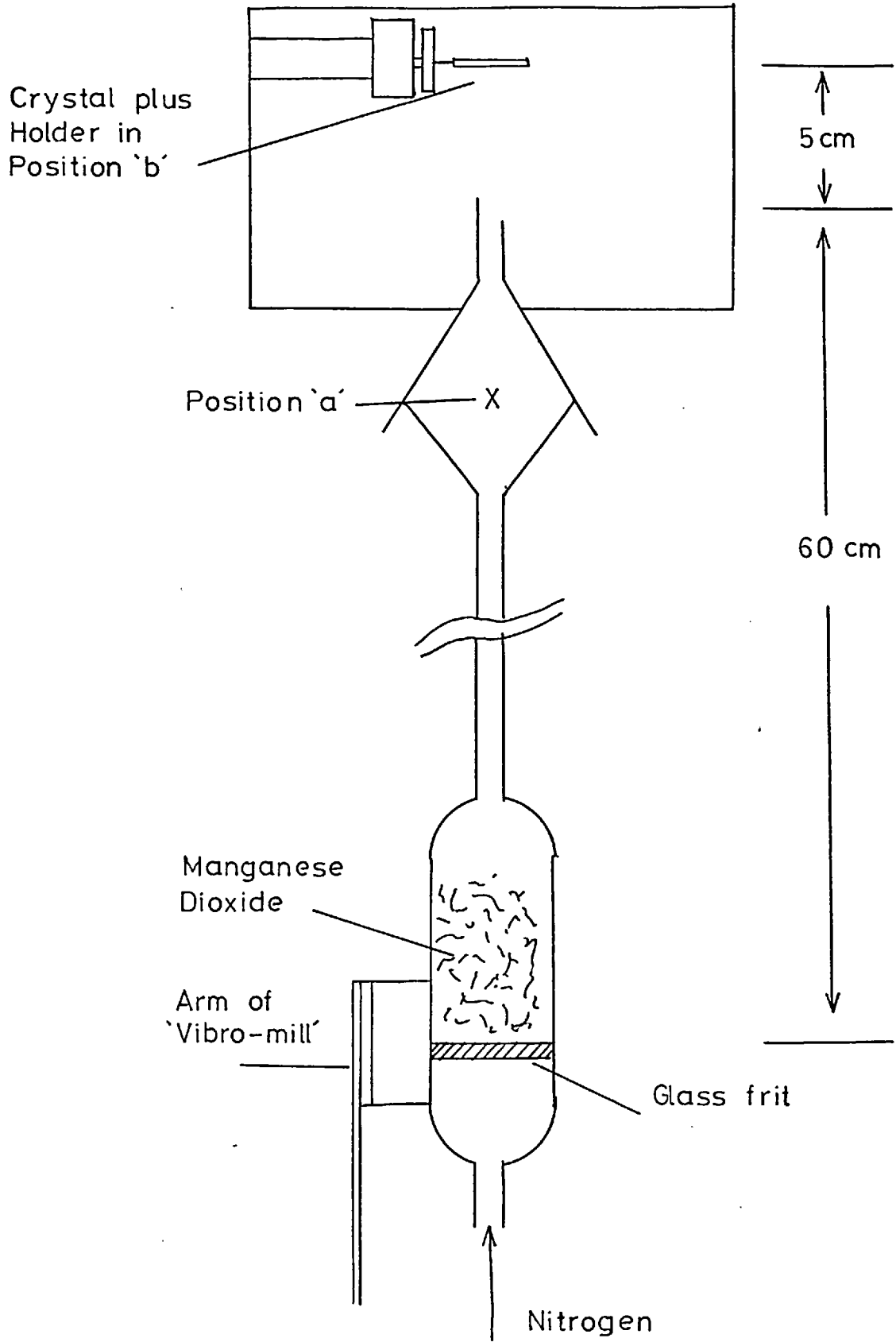
Nitric acid (2 ml of 2M) was added to the solution. The solution was boiled. To the boiling solution ammonium persulphate (2.25g) was gradually added. The solution was boiled for a further five minutes. The solution and precipitate were removed from the source of heat and filtered hot. The precipitate, black manganese dioxide, was washed with copious quantities of hot water and dried at 120°. The dried material was finely ground and sieved through a 300 mesh sieve.

Initial attempts to coat manganese dioxide onto a crystal were made by employing the same technique used to coat the mixture of silver compounds i.e. sieve the coating onto a water drop or a solution of collodion. It was quickly realized that a more reproducible technique was required for applying the manganese dioxide to the adhesive or water drop on the crystal in place of the rather haphazard sieving method.

3.3.2.4. Particle Fractionater

To fulfil this requirement the apparatus depicted in figure 28 was constructed. The lower part of the apparatus consisted of a coarse glass frit sealed in a glass tube. The tube was drawn off as indicated. This glass assembly was secured with adhesive tape to the vibrating arm of a "vibro-mill". (This mill was the type of mill used to prepare KBr discs for infra-red spectrophotometric analysis. The container in which the KBr and sample were usually ground was discarded).

When the manganese dioxide was placed in the glass assembly as indicated, the complete assembly was vibrated by the mill. Nitrogen gas was passed upwards through the glass frit so forming a fluidized bed. The nitrogen flow rate was adjusted so that it was sufficiently rapid to entrain particles of manganese dioxide in the gas stream and carry the smallest particles out of the exit orifice of the equipment. Larger particles were too heavy to be carried out of the apparatus when the



Particle Fractionater

Figure 28

nitrogen flow rate was suitably adjusted. The apparatus was called a particle fractionater because of its ability to separate the larger and smaller particles of a sample placed in the equipment.

When the apparatus was first designed it was intended that the crystal, held with its major surfaces normal to the nitrogen stream, should be placed in the expansion type chamber (a); the crystal face with the water drop or adhesive on it facing upwards. The deposits formed by this method did not permit the crystal to oscillate, although they were even in appearance. Better results were obtained when the crystal was placed (5 cm) above the exit orifice of the device (b), the surface upon which the deposit was to be formed was facing downwards, so that the entrained particles were impacted onto the crystal surface.

The methodology of producing a coating with this technique was:

- i) note the frequency of the clean crystal:
- ii) apply the required quantity of water or adhesive to the crystal surface:
- iii) place the crystal in the device:
- iv) vibrate the glass frit and pass nitrogen through the equipment at a rate of 1-2l/min. for approximately 5-10 seconds:
- v) carefully remove the crystal (now covered with manganese dioxide on the lower face) and dry at 120° for 10 minutes:
- vi) allow the crystal to cool and gently tap the crystal to remove the excess manganese dioxide:
- vii) check the frequency of vibration of the coated crystal in the test oscillator and the cell oscillator.

(It was found necessary to modify the cell oscillators so that they could be plugged directly onto the crystals when the crystals were

in the cell block; this was to avoid using a length of coaxial cable between the crystal and the oscillator thus avoiding the problems of capacitive loading of the crystal by the coaxial cable. This modification also necessitated the abandonment of the upper half of the stainless steel cell block assembly).

In order to evaluate the usefulness of the particle fractionator as an aid to coating crystals, a study was made of the variation of the parameters that control the deposit size, and hence the resultant frequency change that occurred. These parameters were the volume, the area and the nature of the adhesive; both water and collodion solutions were used. The coatings were made on a number of different crystals to ensure that any unpredicted response that may occur was a genuine effect that was shown by a number of crystals and not a peculiar effect attributable to one specific crystal only. The crystals used were also in a variety of conditions i.e. some crystals were new and unused and others had been used extensively with a considerable amount of gold scratched off the electrodes of the crystals. The first study used water to fix the manganese dioxide to the crystal. Volumes between $0.2 \mu\text{l}$ and $0.7 \mu\text{l}$ were used with the diameter of the water spot varied between 1 and 5 mm. The appearance of the deposits varied according to the diameter of the water spot used i.e. a 1 mm diameter deposit stood proud of the crystal surface like a small dome, the 2 and 5 mm. deposits having the appearance of a plate adhering to the surface of the crystal. As reported earlier in this chapter deposits of this nature were readily removable from the crystal by brushing. The results of this study are summarized in table 6.

Two series of deposits on crystals 1, 2, and 3 were prepared with $0.5 \mu\text{l}$ of water spread to 3 and 4 mm. diameter. None of these deposits

Crystal number	Volume of water applied (μl)	Diameter of deposit (mm)	Clean frequency (Hz)	Coated frequency (Hz)	Frequency change $\pm \Delta f$ (Hz)
1	0.5	1.5	9005094	9004204	- 790
1	0.5	2.0	9005094	9004700	- 394
2	0.5	1.0	9006515	9005550	- 965
2 <u>2</u>	0.5	1.0	9005619	9005697	+ 78
2	0.5	2.0	no oscillations		
2 <u>1</u>	0.2	2.0	9005706	9009503	+3,797
3	0.2	1.0	9022200	9023338	+1,138
3 <u>2</u>	0.5	1.0	9022893	9023412	+ 519
3	0.5	1.5	9023293	9021516	-1,777
3	0.7	1.5	9022178	9023266	+1,088
3	0.5	2.0	9023293	9021537	-1,756
3 <u>1</u>	0.5	5.0	9023017	9021657	-1,360
4	0.2	1.0	9019130	9019448	+ 318
4 <u>2</u>	0.5	1.0	9019140	9019291	+ 151
4	0.5	2.0	9019876	9022690	+1,814
5	0.2	1.0	9010654	9010954	+ 300

Table 6

For the significance of the superscripts 1 and 2 see text

would oscillate. The deposits identified in the table with a superscript 1 were similar to those just described, in that they would not oscillate after coating. It was established however, that oscillations could be induced by very gentle removal of some of the coating. This was achieved with a fine camel hair brush. Crystal 3¹ required extensive trimming or removal of coating before oscillations occurred.

These crystal deposits identified by superscript 2 were prepared and the frequency of the coated crystal was noted. No trimming of the deposit was needed to induce oscillations. After the coated frequency was established the deposit on these crystals was slightly trimmed: in all three cases the frequency of the trimmed crystal was lower than the untrimmed frequency. The frequency pattern of these three crystals was as follows; upon coating, i.e. addition of mass to the crystal, the frequency of vibration increased; upon removal of some of the coating from the crystal the frequency of vibration decreased. This behaviour is, in qualitative terms, the exact reverse of the Sauerbrey equation.

When this series of experiments was carried out it was not possible to accurately obtain the weight of the deposit on the crystal. An estimate of this weight was made for a number of crystals using a beam balance capable of weighing to 10^{-5} g i.e. the smallest scale division was equivalent to 10 μ g. Using this balance it was established that deposit weights were of the order 50-100 μ g. A comparison of deposit data and accurate deposit weights, obtained later with a quartz fibre torsion microbalance, showed the original estimates of the deposit weights to be correct.

The significance of the deposit weight is realized when not only the sign of the frequency change obtained on coating is considered, but also the magnitude of the change. On coating, more than 50% of the crystals

changed their frequency, either increase or decrease, by less than 1,000 Hz. This corresponds with loadings between 50 and 100 μg and approximately 2 mm diameter.

A coating of triethanolamine prepared at a later date gave a frequency change of - 6,147 Hz with a loading of 4.6 μg at 1.94 mm. diameter. The triethanolamine coating is a typical "normal" coating and was chosen as an example because the diameter of the deposit was similar to the manganese dioxide coatings. There is however, a great disparity in the frequency changes obtained on coating the two materials.

No correlation was found between the physical condition of the crystals i.e. new or extensively used, and an anomalous frequency response on coating.

The next series of experiments were similar to those just described but in the place of water as an "adhesive" collodion was used. Three solutions of collodion in a mixture of acetone and toluene were used. The volume ratio of the solvents were 2 : 1, 1 : 1 and 1 : 2 of acetone : toluene. These mixtures contained 26 $\mu\text{g}/\mu\text{l}$, 20 $\mu\text{g}/\mu\text{l}$ and 13 $\mu\text{g}/\mu\text{l}$ of collodion respectively. The same experimental procedure as described for the previous experiment was used.

The results of this study are summarized in table 7.

Deposits were prepared of 3 mm diameter on crystals 2, 3 and 4 using 0.5 μl of the 20 $\mu\text{g}/\mu\text{l}$ solution of collodion. The deposits would not permit the crystal to oscillate. It was not possible to trim the deposits in order to induce oscillations as the manganese dioxide was firmly fixed to the surface of the crystal.

When attempts were made to prepare deposits using the most dilute solution of collodion (13 $\mu\text{g}/\mu\text{l}$) it was found that the material was almost

Crystal number	Volume of collodion solution applied (μl)	Diameter of deposit (mm)	Clean frequency (Hz)	Coated frequency (Hz)	Frequency change $\pm \Delta f$ (Hz)
Collodion solution- 2:1 acetone : toluene, 26 $\mu\text{g}/\mu\text{l}$ of collodion					
1	0.5	1.5	9005094	9026327	+21,233
2	0.5	1.5	9004298	9023816	+19,518
3	0.5	1.5	9022355	90041266	+18,911
1	1 μl	2.0	no oscillations were obtained on coating.		
2	1 μl	2.0			
3	1 μl	2.0			
Collodion solution- 1:1 acetone : toluene, 20 $\mu\text{g}/\mu\text{l}$ of collodion					
4	0.5	1.0	9004072	9017790	+13,718
2	0.5	1.25	9004815	9022860	+ 8,045
3	0.5	1.5	9020180	9047180	+27,000
4	0.5	2.0	9004072	9032840	+28,768
2	0.5	2.0	9004262	9029965	+25,703
3	0.5	2.0	no oscillations		

Table 7

dry by the time the crystal plus adhesive was placed in the particle fractionator. Consequently none or very little manganese dioxide was coated onto the crystal.

The deposits prepared using collodion were regular but slightly granular in appearance. In order to remove the deposit the coated crystal was soaked in acetone and then wiped with a tissue.

The clearest difference between the results shown in tables 6 and 7 is that no crystal coated with collodion and manganese dioxide has decreased its frequency on coating. The frequency changes are, in all cases, large increases. This contrasts strongly with the small changes shown in table 6.

A possible explanation of this difference could be that the manganese dioxide coated on a crystal without collodion as an adhesive is not held onto the surface of the crystal firmly enough and thus does not exert the full mass effect expected from a firmly bound coating of the same weight. A similar effect has been reported (111). In this work the authors describe the use of a piezo-electric crystal as the collector in an electrostatic precipitator. This device was designed and used for estimating the particulate content of ambient air. The sample air was passed through a corona discharge in which particulate material in the air became charged particles. These particles passed down a potential gradient (15kV/inch) and were collected on one of the electrodes of the piezo-electric crystal. The crystal was held normal to the direction of sample flow and the collecting electrode was earthed. The charged particles were held on the surface of the crystal by electrostatic attraction where they exerted their influence on the vibrational frequency of the crystal. The frequency of the crystal was reported as decreasing with added mass. As this technique was integrating in its mode of action the total

quantity of dust on the surface of the crystal increased as sampling continued.

Crystals oscillating at 1.5 MHz and 5 MHz were used in this study, the cut off point for both types was established as being 400 μg .

It was observed that when the relative humidity of the sample air was low (<30%) then the experimental sensitivity obtained with the equipment decreased as the load on the crystal increased. With the relative humidity of the sample between 40 and 50% the sensitivity of the device was constant over a much larger range. The authors concluded from this observation that the moisture content of the sample was playing an important part in the bonding or adhesion between the particles and the electrode surface. In the absence of moisture and a partially loaded crystal the particles were not sufficiently firmly bound to the crystal surface to exert their full mass effect, consequently the sensitivity of the equipment decreased. When moisture was present a firmer binding of the particles occurred and the sensitivity remained constant over a greater loading range.

This explanation can be used to account for the difference in magnitude of the frequency changes shown in tables 6 and 7 i.e. between loose coatings and firmly bound coatings.

No conclusion as to the cause of the frequency increase can be drawn from this work except that the cause is not simply due to the weight of the coating alone as loadings of up to 400 μg of particulate material were reported as behaving in a normal manner. Coatings heavier than 400 μg simply stopped the crystal oscillating.

A further technique of securing solid materials to the surface of a crystal was devised and investigated.

3.3.2.5. Latex Bonded Coatings

This method of coating crystals with solid materials entailed the securing of the active solid onto the surface of the crystal with a synthetic latex. This technique was used to prepare deposits of manganese dioxide, lead dioxide silver oxide/silver metavanadate mixtures and also coatings of the decomposition product of silver permanganate.

The latex was applied to the crystal as a dispersion in water. The latex deposit was allowed to dry, leaving a sticky surface on the crystal. A quantity of the active solid was placed on the latex deposit and compressed; the excess material not directly adhering to the latex deposit was brushed away.

The deposits prepared in this way were generally smooth and regular in appearance, the frequency of the crystal always decreased when the latex was applied and generally decreased when the active solid was subsequently applied, although increases in the vibrational frequency of the crystal were observed when the solid material was secured to the crystal.

Three different latex dispersions were examined. These materials were acrylate polymers and termed Acronal 4D, 30D and 35D. The exact nature of these materials is not published by the manufacturers, B.A.S.F. of Ludwigshaven, West Germany. The material which was chosen as being most suitable was Acronal 4D. When dry the surface of this latex was sufficiently tacky to give a good even covering of solid material.

It was established that a dispersion of 10 g/l of Acronal 4D in water containing approximately 0.1% by volume of Dispex N40, a wetting agent, was adequate for providing deposits in the range 1.40 to 3.94 mm

diameter. Generally 0.4 μl of the dispersion were used to form the latex deposit of the required diameter.

When crystals were coated using this technique the frequency changes due to the separate addition of the latex and the active solid were recorded and also the masses of the latex and solid were separately obtained by direct weighing with a microbalance. The diameter of the final deposit was measured with a travelling microscope.

With most of the deposits prepared in this manner it was found necessary to trim the deposit after the excess material, not adhering to the latex, had been removed.

Crystals were also prepared with deposits on one or both major surfaces. The deposit details of a selection of crystals are shown in table 8. It will be noticed that there are some deposits which are obviously not in agreement with Sauerbrey's equation e.g. crystal number 1. The initial deposit of 1.9 μg of latex gave a frequency decrease of 5,482 Hz and subsequent coating of 18.6 μg of manganese dioxide on the same area of the crystal only gave a decrease in frequency of 5,524 Hz.

Crystal number 8 was coated on both sides with manganese dioxide, the frequency of the crystal being checked at each stage of the deposition process. The first deposit was applied with a corresponding decrease in frequency. The application of the latex to the second side of the crystal also gave a decrease in frequency. When the second application of manganese dioxide was complete the frequency change due to this material was + 67,860 Hz giving a total frequency change of the coated crystal of + 48,694 Hz.

The effect demonstrated by crystal number 1 i.e. reduced frequency

Crystal number	Coating material	Frequency change due to Latex (Hz)	Frequency change due to coating (Hz)	Mass of Latex (μg)	Mass of coating (μg)	Diameter of coating (mm)
1	MnO_2	-5,482	-5,524	1.9	18.6	1.86
2	MnO_2	-7,389	-14,805	4.9	29.8	3.92
4	MnO_2	-4,235	-13,046	4.5	28.2	2.92
8	MnO_2					
	side 1	-5,054	-9,787	3.5	20.8	1.90
	side 2	-5,325	+67,860	2.7	18.3	1.58
12	MnO_2					
	side 1	-3,167	-7,268	1.3	16.5	1.62
	side 2	total change	-17,334	1.5	15.6	1.74
7	PbO_2	-3,941	-21,275	4.6	46.3	2.40
9	PbO_2					
	side 1	-3,206	-13,703	2.3	44.3	2.41
	side 2	-4,438	-13,861	3.7	39.4	2.38
14	PbO_2					
	side 1	-2,900	-9,703	4.0	42.5	2.40
	side 2	-2,093	-9,486	4.8	40.9	2.68
15	PbO_2					
	side 1	-4,855	-12,208	5.0	30.8	1.42
	side 2	-8,363	+60,717	10.7	35.4	1.77
18	$\left\{ \begin{array}{l} (\text{Ag}_2\text{O}) \\ (\text{AgVO}_3) \end{array} \right\}$	-4,404	+50,220	4.7	39.0	1.80
19	$\left\{ \begin{array}{l} (\text{Ag}_2\text{O}) \\ (\text{AgVO}_3) \end{array} \right\}$					
	side 1	-3,480	-22,389	4.6	33.9	2.48
	side 2	-5,986	+73,136	2.8	20.9	1.60
21	Decomposed					
	Ag_2MnO_4	-3,258	-16,945	2.9	19.8	2.76

Table 8

response upon application of the active material did occur, to a lesser degree, with all of the crystals coated by this technique. The extent to which this effect was occurring can be expressed mathematically.

The Sauerbrey equation (6) can be expressed simply as

$$\Delta f = - C \cdot \frac{\Delta m}{A}$$

where C contains all the constants of the equation. If the validity of the equation is assumed and the condition of a smooth film exists then an experimental value for C can be calculated as the mass, area and frequency change are known for the latex deposits applied to the crystals.

Using the experimental value of the constant just calculated and knowing the area and mass of the active solid deposited on the crystal it is therefore possible to predict the decrease in frequency that should occur with a coating of such dimensions.

If the experimental frequency decrease obtained on completion of the coating process is then ratio-ed with the predicted frequency decrease

$$\text{i.e. } \frac{\Delta f_{\text{experimental}}}{\Delta f_{\text{predicted}}}$$

then the resultant figure will be a measure of the agreement between the coating and Sauerbrey's equation. Table 9 shows the experimental frequency change obtained on coating, the predicted frequency change and the ratio of the two frequency changes for those crystals listed in table 8.

A possible cause of the deviations from the predicted results could be the unequal distribution of mass on the surface of the crystal.

The significance of this is realized if the work carried out by

Crystal number	Experimental frequency change Δf_E	Predicted frequency change Δf_P	Ratio $\frac{\Delta f_E}{\Delta f_P}$
1	-11,006	-59,147	0.186
2	-22,194	-52,413	0.424
4	-17,281	-30,845	0.560
8, side 1	-14,841	-35087	0.424
side 2	+62,535	-41,415	-
12, side 1	-10,435	-43,363	0.241
side 2	-17,334	-	-
7	-25,216	-43,606	0.583
9, side 1	-16,909	-64,956	0.261
side 2	-18,299	-51,696	0.354
14, side 1	-12,603	-33,716	0.374
side 2	-11,579	-19,926	0.583
15, side 1	-17,063	-34,762	0.493
side 2	+52,354	-36,029	-
18	+45,816	-40,947	-
19 side 1	-25,869	-29,125	0.891
side 2	+67,150	-50,667	-
21	-20,203	-25,502	0.792

Table 9

Sauerbrey (46, 47) is studied. In this work the amplitude distribution of the vibrations occurring in an A.T. cut crystal are determined. As the amplitude of vibration was found to be greatest in the centre of the exciting electrode of the crystal, and almost zero at the periphery of the electrode, it follows that the part of the crystal most sensitive to added mass is the centre of the electrode. Mass at the edge of the electrode contributes to the frequency change to a lesser degree. This has been shown experimentally, to be correct (70, 73) in that deposits of the same mass and area give different frequency changes when placed on different parts of the crystal. The largest frequency change being observed when the deposit is placed in the centre of the electrode.

This variation in sensitivity as a function of position or more accurately as a function of the vibration amplitude distribution is not predicted in the Sauerbrey equation as a constant vibrational amplitude was assumed (44).

Thus if the deposits prepared using latex as the adhesive were more dense at the edge of the deposit than in the centre, as was occasionally evident by the formation of a dark outer ring when deposits of lead dioxide were made, then the frequency decrease of the crystal would not be as great as expected.

The responses of crystal coatings prepared by this method and the response of other solid coatings will be described in the next chapter.

Further investigation of the nature of the high frequency effect and a collection of the information relevant to the occurrence of this effect will be detailed in chapter 5.

4. The Response of Solid Coating Materials

4.1. Introduction

The responses of the solid materials coated by the techniques described in chapter 3 will be described in this chapter. The order in which the materials are to be described is indicative of the response obtained in that the interesting and more useful materials, manganese dioxide and lead dioxide will be described last.

4.2. Sodium Tetrachlormercuriate

As described in chapter 3 this material presented no problems associated with the coating of the crystals.

A number of crystals were coated on both electrodes. The mass of the deposits on each crystal varied between 40 and 155 μg . The deposits were 2-3 mm. in diameter. The response of each of these crystals to sulphur dioxide was checked in both a static and dynamic environment.

To check the response in a static environment the glass cell was used (fig. 19), the coated crystal was placed in the cell, the cell flushed with nitrogen and then sealed whilst the crystal reached an equilibrium frequency.

When the frequency was constant an aliquot of sulphur dioxide was injected into the cell with a microsyringe. The frequency of the crystal was monitored for a period of 15 minutes after the sample introduction. The maximum concentration of sulphur dioxide in the static cell during these experiments was 0.93% by volume: for all of the coated crystals tried in this experiment no frequency change was observed after the sulphur dioxide had been introduced into the cell.

Similarly no response was obtained from any crystal coated with sodium tetrachlormercuriate when exposed to a flow of nitrogen containing sulphur dioxide. As no response was obtained with this coating in a static environment the lack of response in a flowing system

is not surprising.

The lack of any response in a static system is however, not in agreement with reported work (82). In this work authors report a total frequency change of 1,400 Hz when a crystal, coated on one electrode only with sodium tetrachlormercuriate (approximately 14 μg), was exposed to a static atmosphere of sulphur dioxide (0.22% by volume) for a period of 15 minutes.

The response of an uncoated crystal under the same conditions was reported as being a decrease of 30 Hz.

Repeated attempts were made to reproduce the reported results but no response at all was obtained for the sulphur dioxide/dry sodium tetrachlormercuriate system.

It was suspected that the reaction between the two compounds was not occurring as the reactants were dry and not, as is usual, a reaction between gaseous sulphur dioxide and an aqueous solution of sodium tetrachlormercuriate.

It was considered, at this stage of the work, undesirable to include a further variable in the system, i.e. the introduction of water vapour into the crystal environment, therefore no further work with sodium tetrachlormercuriate was carried out.

4.3. Nickel II Hydroxide

It was hoped that the use of nickel hydroxide as a selective coating for sulphur dioxide detection would be more successful than sodium tetrachlormercuriate as, according to Feigl (90), the reaction between nickel hydroxide and sulphur dioxide proceeds readily in the dry state. The test described in Feigl, i.e. the use of dry nickel hydroxide impregnated filter paper to detect sulphur dioxide, was carried out by the author as a preliminary check; the test was found to work; the pale green nickel hydroxide turned black.

After a suitable method of depositing nickel hydroxide on a crystal had been developed, (see chapter 3) a number of crystals were coated on both electrodes with the material. The volume of the solution containing the nickel hydroxide and thus the mass of material was kept constant ($1 \mu\text{l}$ of $4.4 \mu\text{g}/\mu\text{l}$ solution), the area of the deposit was varied from 1.5 to 5.5 mm. After the solution of nickel hydroxide had been deposited on the crystal the solvent, aqueous ammonia, was allowed to evaporate at room temperature.

The deposit details of the first batch of nickel hydroxide coated crystals are shown below. The mass of each deposit, $4.4 \mu\text{g}$, was deduced from the solution concentration not by direct weighing.

Crystal and deposit number	Deposit Diameter (mm)	Frequency change (Hz)
1 a	1.5	No oscillations
b	-	-
2 a	2.0	- 4,406
b	2.0	- 6,545
3 a	3.0	-3,800
b	3.0	-3,900
4 a	4.0	- 4,103
b	4.0	- 4,090
5 a	5.0	- 2,951
b	5.0	- 3,195
6 a	5.5	- 2,525
b	5.5	- 2,967

Table 10

The appearance of the deposits was good, the finest and most evenly distributed deposits were on crystals 5 and 6. The deposits

on crystals 2 and 3 were slightly patchy but smooth whilst small individual particles were becoming evident on crystal 4. The frequency of crystal 3 was unstable on the last three digits (± 100 Hz). The response of these coated crystals were checked in the following manner. The coated crystal was placed in the static cell, the cell was then flushed with nitrogen (400 ml./min. for two minutes) and sealed. The crystal was allowed to reach an equilibrium frequency. When the crystal had come to equilibrium an aliquot of sulphur dioxide (100 μ l) was introduced into the cell. The frequency of the crystal was monitored for 10 minutes; ten minutes after sample introduction the cell was flushed again with nitrogen and the crystal allowed to equilibriate. This procedure was repeated until the response of the crystal had decayed and become constant; the crystal was then changed.

Crystal number 4 would not oscillate when placed in the cell and both crystals 2 and 3 were unstable in frequency when placed in the cell. The results obtained for crystals 5 and 6 were repeated; this required the application of fresh deposits. The two sets of results were in good agreement. The responses of crystals 5 and 6 are shown below; the injection number shown in the table is the number of the consecutive injection of a 100 μ l aliquot of sulphur dioxide, thus for the first injection a larger response was obtained than for the fourth injection.

Injection number	Response of Crystal 5 (Hz)	Response of Crystal 6 (Hz)
1	52	38
2	15	29
3	12	16
4	10	13

Table 11

The rapid decay of the response is to be expected from a coating which reacts irreversibly with sulphur dioxide: the active sites on the coating grow less in number as the interaction between sample and coating proceeds, therefore the response from the next aliquot of sample is very much smaller than the previous sample as the number of free active sites is less. The frequency change obtained as a result of coating/sample interaction was not reversible by flushing the cell with nitrogen as described.

It was suspected that the low initial response of the coated crystals was attributable to contamination of the coating by atmospheric sulphur dioxide prior to the crystal being placed in the sample cell. Although the crystals were stored in a desiccator between the coating preparation and use, the coatings were applied, and the solvent allowed to evaporate, in the open laboratory. The crystals were thus exposed to the laboratory atmosphere for a period of approximately 25 minutes.

In order to test this idea several crystals were coated with nickel hydroxide; the dimensions of the deposits were similar to crystal 5. The time elapsing between the beginning of the coating procedure and the time when the coated crystal was placed in the sample cell was reduced to approximately 5 minutes. This was achieved by drying the deposit at 110° for 3 minutes. The initial response of crystals coated in this manner was improved, a typical initial response was a decrease in frequency of 123 Hz over a 10 minute period after the introduction of 100 μ l of sulphur dioxide into the sample cell. The subsequent pattern of response was very similar to that shown in table 11 i.e. a very rapid decrease in the response as the total quantity of sulphur dioxide presented to the crystal increased.

As the response of the nickel hydroxide coatings was low for a

relatively high concentration of sulphur dioxide (0.37%) and also as the response decreased rapidly after exposure to sulphur dioxide further work with nickel hydroxide was not carried out.

4.4. Silver Compounds

The silver compounds that were screened as possible coating materials were a silver oxide/silver metavanadate mixture and the thermal decomposition product of silver permanganate. These materials were prepared as described in chapter 3 and applied to the crystals using the latex technique. The deposit details for the crystals coated with these materials are shown in table 12. The crystal identification numbers correspond with those given in tables 8 and 9, the details are repeated here for convenience.

Crystal number	Frequency change due to latex $\Delta f_L(\text{Hz})$	Frequency change due to coating $\Delta f_C(\text{Hz})$	Mass of latex (μg)	Mass of coating (μg)	Diameter of coating (mm)
18	-4,404	+50,220	4.7	39.0	1.80
19 1	-3,480	-22,389	4.6	33.9	2.48
2	-5,986	+73,136	2.8	20.9	1.60
20	-4,944	+51,697	3.9	24.0	1.56
21	-3,258	-16,945	2.9	19.8	2.76
22	-4,083	-24,503	1.5	21.5	2.30

Crystals 18, 19 and 20 were coated with the silver oxide/silver metavanadate mixture.

Crystals 21 and 22 were coated with the thermal decomposition product of silver permanganate.

Table 12

Crystal numbers 19 to 21 inclusive were tested for their response to sulphur dioxide in a static environment. The procedure used was similar to that used to check the nickel hydroxide deposits. Investigations of the decay of response as a function of total quantity of sulphur dioxide introduced to the crystal were not carried out as the initial response was too low to warrant further study. Crystal 22 was exposed to a static atmosphere of dilute nitrogen dioxide, the percentage composition of the nitrogen dioxide and sulphur dioxide atmospheres was the same 0.074% i.e. 20 μ l of sample gas injected into the cell.

The results of these experiments are shown in table 13. Blank values, the degree to which the sample gases adsorbed onto clean crystals were also ascertained.

Crystal number	Frequency change 10 min. after sample introduction (Hz)	Frequency change 30 min. after sample introduction (Hz)	Sample gas
19	-45	-84	0.074% SO ₂ in N ₂
20	—	-36	
21	-91	-165	
Blank	—	-5	
22	A decrease of 58 Hz in 4 min. then no further change		0.074% NO ₂ in N ₂
Blank	—	-20	

Table 13

It should be noted that the frequency of crystals 19 and 20 increased on coating but decreased when sample gas was presented to the coated crystal, but crystals 21 and 22 behaved in a normal manner

i.e. the frequency decreased on coating and decreased when sample was presented to the crystal.

Crystal number 18 was checked for response to both nitrogen dioxide and sulphur dioxide in a dynamic environment. The crystal was placed in the stainless steel cell with flow of nitrogen (12 ml/min.) passing through the cell. Aliquots of sample gas (5 to 100 μ l of NO_2 and SO_2) were introduced into the gas stream via an injection port. When sulphur dioxide was introduced into the system no response due to the coating alone was observed. The frequency responses of a clean crystal, a crystal with deposit of latex only and crystal 18 were identical at a sensitivity of -46 Hz/100 μ l of injected sample, this frequency change being due to the injection of sulphur dioxide onto the system. (Information acquired during work with triethanolamine coated crystals suggests that a portion of this frequency change is due to the injection process itself and not entirely due to the adsorption of sulphur dioxide onto the quartz crystal).

When aliquots of nitrogen dioxide were introduced to crystal 18 a response due to absorption of the sample by the coating was observed. The blank response (a clean crystal and a latex only coating) was established as being -50 Hz/100 μ l of injected nitrogen dioxide; the response for the coated crystal was -192 Hz/100 μ l: note also that these responses are decreased^s in the resonant frequency but the crystal increased its frequency upon coating.

As the responses of the silver compounds were so low in the static system further work in a dynamic system was not carried out with these coating materials.

4.5. Manganese Dioxide

4.5.1. Loosely Bound coatings

The first investigations of the suitability of manganese dioxide as a coating material for the detection and determination of nitrogen dioxide were carried out using crystals coated with the aid of the particle fractionator; water was used as the securing agent. The technique used has been fully described in the previous chapter.

Three crystals were coated by this method; the deposit details are shown in table 14. It will be noticed that the frequency changes on coating were typical for crystals coated in this manner;

Crystal number	Diameter of deposit (mm)	Thickness of deposit (mm)	Mass of deposit (μg)	Frequency change (Hz)
1	0.84	0.11	55.5	- 333
2	1.38	0.04	68.5	+2,147
3	2.14	0.16	194.3	+6,100

Table 14

i.e. the frequency change was not very great in comparison to the load on the crystal. The mass of each deposit was determined by direct weighing, the diameter and thickness of the deposit were measured with a travelling microscope.

The response characteristics of these crystals to aliquots of nitrogen dioxide were determined in a flowing system after a satisfactory preliminary examination of a similarly coated crystal in a static environment. (A decrease of 1,924 Hz in 10 minutes was obtained when a manganese dioxide coated crystal was exposed to a static atmosphere of nitrogen dioxide in nitrogen (0.37%).)

To determine the dynamic response of the 3 coated crystals the stainless steel cell block was used with a clean uncoated crystal in the reference cell. The ratio mode of operation was used to compare the reference and sample crystal frequencies. A simultaneous check was occasionally made with a single sided measurement as to whether the frequency of the sample crystal was increasing or decreasing when sample was presented to the crystal.

Unless otherwise stated 100 μ l samples of nitrogen dioxide were injected into the gas stream before the carrier gas entered the sample cell. The frequency and/or the frequency ratio of the sample crystal was monitored as a function of time so that the peak shape representing the sample/coating interaction could be studied. The nitrogen carrier gas flow rate was maintained at 12 ml/min. through the sample and reference cells; the flow rate was kept at this value for the experiments carried out with all 3 crystals unless stated otherwise.

The frequency of these crystals did not drift as a result of carrier gas/coating interaction.

The responses of these crystals to successive samples of nitrogen dioxide, though not identical, were similar in several respects.

1. All 3 crystals increased their vibrational frequency when sample gas was introduced into the carrier gas stream.
2. The peak shape representing the sample/coating interaction changed for each crystal as the total quantity of sample gas introduced to the crystal increased. Similarities in the changes of peak shape that occurred for each crystal were observed.
3. The magnitude of the frequency changes reflected the different dimensions of the deposits.

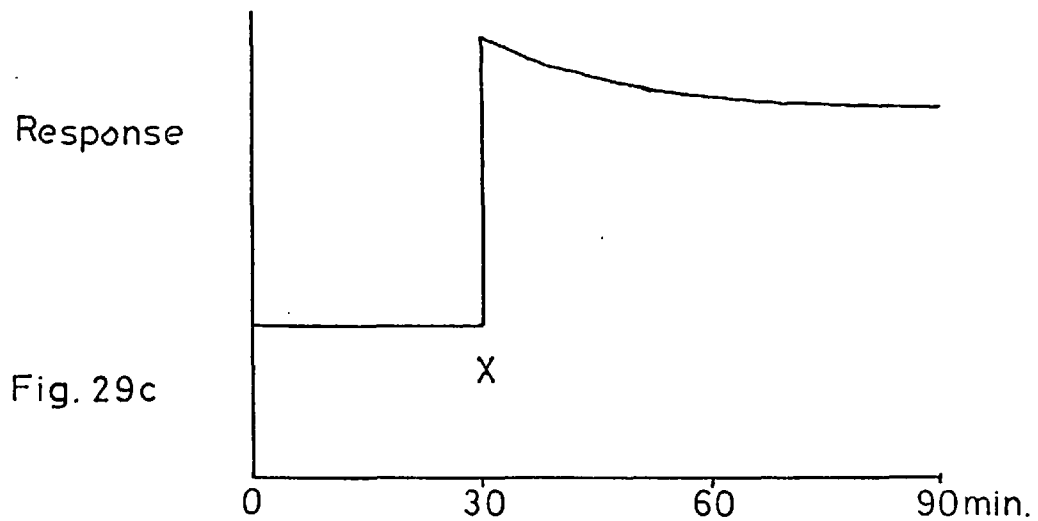
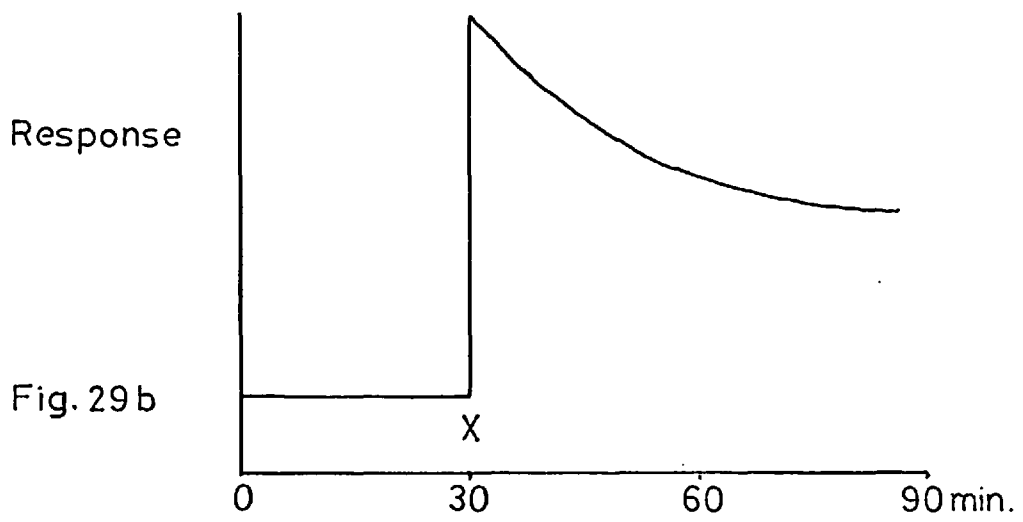
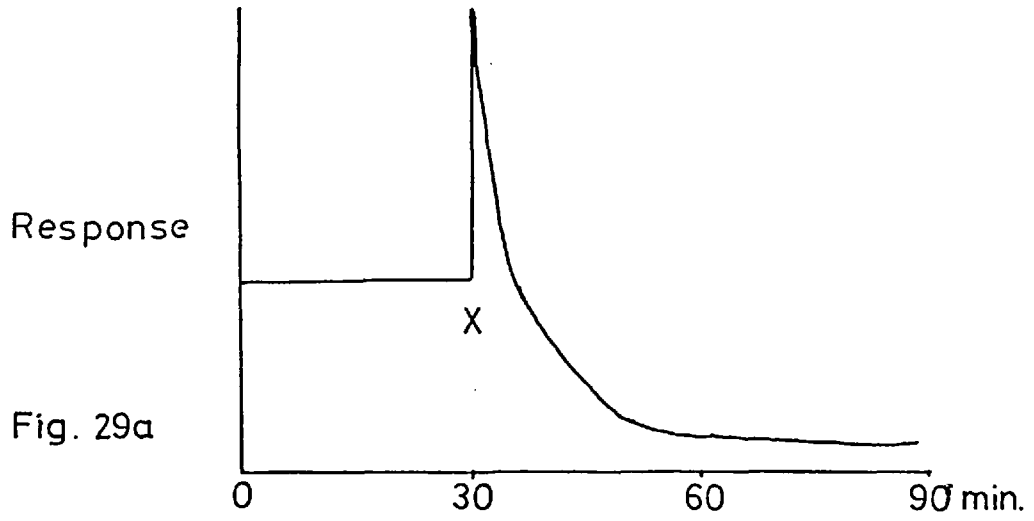
The various peak shapes obtained during this investigation are shown schematically in figure 29 (a-f). The variation in shape and magnitude of these peaks was a function of change in the nature of the coating material and not a change in the quantity of sample introduced into the system.

Note that the frequency of the crystals, without exception, increased very rapidly when the sample was introduced into the system. (Sample introduction in figure 29 (a-f) is depicted by a cross) and also that when the sample/coating interaction was of the type shown in figure 29 (a) then the frequency of the crystal first increased after sample introduction and then decreased to a frequency lower than the pre-sample introduction frequency.

The increase in frequency obtained when the first 3 injections of nitrogen dioxide were made into the flowing environments of crystals 1, 2 and 3 are shown in table 15. Also shown in this table is the peak shape associated with any particular sample introduction; i.e. crystal number 2 on the second injection of 100 μ l of nitrogen dioxide had a peak shape of the type shown in figure 29 (b).

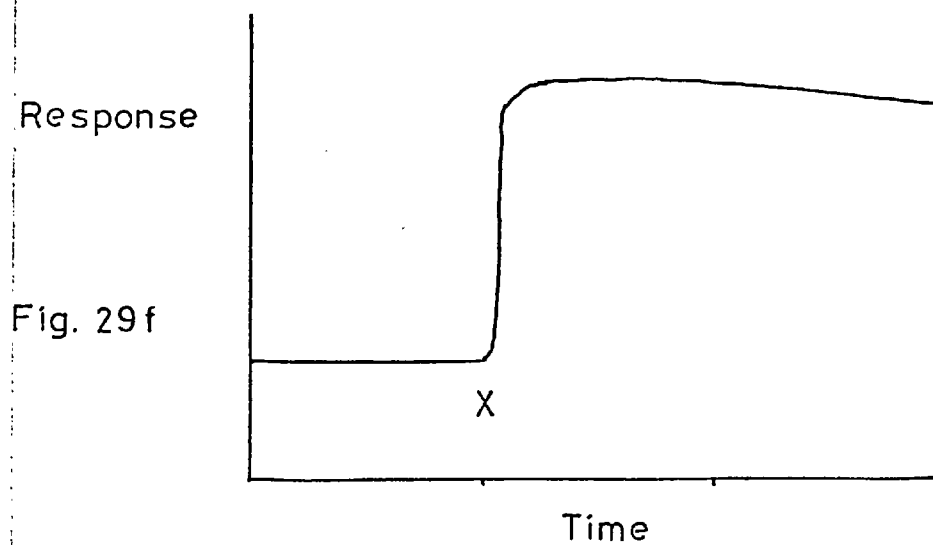
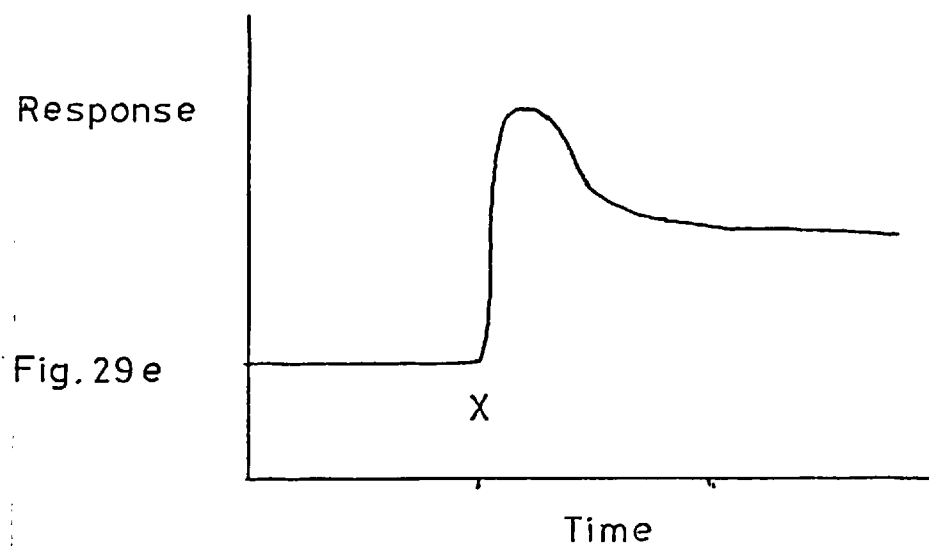
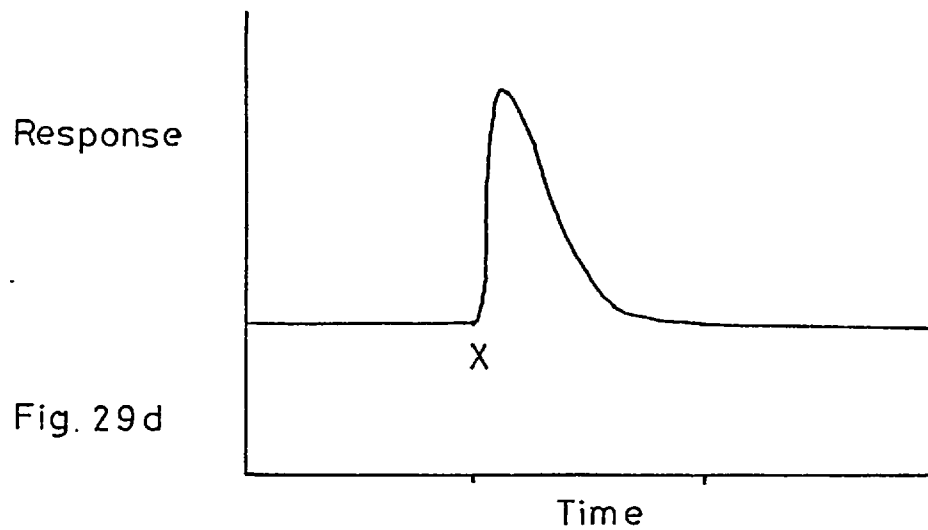
Crystal number	Injection number			
	1	2	3	nth
1	325Hz 29(a)	169Hz 29(a)	140Hz 29(a)	113 Hz 29(d)
2	575Hz 29(a)	704Hz 29(b)	305Hz 29(c)	129Hz (29(e))
3	597Hz 29(a)	905Hz 29(b)	420Hz 29(c)	142Hz 29(f)

Table 15



Peak Shapes Representing Interaction between Manganese Dioxide
Coated Crystals and Nitrogen Dioxide

Figure 29 a-c



Peak Shapes Representing Interaction between Manganese
Dioxide Coated Crystals and Nitrogen Dioxide

Figure 29 d-f

The n^{th} injection represents the peak value when the response became constant, i.e. no further decrease in the response of the crystal was observed for subsequent injections of 100 μl aliquots of nitrogen dioxide.

For crystal number 1, $n = 6$; for crystal 2, $n = 10$; and for crystal number 3, $n = 15$.

The change in the peak shape from the third injection to the n^{th} injection was gradual, i.e. the magnitude of the frequency change decreased for successive injections and the peak shape altered slightly. This process occurred for all three crystals, the actual change in the peak shape is best appreciated by comparing the peak shape of the third injection with that of the n^{th} injection.

If the peak shapes obtained for the n^{th} injections are compared a trend will be observed. Crystal number 1 was behaving in a readily reversible manner, i.e. the nitrogen dioxide sorbed onto the deposit was removed by the nitrogen carrier gas (fig. 29 (d)). Crystal number 3 however did not readily release the nitrogen dioxide sorbed onto the crystal (fig. 29 (f)) whilst crystal number 2 showed characteristics of crystals 1 and 3.

It was established that the rate of frequency decrease after sample sorbtion for crystal 3, (peak 29, f) could be increased from 18 Hz/10 min. to 39 Hz/10 min. by increasing the carrier gas flow rate, after sample sorbtion, from 12 ml/min. to 50 ml/min. No significant frequency change was observed when the carrier gas flow rate was increased and the crystal was oscillating at an equilibrium frequency.

This change in the rate of frequency decrease by an increase in the carrier gas flow was interpreted as being the removal of sorbed sample from the deposit, thus the nitrogen dioxide was only weakly bound or physisorbed onto the manganese dioxide. This is in agreement with

the concept that the manganese dioxide reacts chemically with nitrogen dioxide and therefore has a finite capacity, when the manganese dioxide is exhausted further sorbtion of nitrogen dioxide will be a weak physisorbtion onto a complex mixture of MnO_2 and $Mn(NO_3)_2$ as opposed to the strong chemisorbtion that has been reported for fresh manganese dioxide and nitrogen dioxide.

If the above discussion were applied to peak shapes 29b and c i.e. a frequency decrease after the initial increase as a result of loss of sorbed sample to the carrier gas, then an increase in the carrier gas flow should increase the rate of loss of material from the crystal. This however, is not the case, the rate of frequency decrease for peak shapes 29b and c was found to be quite independant of carrier gas flow.

Similarly the simple loss of sorbed nitrogen dioxide cannot be applied to peak shape 29a as the final frequency of this crystal is lower (by 305 Hz for crystal 3 injection 1) than the start frequency; this idea also conflicts with the idea of chemisorbtion of nitrogen dioxide on fresh manganese dioxide.

The frequency decrease could be caused by the loss not of nitrogen dioxide, but of perhaps water which may have been sorbed on the manganese dioxide, the water being released as the more strongly retained nitrogen dioxide is sorbed onto the surface of the deposit. If this idea was correct then every mole of nitrogen dioxide sorbed onto the manganese dioxide would have to displace 2.56 moles of water simply to maintain a constant frequency and more than 2.56 moles to cause an overall decrease in frequency.

A characteristic of crystals oscillating high, which dealt with in more detail in the next chapter, gives rise to another possible

explanation of the peak shapes.

It has been established that when mass is placed in a thin uniform film on the surface of a high oscillating crystal then the frequency of that crystal will decrease although the final frequency is still higher than the frequency of the clean crystal.

Consequently, as the decrease in frequency after the introduction of nitrogen dioxide was independent of carrier gas flow rate it is possible that the frequency decrease is attributable to movement of sorbed nitrogen dioxide through the manganese dioxide deposit; from the outside of the deposit, where it is giving the initial large increase in frequency, to the centre of the deposit closer to the crystal itself. This movement of nitrogen dioxide could act either as mass moving away from the surface causing a decrease in the anomalous frequency or mass moving into close proximity of the crystal where, as just described it will cause the crystal to decrease its frequency in a normal manner. After repeated injection this movement or equilibration will cease due to saturation of the available sites for sorption.

During this period of repeated injections the frequency of the crystals was generally increasing, showing the integrating nature of the coating.

Once the coatings had been saturated with nitrogen dioxide the frequency response obtained by the physisorption of sample was linearly related to the quantity of sample injected into the system. The sensitivity of each crystal, when saturated, is shown in table 15, the response per 100 μ l of injected nitrogen dioxide is shown in the column "nth injection".

Since the changing peak shapes of these crystals were thought to be due to a bulk effect of the coating material, and the frequencies

of the coated crystals increased when sample had been introduced to the crystal, (both effects were thought to be due to the geometry of the large deposits) it was decided to change the coating technique to provide thin film type deposits.

4.5.2. Firmly Bound Coatings

These deposits were achieved using latex as the securing agent. This technique has been previously described; six crystals were coated with manganese dioxide with this method, four deposits were single side deposits and two crystals were coated on both sides. The details of the deposits are shown in table 16, some of these details have been listed elsewhere but are repeated here for convenience.

The responses of these crystals were checked in a manner similar

Crystal number	Frequency change due to latex Δf_L (Hz)	Frequency change due to coating Δf_C (Hz)	Mass of latex (μg)	Mass of coating (μg)	Diameter of coating (mm)
1	-5,482	-5,524	1.9	18.6	1.86
2	-7,389	-14,805	4.9	29.8	3.92
4	-4,235	-13,046	4.5	28.2	2.92
6	-3,569	-9,952	4.5	19.9	1.88
8	-5,054	-9,787	3.5	20.8	1.90
2	-5,325	+67,860	2.7	18.3	1.58
12	-3,167	-7,268	1.3	16.5	1.62
2	-17,334		1.5	15.6	1.74

Table 16

to that used for the previous manganese dioxide coated crystals; i.e. the stainless steel cell with a clean reference crystal, a nitrogen carrier gas flow of 12 ml/min. through each cell and the ratio mode of

frequency monitoring, Various aliquots of nitrogen dioxide (5-100 μ l) were introduced into the system, the resultant frequency change was noted as a function of time after the sample injection. Replicate injections were made, between 3 and 10 injections were made to obtain each mean response.

The first difference observed with the latex/manganese dioxide coated crystals was in the frequency change obtained upon coating: all crystals, except number 8, had decreased their frequency. (See chapter 3 for further discussion).

Another major difference between the two types of manganese dioxide coatings was the total absence of any variation of peak shape and magnitude as described for the previous coatings. The shape and magnitude of a peak due to any given quantity of injected sample was generally constant throughout the experimental life of the crystal; there were one or two special exceptions, which will be explained later.

When these manganese dioxide/latex coated crystals were exposed to samples of nitrogen dioxide the sign of the frequency change that accompanied the sample injection was not constant from one crystal to another; some crystals decreased their frequency when sample was presented, others increased their vibrational frequency when exposed to sample.

Crystal number	Direction of frequency change due to:-	
	i) coating	ii) sample presentation
1	decrease	increase
2	decrease	increase
4	decrease	decrease
6	decrease	decrease
8	increase	decrease
12	decrease	initial decrease see text

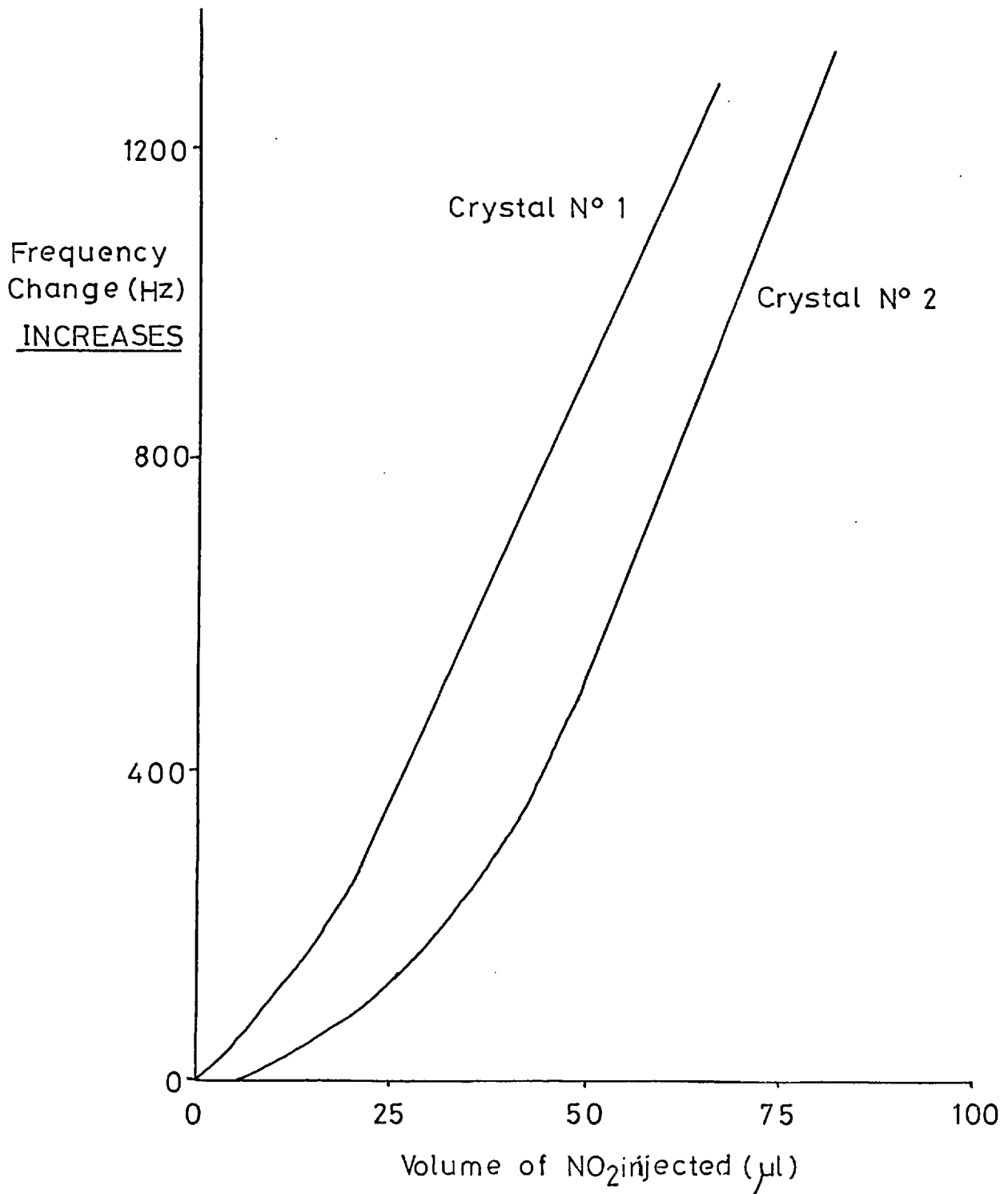
Table 17

The pattern of frequency change obtained for these crystals i.e. increase or decrease of frequency upon coating and increase or decrease of frequency upon presentation of sample is shown in table 17. Crystal number 12 changed its vibrational state during its experimental life in that the crystal decreased its frequency upon coating and the frequency also decreased when sample was presented to the crystal, but after a period of continuous use, the response of the crystal for samples of 50 μ l and more began to decrease and become erratic. During this period the crystal changed its vibrational mode from a decrease in frequency to a considerable increase i.e. the crystal began vibrating 49.3 KHz higher than the clean frequency, compared with the original decrease of 27.7 KHz obtained when the crystal was coated. The only change in the system during this period was the further introduction of sample gas, no other parameter connected with the system was changed.

The response of this high vibrating crystal to injected samples, unfortunately, could not be ascertained as the frequency of the crystal was not stable, a random variation of frequency of approximately \pm 100 Hz about a mean frequency was observed.

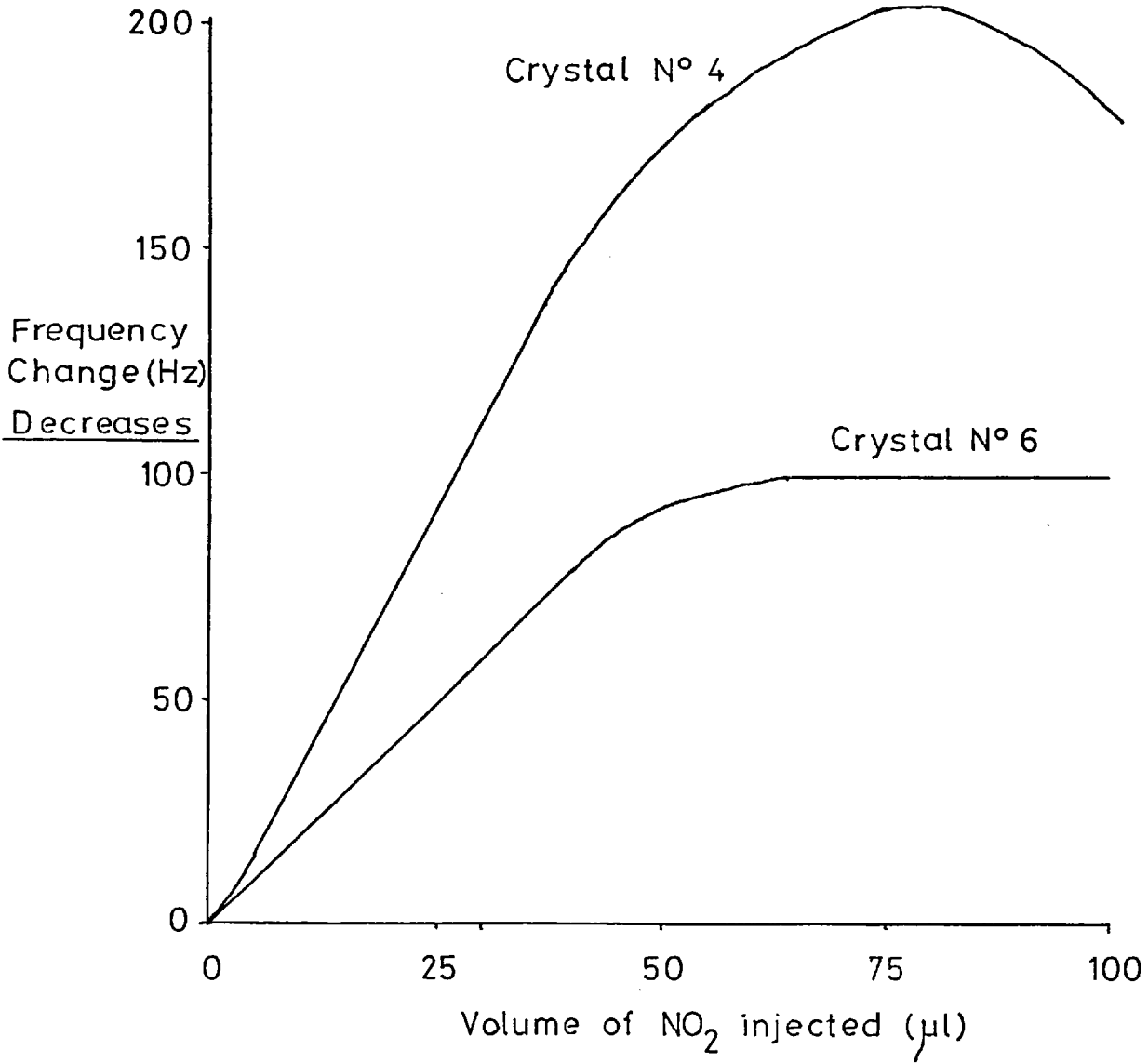
The responses of these manganese dioxide coated crystals are presented graphically; the responses of crystals 1 and 2 are shown in figure 30, 4 and 6 in figure 31 and 8 and 12 in figure 32.

It is readily seen by comparing the details contained in table 16 and the graphs in figures 30, 31 and 32 that for these crystals no direct correlation of the type indicated by Sauerbrey exists between the coating dimensions and the responses obtained. This can be illustrated by the following comparisons; crystals 1 and 6 had very similar deposits upon them i.e. mass and area of deposit, but the responses of these crystals were totally dissimilar, both the magnitude



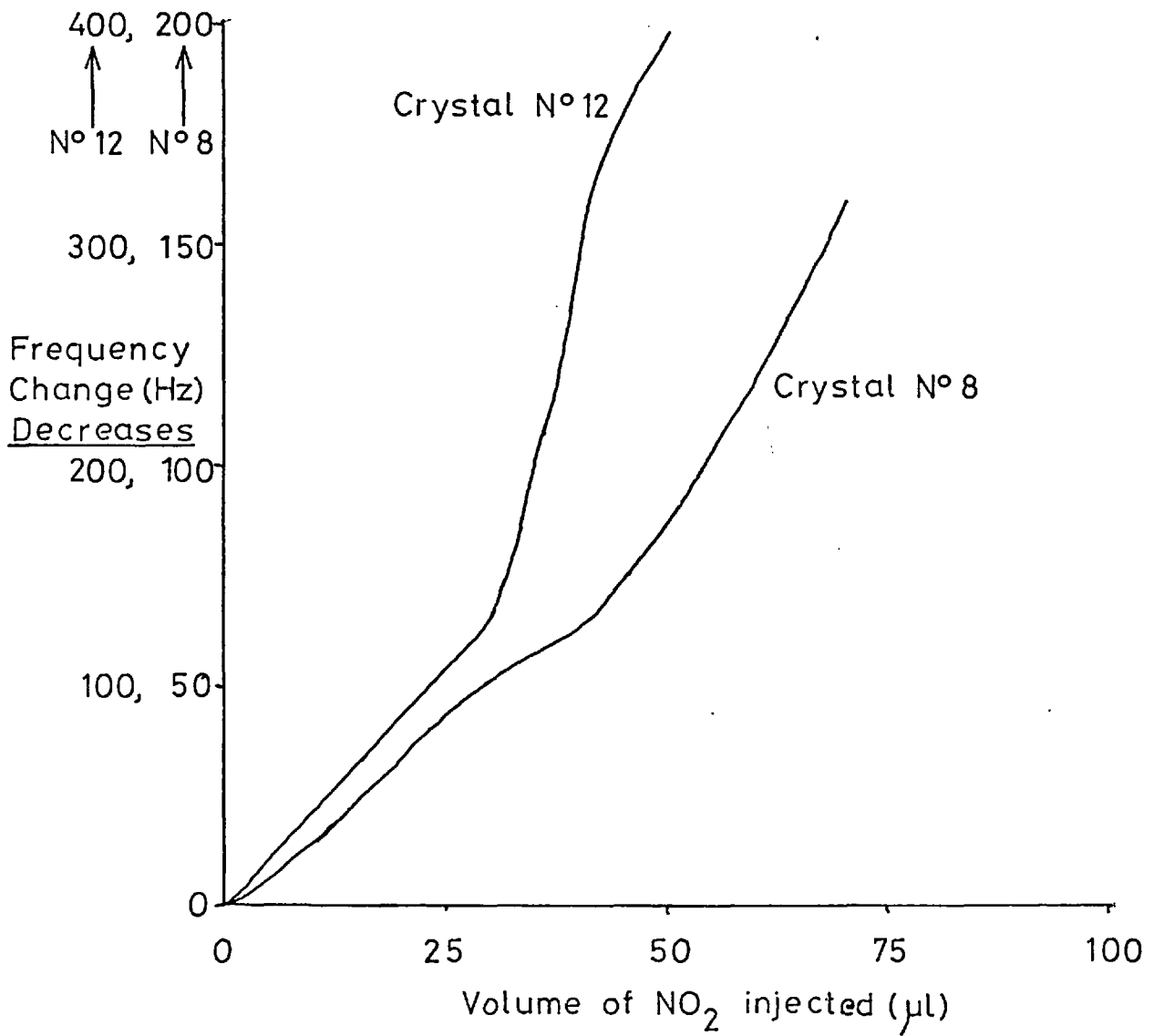
Calibration Graphs of Crystals 1 and 2

Figure 30



Calibration Graphs of Crystals 4 and 6

Figure 31



Calibration Graphs of Crystals 8 and 12

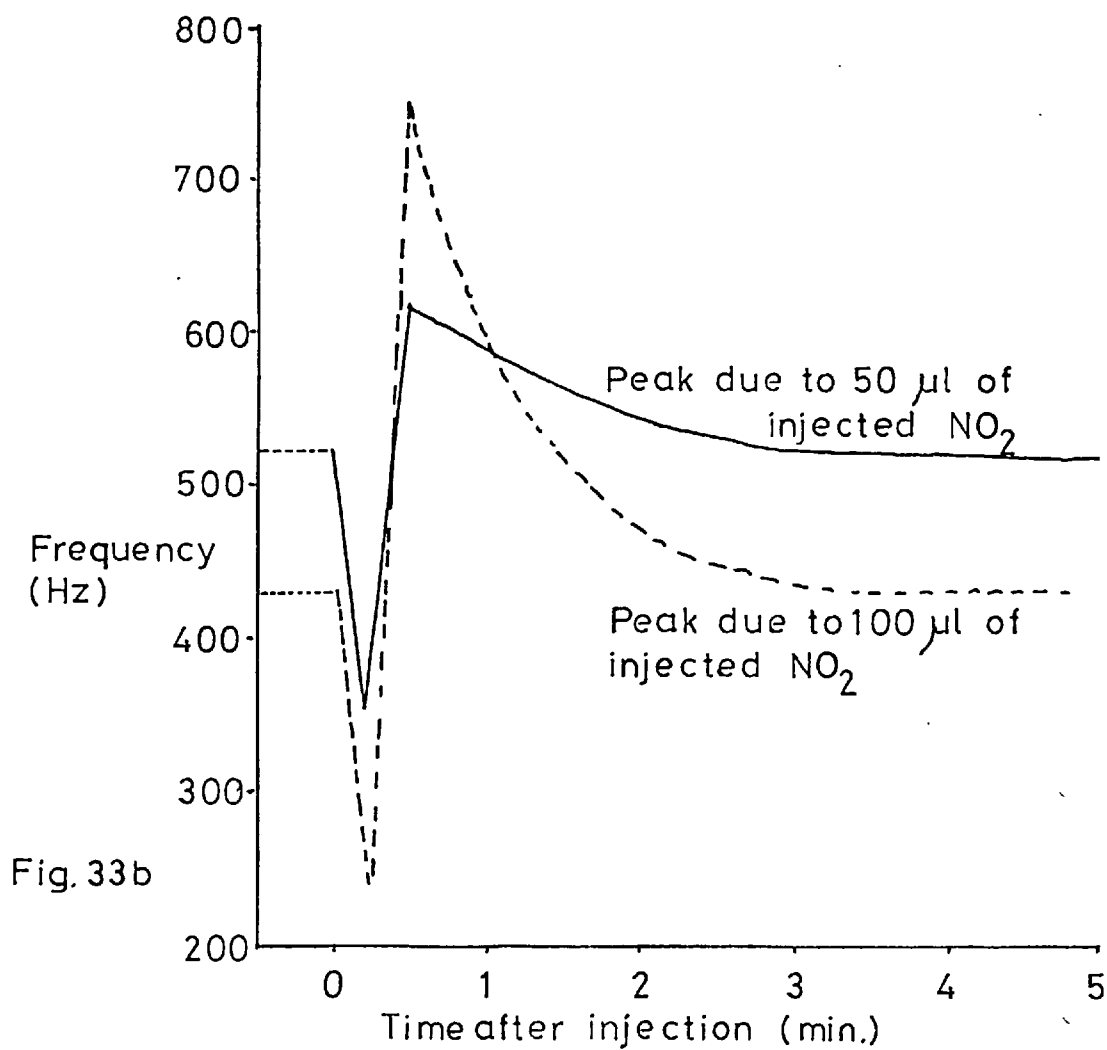
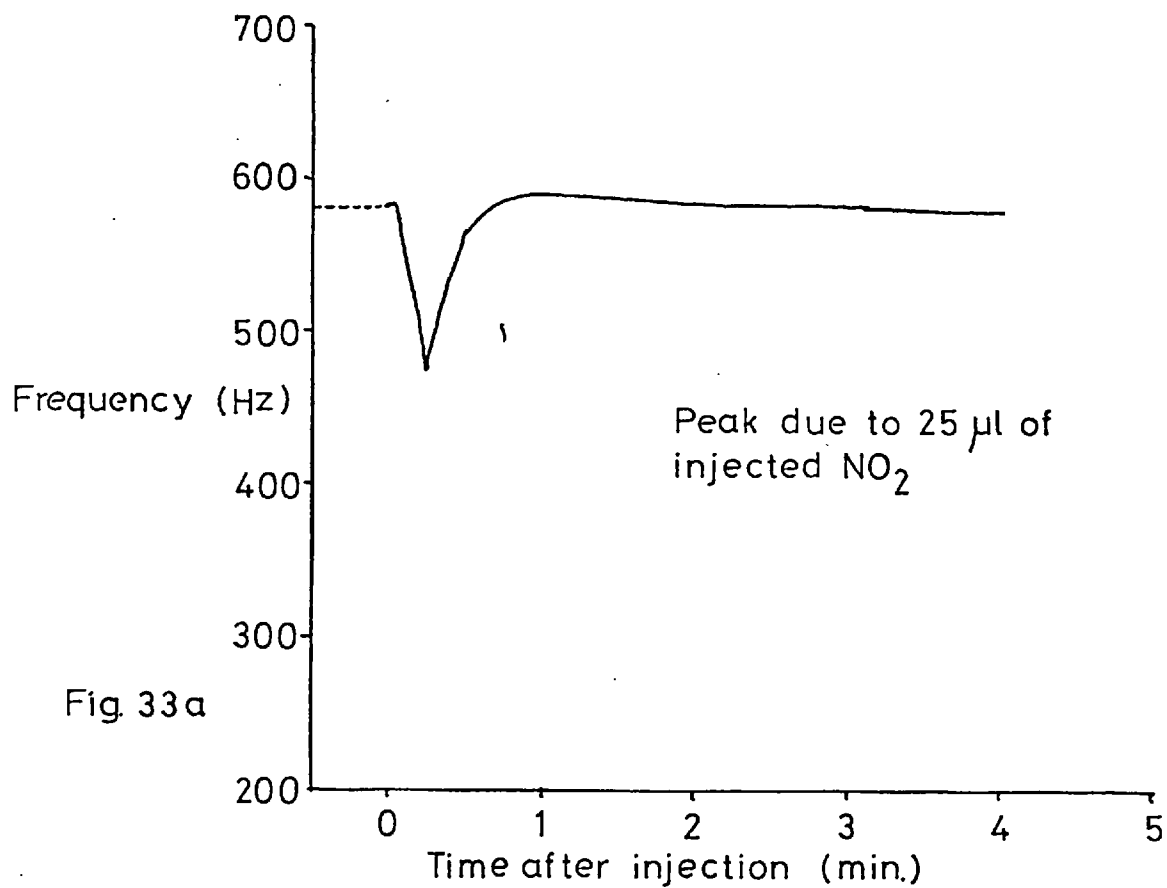
Figure 32

and direction of the frequency change obtained upon sample presentation were different.

Similarly the responses of crystals 1 and 2 were very similar but the coatings were not. The responses of crystals 4 and 6 however were similar and so were the coatings upon these crystals. Both crystals decreased their frequency when coated and when sample was presented to the crystal. Both calibration graphs curve off, crystal 6 reaching a plateau region and crystal 4 actually decreases as the quantity of injected nitrogen dioxide was increased. The cause of this curvature was the same for both crystals and can be readily appreciated by studying the peak profile obtained after injection of a sample. Figure 33a shows the variation of frequency of crystal 4 plotted as a function of time elapsed after the sample of nitrogen dioxide (25 μ l) had been injected. The maximum frequency decrease i.e. peak height, is the value plotted in figure 31. If the profiles obtained for 50 and 100 μ l samples are studied (fig. 33b) it will be observed that the frequency first decreases, then rapidly increases and finally decreases gradually to a value very similar to the frequency immediately prior to injection. The magnitude of the increase increases as larger quantities of sample are injected.

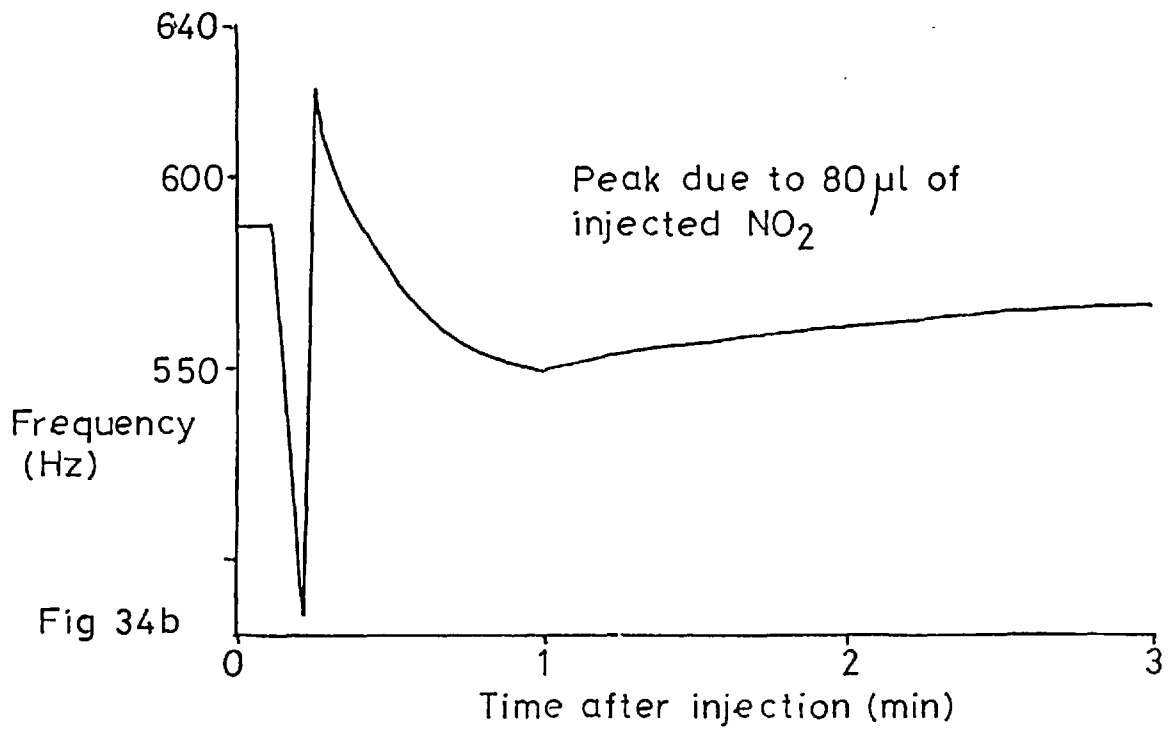
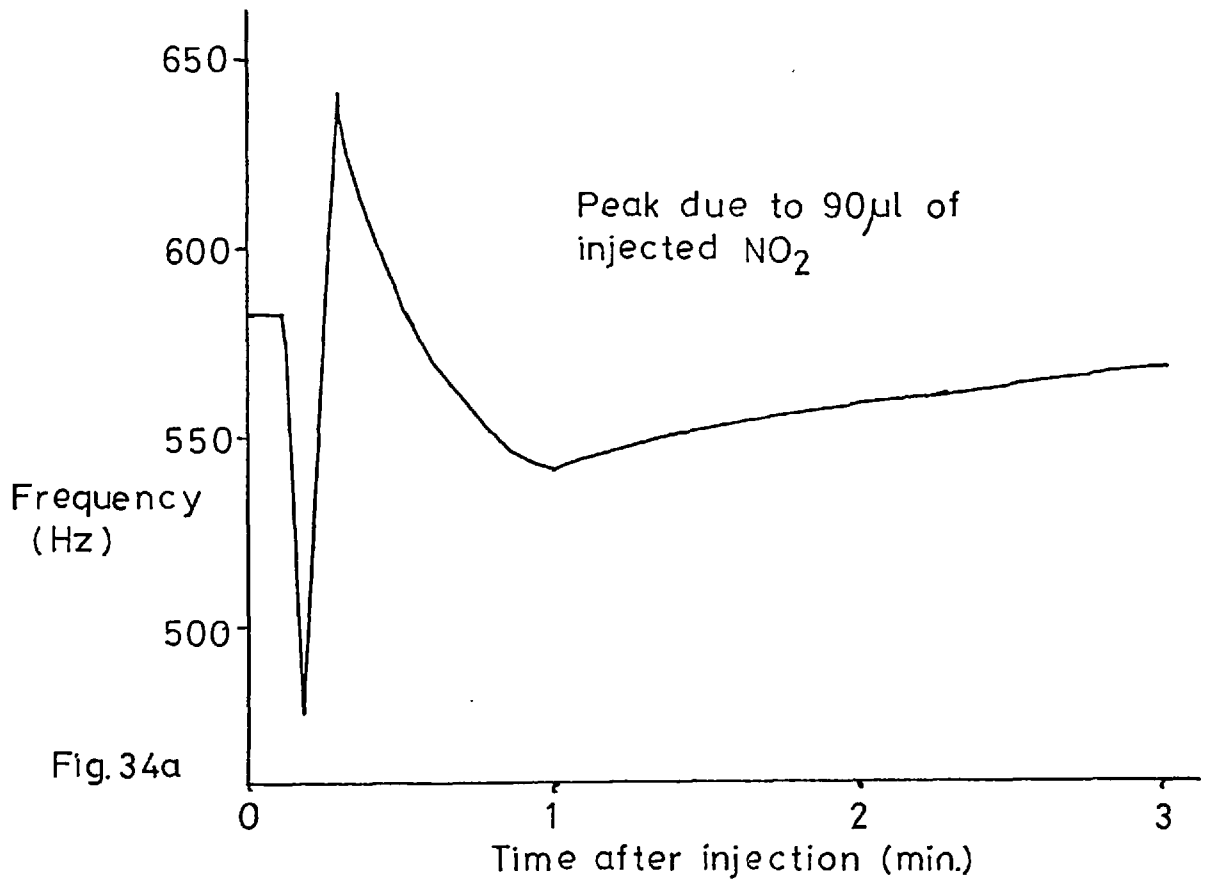
If the profiles obtained from crystal 6 are studied then the same basic shape is seen although the shape of the recovery after the increase is different (figure 34 a and b).

The shapes of the calibration graphs for crystals 8 and 12, both crystals were coated on both sides, are similar. Neither graph is a good calibration, nor are there any notable features of these graphs that can be explained. Note that crystal 8 had increased its frequency upon coating but the frequency decreased when sample was



Peak Profiles of NO_2 on Crystal 4

Figure 33 a,b



Peak Profiles of NO_2 on Crystal 6

Figure 34 a,b

presented to the crystal.

Crystal number 12, as stated earlier, increased its frequency by 77.0 KHz after a period of several weeks. The data presented in figure 32 was obtained before the change occurred.

Immediately prior to the increase in frequency of this crystal 50 μ l aliquots of nitrogen dioxide were injected; the frequency decreases obtained were 213, 211, 194, 159 Hz. These are results obtained in sequence. They compare with a mean response of 390 Hz obtained in the early life of the crystal. Although the latex/manganese dioxide crystals behaved in a generally reversible fashion there was a build up of nitrogen dioxide on the crystal i.e. small quantities of sample that were never removed by the carrier gas. In the case of crystal 12 this caused a decrease of approximately 1,300 Hz over several weeks. It is suspected that the last series of 50 μ l injections and the gradual decrease in the frequency of the crystal caused the crystal to reach some specific frequency or coating condition to induce the high frequency system of vibrations. The peak profiles of the last injections prior to the large frequency increase do not however, give any indication of the change that occurred shortly after the injections, i.e. there was no shape similar to those shown in figures 33 and 34.

The effect of sulphur dioxide on manganese dioxide was checked using crystals 1 and 2. The same experimental procedure was used as has been previously described. It was found that the crystals were less sensitive to sulphur dioxide but the experimental points on the graph were a good fit to a straight line passing through the origin. The sensitivities were 72 Hz/10 μ l of injected sulphur dioxide and 33 Hz/10 μ l for crystal 1 and 2 respectively.

The different affinities of these crystals to sulphur dioxide and nitrogen dioxide is illustrated by comparing the peak shapes obtained from the separate injections of 5 μ l aliquots of nitrogen dioxide and sulphur dioxide onto crystal number 1 (figure 35).

It is clear from this comparison that affinity of manganese dioxide for nitrogen dioxide is much stronger than the manganese dioxide/sulphur dioxide system. This is shown by the very short time required to remove the sulphur dioxide from the crystal surface in comparison with the much longer time required to remove the nitrogen dioxide.

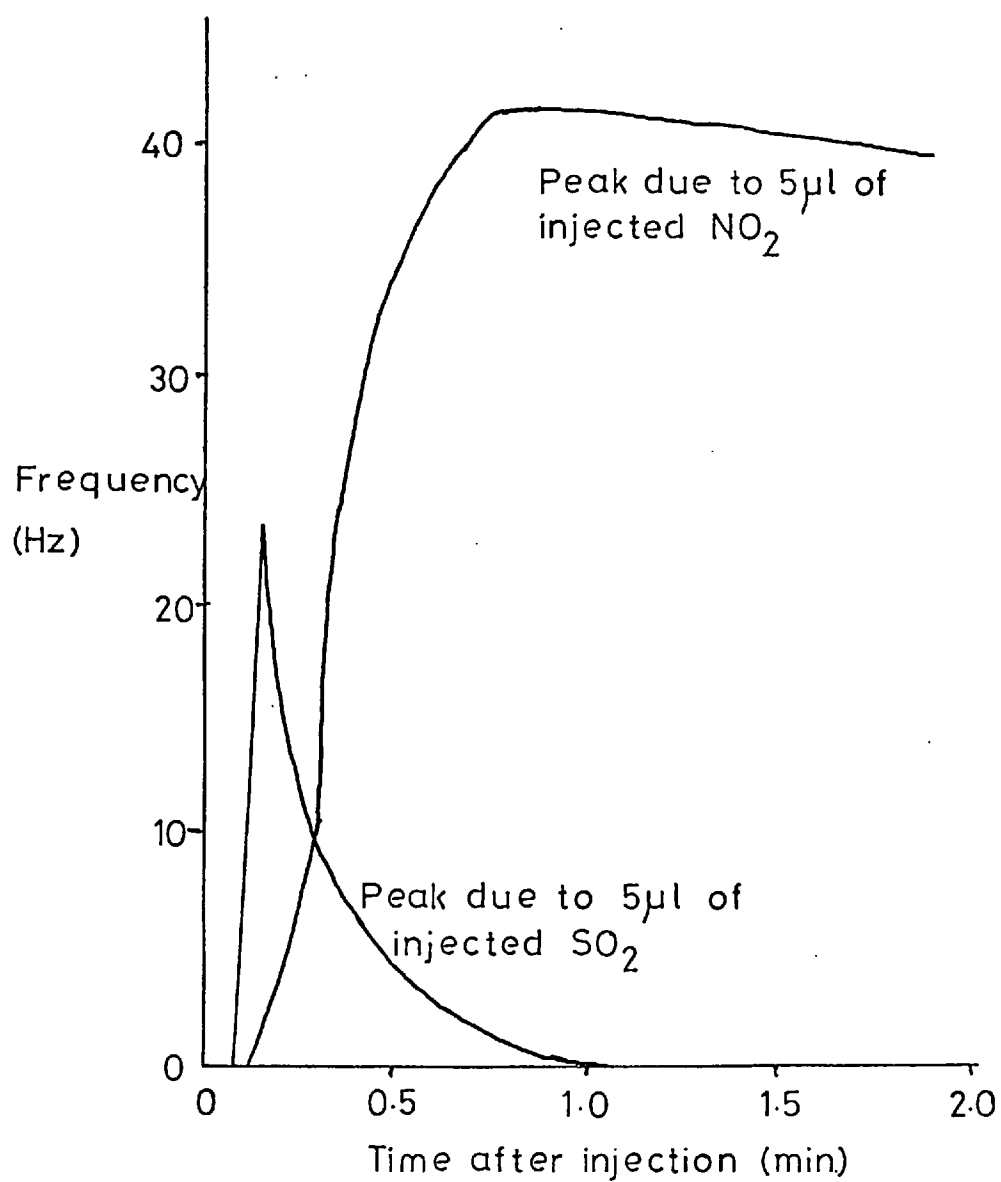
A study was carried out to establish if there was any effect on the response of these crystals to nitrogen dioxide when immediately prior to the injection of nitrogen dioxide the crystal surface had been exposed to sulphur dioxide. The opposite effect was also studied i.e. the effect of previous exposure to nitrogen dioxide on the determination of sulphur dioxide.

It was found that previous exposure to replicate 100 μ l aliquots of nitrogen dioxide had no effect on the frequency change of a 20 μ l aliquot of sulphur dioxide; no enhancement or suppression of response was observed. Similarly no effect due to the prior exposure of a crystal to sulphur dioxide was observed when nitrogen dioxide was injected into the system.

No further experimental work was carried out with manganese dioxide coated crystals.

At this point it is relevant to give a summary of the information relating to manganese dioxide coated crystals.

- i) With the study of manganese dioxide coatings applied with latex and with the aid of the particle fractionater all



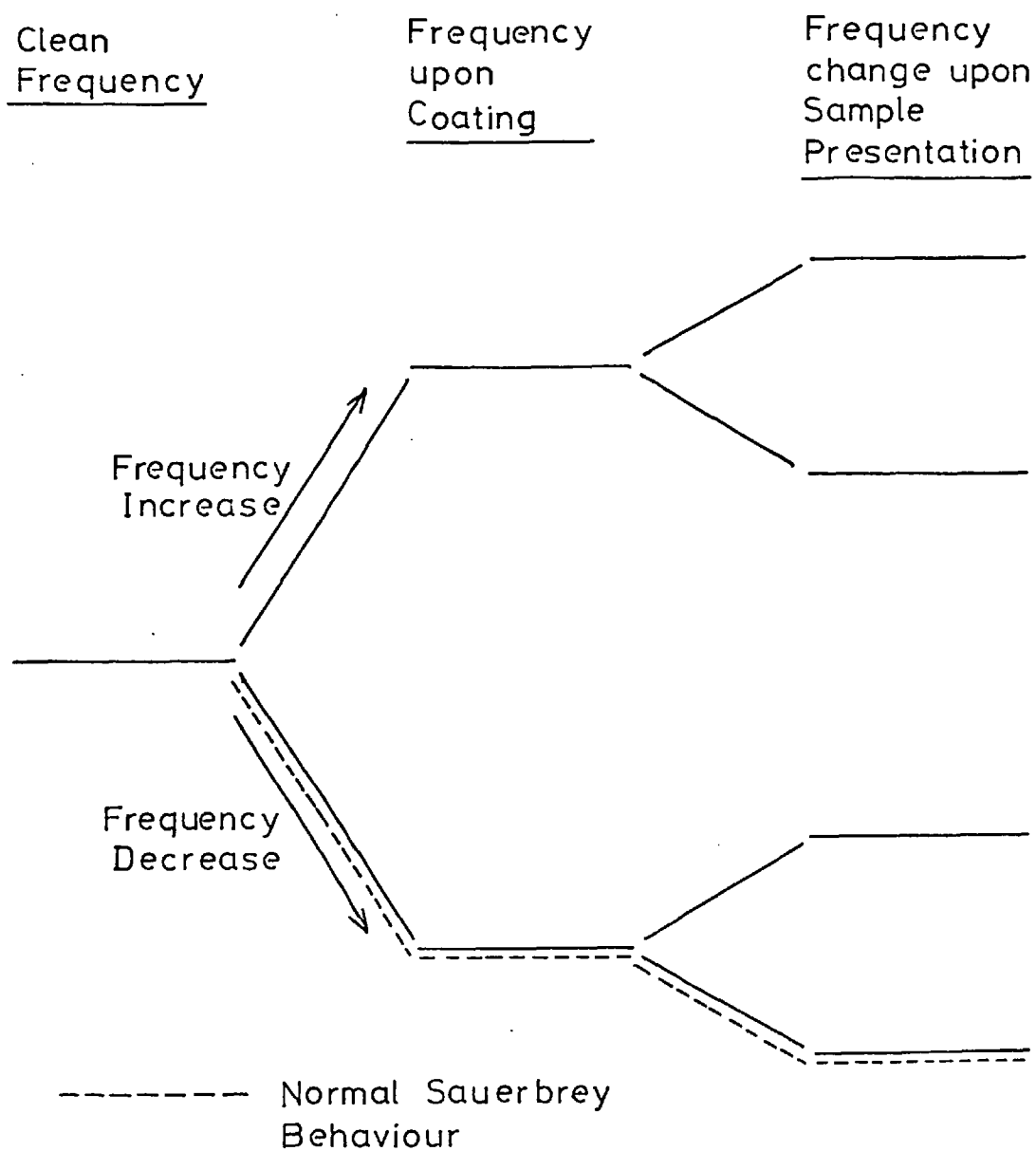
Comparison of Peak Shapes for NO₂ and SO₂

injected onto Crystal 1

Figure 35

possible combinations of frequency change have been seen; these changes are depicted schematically in figure 36.

- ii) The exact manner in which a coated crystal will behave, especially those crystals using latex, is very difficult to predict.
- iii) The initial responses of the crystals coated with the particle fractionater were quite large but rapidly decreased. This decrease is attributed to the filling of the most active sites for sorbtion, probably chemisorbtion of sample, the lower responses being due only to a more weakly bonded species i.e. physisorbtion of the sample.
- iv) The change in the shapes of the peaks obtained from these crystals was thought to be due to not only a change from chemisorbtion to physisorbtion but also either a bulk effect was operating, i.e. movement of sorbed sample through the deposit or to the expulsion of adsorbed water from the deposit by the more strongly adsorbed sample gas.
- v) The responses obtained from the crystals coated with the aid of latex, in general, did not vary throughout the experimental life of the crystal.
- vi) The peak shapes obtained from the latex crystals did not vary as did the more loosely bound deposits. As the same sample of manganese dioxide was used to prepare both deposit types and as the latex deposits were very thin in comparison to the loosely bound deposits it would appear that the change in peak shape that has been reported was caused by some bulk effect and not the desorbtion of water or the loss of some other material.



Frequency Change Combinations

Figure 36

- vii) If the responses of the latex/manganese dioxide coated crystals are compared it will be observed that crystals 1 and 2 are more sensitive than any of the other crystals. As the deposit dimensions of crystals 1 and 2 are quite different but yet they were similar with other crystals that gave lower responses, then the particular pattern of frequency response shown by crystals 1 and 2 i.e. decrease in frequency upon coating but increase in frequency upon sample presentation, may give rise to a more sensitive mass response.
- viii) The frequency response of a manganese dioxide coated crystal to sulphur dioxide was less than its response to equal volumes of nitrogen dioxide even though the actual mass of sulphur dioxide introduced into the system was higher.
- ix) No enhancement or suppression effects were observed when alternate samples of nitrogen dioxide and sulphur dioxide were determined.

Further discussion as to the suitability of manganese dioxide as a coating material for atmospheric nitrogen dioxide will be set out in the conclusion of this thesis.

4.6. Lead Dioxide

Several crystals were coated with lead dioxide using the latex technique. Both single and double sided deposits were prepared. It was observed, as with the manganese dioxide coatings, prepared by the same technique, that the incidence of a high frequency occurring upon coating was low. Details of the deposits prepared are shown in table 18.

Crystal number	Frequency change due to latex (Hz)	Frequency change due to coating (Hz)	Mass of latex (μg)	Mass of coating (μg)	Diameter of coating (mm)
7	-3,941	-21,275	4.6	46.3	2.40
9 1	-3,206	-13,703	2.3	44.3	2.41
2	-4,438	-13,861	3.7	39.4	2.38
11 1	-4,197	-17,080	2.5	32.8	2.76
2	-4,480	-11,767	4.8	31.1	2.38
14 1	-2,900	-9,703	4.0	42.5	2.40
2	-2,093	-9,486	4.8	40.9	2.68
15 1	-4,855	-12,208	5.0	30.8	1.42
2	-8,363	+60,717	10.7	35.4	1.77

Table 18

The responses of crystals 7 and 9 to sulphur dioxide were checked in a static environment, numbers 11, 14 and 15 were checked in a flowing system in the usual manner.

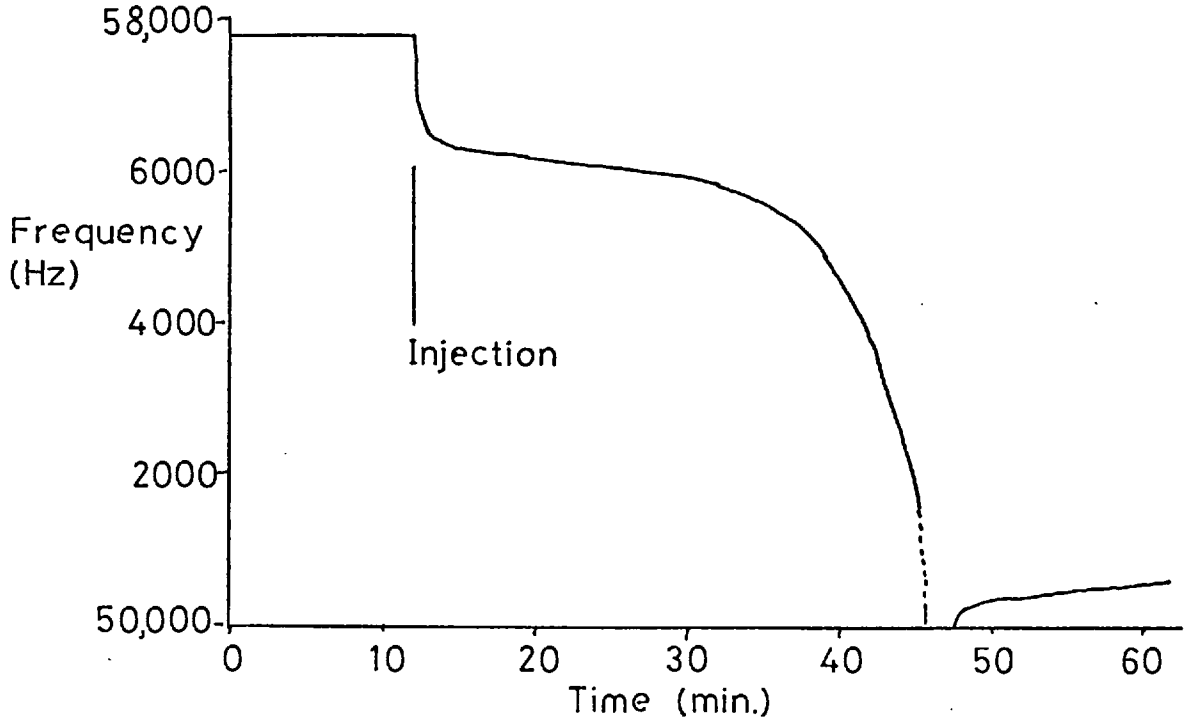
4.6.1. Static Assessment, Critical Leading Percentage

Crystal number 7, a single deposit, was placed in the glass cell, the cell was flushed with nitrogen and the crystal allowed to reach an equilibrium frequency. An aliquot of sulphur dioxide (100 μ l) was injected carefully into the cell, not directly onto the crystal surface, and the frequency of the crystal was monitored. A single sided measurement system was used. The resultant frequency change that was obtained is shown in figure 37. In this graph the stable frequency prior to injection is shown between times $t = 0$ and $t = 12$ minutes. At $t = 12$ minutes the sample of sulphur dioxide was injected. The frequency of the crystal decreased as shown i.e. 1,600 Hz in the first 10 minutes of exposure. At time $t = 25$ minutes the frequency of the crystal began to rapidly decrease. No further sample had been introduced. At $t = 45$ minutes the frequency of the crystal fell very rapidly and oscillations stopped.

The cell was flushed with nitrogen (3 minutes at 400 ml/min.) and resealed. The oscillations restarted as shown.

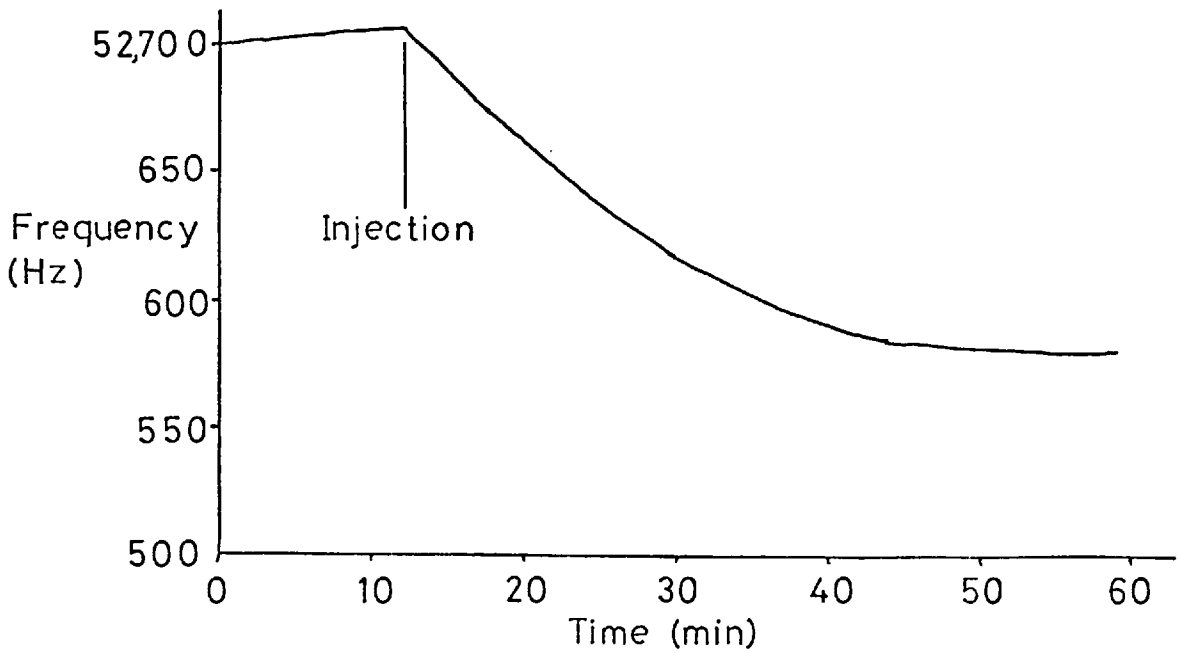
The crystal was again allowed to come to an equilibrium frequency and a further 10 μ l of sulphur dioxide was introduced into the cell. The frequency response due to this injection is shown in figure 38. The frequency of the crystal did not decrease as quickly as the original injection, neither did it suddenly decrease for no apparent reason once a steady frequency had been reached.

Crystal number 9 was also examined in a static environment, the same procedure as just described for crystal 7 was used. The first aliquot of sulphur dioxide (20 μ l) was injected and the frequency res-



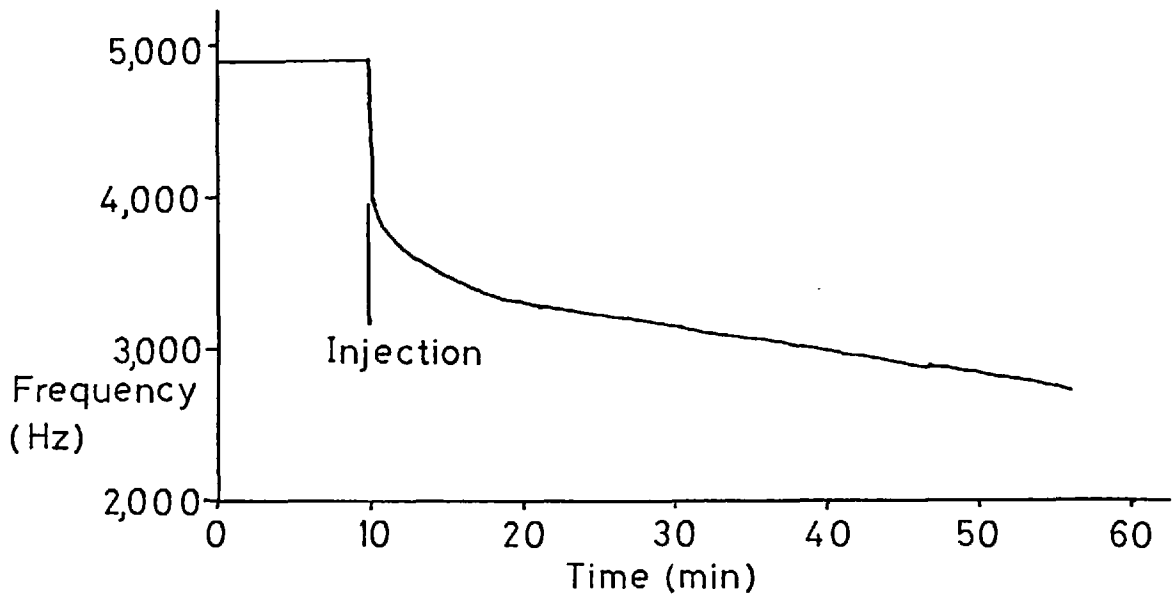
Frequency Change due to 100 µl of SO₂
injected into Static Environment of
Crystal 7

Figure 37



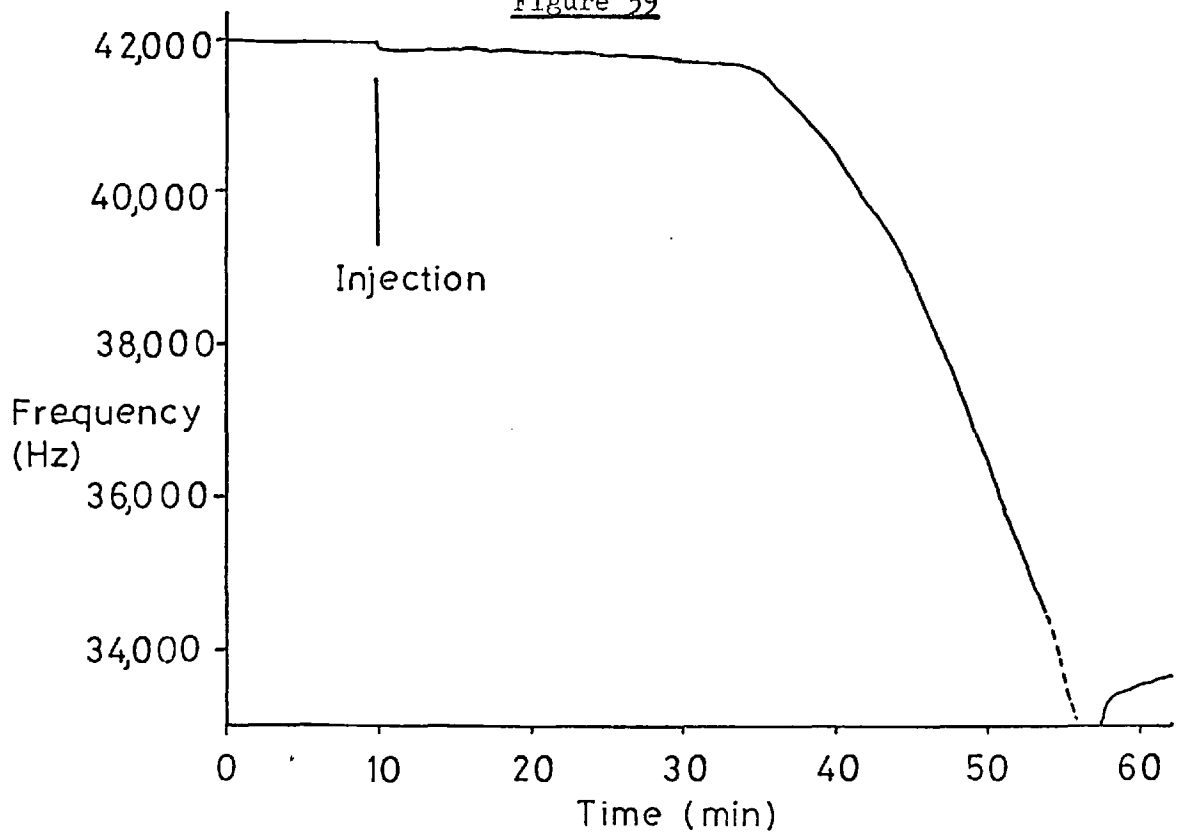
Frequency Change due to 10 µl of SO₂
injected into Static Environment of
Crystal 7

Figure 38



Frequency Change due to first 20 μ l of SO_2
injected into Static Environment of
Crystal 9

Figure 39



Frequency Change due to second 20 μ l of SO_2
injected into Static Environment of
Crystal 9

Figure 40

ponse monitored. The result is shown in figure 39. The frequency was monitored for 4 hours, but no further decrease was obtained as with the first injection onto crystal 7. The cell was flushed with nitrogen and a second 20 μ l injection of sulphur dioxide was made.

A decrease of 195 Hz was observed in the 10 minutes immediately after the injection; 25 minutes after the injection the frequency of the crystal began to decrease rapidly in an identical manner to that described for crystal 7. A plot of the frequency of crystal 9 against time for this second 20 μ l injection of sulphur dioxide is shown in figure 40. The crystal stopped oscillating as the frequency decreased but started again after the cell had been flushed.

This sudden and dramatic fall in the frequency of the crystal was only seen in a static environment. Note also that the time elapsed from the injection point to the "knee" of the sudden decrease is approximately the same for both crystals i.e. 25 minutes. The fact that no rapid decrease of this nature occurred with the first injection onto crystal number 9 suggests that some preconditioning of the surface of the lead dioxide is necessary before the decrease occurs. The decrease could be due to some condensation of sulphur dioxide onto the crystal surface. No specific work was carried out to elucidate the exact nature of this rapid frequency change.

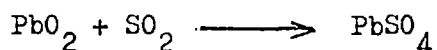
In the literature pertaining to the use of the lead dioxide candle for the sampling of atmospheric sulphur dioxide the term "critical loading percentage" is used (33). This term is used to represent the percentage of lead dioxide with which sulphur dioxide can be reacted while still maintaining the condition of proportionality between sulphation and concentration.

The value of this percentage is determined by monitoring the uptake

of sulphur dioxide from an atmosphere of dilute sulphur dioxide by a standard sample of lead dioxide. Previous techniques used to determine this value have required the immersion of a standard lead dioxide sample into a standard sulphur dioxide atmosphere for a period of time. After the exposure was complete the lead dioxide sample was removed and the sulphate content of the sample determined gravimetrically.

This procedure was repeated, with fresh lead dioxide samples for a series of different exposure times. A variation of the quantity of sulphur dioxide absorbed against time of exposure of sample was then plotted.

If the reaction between lead dioxide and sulphur dioxide is:



and it is assumed that all sulphur dioxide absorbed onto the lead dioxide has reacted with it then the information relating to the mass of sulphur dioxide absorbed can be translated into a percentage of lead dioxide that has reacted with the gas.

Previous workers have established that the absorption of sulphur dioxide onto lead dioxide proceeds at two quite distinct rates, the first being a quite rapid absorption, changing to a slower rate. The percentage of lead dioxide which has reacted with the sulphur dioxide at the point where the rate of absorption changes is the critical percentage.

From the initial experiments carried out with crystals 7 and 9 it is possible to translate the frequency decrease, obtained by the introduction of sample to fresh lead dioxide, into a mass of sulphur dioxide absorbed and therefore a plot of the percentage of lead dioxide that has reacted at any given time during the absorption process. By

using the quartz crystal microbalance with lead dioxide coated on the surface of the crystal it is a simple matter to establish the critical percentage as only one coating of lead dioxide and one sample introduction is required; the quantity of sulphur dioxide absorbed being continuously monitored.

By using the coating data for crystals 7 and 9 an experimental value of the constant in the Sauerbrey was calculated. The experimental value of this constant was then used to calculate the mass of sulphur dioxide absorbed and therefore the percentage of lead dioxide reacted, from the frequency change.

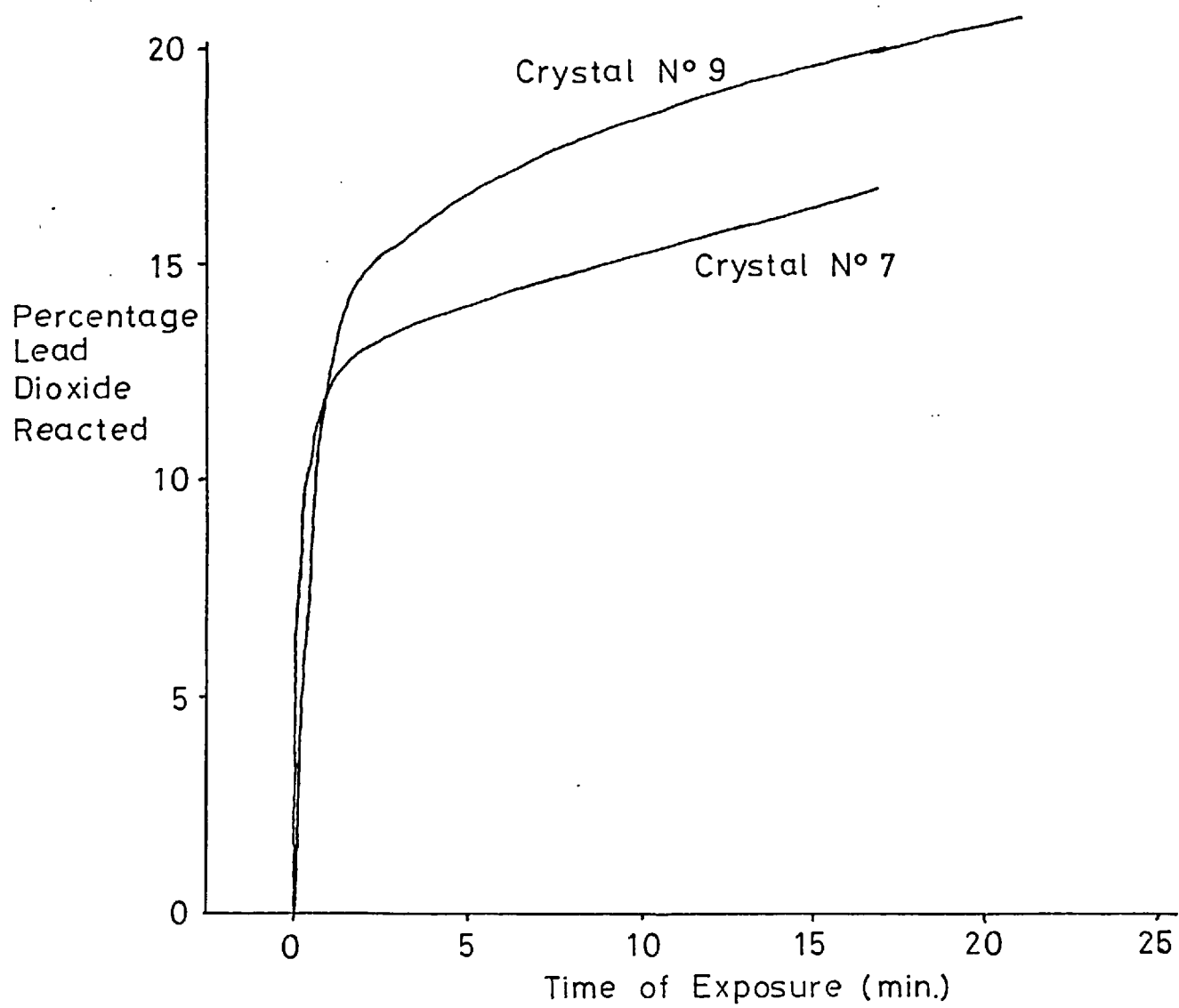
The results of these calculations are shown in figure 41. From these graphs it will be seen that the critical percentage was, for crystal number 7 approximately 12-13% and for crystal number 9 approximately 15%. These values are in good agreement with previous reported values, those being 15% (32) and different values between 4% and 16% (33). The different results reported in reference 33 were due to the different particle sizes of the sample of lead dioxide.

From this work it was expected that the performance of a lead dioxide coated crystal acting in an integrating mode would be severely restricted if the absorption of sulphur dioxide was a linear function of concentration until only 15% of the lead dioxide on the crystal had reacted with the sample gas.

4.6.2. Dynamic Studies

Crystal numbers 11, 14 and 15 were used to check the performance of lead dioxide as a detector of sulphur dioxide in a flowing system.

The flowing system was as usual, a nitrogen flow rate of 12 ml/min. through the reference and sample cells. A clean reference crystal and the ratio mode of measurement was used. Frequency recordings were



Determination of Critical Percentage

Figure 41

made as a function of time after the sample injection so that the peak height and shape, as a result of the sample/coating interaction, could be studied. Small replicate injections of sulphur dioxide ($10 \mu\text{l}$) were made into the gas stream flowing over crystal number 11 so that the expected decrease in response, for a constant sample size, and the change in peak shape, as a result in the change from chemisorption to physisorption could be studied.

The frequency change, or peak height for each successive injection of $10 \mu\text{l}$ is shown in figure 42. The frequency of the crystal decreased when sample was presented to it.

The peak shape representing each of the injections made did change; the peak due to the first injection i.e. a peak height of 309 Hz, was a clean step with no signs of loss of material from the crystal surface after the initial absorption.

This stepwise decrease was maintained until injection number 7, when the crystal began to behave in a reversible fashion with some, though not all, of the absorbed sample being removed by the carrier gas. The amount of material removed after the initial absorption increased between injections 7 and 11 by which time the crystal was operating in a totally reversible manner and giving a constant response to further $10 \mu\text{l}$ injections.

An attempt was made to construct a calibration graph when the crystal was operating in the reversible manner but a 10 fold increase in sample size i.e. $10 \mu\text{l}$ to $100 \mu\text{l}$ only produced a 3 fold increase in response i.e. 13 Hz to 38 Hz; frequency changes of this order were considered, for practical purposes of very little use.

A similar series of experiments were carried out with crystal 14 i.e. the lead dioxide was slowly exhausted and a calibration graph

Crystals
Decrease in Response of Lead Dioxide Coated

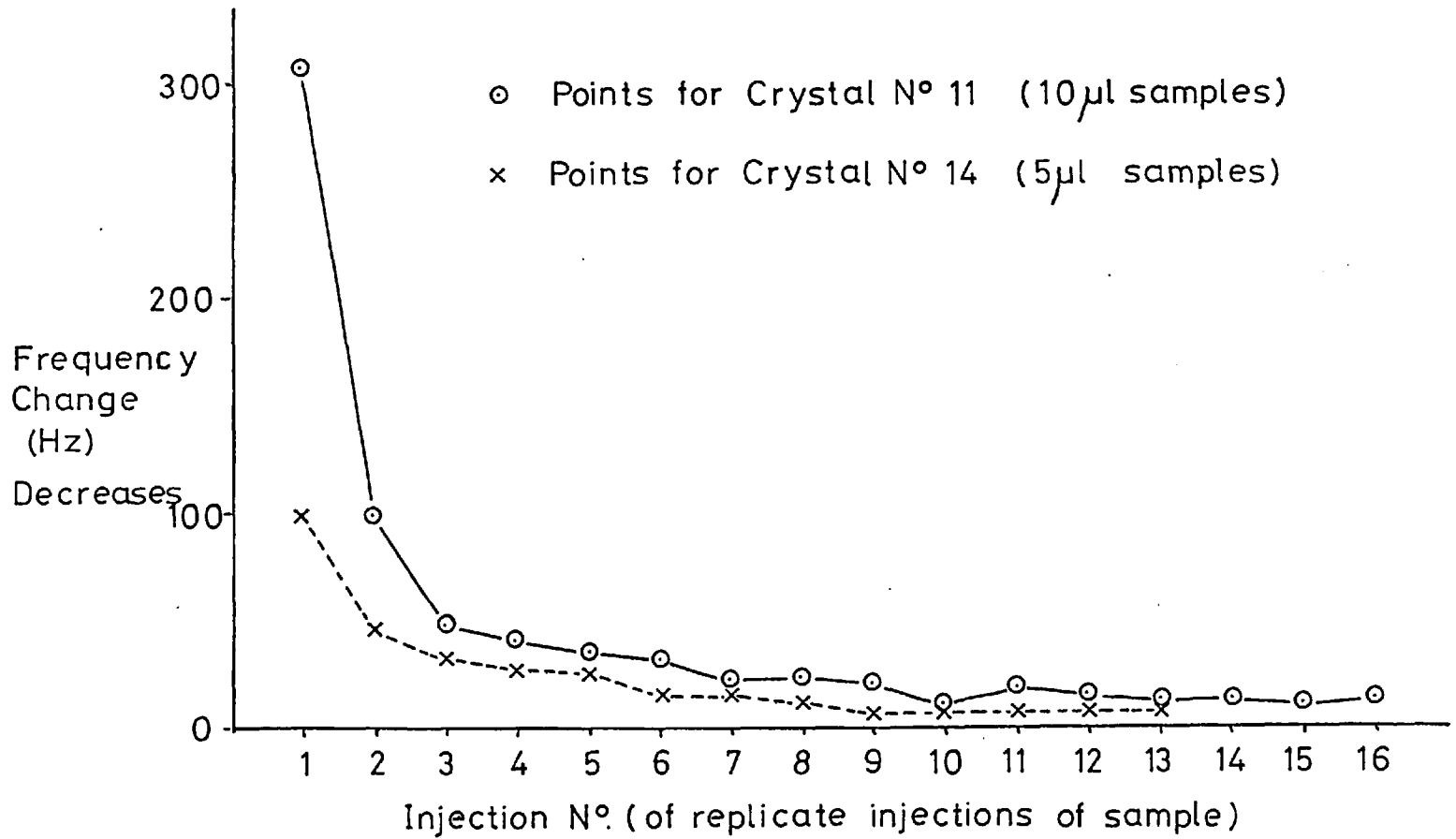


Figure 42

prepared with the crystal behaving reversibly.

With crystal 14 smaller aliquots of sample (5 μ l) were injected in an attempt to "level out" the response obtained with crystal 11.

The results of the replicate injection series is shown in figure 42. It will be noticed that no leveling out was obtained and the rate at which the response decreased was similar for both crystals 11 and 14.

The peak shapes obtained from crystal 14 were of the same pattern obtained for crystal 11, injections 1 to 4 showed a totally integrating mode of action, injections 5 to 10 changed the peak shape gradually to a completely reversible nature and subsequent injections being of constant peak height and totally reversible.

As with crystal 11 attempts to produce a calibration graph with the crystal operating reversibly were not successful.

The irreversible frequency drop of crystals 11 and 14 represents the total quantity of sulphur dioxide permanently absorbed onto the coating. This frequency drop is the difference between the crystal frequency prior to sample introduction and when the lead dioxide on the crystal had been saturated and the crystal was behaving totally reversibly.

The mass of sulphur dioxide irreversibly absorbed onto each crystal was calculated and the percentage of available lead dioxide that had reacted with the sulphur dioxide was also calculated.

For crystal number 11, 1.18 μ g of sulphur dioxide was irreversibly absorbed over the first 11 injections; this mass of sulphur dioxide corresponds to 6.4% of the available lead dioxide reacted.

For crystal number 14, 0.96 μ g of sulphur dioxide were irreversibly absorbed over the first 9 injections; this mass corresponds to 3.9% of the available lead dioxide reacted.

Note that these percentages of reacted lead dioxide are considerably lower than the critical percentages obtained for crystals 7 and 9 but also the values for crystals 7 and 9 were obtained in a static environment not a flowing gas stream.

Crystal number 15 was a crystal which, upon coating, had increased its resonant frequency. The response of this crystal was checked in a similar manner to number 14 however, no decay in response of the type shown in figure 42 was observed for this crystal. Upon injection of 5 μl of sulphur dioxide the frequency of the crystal decreased by only 9 Hz. The decrease was irreversible and repeatable. This response was constant in size and peak shape until the seventh injection of sample, the sample/coating interaction then began to show a reversible nature. The change in peak shapes obtained with this crystal was very similar to those obtained with crystals 11 and 14; i.e. a period of integrating action, a final reversible mode with a transitional stage between the two extremes.

A calibration graph was prepared; this was linear with a sensitivity of 21 Hz/20 μl of injected sample. The graph passed through the origin. This result contrasts sharply with the responses seen for crystals 11 and 14. All three coatings were prepared from the same sample of lead dioxide and kept in a sulphur dioxide free atmosphere.

The most obvious difference was that crystal 15 had increased its frequency upon coating, although its frequency decreased when sample was presented to it. This will be discussed further in the next chapter.

The responses of crystals 11, 14 and 15 were checked, after the experiments with sulphur dioxide, for their responses towards nitrogen dioxide.

Aliquots of nitrogen dioxide (5-100 μl) were injected into the

flowing gas stream.

Linear calibration graphs were produced for all three crystals, the sensitivity being identical in each case at a change of 71 Hz/20 μ l of injected nitrogen dioxide. The graph passed through the origin.

The peak shape representing the nitrogen dioxide/lead dioxide interaction was very similar to the nitrogen dioxide/manganese dioxide system shown in figure 35 i.e. the maximum frequency change was quickly reached but desorption of the sample was slow. A typical recovery for a lead dioxide coating, after the injection of a 50 μ l sample of nitrogen dioxide is 75% recovery in 7 minutes.

The suitability of lead dioxide as a coating material for the analysis of atmospheric sulphur dioxide will be discussed in the conclusion of this work.

5. Investigation of High Frequency Effect

5.1. Introduction

In the preceding two chapters the occurrence of the high frequency effect has been detailed with all of the possible frequency change combinations being observed. This was shown schematically in figure 36. It was suggested in chapter 3 that the occurrence of a high frequency oscillation could be due to a loose particle effect, but with collodion and latex to secure the deposits the effect persisted. The geometry of the deposit was also suspect on the first crystals coated with manganese dioxide using the particle fractionater. These deposits, although regular in appearance, stood proud of the crystal surface (see chapter 4 for details).

The use of latex to bind the active solid to the crystal gave deposits which were very thin and smooth in comparison to the deposits prepared using the particle fractionater but the high frequency effect persisted.

The probability of this effect being due to some manufacturing process is low, as crystals made in Great Britain and America gave the same effect; similarly the condition of the crystal appears to have no significance. If the deposit details shown in table 8 are examined it will be observed that those crystals oscillating high e.g. crystals number 8 do not have an exceptionally heavy or light deposit upon them, thus the rather ill defined overload region suggested in chapter 3 is not a simple function of the mass of the deposit.

It was decided to investigate the possibility that the mass per unit area of the deposit was the important parameter which controlled the high frequency effect.

5.2. Experimental Investigation

5.2.1. Collodion Deposits

In this investigation the crystals used were coated with collodion only. No attempts were made to bind any active solid onto the collodion deposit.

Collodion was chosen as the deposit material because of the highly reproducible nature with which the deposits could be formed. The deposits were tightly bound to the crystal surface, they were flat, not standing proud from the crystal surface (as discernible by the naked eye) and when viewed obliquely under a strong light very few irregularities in the surface could be seen.

No active solid material was fixed to the collodion as this process was not as reproducible as the formation of the collodion deposit. If the mass per unit area measurement alone was the controlling parameter of the high frequency effect, then it could be readily investigated with collodion deposits.

Two collodion in acetone solutions were prepared; the concentrations were 40 $\mu\text{g}/\mu\text{l}$ and 24 $\mu\text{g}/\mu\text{l}$. Using 1 or 2 μl aliquots of these solutions deposits of various areas and masses were prepared. The details of these deposits are shown in table 19. Deposit numbers 21 to 24 inclusive were prepared by the addition of more collodion to deposit numbers 6, 8, 9 and 12 respectively. The frequencies of crystals 6, 8, 9 and 12 had decreased upon coating. When more collodion was added to deposits 6 and 12 the frequency change due to the new deposits, 21 and 24, were substantial increases in frequency. Deposit numbers 22 and 23 would not oscillate. It is probable that the relatively large original deposits were badly disturbed by the second coating process thus not permitting oscillations to occur. The inter-relationship between the frequency change and the mass per unit area of the deposit is shown in

Deposit number	Area of deposit (mm ²)	Mass of deposit (µg)	µg/mm ²	frequency change (Hz)
1	4.01	70.8	17.7	+28,119
2	10.64	176.0	16.54	+51,238
3	12.82	174.0	13.57	+66,594
4	16.05	82.7	5.15	-62,500
5	1.13	45.0	39.8	+23,926
6	7.84	49.3	6.29	-68,790
7	2.60	41.4	15.92	+24,004
8	10.64	40.8	3.83	-51,880
9	11.70	52.7	4.50	-57,380
10	3.33	54.4	16.32	+37,740
11	7.45	50.6	6.79	+68,366
12	9.61	53.4	5.55	-59,729
13	5.89	53.4	9.02	+41,778
14	8.55	50.9	5.95	-61,433
15	4.23	145.2	34.33	+11,850
16	5.47	151.9	27.77	+28,320
17	6.70	147.0	21.94	+27,673
18	10.99	157.2	14.30	+49,045
19	2.11	104.8	49.67	+12,588
20	17.80	104.8	5.89	+27,100
21	7.84	68.7	8.76	+40,788
22	10.64	90.1	8.47	-
23	11.70	177.2	15.20	-
24	9.61	111.4	11.58	+46,019

Table 19

Dependence of Frequency Change upon Loading

Figure 43

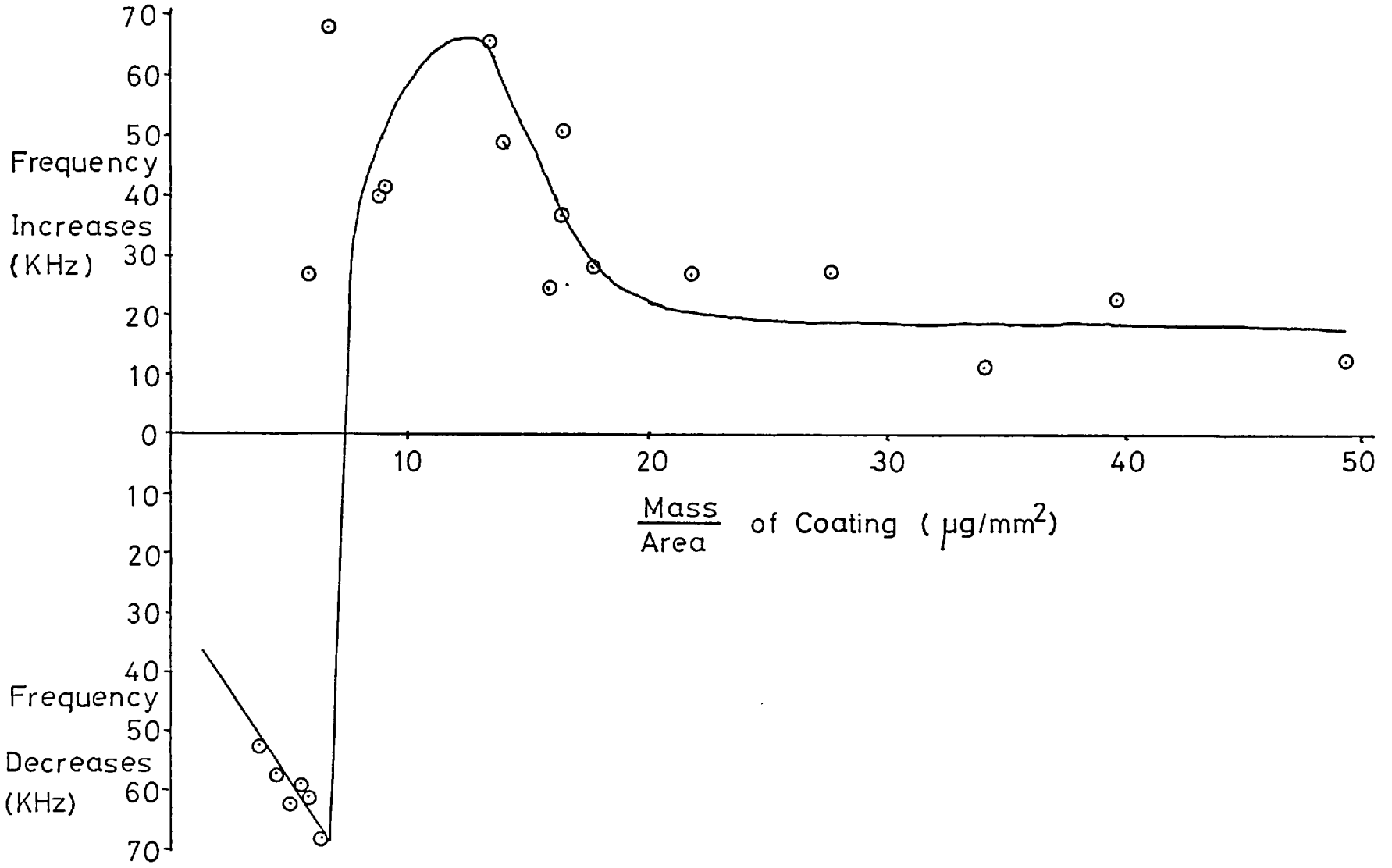


figure 43. It will be observed that those crystals which decreased in frequency upon coating are in general agreement with Sauerbrey's equation i.e. a straight line relationship. When the crystal frequency increased with coating then no simple relationship between the frequency change and the loading was operating. This is clearly indicated by figure 43.

In figure 43 it is also obvious that the critical value for the loading on the crystal is approximately $7 \mu\text{g}/\text{mm}^2$; below this value the crystal frequency decreased and above this value the frequency increased upon loading.

5.2.2. Apiezon Deposits

As the collodion experiments had demonstrated that the high frequency effect is not caused only by deposits of particulate material, Apiezon M grease was used in an attempt to achieve the same effect i.e. a crystal increasing its vibrational frequency after the application of a coating. This material has been used by previous workers (69, 82) but no anomalous behaviour was reported. Apiezon grease also offered the possibility of varying the coating density i.e. $\mu\text{g}/\text{mm}^2$ of a deposit on a crystal without removing the deposit and recoating as was necessary with the collodion deposits. This was possible as a deposit of apiezon can be spread over a greater area simply by heating the material in an oven. Similarly more material can be added to an existing coating and a smooth deposit obtained, unlike the deposition of collodion where a further deposit disturbs the initial deposit to too great an extent thereby stopping the crystal vibrating.

In the experiments with apiezon two approaches were used to obtain crystals that would increase their vibrational frequency after coating. The two methods assume that the important condition for an increase in

vibrational frequency is a high mass per unit area value for the coating as was experienced with the collodion deposits. This condition may be achieved by starting the experiment with a deposit of small area and high mass, (under which circumstances the crystal will probably not oscillate) and then heat spreading the deposit until oscillations occur. Alternatively a coating of modest dimensions may be prepared with a resultant decrease in the crystal frequency. The mass of this deposit can be increased by adding further apiezon, but the area of the deposit maintained constant thus increasing the mass per unit area value of the coating.

In order to test these methods of producing a crystal with increased vibrational frequency two solutions of apiezon in chloroform were prepared; the concentrations were 40 $\mu\text{g}/\mu\text{l}$ and 4 $\mu\text{g}/\mu\text{l}$; volumes of solution used to prepare the deposits ranged from 0.5 μl to 3 μl .

The deposit prepared on crystal number 1 was a small area/moderately high mass deposit prepared by placing 3 μl of 4 $\mu\text{g}/\mu\text{l}$ apiezon solution slowly on the crystal surface. After the deposit had been prepared and the relevant details recorded (mass of deposit, diameter and frequency change) the crystal was placed in an oven at 94° for ten minutes. The crystal was removed and allowed to cool for 30 minutes when the larger deposit diameter and new frequency change were recorded. The results are shown below in table 20.

Crystal and deposit number	Area of deposit (mm^2)	Mass of deposit (μg)	$\mu\text{g}/\text{mm}^2$	Frequency change (Hz)
1 (a)	4.22	11.4	2.22	+59,316
heat (a) at 94° for 10 min. to give (b)				
(b)	16.06	11.4	0.71	-10,601

Table 20

Crystal and deposit number	Area of deposit (mm ²)	Mass of deposit (μg)	μg/mm ²	Frequency change (Hz)	Time* heated (min.)
2 (a)	2.84	21.9	7.73	-	2
(b)	3.94	21.9	5.56	-	3
(c)	6.61	21.9	3.32	-	3
(d)	8.97	21.9	2.44	-	5
(e)	10.41	21.9	2.11	-	7
(f)	15.62	21.9	1.40	-	10
(g)	20.11	21.9	1.09	-	10
(h)	23.41	21.9	0.94	+46,885	-

Note:

*The time indicated in the last column is the length of time that coating was heated at 91° to prepare the next coating.

i.e. coating (a) was heated for 2 min. at 91° to prepare coating (b) etc.

Table 21

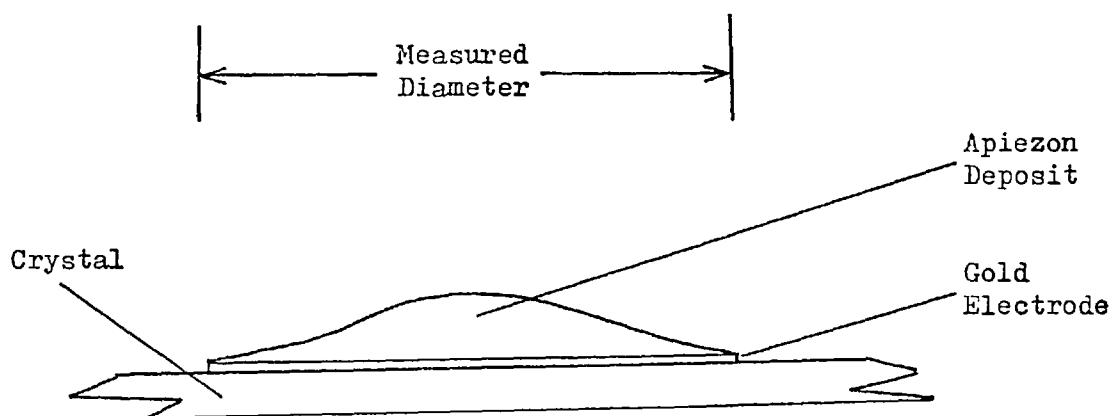
The deposit prepared on crystal number 2 was also of a small area but higher mass; 0.5 μl of 40 $\mu\text{g}/\mu\text{l}$ of apiezon solution were used to form the first deposit. This deposit required extensive heating before oscillations occurred. The details of the deposits and the heating required to produce them are shown in table 21. The crystal was allowed to cool for 30 minutes before the details of the new deposit were recorded. The mass of the deposit was established at the beginning of the experiment and checked at the end. There was no detectable difference in the deposit mass after heating.

The deposit formed on crystal number 3 was of moderate dimensions; 1 μl of 4 $\mu\text{g}/\mu\text{l}$ apiezon solution was used to form the initial deposit. Further quantities of apiezon were added to this deposit until the crystal ceased to vibrate. The crystal was then heated in an identical manner to crystal number 2 until oscillations occurred. The details of this deposit are shown in table 22.

Crystal and deposit number	Area of deposit (mm^2)	Mass of deposit (μg)	$\mu\text{g}/\text{mm}^2$	Frequency change (Hz)	Time heated at 91° (min)
3 (a)	3.73	5.9	1.58	- 7,589	-
(b)	3.73	9.3	2.64	-10,122	-
(c)	3.73	12.6	3.57	-	2
(d)	9.95	12.6	1.27	-	4
(e)	12.69	12.6	0.99	-11,272	-

Table 22

If the frequency changes and the corresponding mass per unit area values are studied for the apiezon deposits it will be observed that there is no apparent relationship existing between these quantities as has been shown to exist for the collodion deposits; even deposits which decreased the resonant frequency of the crystal do not appear to obey Sauerbrey's equation. The reason for this non-obeyance of the Sauerbrey equation is the fact that the deposits, although regular and smooth, are not flat. When the coatings prepared on crystals 1, 2 and 3 were examined by viewing them obliquely under a strong light a distinct mound was observed in the centre of the deposit. This is shown schematically below:-



Cross section through an apiezon deposit

This deposit shape was as a result of heating the deposit in order to spread the apiezon. As the deposits which did give a decrease in the frequency of the crystals were of different dimensions, then because of the concentration of mass in the centre of the deposits, the radial mass distributions were also different. According to the Sauerbrey equation the change in frequency, Δf , upon coating is directly proportional to $\frac{\Delta m}{A}$. It is a precondition that the mass which causes this frequency

change lies in a uniform flat film. As this is clearly not the case with the apiezon deposits then the values given for the coating densities in tables 20, 21 and 22 are only average values and cannot be used in the Sauerbrey equation. As this average value was, for the apiezon deposits, misleading the radial mass per unit area distribution was determined for crystals 2(h) and 3(e). These crystals were chosen as there was an obvious conflict contained in the information of tables 21 and 22 and the hypothesis that the mass per unit area of a deposit was the parameter controlling the incidence of a crystal increasing its vibrational frequency.

Specifically crystal 2(h) had an apparent coating density of $0.94 \mu\text{g}/\text{mm}^2$ with an increase in the vibrational frequency of 46,885 Hz but crystal 3(e) which had a coating density of $0.99 \mu\text{g}/\text{mm}^2$ had decreased its vibrational frequency by 11,272 Hz; also crystals 3(a) and (b) had higher coating densities than 2(h) i.e. 1.58 and $2.64 \mu\text{g}/\text{mm}^2$ respectively, but had decreased the frequency of the crystals after coating. The method used to determine the mass per unit area as a function of the deposit radius for these deposits was as follows.

The weight of the crystal plus deposit and also the diameter of the deposit was noted. The diameter of the deposit was reduced, stepwise, by carefully removing the edge of the deposit with a fine brush dipped in chloroform. The ring of deposit thus removed was concentric with the centre of the deposit. All traces of the apiezon contained in the ring were removed from the crystal by brushing with chloroform.

The reduced diameter of the deposit was recorded and also the weight of the crystal and now lighter deposit was noted.

This stepwise removal of the deposits was continued, recording each new weight and smaller diameter, until the deposits had been completely removed. The diameter of the deposit was reduced by

approximately 0.5 mm at each removal stage.

The results of this determination for crystals 2 and 3 are shown in tables 23 and 24 respectively. The mass per unit area of each section of the deposit removed was calculated; this calculated value was plotted as a function of the radius of the deposit to construct the profiles shown in figure 44.

It will be observed that in the area contained by a circle approximately 1 mm radius the mass per unit area profile for crystal number 2 is significantly different from crystal number 3. The percentage of the total deposit contained within the 1 mm. radius circle for both crystals is very similar with 55% of the deposit mass of crystal 2 contained in this area and 56% of the deposit of crystal number 3 contained in the same area. The actual masses, and therefore the average mass per unit area, are however quite different. The values over this central area of the crystals were; crystal 2, mass 13.7 μg , mass per unit area 4.33 $\mu\text{g}/\text{mm}^2$; crystal 3, mass 5.80 μg , mass per unit area 1.53 $\mu\text{g}/\text{mm}^2$.

As the central area of the crystal is the most active portion it would appear that the exact manner in which mass was distributed over this area was a prime cause of the high frequency effect. This explanation does not, however, take into account the part played by the edges of a deposit. If table 21 is examined it will be seen that the increase in area between deposit 2 (g) and 2 (h) is very small i.e. 3.30 mm^2 or an increase in the diameter of the deposit of 0.40 mm. This difference in the diameter of the deposit was sufficient to allow the crystal to vibrate in a high state. It is very likely that the 10 minute heating period between deposits 2 (g) and 2 (h) also changed the mass distribution at the centre of the deposit, which could also have induced the high oscillation state. When the first portion of the

Mass removed (μg)	r_1 (mm)	a_1 (mm^2)	r_2 (mm)	a_2 (mm^2)	$(a_1 - a_2)$ (mm^2)	$\frac{M}{a_1 - a_2}$ ($\mu\text{g}/\text{mm}^2$)
1.2	2.72	23.24	2.07	13.46	9.78	0.12
6.6	2.07	13.46	1.61	8.14	5.32	1.24
2.0	1.61	8.14	1.26	4.99	3.16	0.63
1.5	1.26	4.99	0.97	2.96	2.03	0.74
5.4	0.97	2.96	0.75	1.77	1.19	3.06
4.6	0.75	1.77	0.69	1.50	0.27	3.08
1.0	0.69	1.50	0.54	0.92	0.58	1.09
2.7	0.54	0.92	-	-	0.92	2.95

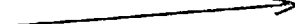
r_1 = radius of outer circle

a_1 = area of outer circle

r_2 = radius of inner circle

a_2 = area of inner circle

$(a_1 - a_2)$ = area of deposit removed

Deposit: 
(Shaded area represents
deposit removed)

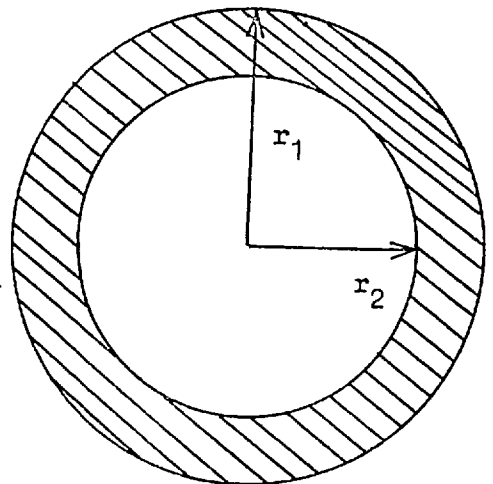
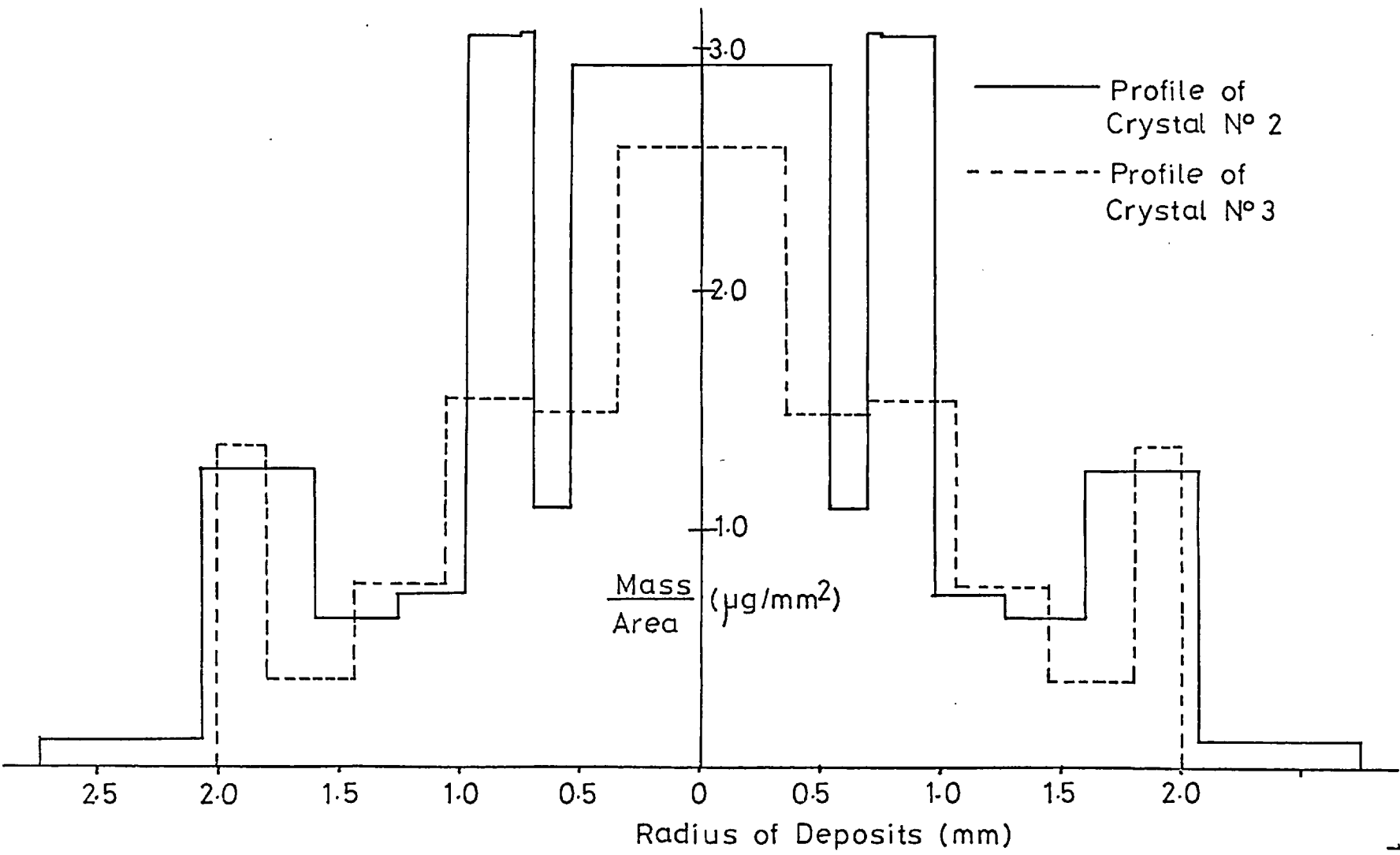


Table 23

Mass removed (μg)	r_1 (mm)	a_1 (mm^2)	r_2 (mm)	a_2 (mm^2)	$(a_1 - a_2)$ (mm^2)	$\frac{M}{(a_1 - a_2)^2}$ ($\mu\text{g}/\text{mm}^2$)
3.1	2.00	12.57	1.81	10.29	2.27	1.36
1.4	1.81	10.29	1.44	6.51	3.78	0.37
2.3	1.44	6.51	1.06	3.53	2.96	0.78
3.2	1.06	3.53	0.68	1.45	2.08	1.54
1.6	0.68	1.45	0.35	0.39	1.07	1.50
1.0	0.35	0.39	-	-	0.39	2.60

r_1 , a_1 , r_2 and a_2 have an identical significance as in table 23

Table 24



Deposit Profiles of Apiezon Deposits on Crystals 2 and 3

Figure 44

deposit was removed, in the establishment of the deposit profile, the crystal stopped vibrating. The centre of the deposit had not been disturbed.

This fact demonstrates that the mass distribution in the centre of the crystal is not the sole cause of crystals vibrating in a high state and that the edge of the deposit, which in this case constituted only 4.8% of the deposit mass, play an important role.

5.3. Anomalous Responses of Stationary Phase Coated Crystals

A very brief examination of the responses of crystals 2 and 3 was made before the deposit profiles of these crystals was established.

The experimental procedure used was identical for both crystals. The crystals were placed in the stainless steel cell with a nitrogen flow rate of 5 ml/minute. Samples of chloroform vapour in air (40 μ l of 15% v/v) were injected into the gas stream over a period of four seconds. Crystal number 3 which had decreased its frequency upon coating, responded in a normal manner i.e. the frequency decreased further when the sample partitioned into the coating. The magnitude of the change was 23 Hz.

Crystal number 2, which had increased its frequency upon coating, also decreased its frequency when exposed to sample. The frequency change was of the same order as crystal 2 i.e. a decrease of 20 Hz.

Other experiments reported to the author (112) demonstrated that a crystal coated with a stationary phase, and behaving in a normal manner, could be induced to increase its frequency when exposed to large quantities of sample. This effect was demonstrated using a crystal coated with squalane in both a static and a dynamic environment.

A squalane coated crystal was placed in the glass cell (figure 19) and allowed to reach an equilibrium frequency. The atmosphere in the

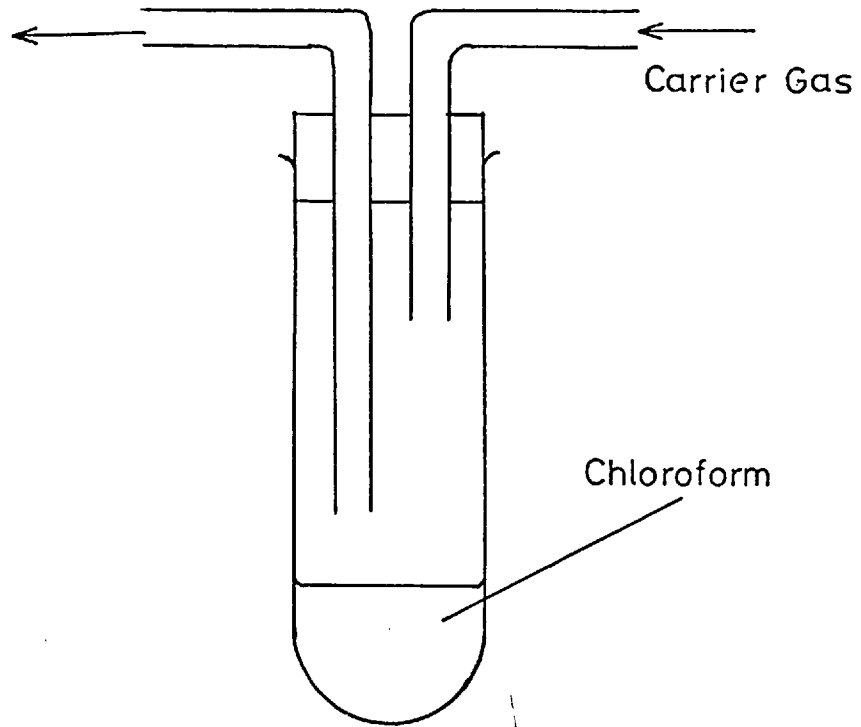
cell was dry nitrogen. A quantity of liquid benzene was introduced into the cell so that there was an excess of liquid benzene present when the cell atmosphere was saturated with benzene vapour. When the benzene was introduced into the cell the frequency of the crystal began to decrease. The rate of decrease was quite rapid. After a short period of time, approximately one minute, the rate of decrease decreased shortly after which the crystal frequency began to increase. When the frequency had increased by a few hundred hertz the crystal stopped oscillating. The crystal did not start oscillating again until the cell had been flushed with nitrogen and the concentration of benzene in the cell greatly reduced.

When the crystal did begin oscillating it was observed that the frequency was decreasing as the cell was being flushed out; the magnitude of the decrease was a few hundred hertz. The crystal frequency then began to increase as the flushing of the cell continued.

A similar effect was observed with a flowing system, the sample being chloroform vapour. The crystal was coated with squalane. The sample vapour was obtained from a device shown in figure 45. The nitrogen flow rate used was 12 ml/minute. A bypass arrangement was used so that either nitrogen or nitrogen plus chloroform vapour could be passed through the sample cell.

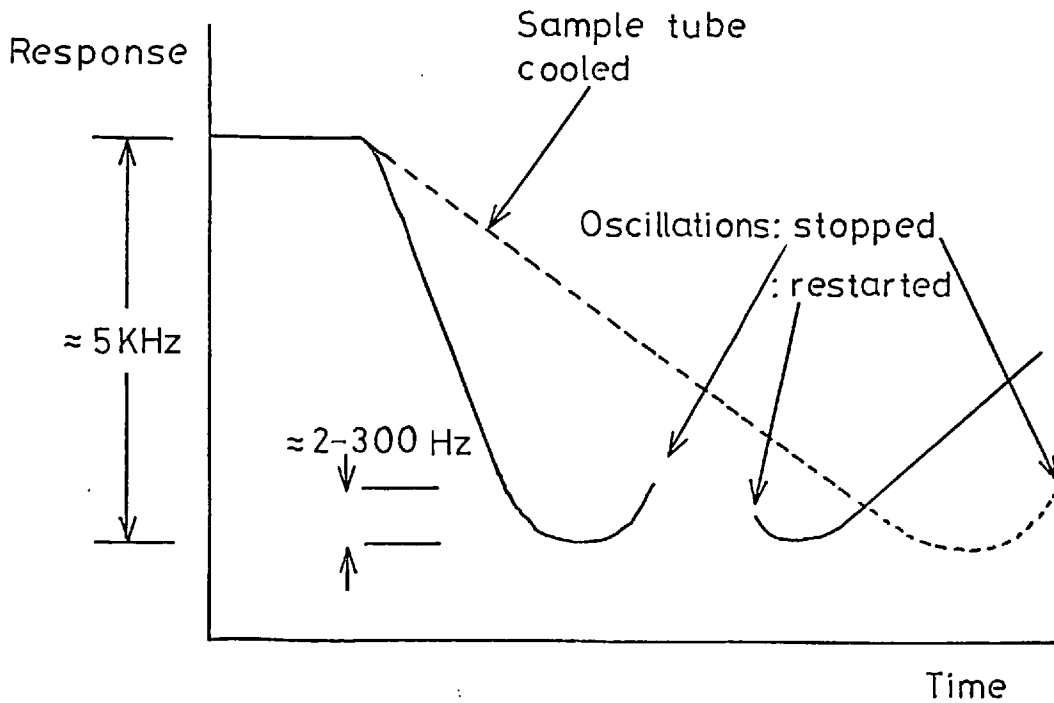
Whilst passing nitrogen only through the cell a stable baseline frequency of the coated crystal was obtained.

The chloroform sampling device was then switched into the carrier gas line. The change in frequency of this crystal as a function of time is shown schematically in figure 46. It will be observed that as the sample dissolves in the coating the frequency of the crystal decreases until some specific point or parameter is exceeded when the



Chloroform Vapour Sampling Device

Figure 45



Response of Squalane Coated Crystal to Chloroform Vapour

Figure 46

crystal frequency then increases. The sample chloroform was still being presented to the crystal when the frequency started to increase. Soon after the frequency began to increase oscillations stopped. When the crystal had stopped oscillating the supply of sample was terminated and nitrogen carrier gas was passed through the cell thus reducing the concentration of chloroform vapour in the environment of the crystal. When the crystal began to oscillate the frequency was decreasing as described for the squalane/benzene system. As the flushing of the cell was continued the frequency of the crystal began to increase. This is shown in figure 46.

A similar experiment was carried out but with the chloroform sampling tube immersed in an ice bath. This reduced the concentration of chloroform vapour in the nitrogen carrier gas.

The frequency changes that occurred in this experiment are shown by the dotted line in figure 46. The shape of this curve is similar to that obtained in the previous experiment except that the time required to reach the critical point, where the frequency increases, is longer; this is because of the reduced chloroform concentration.

Unfortunately no quantitative data is available for these experiments, only a qualitative description can be given.

The magnitude of the frequency changes and the time scale of the changes shown in figure 46 are intended only as a guide and do not represent accurate measurements.

Another feature of a crystal oscillating in a high state was ascertained.

A single collodion deposit was prepared on a crystal so that the crystal would oscillate high. A frequency increase of 41.9KHz was obtained with the deposit placed centrally on the electrode.

On the remaining clean electrode of this crystal a light deposit

of apiezon ($4 \mu\text{g}$) was made, the frequency change accompanying this deposition was a decrease in frequency of 2.5 KHz. The crystal frequency with the two deposits was $(41.9 - 2.5)$ KHz higher than its clean frequency i.e. 39.4 KHz.

A further smaller deposition of apiezon ($1.6 \mu\text{g}$) on the crystal was made. This deposit was placed on the same electrode as the colloidion deposit, as close as possible to the deposit without disturbing it. The apiezon deposit was off-centre but still completely contained upon the electrode surface. The frequency change due to this deposit was $- 0.8$ KHz, the crystal frequency was then $(39.4 - 0.8)$ KHz or 38.6 KHz higher than the clean frequency of the crystal.

This fact demonstrates that even when a crystal is oscillating in a high state it is still capable of decreasing its frequency when mass is placed in a smooth film on its surface.

5.4. Discussion of High Frequency Effect

In the preceding pages it has been shown that not only deposits of solid material can give rise to a high oscillating crystal but also materials which had previously behaved in a "normal" manner can cause a similar effect.

Similarly the responses obtained from crystals coated with g.c. stationary phases, when exposed to sample gas, fit the same pattern as those coated with a solid i.e. three of the four possible combinations of frequency changes, as shown in figure 36 chapter 4, have been observed. There are, however, significant differences in the behaviour of these two types of coating materials.

- i) In order to make the frequency of a squalane coated crystal increase when exposed to sample very high concentrations of sample were required. This was not so with crystals coated

with manganese dioxide, where only small (by comparison) quantities of sulphur dioxide were sufficient to increase the frequency of the crystal.

The frequency of manganese dioxide coated crystals increased either directly any sample was presented to the crystal or a change in the sign of the frequency response occurred as larger samples of sulphur dioxide were presented to the crystal, e.g. crystal numbers 4 and 6 of the manganese dioxide/latex series of crystals.

These crystals were similar to the squalane/benzene and squalane chloroform systems, in that the frequency change that occurred was of the same pattern but the quantity of sample necessary to produce these changes were quite different.

ii) The squalane/benzene and squalane/chloroform systems did not increase their frequencies by a large amount before the crystals ceased to oscillate. The manganese dioxide/sulphur dioxide system would however, sustain the high vibrational state of oscillations as demonstrated by crystal 12 of the manganese dioxide/latex series. This crystal increased its frequency after repeated sample introduction such that it was oscillating 49.3 KHz higher than the clean uncoated frequency.

iii) The incidence of the high frequency effect is much greater with solid coatings and sample sorbtion than with g.c. stationary phase type coatings. This statement is based on the author's experience of using carbowax, apiezon and triethanolamine and also the experiences of a fellow

worker (112)

At this point a summary of the information relating to the incidence of the high frequency effect will be given.

- i) The frequency of a clean crystal may increase or decrease upon coating.
- ii) The frequency of a coated crystal may increase or decrease on sample presentation irrespective of the frequency change obtained on coating.
- iii) The high frequency effect occurs when one or both sides of the crystal are coated.
- iv) The high frequency effect is not specifically caused by solid coatings.
- v) The effect may be enhanced when solids are tightly bound to the crystal.
- vi) The incidence of this effect is greater with solid coatings but does not always occur when solids are coated on a crystal.
- vii) There appears to be some connection with the coating density i.e. mass per unit area, and the appearance of a high frequency.
- viii) This effect is not due simply to an unevenness of the deposit or simply the mass of the deposit.
- ix) When a crystal which is oscillating high has mass applied to it in a thin film then the frequency of the crystal will decrease.

The fact that the high frequency effect can occur with coatings of quite different physical and chemical properties suggested that the effect was caused by the process of coating the crystal and not

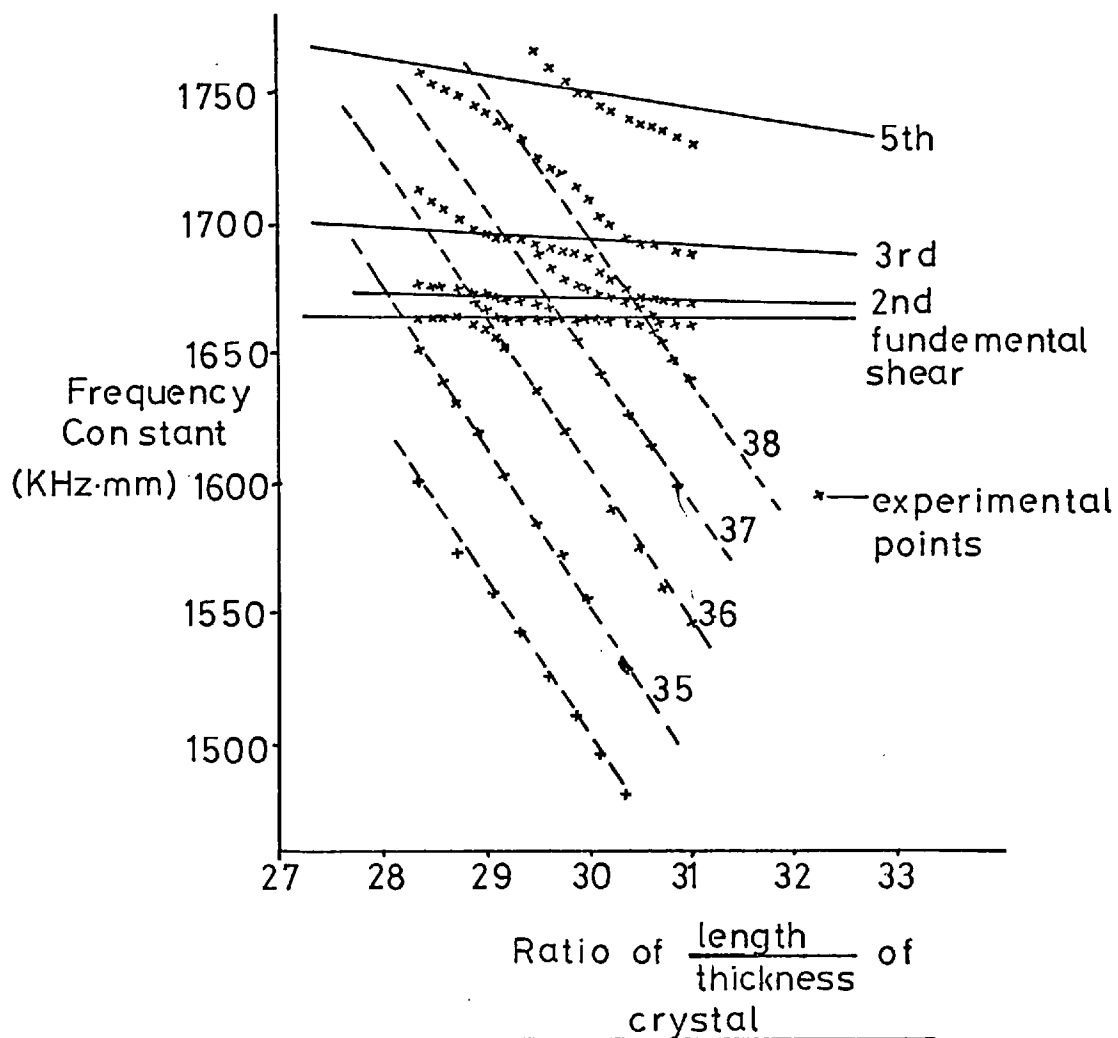
the material with which the crystal was coated, although the nature of the coating material could in some cases actively contribute to the effect.

5.4.1. The Coupling of Vibrational Modes

It is known that the A.T. cut crystal does not vibrate totally in shear mode. This was illustrated in figure 9. In this illustration the maximum and minimum points represent the angle of cut where the elastic constant which relates low frequency shear to the required high frequency shear is zero. This elastic constant does however have a small but significant value at the angle of cut required to produce an A.T. cut crystal. Thus the frequency of a clean uncoated A.T. cut crystal is a combination of high frequency shear and some overtone of a low frequency shear.

A similar situation exists with coupling between high frequency flexural vibrational mode and the high frequency shear mode of an A.T. cut crystal. The high frequency flexural mode of motion occurs in the plane of the length and width of the crystal and naturally has overtone modes. The higher overtone orders coincide with the fundamental shear mode frequency at frequencies dictated by the actual dimensions of the crystal. This is illustrated in figure 47. The solid lines show the variation of the frequency constant with the crystal dimensions for high frequency shear resonances; the values for the 1st, 2nd, 3rd and 5th overtone modes are shown.

The broken lines plot the same variation for the high frequency flexure mode. These variations for the shear and flexural modes are calculated. Experimentally determined resonant frequencies are indicated by crosses. A large degree of coupling between these two modes of motion will be observed where odd shear mode orders and



High Frequency Shear and Flexure Resonances
in an AT Cut Quartz Plate

Figure 47

even flexure mode orders coincide.

In the region of these areas of high coupling it will be observed that a crystal of given dimensions may have two values of frequency constant and hence two vibrational frequencies for the same dimensions. The complex aspects of modes of motion in quartz crystals and coupling that takes place between various modes is dealt with in detail in Heising (113).

This process of coupling was considered as being a possible cause of the high frequency effect; the reasoning that led to this consideration was as follows: if a clean uncoated crystal was vibrating in the vicinity of one of the coupling regions and as the high frequency effect is due to the coating process itself, then the application of a coating to a crystal might induce a greater coupling effect or cause a "jump" from one experimental frequency curve to another in the coupling region.

In order to test this hypothesis it was decided to change the frequency of a crystal, which had previously increased its frequency upon coating, by electroplating nickel onto the gold electrodes. This would have the effect of increasing the thickness of the crystal and thus decrease the frequency; as predicted by the Sauerbrey equation. It was anticipated that by decreasing the frequency in this manner the operating region of the crystal would be moved away from any point where coupling might occur.

The crystal that was used had, prior to the electrodeposition of the nickel, been coated with manganese dioxide using the particle fractionator with both water and collodion as deposit securing agents. The frequency changes after coating were typical for the technique used, i.e. small increases with water as adhesive and increases of several kilohertz when collodion was used.

Nickel was deposited on the electrodes of the crystal by electroplating the metal from an ammoniacal solution of nickel sulphate. The frequency change after deposition was a decrease of 94.6 KHz. The crystal was then recoated with manganese dioxide by the two techniques. The frequency changes obtained by coating manganese dioxide on the nickel coated crystal were the same as those obtained by coating on the clean crystal; neither magnitude nor sign of the frequency changes were significantly changed.

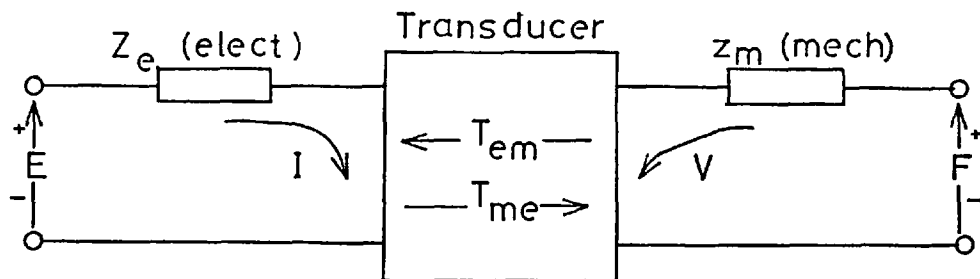
No further work was carried out to investigate the possible connection between the high frequency effect and the coupling of vibrational modes of motion.

A more likely cause of the high frequency effect was considered to be linked with the fundamental nature of a vibrating quartz crystal.

In the following section no attempt will be made to present a quantitative explanation but similarities between the theory of electromechanical devices and experimental evidence of coated piezoelectric crystals will be pointed out and thus hopefully identify the area of importance responsible for the high frequency effect.

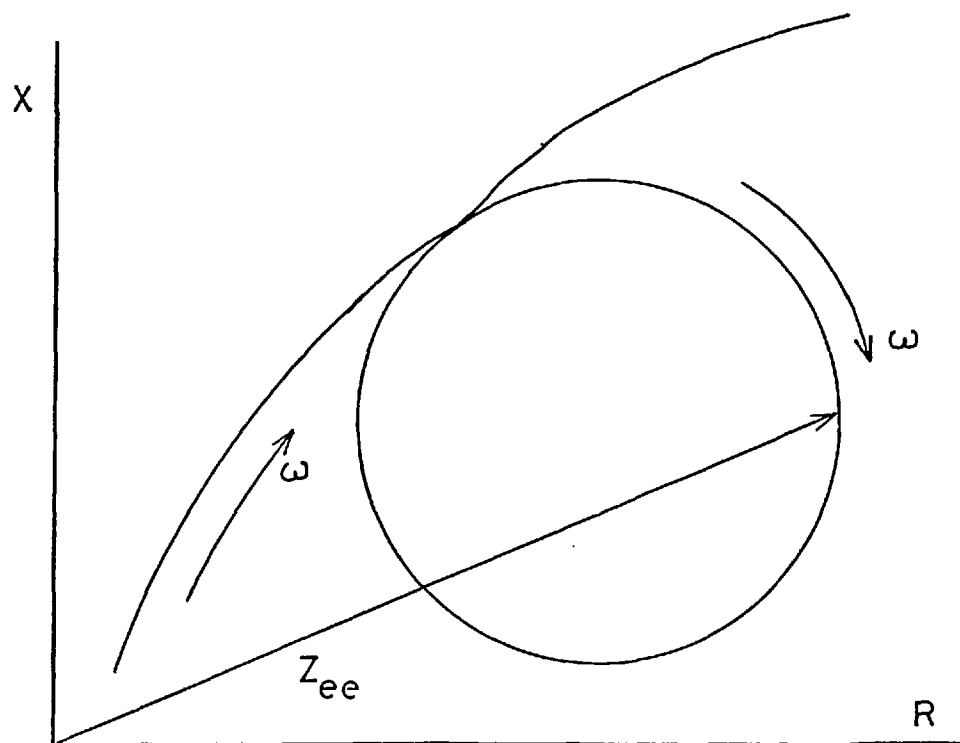
5.4.2. General Considerations of Electromechanical Transducers

An electromechanical transducer is a device which provides a definite functional relationship between the variables of an electrical system and the variables of a mechanical system. Two general equations may be written to describe the simple transducer system shown in figure 48. One equation is written in terms of the electrical variables and includes the electrical effects due to motion in the mechanical system, the other equation is written in terms of the mechanical variables and includes all the mechanical effects arising from currents or voltages in the electrical system.



Schematic Representation of an Electro-
Mechanical Transducer

Figure 48



Vector Impedance Locus

Figure 49

These equations are:

for the electrical system,

$$E = Z_e I + T_{em} v \quad (1)$$

for the mechanical system,

$$F = T_{me} I + z_m v \quad (2)$$

In these equations and figure 48 the symbols T_{me} and T_{em} represent the transduction coefficients that describe the electro-mechanical coupling, the direction of transfer being indicated by the subscripts.

Important properties of the electromechanical interaction of a transducer can be revealed by studying the electric driving point impedance of the system at its electrical terminals. The electric driving point impedance is defined as the complex ratio of the voltage across the terminal pair to the current entering or leaving the terminals when all other electromotive forces and current sources are suppressed. For the general system of figure 48 the driving point impedance can be found by setting $F = 0$ in equation 2 and solving for I in terms of the terminal voltage E . This leads to

$$Z_{ee} = \left[\frac{E}{I} \right]_{F=0} = Z_e + \frac{-T_{em}T_{me}}{z_m} \quad (3)$$

Equation (3) may be rewritten as

$$Z_{ee} = Z_e + Z_{mot} \quad (4)$$

where

$$Z_{mot} = (-T_{em}T_{me}) \cdot \frac{1}{z_m}$$

= motional impedance

The additive term that appears in the equation represents the modification of the electrical impedance of the transducer caused by

the electromechanical coupling, the term z_m representing the mechanical impedance of the system. In relationship to coated quartz crystals it is this term, z_m and its frequency dependence that is of interest.

As the mechanical impedance is of the complex type a general expression may be written of the form,

$$z_m = r_m + j \omega l_m + \frac{1}{j \omega c_m}$$

The significance of r , l and c , (usually resistance, inductance and capacitance of an electrical circuit,) are respectively, in this equation describing a mechanical system, the mechanical losses of the system, the mass and the reciprocal of the elasticity of the system (114).

The most informative way of presenting the variation of the mechanical impedance with frequency is to represent the impedance as a vector, in the real-imaginary plane, the magnitude and direction of which change with frequency. As the frequency changes then the tip of the impedance vector will trace a curve which is known as the motional impedance locus. When the variation of the electrical impedance, Z_e , is also presented as a vector and summed with Z_{mot} , as indicated in equation 4, then the total impedance locus for the electromechanical system is produced; for the simple system at present under consideration the appearance of this impedance locus is as shown in figure 49. The loop on the curve is entirely due to the effect of the mechanical impedance of the system. A detailed development of the vector impedance locus is given in Hunt (115).

An illustrative example of the effect of mechanical impedance upon the impedance of telephone receivers has been reported (115). Measurements of the variation of impedance with frequency for a telephone receiver were carried out. Two workers, using the same equipment but working independently made the measurements but there was a complete

lack of agreement between their results in the neighbourhood of the resonance point of the receiver.

Only when the two workers watched each other carry out the experiment did the cause of the discrepancy become obvious; one worker would place the receiver on its side whilst making the measurements, the other placed the receiver face down thus altering the acoustic loading on the diaphragm, its motion and thus its electrical impedance.

A very similar effect has been observed, by the author, with a coated piezoelectric crystal. A clean crystal was coated with potassium iodate ($8 \mu\text{g}$ - deposit diameter 1.48 mm), the intention being to examine the reaction between potassium iodate and sulphur dioxide. It was observed with this crystal that the frequency change of the coated crystal could be changed from an increase, relative to the clean frequency, to a decrease by changing the inductance of the tuning coil in the oscillator i.e. by moving the ferrite core of the coil. An identical effect was also achieved by changing not the parameters of the electrical circuit connected to the crystal but the mechanical environment of the crystal.

It was found that with the tuning core of the oscillator in a specific place the crystal could be made to increase or decrease its resonant frequency by removing the outer can of the crystal.

The removal of this covering can changed the environment and hence the mechanical load upon the crystal. The crystal was vibrating with a decrease in the resonant frequency of 23KHz when the can was in place; when the can was removed the resonant frequency of the crystal was 52KHz higher than the clean frequency. The magnitude of the frequency changes that were obtained when induced by changing the oscillator

inductance were the same i.e. a decrease of 23KHz and an increase of 52KHz.

It had been found on many occasions that a coated crystal would oscillate without the covering can but when the can was in place or the crystal placed in the sample cell then oscillations ceased. This occurred with crystals that were oscillating both at a frequency higher than the clean frequency and also crystals that had decreased their frequency upon coating.

By comparing the general theory of electromechanical transducers and the experimental evidence reported it would appear that because of the exact nature of the potassium iodate deposit on the crystal a very small change in the mechanical environment, and thus a change in the mechanical impedance of the crystal, was sufficient to induce the high frequency system of vibration. Similarly as the electrical and mechanical systems are interconnected then a small change in the electrical environment of the crystal was also sufficient to induce the change from a high to low frequency system of oscillation. It would, therefore, seem likely that the variation of the mechanical impedance of a coated crystal is responsible for the high frequency effect and that the difference between coatings that oscillate high and low need only be small, as evident by the small change in the environment caused by the removal of the covering can.

This sensitivity around the critical region would account for the difficulty experienced when trying to produce solid coatings that behaved in a similar manner; in that the exact nature of the deposit i.e. mass, area, mass distribution, surface roughness etc., is very difficult to reproduce.

6. The Response of Organic Coating Materials

6.1. Introduction

The response of crystals coated with organic materials was the first and also the last work carried out with coated piezoelectric crystals.

The initial work with carbowax 20M was carried out in order to obtain some basic experience with the equipment; no attempt was made to thoroughly investigate all of the parameters involved in the system i.e. the variation of coating mass and area were not investigated, neither was the mathematical performance of the partition system between sulphur dioxide and carbowax studied.

Triethanolamine was the last coating material to be investigated, the work being inspired by Hartigan as discussed in chapter 3.

The work with triethanolamine involved the presentation of dilute sample gas to the crystal in a long continuous flow as opposed to the short sample/coating interaction obtained when samples were injected manually, by microsyringe into the carrier gas stream.

6.2. Carbowax 20M

6.2.1. Static Studies

The crystals used in this study were coated on both electrodes using the technique described in chapter 3 i.e. the deposition of carbowax from a chloroform solution. The mass of the deposit applied to each crystal was 30 $\mu\text{g}/\text{side}$ i.e. a total loading of 60 μg .

The glass cells were used to check the static response of these crystals; the reference and sample cells were connected in parallel with respect to the nitrogen gas line used to flush the cells. The reference crystal was uncoated. The mixer circuit was used to monitor the frequency change of the sample crystal; the frequency difference, between reference and sample crystal, obtained from the mixer was

monitored as a function of time.

In order to study the absorption or partition of the sample gas, sulphur dioxide, into the coating on the crystal the following experimental procedure was used:-

The sample crystal was placed in the cell, which was then flushed with nitrogen, (2 min. at 250 ml/min.). After flushing, the crystal was allowed to reach an equilibrium frequency.

The frequency stability was monitored for a period of 15 minutes prior to the introduction of sample into the cell. An aliquot of sulphur dioxide (60 μ l to 250 μ l) was injected into the cell and the resultant frequency change monitored; 10 minutes after the sample injection the cell was flushed with nitrogen (10 minutes at 250 ml/min) in order to desorb the sample from the coating. The crystal was then allowed to equilibrate in a static atmosphere of nitrogen.

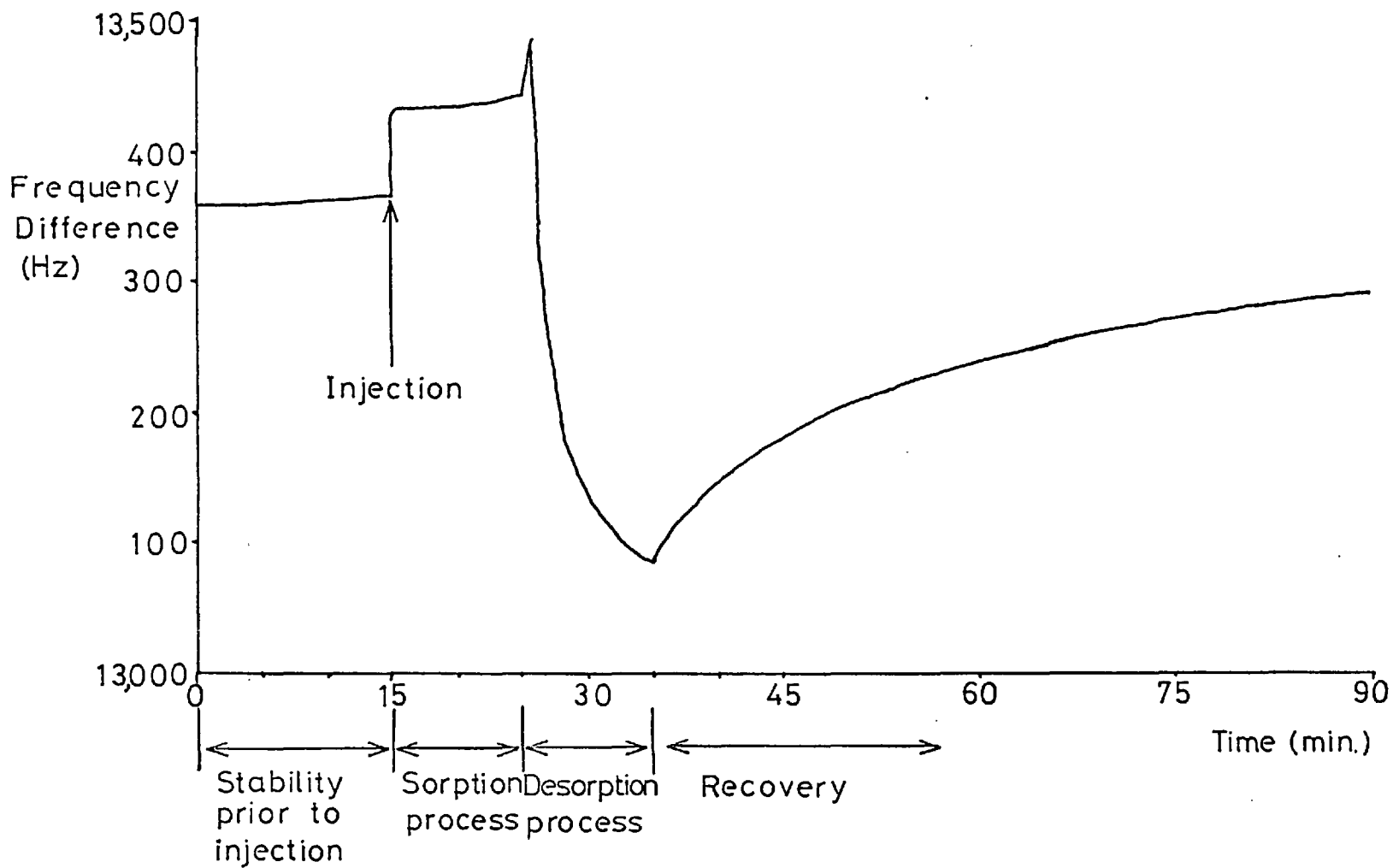
A typical plot of the variation of frequency difference as a function of time for the sequence of events just described is shown in figure 50.

The time period $t = 0$ to 15 minutes shows the stability of the crystal frequency prior to injection. At $t = 15$ minutes an aliquot (250 μ l) of sulphur dioxide was injected. The frequency of the sample crystal rapidly decreased. (The graph shows the frequency difference increasing; this has been explained in chapter 2 and figure 18a and b). After the initial rapid decrease in the sample crystal frequency the frequency decreased only slightly (10 Hz in 10 minutes) before the sample was desorbed.

The cell was flushed with nitrogen from $t = 25$ minutes to $t = 35$ minutes, the recovery of the crystal being shown from $t = 35$ minutes onwards. It will be noticed that the frequency difference after the

Carbowax Coated Crystal
Absorption and Desorption of SO₂ from a

Figure 50



crystal has recovered is smaller than the difference at the beginning of the experiment i.e. the frequency of the sample crystal is higher. This is indicative of bleed of the coating material during the desorption of the sample.

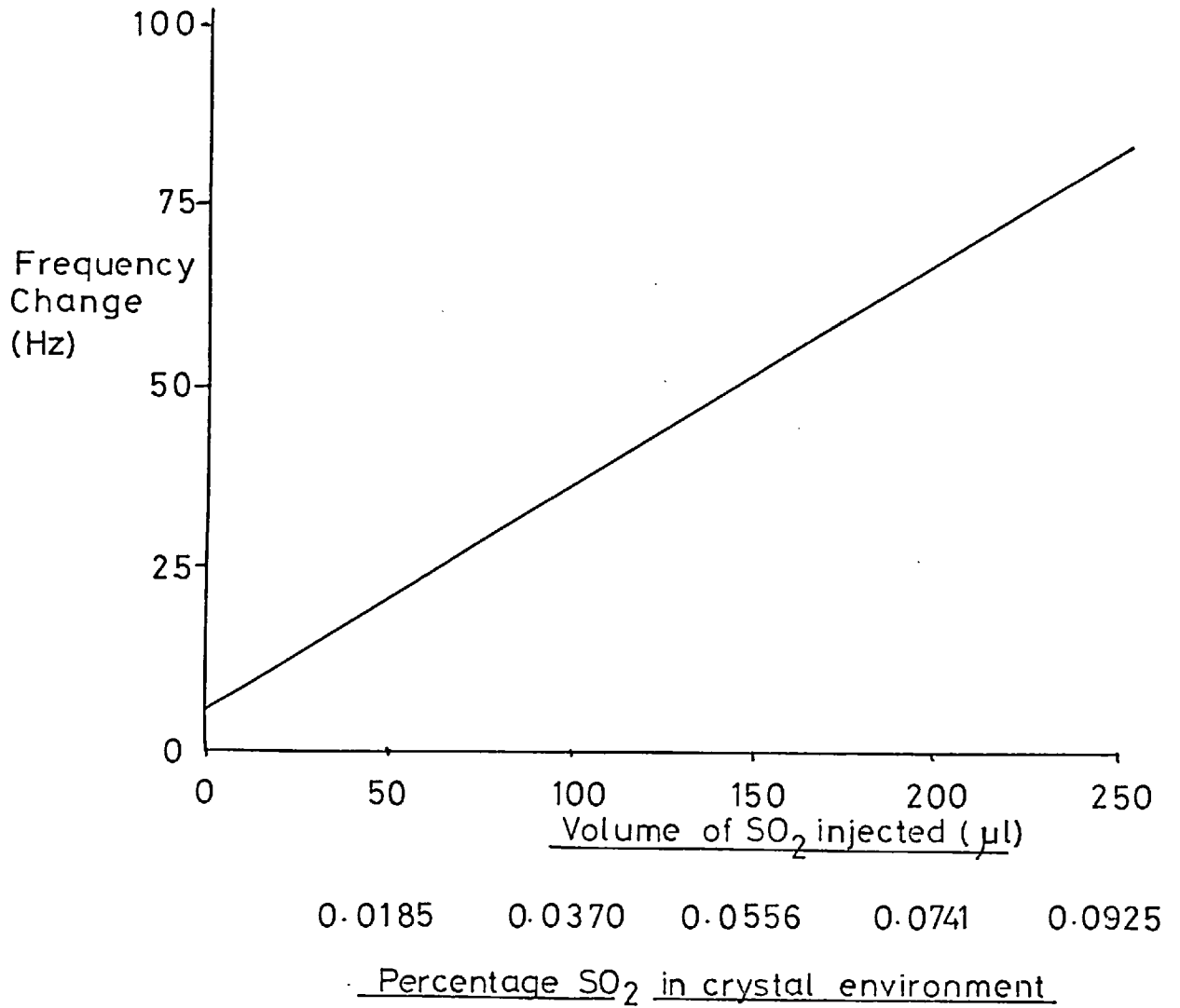
The determined response of these crystals was a 35 Hz decrease in frequency after a 10 minute exposure to dilute sulphur dioxide (0.37%). The total load on the crystal was 60 μg . The response of carbowax coated crystals to sulphur dioxide determined in the manner just described compares very well with normalised data presented in reference 82.

By normalising the data presented in reference 82 a response of 40 Hz would have been obtained if the same conditions of exposure and crystal loading had been employed.

A calibration graph of the response of a carbowax coated crystal in a static environment to a sulphur dioxide was constructed. The same experimental technique as just described was used to establish the frequency change for each separate aliquot of sample gas. The resultant graph is shown in figure 51.

6.2.2. Dynamic Studies

The response of a carbowax coated crystal to sulphur dioxide in a flowing gas stream was also checked using the glass cell. The injection port, shown in figure 23, was included in the gas line immediately before the sample cell.



Response of Carbowax Coated Crystal to SO₂

in a Static Environment

Figure 51

The flow rate of the nitrogen carrier gas was initially set at a flow of 60 ml/min. through each cell. The coated crystal was allowed to come to a steady state, where the bleed rate of carbowax from the crystal surface was constant at 10 Hz/hour, i.e. the frequency difference between the sample and reference crystals was decreasing at the rate of 10 Hz/hour.

Various aliquots (60 μ l to 250 μ l) of sulphur dioxide were injected into the gas stream and the resultant change in the frequency difference was noted. Replicate injections of each sample were made.

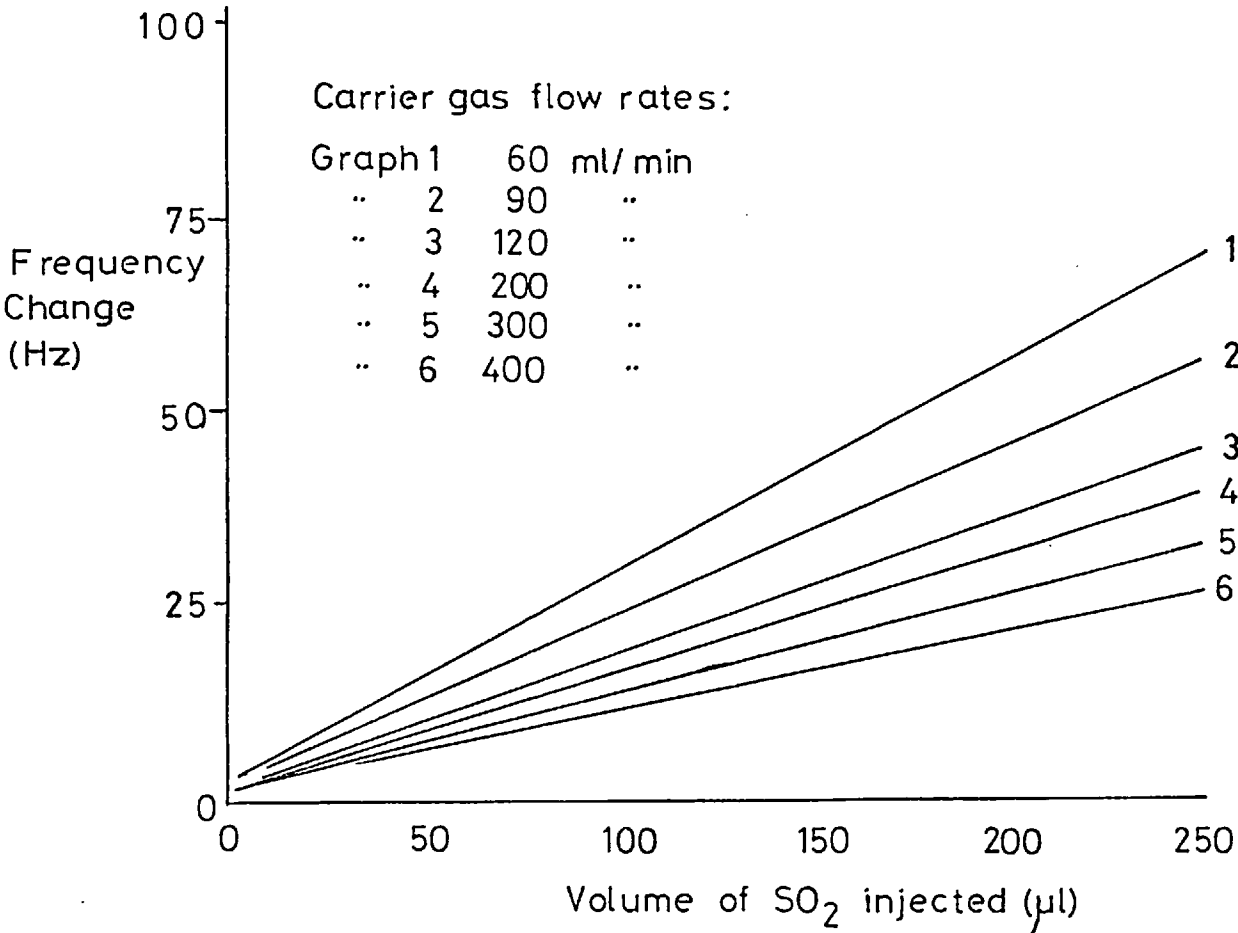
The effect of the carrier gas flow rate upon the response of the coated crystal was examined by increasing the flow rate to 90 ml/min. and constructing a fresh calibration graph.

This process was repeated for flow rates of 120, 200, 300 and 400 ml/min. The six calibration graphs are shown in figure 52.

The dependence of the response upon flow rate is shown in figure 53; in this graph the decrease in the response obtained, after the injection of 250 μ l aliquots of sulphur dioxide, is shown as a function of flow rate.

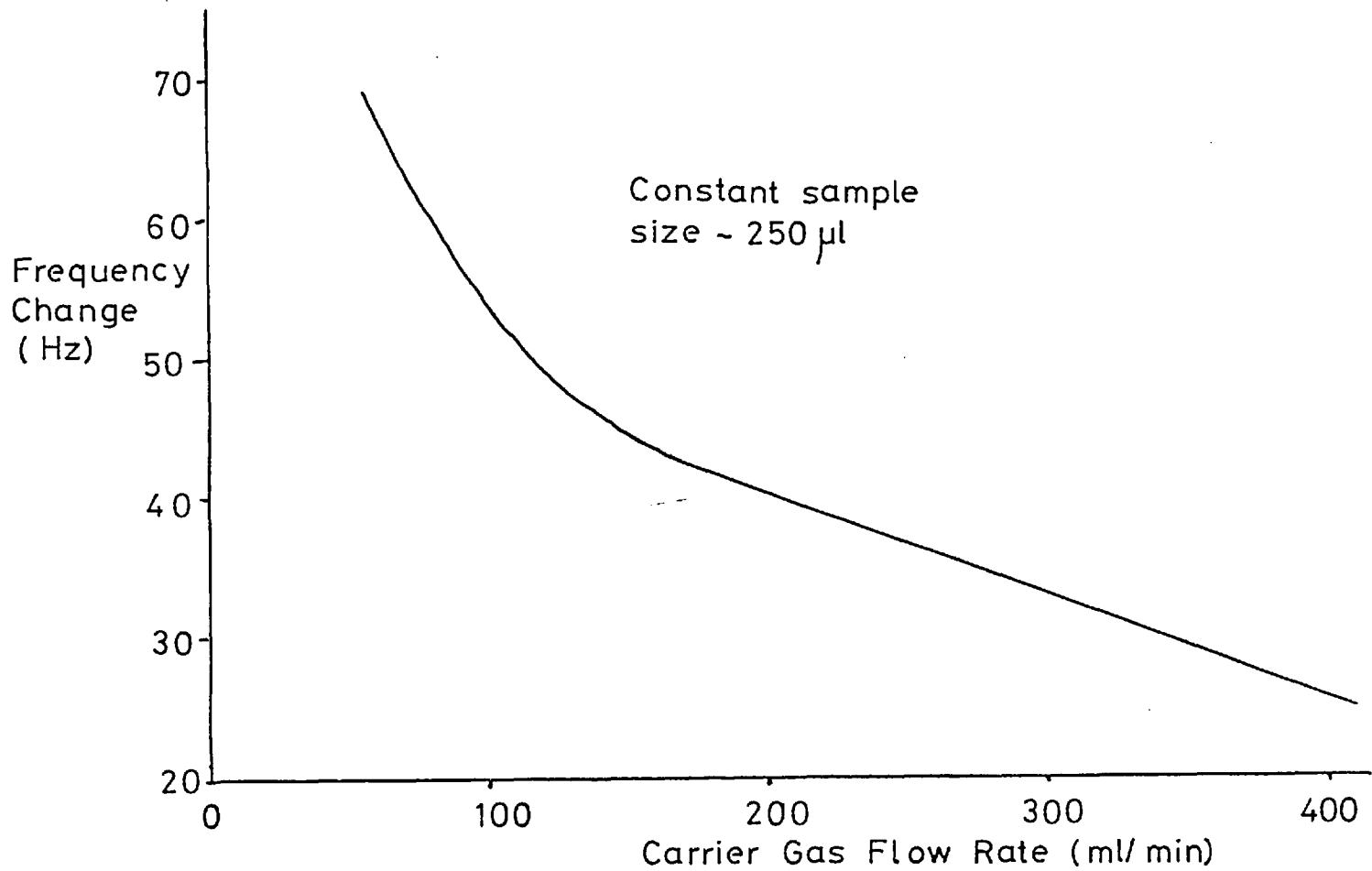
The peak shapes representing the sample/coating interaction show that the system is totally reversible, the baseline frequency of the coated crystal was re-established in 3 minutes after a 250 μ l sample of sulphur dioxide had been introduced into the system; the carrier gas flow rate was 60 ml/min. When the flow rate was increased the recovery time decreased, i.e. for the same sample size but a flow rate of 300 ml/min. the recovery time was only 30 seconds; this is shown in figure 54.

As has been previously stated, the work with carbowax was not intended to be a rigorous assessment of the system. After the cursory examination of the dynamic system no further work was done to examine



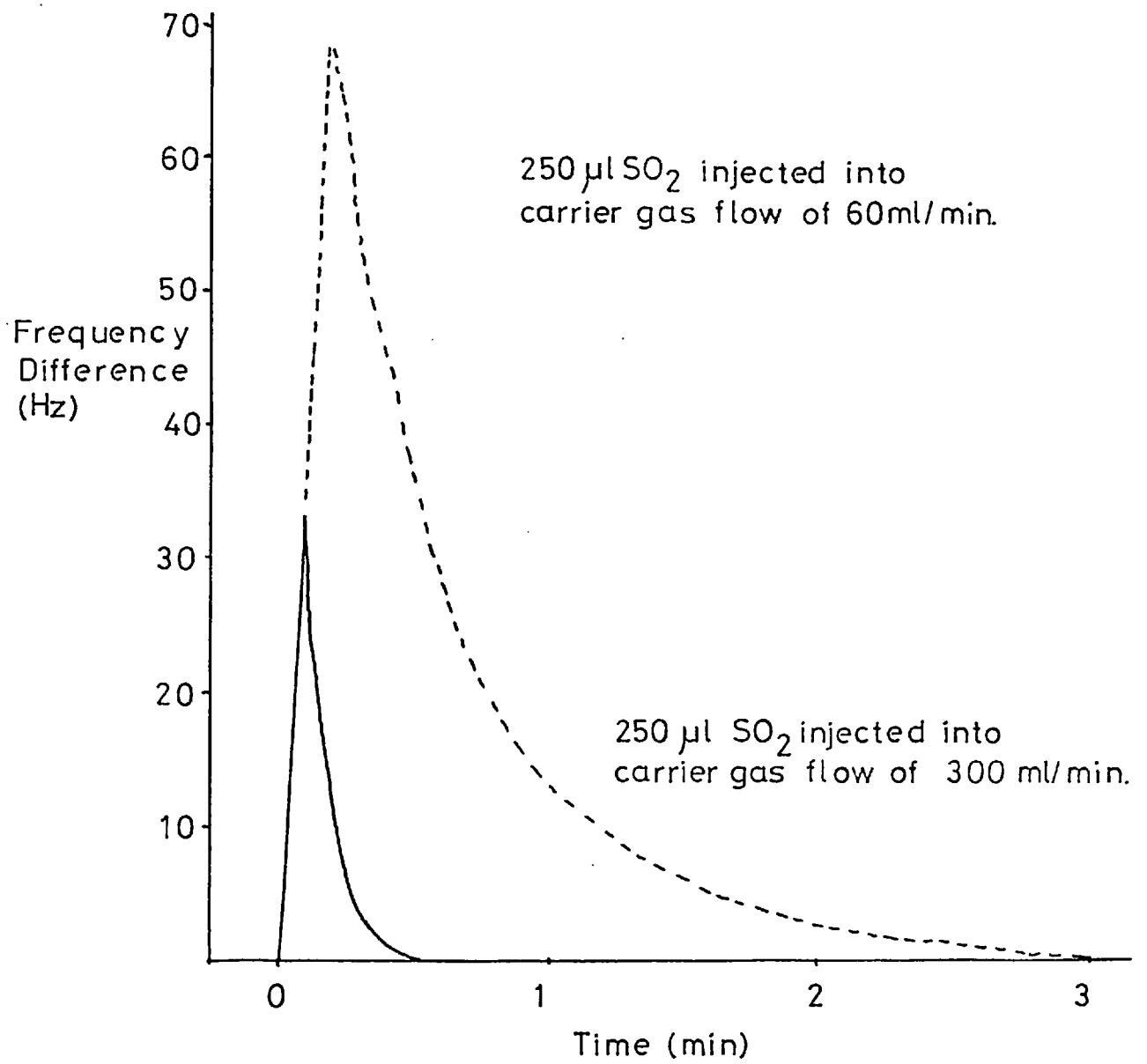
Response of a Carbowax Coated Crystal to SO₂
in a Dynamic Environment (Six flow rates)

Figure 52



Dependence of Response of a Carbonyl Wax Coated Crystal
upon Carrier Gas Flow Rate

Figure 53



Decreased Recovery Time and Response as a Function
of Flow Rate

Figure 54

the suitability of the system to the analysis of low concentrations of sulphur dioxide. The system was used however to establish the level of precision that could be expected from the complete experimental technique and also to assess different cell designs.

Different measuring techniques i.e. peak area and peak height measurements were also investigated with the carbowax/sulphur dioxide system. These experiments have been described in chapter 2.

6.3. Triethanolamine

In the study of triethanolamine as a coating material only one static study was made and the introduction of sample via a micro-syringe was not extensively used. A syringe pump was available which, in conjunction with a 5 ml. syringe, made possible the slow introduction of dilute sample gas into the nitrogen carrier gas. Upon entry into the carrier gas stream the sample gas was further diluted before the gas mixture entered the sample cell. As the concentration of the sample in the syringe was known and also the carrier gas flow rate and the sample delivery rate from the syringe was known it was possible to readily calculate the concentration of the sample gas in the sample cells.

The presentation time of the sample gas to the coated crystal could be made as long or as short as required, this contrasts sharply with the microsyringe method of sample introduction where the sample introduction into the carrier gas stream was complete within 0.5 sec.

The use of the syringe pump for sample introduction therefore permits a more realistic operation of the detector in that it is exposed to a constant concentration of sample for a considerable period of time.

The coating details of the crystals that were used in the evaluation of triethanolamine are shown in table 25. Crystals 1, 2 and 3 were coated on one side only, the rest were coated on both sides.

Crystal number	Frequency change due to coating (Hz)	Mass of coating (μg)	Diameter of deposit (mm)
1	-12,054	24.8	6.50
2	-11,679	53.9	6.98
3	- 6,837	28.2	7.02
4 1	-19,544	38.7	5.82
2	- 9,837	20.7	5.42
5 1	-14,755	37.0	6.00
2	-10,836	28.6	6.00
6 1	-14,981	41.9	6.24
2	-11,338	32.8	6.24
7 1	-12,698	105.9)	Both sides of crystal completely covered
2	-11,778	80.4)	
8 1	- 8,312	9.9	2.48
2	-4,447	6.5	2.50
9 1	- 6,147	4.6	1.94
2	- 7,474	7.2	2.26
10 1	- 6,287	6.2	2.60
2	- 4,515	9.7	2.56
11 1	- 3,187	9.7	1.30
2	- 3,348	3.1	1.66

Table 25

6.3.1. Static Studies

The response of a triethanolamine coated crystal to a static atmosphere of dilute sulphur dioxide was carried out in the usual manner.

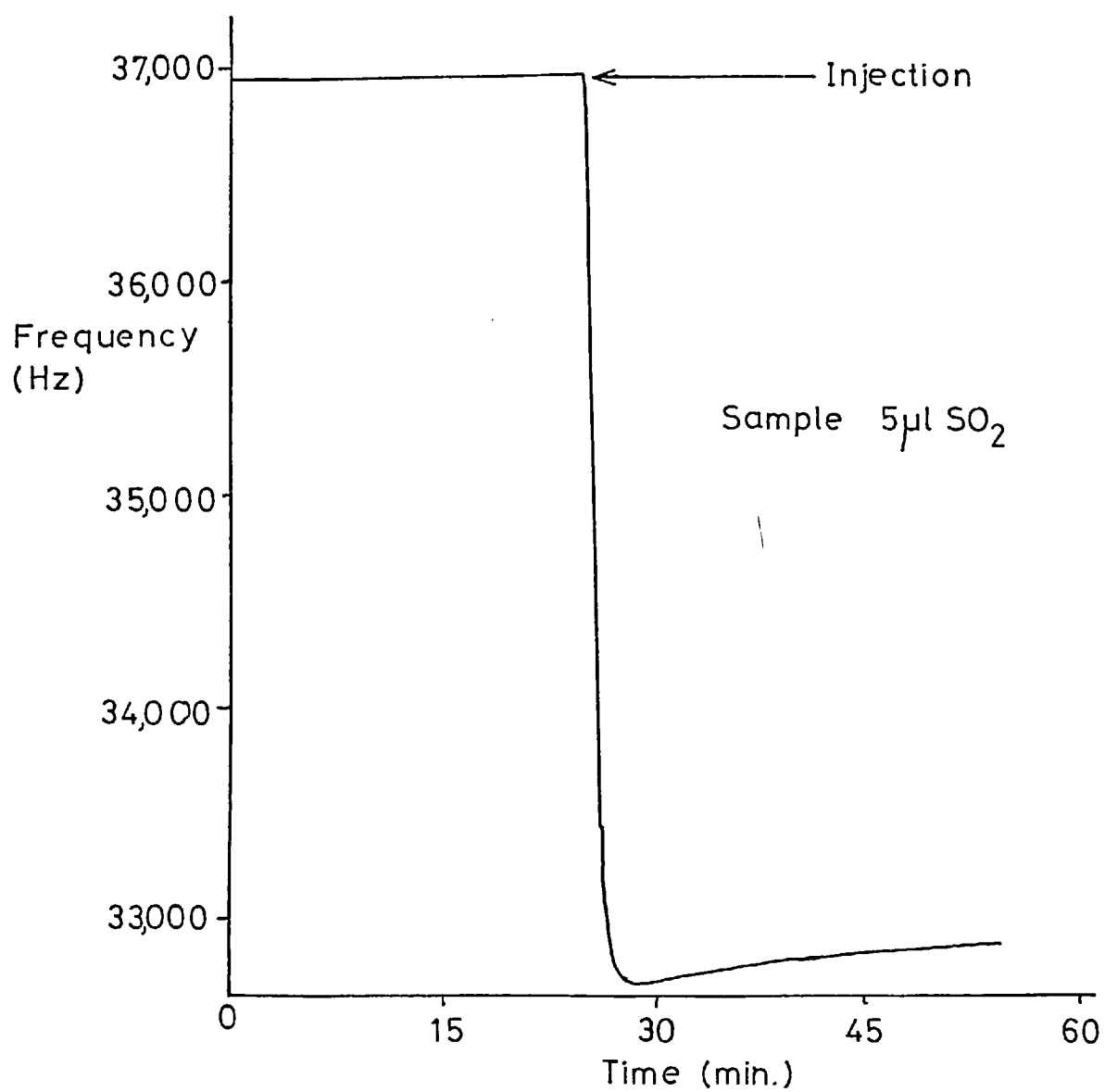
Crystal number 1 (table 25) was placed in the glass cell which was then flushed with nitrogen (2 min. at 100 ml/min.). The crystal was allowed to come to an equilibrium frequency. A simple single sided system of frequency measurement was used i.e. no reference crystal was employed.

When the frequency of the crystal was constant an aliquot of sulphur dioxide (5 μ l) was injected slowly into the cell. The percentage composition of the atmosphere was 0.0185% sulphur dioxide.

The frequency of the crystal was monitored as a function of time the resultant frequency change is shown in figure 55. This figure shows a large and rapid decrease in frequency of 4,216 Hz in 3 minutes.

Using the coating data i.e. the mass and diameter of the deposit and the accompanying frequency change, an experimental value of the constant in Sauerbrey's equation was calculated, which was then used to calculate the mass of sulphur dioxide that was sorbed onto the crystal. This value was 8.67 μ g. As the quantity of sulphur dioxide sorbed onto the crystal was so large, the change in mass of the crystal was checked by direct weighing of the crystal. This operation was carried out quickly to minimise possible loss of sample from the crystal surface. The gain in weight of the crystal determined by direct weighing was in excellent agreement with the calculated value at 8.6 μ g.

As the triethanolamine/sulphur dioxide system was so sensitive (the best previous performance of a coated crystal in a static environment was a frequency decrease of 1,924 Hz in 10 minutes by a manganese



Response of a Triethanolamine Coated Crystal to SO₂
in a Static Environment

Figure 55

dioxide coated crystal in an 0.37% sulphur dioxide atmosphere) no further work was carried out in a static environment. Crystal number 1 was transferred to the stainless steel cell for examination in a dynamic system.

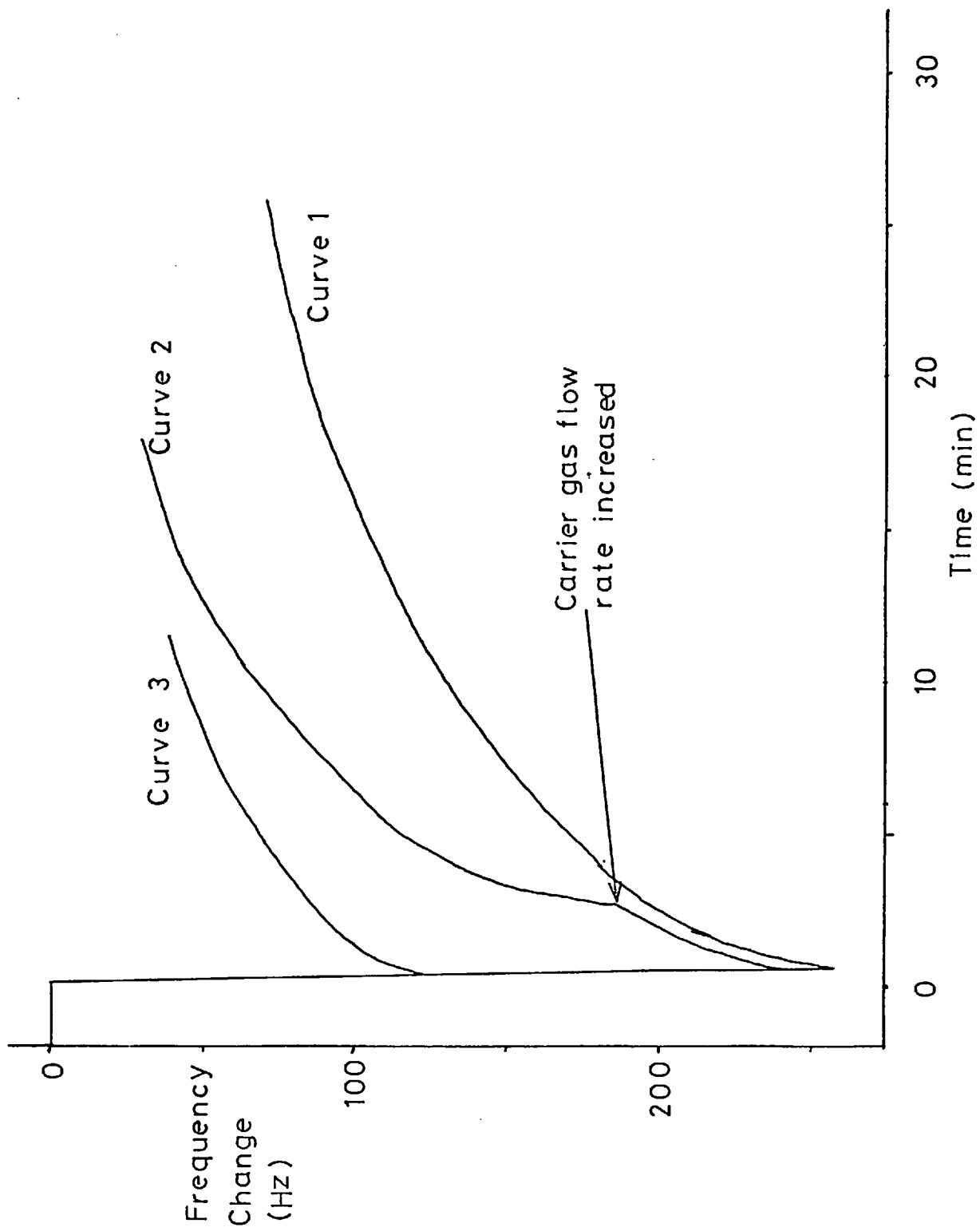
6.3.2. Dynamic Studies

Crystal 1 was placed in the flow cell with nitrogen passing through the cell at 12 ml/min. The frequency of the crystal was again monitored without a reference crystal. The crystal was allowed to reach an equilibrium frequency. When the frequency was steady, an aliquot of sulphur dioxide (5 μ l) was injected into the carrier gas stream, the resultant frequency change was monitored as a function of time. The peak height or maximum frequency decrease was 258 Hz. The recovery of the crystal was slow. A replicate injection was made after 1 hour, the carrier gas flow was increased to 20 ml/min. 2.5 minutes after the sample injection. This was done to increase the rate of recovery of the crystal. The peak response obtained for the second injection was 239 Hz.

The peak profiles for these injections are shown in figure 56, curves 1 and 2. The increased flow rate removed sulphur dioxide from the surface of the crystal more quickly, but the recovery of the crystal was still slow. The carrier flow rate was reduced to its previous rate of 12 ml/min.

As the response of this crystal to small samples of undiluted sulphur dioxide was large, a calibration graph was prepared by injecting aliquots (5 μ l to 100 μ l) of dilute sulphur dioxide (5,000 ppm in air) into the system.

The dilute solution of sulphur dioxide was prepared by injecting, with an all glass, grease free syringe, 5 ml. of sulphur dioxide into



Peak Profiles Representing Dynamic Interaction between
Triethanolamine Coated Crystal and SO₂

Figure 56

the 1l gas reservoir which had been previously flushed with air and evacuated. After the 5 ml. sample of gas had been introduced into the vessel, the pressure in the vessel was released and allowed to rise to atmospheric pressure by opening a tap to the atmosphere. The sulphur dioxide/air mixture was allowed to mix, by diffusion, for 5 minutes before the first aliquot of sample was removed.

The resultant calibration curve of crystal number 1 using dilute sulphur dioxide is depicted in figure 57, a typical peak profile obtained during the construction of this calibration graph is depicted by curve 3, figure 56. This profile represents the frequency change that occurred after the injection of 100 μ l of 5,000 ppm sulphur dioxide in air into the system.

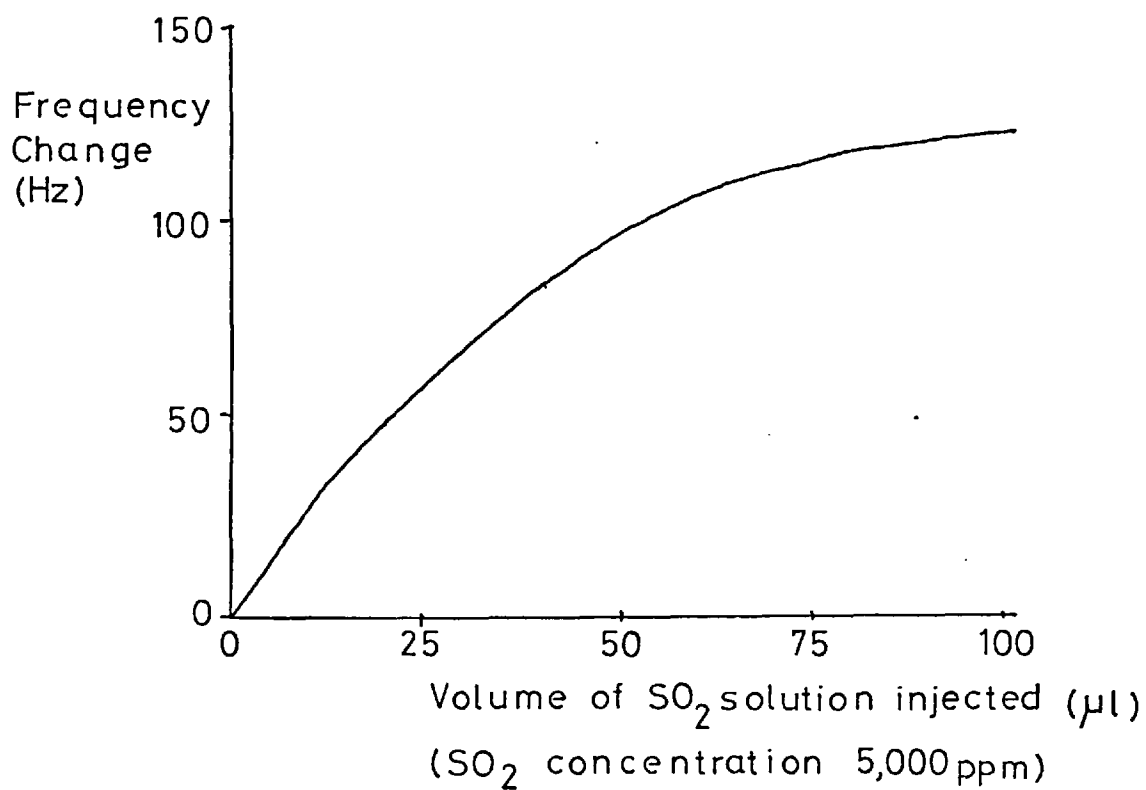
The calibration graph shown in figure 57 demonstrates that the system is very sensitive to sulphur dioxide.

Before a more detailed study of the response of triethanolamine coated crystals to dilute sulphur dioxide was carried out the rate of bleed of the material from a crystal surface was ascertained.

This work has already been reported in chapter 2 in order to demonstrate the effectiveness of a double sided measurement system to correct for frequency changes due to bleed.

In this experiment it was ascertained that the rate of bleed was dependent upon the area and mass of the coating and also decreased as the crystal aged. Typical values of bleed for a freshly coated crystal were between 72 and 44 Hz/hour. After 12 days in a flowing gas stream (12 ml/min.) this reduced typically to 7 Hz/hour; with 83% of the original coating mass still remaining on the crystal.

For the initial experiments exposing a coated crystal to dilute sample gas for a longer period of time crystals 2 and 3 were placed in the flow cells; the carrier gas flow rate was regulated at 12 ml/min.



Calibration Graph of Triethanolamine Coated

Crystal with Dilute SO₂

Figure 57

through each cell. The ratio method of monitoring the frequency changes was used, the sample was injected into the gas stream of crystal 3, crystal 2 being the reference crystal.

The dilute sulphur dioxide used in this study was prepared by the further dilution of an aliquot of 5,000 ppm solution with air. The technique used was the same as the method used to prepare the 5,000 ppm solution i.e. removal of an aliquot of gas from the 11 reservoir, flushing and evacuation of the reservoir and subsequent re-introduction of the previously removed aliquot and dilution with air.

The aliquot sizes were chosen so that solutions of 5, 10 and 25 ppm sulphur dioxide in air were produced. 5 ml aliquots of the sample gas prepared in the manner just described were injected, manually, using an all glass, grease free syringe with a flexible teflon needle over periods of 1, 2 and 3 minutes into the carrier gas stream, the sample gas was thus further diluted before reaching the crystal. The theoretical range of concentrations to which crystal 3 was exposed during these experiments was 0.86 ppm for 2 minutes to 7.35 ppm for 1 minute.

The response of the crystal to numerous injections of sample gas of various concentrations was always found to be of the same order i.e. the frequency of the crystal decreased between 1 and 2 KHz, regardless of the injection time and sample concentration in the syringe. A 5 ml. injection of laboratory air over a period of 2 minutes however, only gave a total decrease of 97 Hz. This indicated that the sulphur dioxide solutions were heavily contaminated; this was finally attributed to the grease used on the taps of the glass reservoir.

In order to overcome this problem a new reservoir was constructed with teflon taps thus eliminating the need for greased taps. A nitrogen line was also sealed to the reservoir so that the samples of sulphur dioxide could be diluted with nitrogen not air. This reservoir was

also fitted with a mercury levelling device so that dilution of the sample in the flask could be avoided when an aliquot of gas was removed. This equipment is depicted in figure 24b.

After the establishment of the contamination of the sulphur dioxide solutions crystal 3 was no longer sensitive to sample gas. The frequency of the crystal had increased such that the vibrational frequency was only 4.9 KHz lower than the clean uncoated frequency. This frequency increase, a change of 72% of the original frequency change that occurred upon coating, was due probably to a combination of bleed of coating and chemical exhaustion i.e. sulphur dioxide retained on the surface of the crystal.

Crystal number 4 was placed in the flow cell with a carrier gas flow of 12 ml/min. No problems with contaminated gas samples were experienced with this and subsequent crystals.

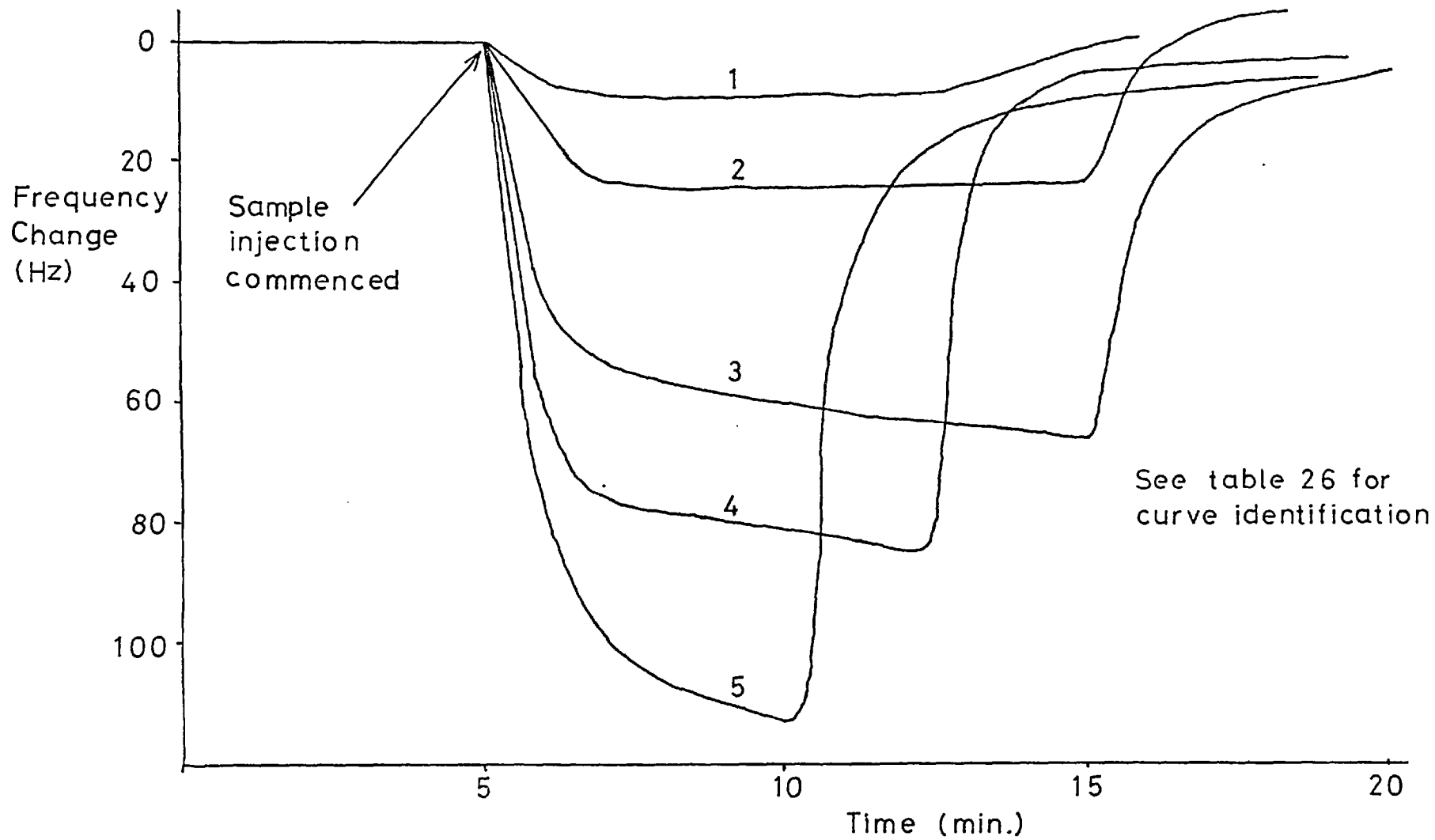
The syringe pump was used to deliver the sample gas into the carrier gas stream. As with the manual injections, the initial work with the syringe pump obtained different concentrations of the sample gas in the sample cell by injecting a constant volume of the same concentration of sample gas into the carrier gas stream at different rates thus effecting a different dilution of the sample gas.

For crystal number 4, 5 ml. aliquots of sulphur dioxide in nitrogen (1 ppm) were injected into the carrier gas stream at 4 different rates. The time taken to inject the samples into the carrier gas stream and the resultant concentration of the sample are shown in table 26.

During the sample injection and crystal recovery the frequency of the crystal was monitored as a function of time, the changes in frequency that occurred during and after each sample injection are shown in figure 58. The identification numbers of the curves correspond to the

Coated Crystal 4
Long Sample Presentation (SO_2) to Triethanolamine

Figure 58



identification numbers in table 26, thus curve 5 represents the frequency change that occurred as a result of injecting 5 ml. of 1 ppm sulphur dioxide into the carrier gas stream over a period of 5 minutes.

Note that the actual time for which the crystal was exposed to 0.020 ppm sulphur dioxide was only 10 minutes not 20. The sample supply was terminated as the crystal had reached a constant frequency after its initial decrease.

The actual shape of the frequency profiles and the significance of these shapes will be discussed after the results of crystal number 5 have been presented

Identification number	Time taken to inject sample (min.)	Flow rate of sample (ml/min)	Concentration of sample in cell (ppm)
2	20	0.25	0.020
3	10	0.5	0.040
4	7.5	0.66	0.052
5	5	1	0.077

Curve 1, figure 58 was a result of injecting nitrogen into the carrier gas stream at a rate of 0.25 ml/min.

Table 26

Injections of pure nitrogen were made to establish if any change in frequency resulted from the injection of diluant gas. The syringe that was used in these injections was washed well in water and dried at 110° to prevent any sulphur dioxide that may be adsorbed on the walls of the syringe from being inadvertently introduced to the sample crystal.

The syringe was filled with nitrogen by withdrawing the gas from the gas line connected to the sample cell via the injection port. This procedure was used to reduce the possibility of contamination.

The injections of nitrogen only were carried out at two flow rates; these were 0.25 ml/min. and 1 ml/min.

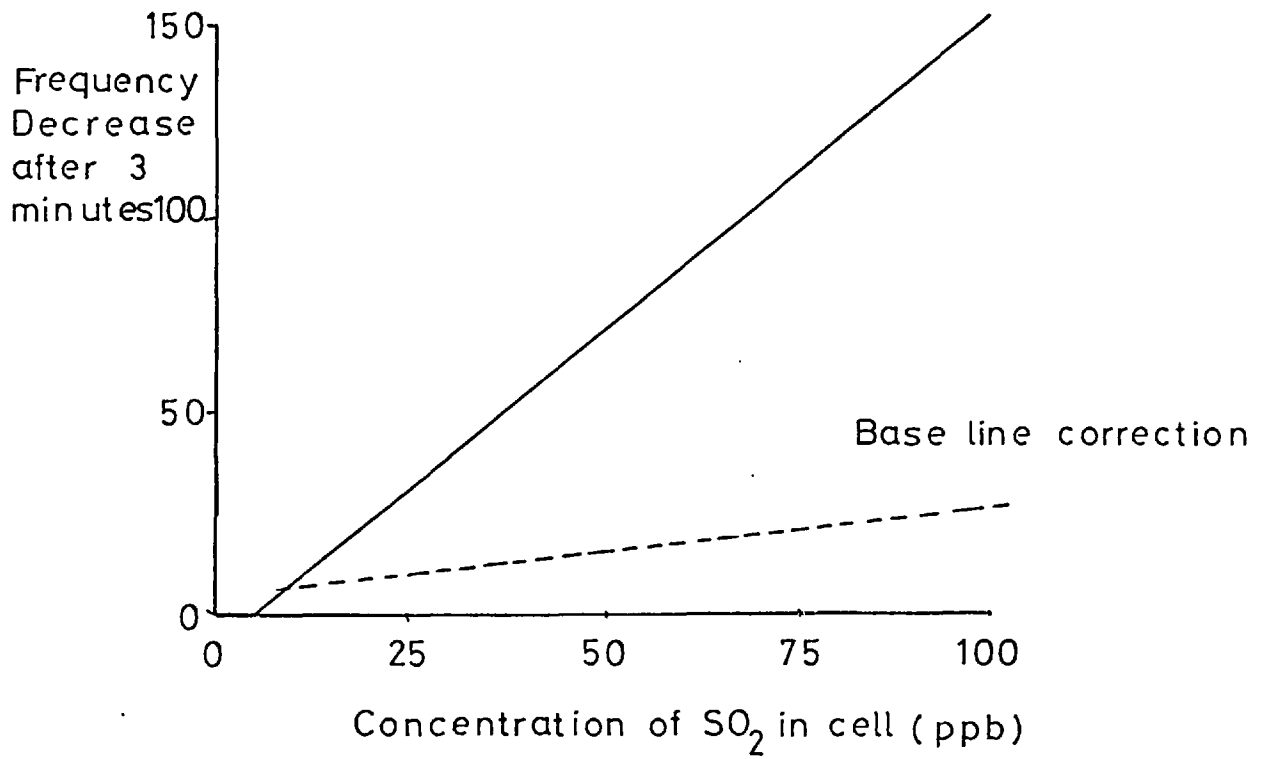
The responses that were obtained from the injection of nitrogen were small but definite decreases in the frequency of the crystal; when the injection was terminated the frequency recovered to its baseline frequency. The frequency changes were probably due to the increase in flow rate; when the injection rate was 1 ml/min. the flow rate increase was 8%, at 0.25 ml/min. the increase was 2%.

With the knowledge of the responses due to the process of injection and also the responses of the crystal to various concentrations of sample gas a calibration graph was constructed, this is shown in figure 59. In order to remove the need for a sloping baseline correction as shown in figure 59 and also to rationalise the sample presentation, it was decided that further sample introduction into the carrier gas stream would be made at a fixed rate of 0.5 ml/min. The concentration of the sample gas in the sample cell would be varied by changing the concentration of sulphur dioxide in the syringe not by changing the duration of sample introduction.

This technique was first used with crystal number 5.

Crystal number 5 was placed in the sample cell with a carrier gas flow rate of 12 ml/min. The frequency of this crystal was monitored without the use of a reference crystal i.e. a single sided measurement only was used.

The response of this crystal to sulphur dioxide was checked by the injection of 5 ml. of dilute sample over a 10 minute period into the carrier gas stream.



Calibration Graph of Triethanolamine

Coated Crystal 4

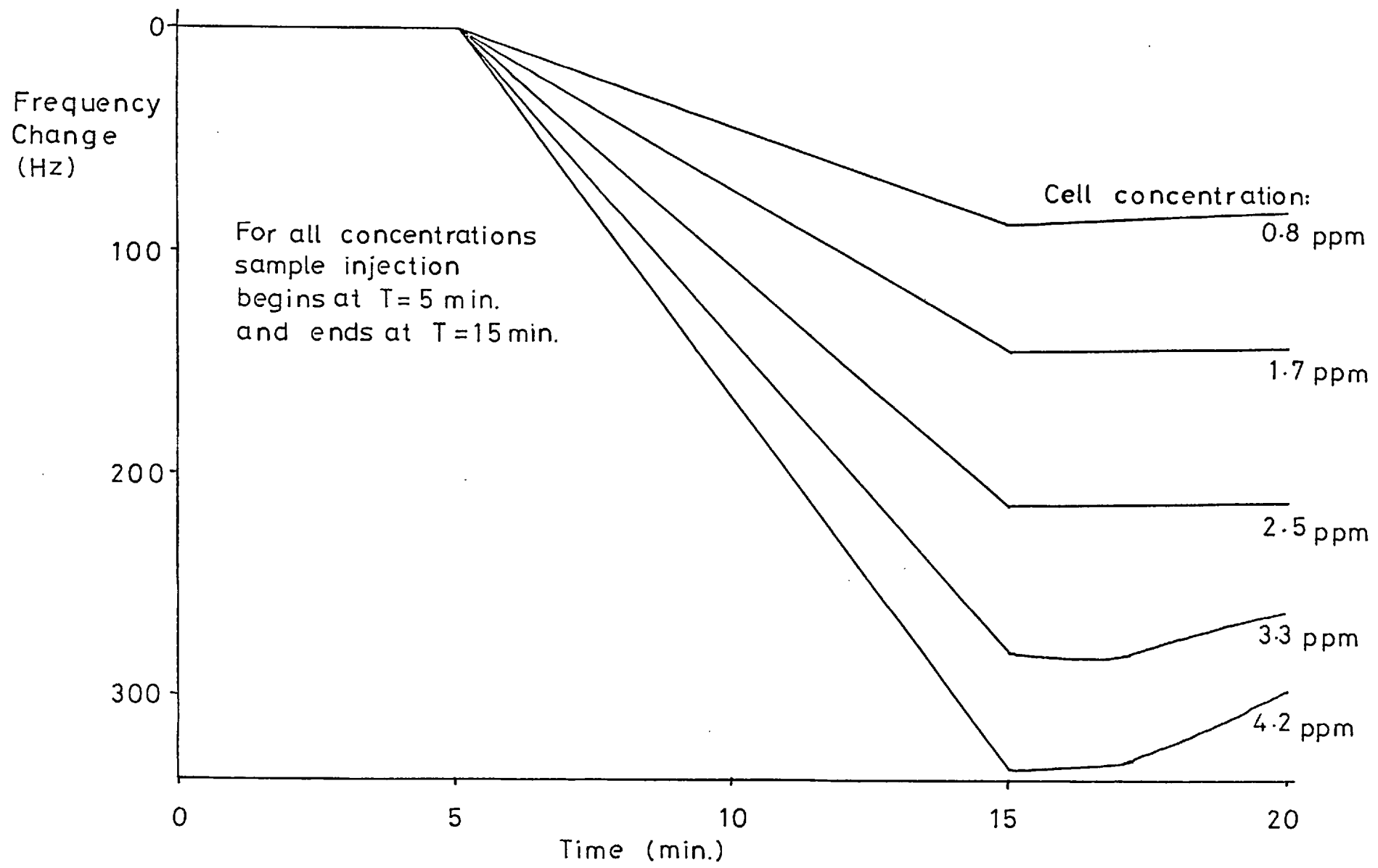
Figure 59

The concentration of sample gas in the sample cell varied from 0.15 ppm to 4.20 ppm. The manner in which the frequency of crystal number 5 changed as samples of sulphur dioxide of varying concentrations were injected into the carrier gas stream are shown in figure 60. The frequency change that occurred between the commencement and cessation of the sample injection was plotted as a function of concentration of the sample in the sample cell. This calibration graph is shown in figure 61. The points plotted in figure 61 are the mean of triplicate injections.

In order to establish the response of this crystal to higher concentrations of sulphur dioxide, aliquots of sample, between 200 ppm and 1,000 ppm, were injected into the system; the concentration of sample in the carrier gas and thus in the sample cell was between 8.3 and 41.6 ppm respectively.

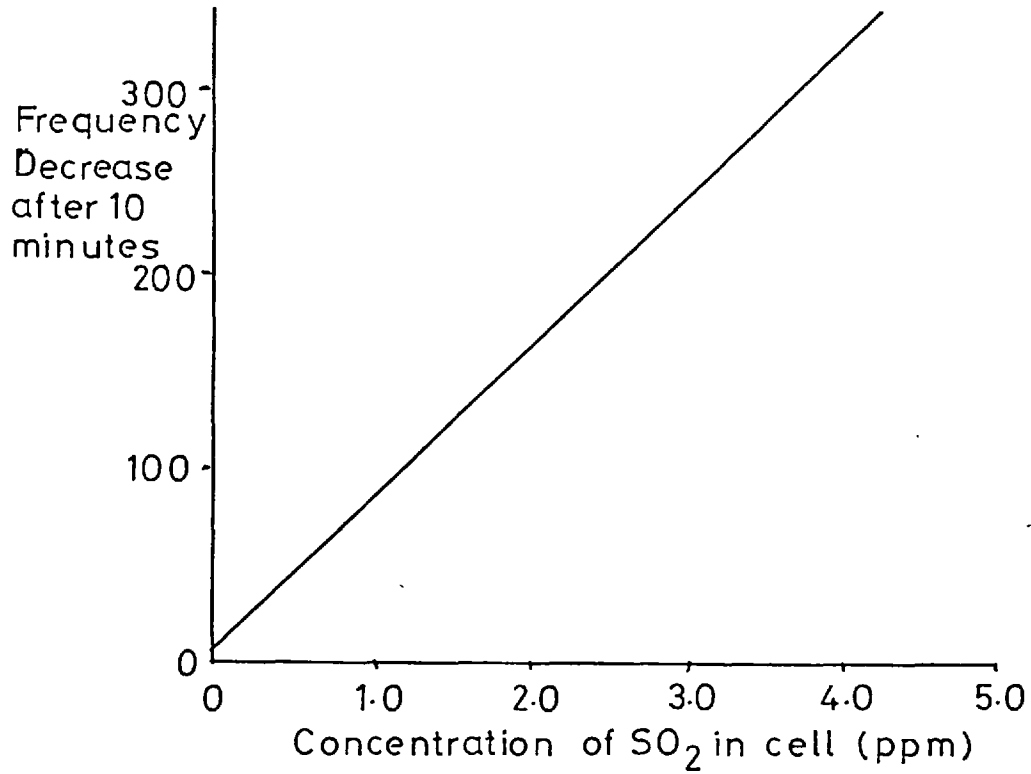
The calibration graph obtained from the introduction of more concentrated samples is shown in figure 62; the cause of the curving off of the graph at higher concentrations is apparent when the peak profiles for the more concentrated samples are studied. These profiles are shown in figure 63. The variation in profile shape shown in figure 63 and also the shapes shown in figures 58 and 60 can be explained by consideration of the concentration of sulphur dioxide in the environment of the coated crystal and the quantity of triethanolamine on the crystal.

At the interaction between sulphur dioxide and triethanolamine is of a chemical nature then, in a closed environment the reaction between a quantity of triethanolamine and a given concentration of sulphur dioxide will proceed to a point defined by the equilibrium constant of the reaction. As a reaction at equilibrium is not static but dynamic then the rate of the forward reaction i.e. to form the product is the



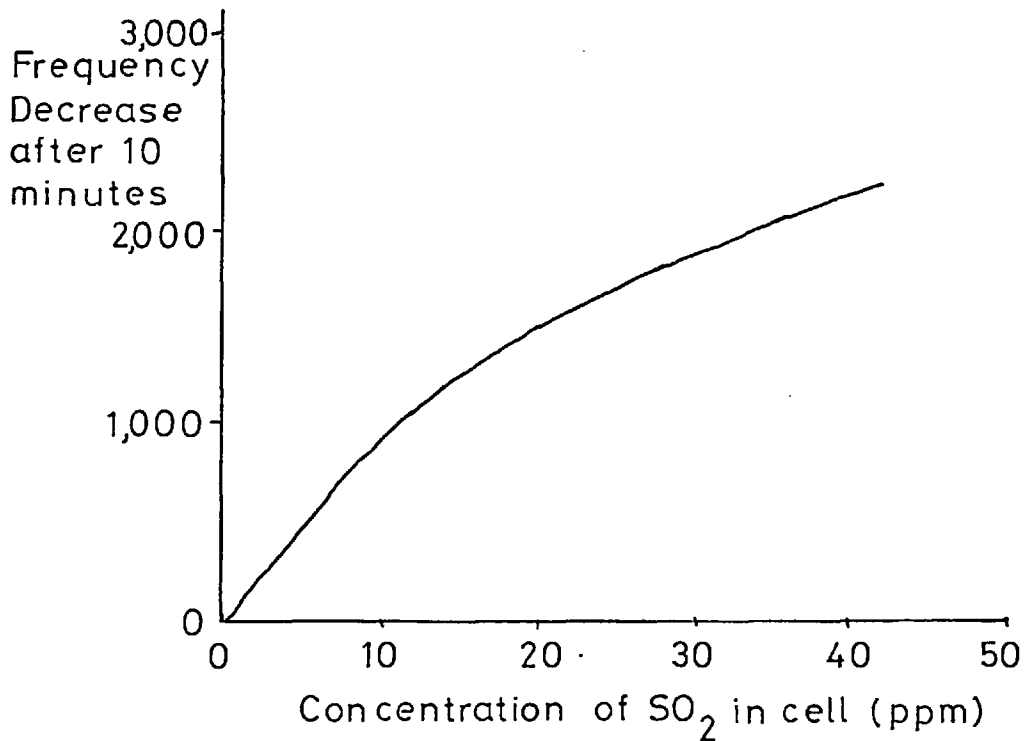
Response of Triethanolamine Coated Crystal 5 to 10 minute Samples of SO₂ (low concentrations)

Figure 60



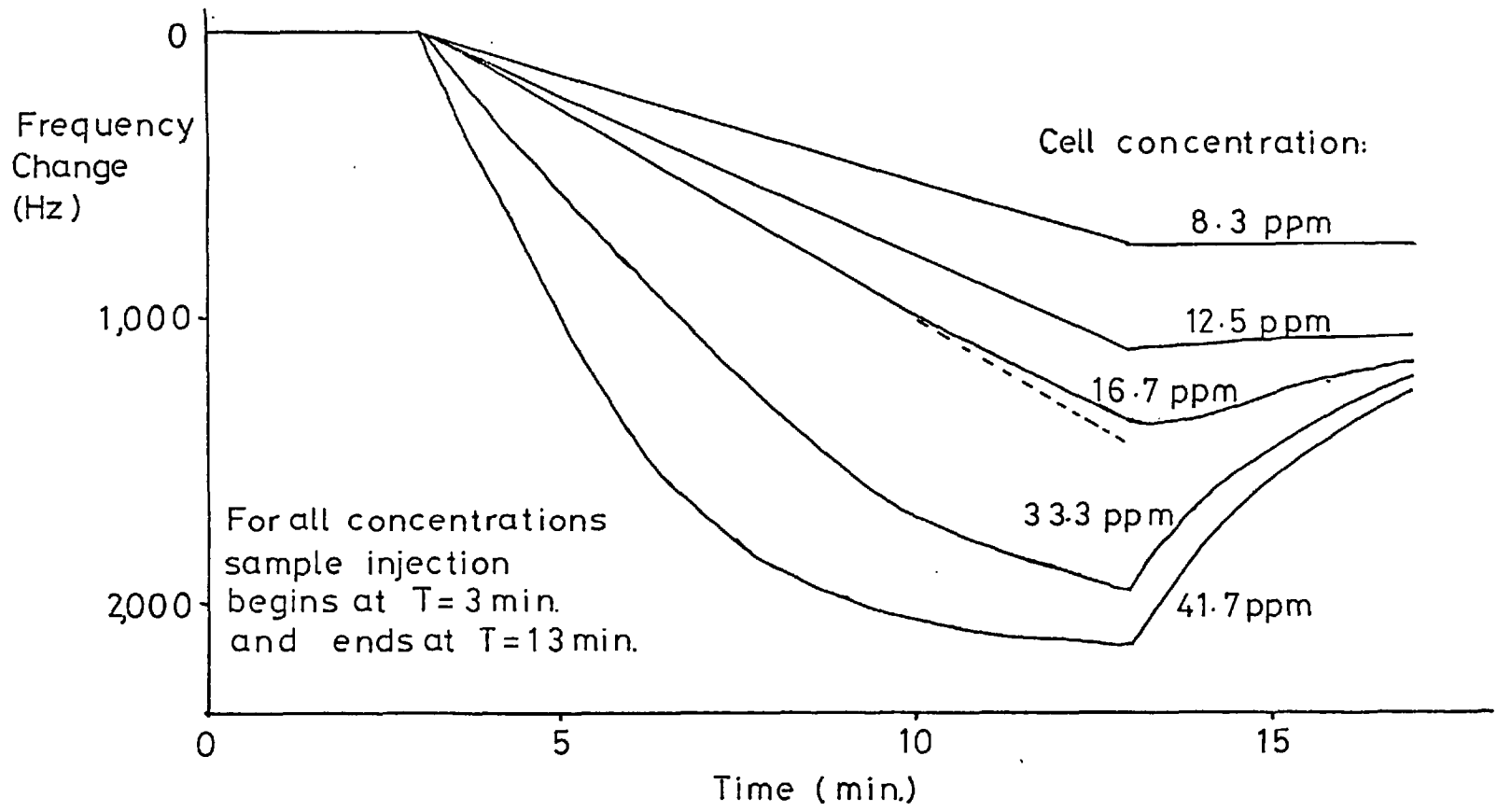
Calibration Graph of Triethanolamine Coated
Crystal 5 (low concentrations)

Figure 61



Calibration Graph of Triethanolamine Coated
Crystal 5 (high concentrations)

Figure 62



Response of Triethanolamine Coated Crystal
5 to 10 minute Samples of SO₂ (high concentrations)

Figure 63

same as the rate of the backward reaction i.e. the dissociation of product back to reactants, the net result being no apparent change in the concentrations of the materials present.

This equilibrium situation is occurring in the sample/coating interaction depicted in figure 58. In these experiments the concentration of sulphur dioxide presented to the crystal was so low that the sulphur dioxide/triethanolamine reaction was coming to equilibrium in the time that the sample was presented to the crystal. This meant that further presentation of sulphur dioxide at the same concentration had no effect on the crystal i.e. no further product was formed and consequently no frequency change observed.

The decrease in the absorption rate of sulphur dioxide by the crystal was due to the build-up of reaction product and therefore, the increase in the rate of the backward reaction with the subsequent decrease in the overall reaction rate.

The situation depicted in figure 60 is an extension of the conditions just described.

In these experiments it is obvious that no equilibrium conditions have been reached but the rate of absorption of sulphur dioxide for each sulphur dioxide concentration is linear and also the variation of the absorption rate is a linear function of concentration. It is likely, therefore, that under the given conditions then the reaction occurring between sulphur dioxide and triethanolamine is a pseudo 1st order reaction; i.e. the rate of the reaction is linearly dependent upon the concentration of one reactant. This statement is justified as the concentration of sulphur dioxide is low compared with the total quantity of triethanolamine available; the quantity of unreacted triethanolamine will therefore effectively remain constant during the sample presentation.

The profiles represented in figure 63 represent the opposite conditions to those that existed in figure 58; the concentration of sulphur dioxide in the environment of the crystal was high. The initial injections producing 8.3 and 12.5 ppm sulphur dioxide showed a linear absorption of sample, with the introduction of a 16.7 ppm sample into the crystal environment a departure from linearity was observed. This departure from linearity increased as the sample concentration increased. This curvature of absorption represents the point where the reaction is no longer pseudo 1st order i.e. the removal of unreacted triethanolamine by the large quantities of sulphur dioxide in the environment of the crystal is becoming important in determining the rate of the reaction.

As the quantity of unreacted triethanolamine on the crystal surface is finite then the quantity of product that can be formed by reaction with sulphur dioxide is also finite, the approach of the maximum absorption of sulphur dioxide is seen in the calibration graph shown in figure 62 i.e. a flattening of the curve as saturation approaches.

The final study carried out with triethanolamine coated crystals was the establishment of the dependence of response upon the area of the coating. For this study crystals 6 to 11 (table 25) were used. These crystals were prepared with a variety of coating dimensions. Crystal number 7 was coated all over both major surfaces of the crystal. This was done in an attempt to stop the triethanolamine "creeping"; as triethanolamine was a very viscous liquid there was a slight tendency for the deposit to spread out on the crystal surface after an extended period of time. The results obtained from the calibration of this crystal showed however that a large loss in sensitivity was obtained.

The calibration of crystals 6 to 11 was carried out in the same

manner as crystal number 5, i.e. the crystal was placed in the flow cell with a carrier gas flow of 12 ml/min. When the crystals had reached a steady state 5 ml. samples of dilute sulphur dioxide solutions were injected into the carrier gas stream over a period of 10 minutes. The range of concentrations to which each crystal was exposed was 0.83 to 4.2 ppm.

The calibration graphs of crystals 5 to 11 are shown in figure 64.

In order to compare the response of these crystals as a function of area of the coating then the mass which causes the frequency change must be the same, the mass which causes the frequency change being the mass of absorbed sulphur dioxide.

As these crystals were behaving in a normal manner the mass of sulphur dioxide that was absorbed onto each crystal after exposure could be calculated; this mass was calculated for each crystal after a 10 minute exposure to 4.2 ppm sulphur dioxide. The frequency change that occurred upon absorption of this calculated mass of sulphur dioxide was normalized so that a frequency change that would be caused by the absorption of 1.00 μg of sulphur dioxide was obtained i.e. for crystal number 11 1.65 μg of absorbed sulphur dioxide caused a frequency change of 420 Hz, therefore an absorbed mass of 1.00 μg on the same deposit would cause a frequency decrease of 255 Hz. The frequency change obtained on absorption of a mass of sulphur dioxide for crystal numbers 5-11 is shown below in table 27. Also tabulated is the normalized frequency response and the mass per unit area of the absorbed sample.

Crystals 5-11
Calibration Graphs of Triethanolamine Coated

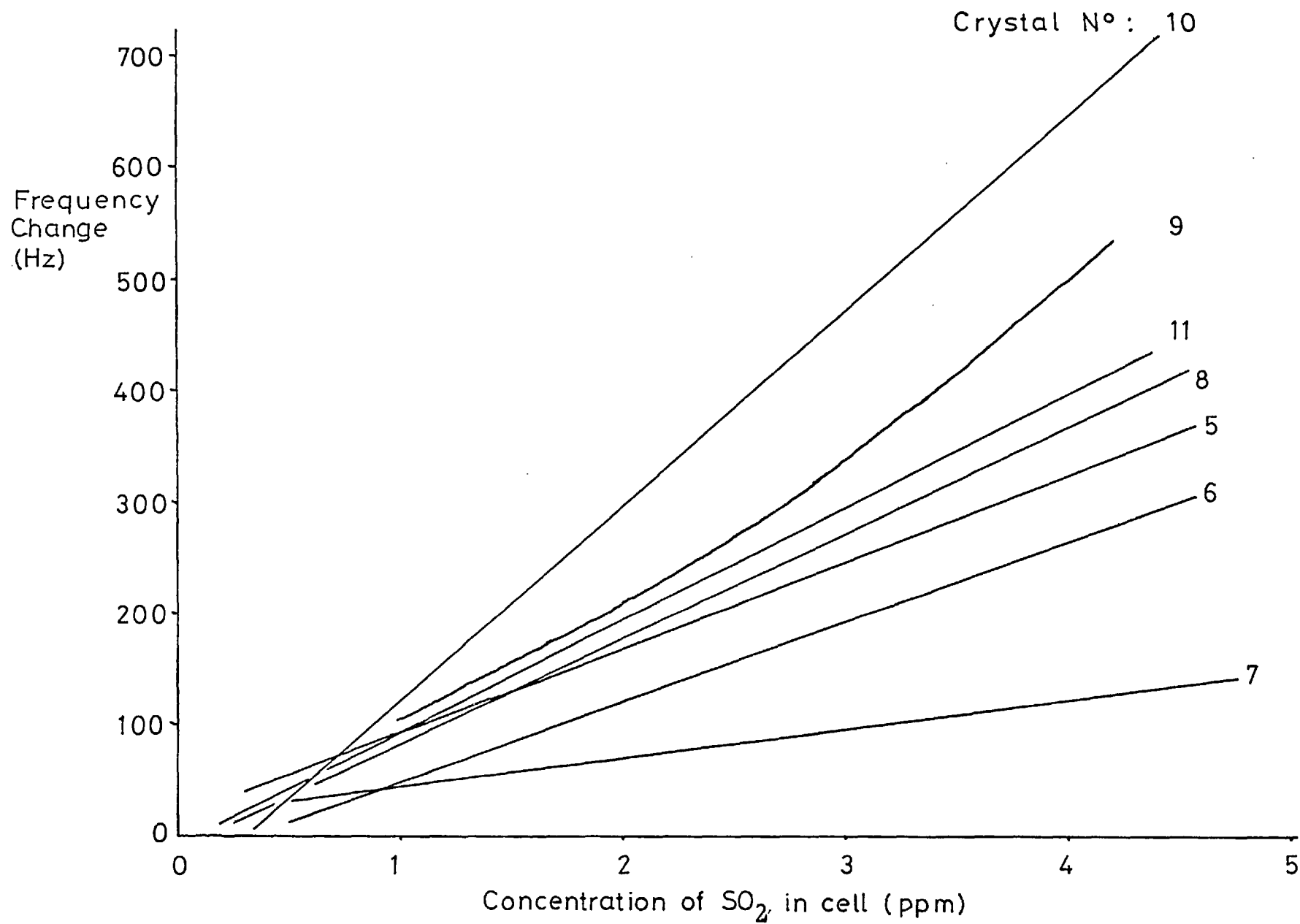


Figure 64

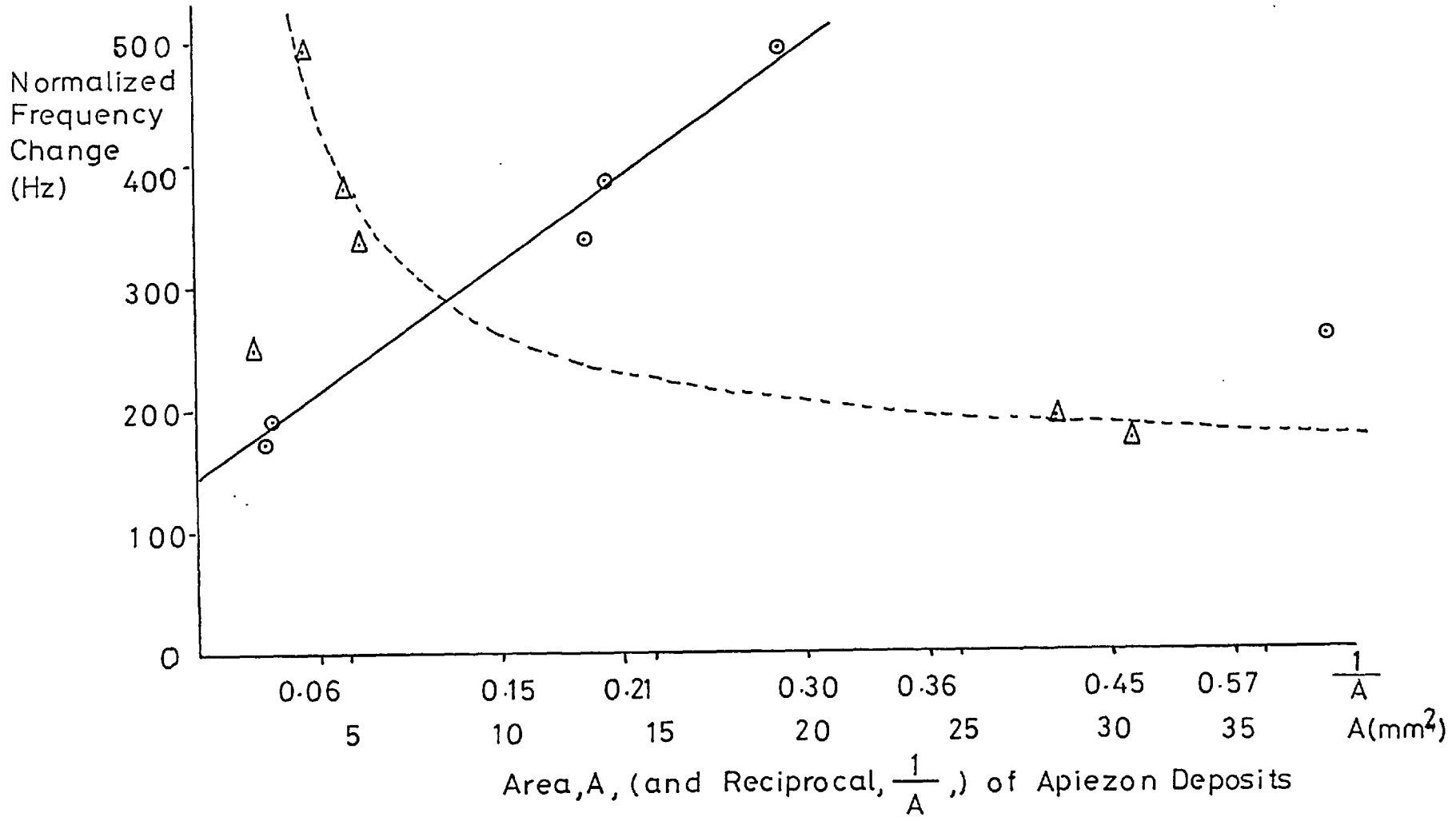
Crystal number	Δf_{SO_2} (Hz)	m_{SO_2} (μg)	Δf_{N} (Hz)	$\frac{m}{A}$ $\mu\text{g mm}^{-2}$
5	340	1.74	195	0.0615
6	280	1.59	176	0.0520
8	387	1.00	387	0.205
9	534	1.08	494	0.310
10	687	2.02	340	0.386
11	420	1.65	255	0.917

Table 27

The dependence of the frequency change upon the area of the deposit is shown in figure 65. The straight line graph is a plot of Δf vs $\frac{1}{A}$; this linear response is predicted by the Sauerbrey equation. The dotted curve is a plot of Δf vs A and was constructed from values obtained from the straight line plot. The experimentally determined points are shown as Δ . Note that on this plot one point due to crystal 11 occurs at $f = 255$ Hz and $A = 1.88 \text{ mm}^2$. This point represents the rapid decrease in response that is obtained when the area of the deposit becomes very small; under these conditions then the area of deposit available for reaction with the sample gas is more important than the Sauerbrey requirement of a small area for maximum frequency response. From the plot of Δf vs A it would appear that the maximum

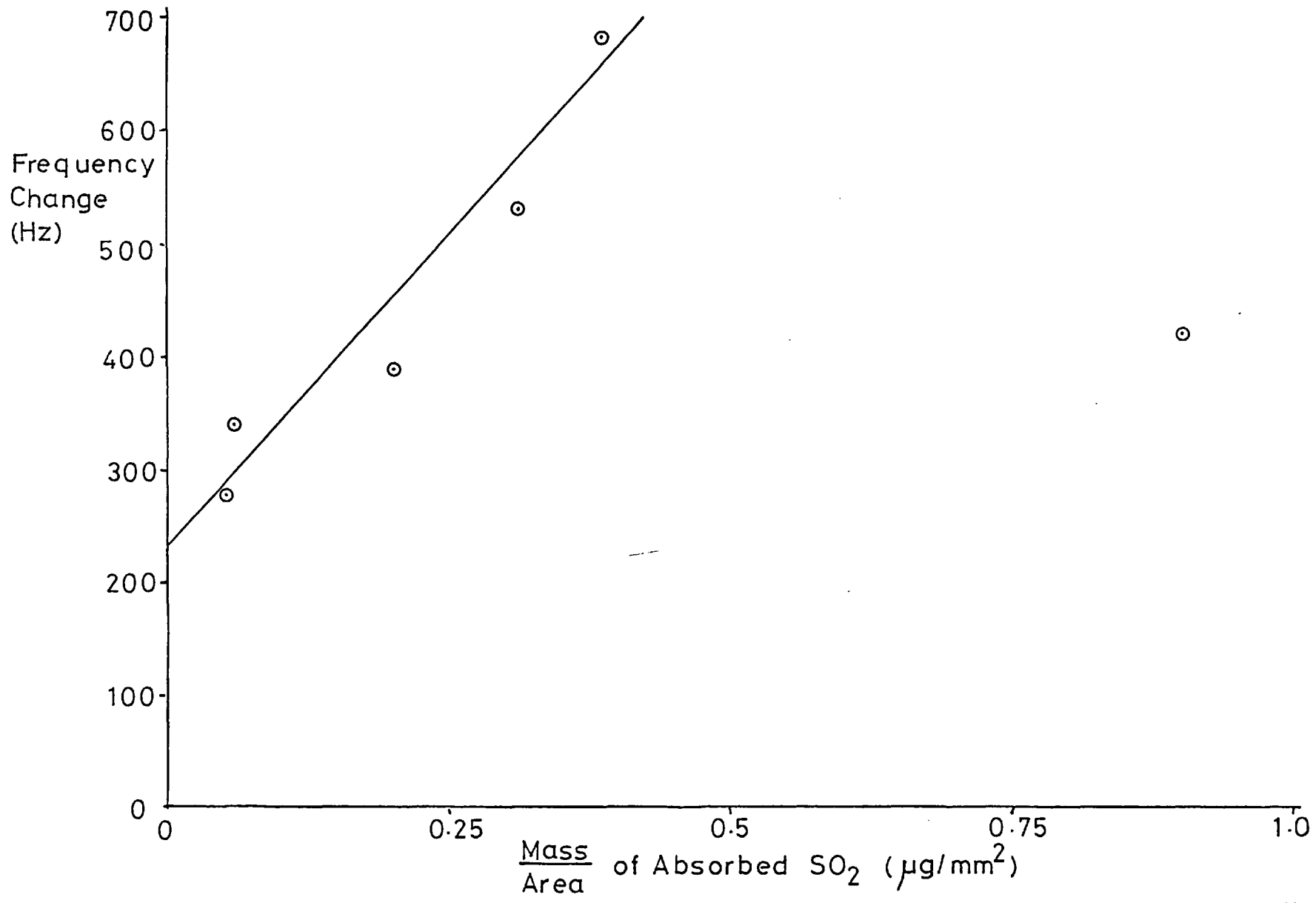
Figure 65

Dependence of Frequency Change upon Area of Coating



Frequency Change as a Function of Mass/Area of Absorbed Sample

Figure 66



response of a triethanolamine coating would be obtained if the area of the deposit were approximately 3 mm^2 .

If a series of crystals were required with the same response it would be more difficult to reproduce this response with such a small area as the response vs area curve is steep in this particular region.

An additional check on the Sauerbrey equation was made by plotting the mass per unit area of the absorbed sample gas as a function of the frequency change obtained upon sample introduction. This plot gave a straight line graph (figure 66), the only point severely in error being due to crystal number 11 where, as mentioned previously, the area of the deposit was too small for maximum response. The values for the various mass per unit areas plotted are shown in table 27.

7. Conclusion

7.1. Introduction

In the first chapter of this thesis it was stated that one of the intentions of this work was to demonstrate how the piezoelectric crystal detector can help solve some of the problems of air pollution analysis; these problems being the large outlay in equipment and/or manpower necessary to obtain an intimate knowledge of the variation of pollution levels in our environment.

The work with triethanolamine coated crystals has in fact demonstrated that this device is capable of determining low levels of sulphur dioxide without the need for preconcentration of the sample and with instrumentation which is (by today's standard) very simple.

The application of solid materials to a vibrating quartz crystal led to the discovery of unpredicted frequency changes in that the frequency of the crystal increased, not decreased, when mass was placed on the surface of the crystal; it was later established that this effect was not confined to solid coatings but less frequently observed with other coatings.

A change in the nature of the coating/sample interaction from chemisorption to physisorption has been observed for most of the solid coatings investigated, this change, which also implies a change from irreversible to reversible interaction, was also accompanied by a decrease in response of the coated crystal.

Generally the sensitivity of a crystal coated with a solid material was not sufficiently high to permit direct analysis of pollutant gases present in the atmosphere and also the problems encountered when trying to coat crystals reproducibly with active solids were more difficult than coating the crystals with non-solids.

The points that arose as a result of this work will now be considered in more detail.

7.2. Instrument Evaluation and Coating Techniques

In the second chapter the instrumentation required for this system was described and the combined precision of the sample injection and subsequent determination was determined as being of the order of $\pm 9\%$ r.s.d. Similar results were obtained throughout the duration of this work whenever the crystal and sample interaction was of a stable nature i.e. when the mode of sorption was not changing from chemisorption to physisorption, or the coating on the crystal was not being saturated, as occurred with the triethanolamine/sulphur dioxide system.

The degree of correction of spurious frequency changes achieved by the double sided system was shown to be appreciable, although to correct for bleed of coating from a crystal extreme care is required to ensure that both sample and reference crystals have very similar coatings.

The ease of preparation of coatings varied greatly, dependant upon the nature of the coating material. As described in chapter three deposits prepared from solutions were easy to prepare but care must be exercised to ensure an even distribution of the coating mass. This point was emphasised with the apiezon deposits and a lack of correlation with the Sauerbrey equation, even though the frequencies were decreasing with added mass.

The coating of insoluble solid materials was, initially, by no means as easy as using a solution to prepare the active surface; initial problems being to prepare a secure deposit that would permit the crystal to oscillate and the appearance of the high frequency effect. A technique was developed, using latex as an adhesive, to successfully

secure solid materials to the crystal surface but the frequency change that resulted from the coating procedure and subsequent coating/sample interaction was difficult to predict.

7.3. High Frequency Effect

It has been postulated that the cause of the high frequency effect was a change, past some critical limit, in the mechanical impedance of the electromechanical transducer system i.e. the quartz crystal.

The evidence to support this posulation is not direct but may be inferred from the various experimental facts observed during this study. This evidence may be summarized as follows.

i) Active Participation of Coating

The coating on a crystal which is oscillating high plays a more active role in controlling the conditions for oscillation than does the coating on a crystal which is oscillating normally; this is demonstrated by the fact that the removal of the outer 0.65 mm of an apiezon deposit (4.8% of the total mass of deposit), from a crystal that was oscillating high was sufficient to stop the crystal oscillating. If mass is removed in a similar fashion from a normally oscillating crystal then the frequency of the crystal will increase.

A more general indication of coating participation in determining whether the high frequency effect is observed or not is that solid coatings applied to a crystal using the techniques described in the text give rise to the high frequency effect much more frequently than the application of non-solid coatings, thus the solid coatings must in some way have a greater influence on the important parameter controlling the high frequency effect.

These observations reflecting the active participation of a coating contrast with the more passive role assumed to be played by

coatings in the derivation of the Sauerbrey equation; in this derivation the coating is assumed to influence the frequency of the crystal only by its mass and not by its bulk or elastic properties. This assumption can be made only as a result of the mode of motion of a vibrating AT cut crystal and applied when the coating is thin, compared to the thickness of the crystal, uniform, and tightly bound to the crystal surface.

ii) Alternative Frequency Changing Mechanism

Further information to support the postulation stems from the probability that when the frequency changes that occur, as a result of coating the crystal and/or coating sample interaction, are anything but normal, (i.e. anything other than a decrease in frequency upon coating and a decrease in frequency upon sample presentation) then the frequency change that occurs is doing so by a quite different mechanism to the frequency changes that occur with a "normal" crystal.

It is necessary to consider a different mechanism in order to account for the similarity in response for crystals that have deposits of the same material but of totally different dimensions e.g. crystals numbers 1 and 2 of the manganese dioxide/latex series (chapter 4).

A similar situation arises when crystals 11, 14 and 15 of the lead dioxide/latex series are considered i.e. both crystals 11 and 14 behaved normally with a change in the nature of the sample/coating interaction from chemisorption to physisorption as the total quantity of sample presented to the crystals increased, this change was accompanied by a decrease in response. When the physisorption state was reached neither crystal would produce a calibration graph: Crystal 15, which had increased its frequency on coating but decreased its frequency when sample was presented, gave the same trend in peak shape as the nature of the interaction changed but the magnitude of the response was quite

different, i.e. much lower for the same sample size with no decrease in response observed for replicate sample injections. It was also possible to construct a calibration graph when the coating was acting reversibly - unlike crystals 11 and 14.

These comparisons of the manganese dioxide crystals and the lead dioxide crystals strongly suggest that the frequency changes that are occurring are doing so by a mechanism different to that assumed in the Sauerbrey equation.

iii) Changing Electrical and Mechanical Environment

The most obvious evidence that the high frequency effect is due to some unspecified change in the mechanical impedance of the crystal comes from the behaviour of the crystal coated with potassium iodate and the strong dependence of the frequency of this crystal upon its electrical and mechanical environment.

The potassium iodate coated crystal was capable of oscillating normally i.e. a decrease in frequency as a result of the coating and was also capable of oscillating at a frequency higher than the clean uncoated frequency. This change could be prompted by changing the electrical or the mechanical environment of the crystal. The change in the mechanical environment consisted of removing or replacing the outer covering can of the crystal thus changing the acoustic loading on the vibrating plate. This change in the mechanical environment of the crystal and subsequent frequency change compares directly with the measurement of the electrical parameters of telephone receivers (see chapter 5) and the dependence of these parameters upon the mechanical environment of the diaphragm of the instrument; both telephone diaphragms and piezoelectric crystals are electro-mechanical transducers; mechanical impedance being a parameter of such devices.

As piezoelectric crystals are electro-mechanical transducers it follows that by changing the electrical environment of the crystal then the same frequency change should be obtained as was obtained by changing the mechanical environment; this was found to be correct, the change being effected by varying the inductance of the driving oscillator. (Changing the inductance of the oscillator with a "normal" crystal in circuit caused a change in frequency of only 2 - 3 KHz as opposed to the jump of 75 KHz obtained with the potassium iodate coated crystal).

It was stated in chapter 5 that the purpose of this section was to attempt to identify the general cause of the high frequency effect and not give a detailed analysis of the precise nature of the effect. By combining the information summarized here in this chapter and comparing this total information with the general theory of electro-mechanical transducers then the resultant conclusion strongly suggests that the variation of the mechanical impedance of the oscillating crystal is responsible for the high frequency effect.

7.4. Response of Various Coatings

With the piezoelectric detector one of the main factors in limiting the sensitivity is the strength of the coating/sample interaction i.e. has the coating material the ability to interact measurably with low concentrations of sample gas?

Of the coatings tried only triethanolamine was found to be capable of measurably interacting with concentrations of sulphur dioxide that are likely to be found in the atmosphere.

With the technique used for sample presentation i.e. sample presentation with the aid of a syringe pump, it was possible to determine sulphur dioxide in nitrogen, in the sample cell, at a concentration of

0.025 ppm, the frequency change obtained with a ten minute presentation of the sample was twice the frequency change obtained by injecting nitrogen only into the carrier gas stream.

The linear range of a triethanolamine coated crystal was not great at two orders of magnitude i.e. 0.025 ppm to 12 ppm.

When higher concentrations of sample gas were presented to the crystal i.e. greater than 12 ppm then saturation of the coating became more important with a subsequent loss of linearity and sensitivity.

This small linear range is not too great a disadvantage however as concentrations greater than 2 - 3 ppm very seldom occur in the environment (excluding enclosed industrial environments) and as the device is linear up to a concentration of twice the threshold limit value for sulphur dioxide (5ppm) it could still be applied as a warning device in an industrial environment to indicate that the T.L.V. has been exceeded.

The major disadvantages of triethanolamine coated crystals are; the finite working life of a crystal, 2 - 3 weeks of continuous exposure to sample and the difficulty of preparing identical coatings that have the maximum response i.e. the optimum area of coating.

The finite life of the crystal is as a result of bleed of material from the crystal surface and also due to sulphur dioxide accumulating in the coating (the sorbtion process is not 100% reversible).

No study was made regarding the selectivity of triethanolamine.

With the other stationary phase type material that was used i.e. carbowax 20M it is difficult to come to any conclusion about the applicability of this material to the detection of sulphur dioxide as only a brief study was carried out. It is not meaningful to compare the results of the "single shot injection" of sample into the environment of a triethanolamine coated crystal and the carbowax coated

crystals as the carrier gas flow rates and cell geometry were quite different for the two coating materials, a simple inspection of the responses yields the following; triethanolamine coated crystal, 5 μ l injection of sulphur dioxide into a carrier gas stream flowing at 12 ml/min gave a response of 258 Hz; a carbowax crystal gave a response of only 15 Hz when 50 μ l of sulphur dioxide were injected into a carrier gas flow of 60 ml/min. Only by further experiment could the applicability be correctly ascertained.

The decision to investigate solid coatings on a crystal was made in order to obtain a more selective sample absorption than was possible with g.c. stationary phases. It was realized that the life of these solid coatings would be limited as the nature of the sample/coating interaction would probably be irreversible.

The actual use of these materials on crystals however revealed more disadvantages than at first realized, not the least of which was the high frequency effect. More important than the high frequency effect, to the analytical applicability of these coatings was the lack of sensitivity exhibited; this lack being so great as to render all of the solid coatings examined as being unsuitable for the analysis of environmental sulphur dioxide and nitrogen dioxide without pre-concentration of the sample. This lack of sensitivity shown by all of the solid coatings is readily appreciated by comparing the response of these materials with the single shot injections of sulphur dioxide into the environment of a triethanolamine coated crystal under identical experimental conditions i.e. same cell and undiluted sulphur dioxide being injected into the environment of each crystal. This comparison is made in table 28; in this table the best frequency change obtained with any coating when exposed to sample in a static environment is listed with the time taken to achieve the frequency change. The cell used for each crystal was the glass cell, each crystal was in a nitrogen

atmosphere.

Coating Material	Sample + Quantity	Best Response	Time taken to achieve response
NaHgCl_4	SO_2 , 100 μl	nil	-
Ni(OH)_2	SO_2 , 100 μl	-123 Hz	10 min.
$\text{AgVO}_3/\text{Ag}_2\text{O}$	SO_2 , 20 μl	-84 Hz	30 min.
Decomp. prod) of AgMnO_4	SO_2 , 20 μl	-165 Hz	30 min.
	NO_2 , 20 μl	-58 Hz	4 min.
MnO_2	NO_2 , 100 μl	-1,924 Hz	10 min.
$(\text{C}_2\text{H}_4\text{OH})_3\text{N}$	SO_2 , 5 μl	-4,216 Hz	3 min.
PbO_2	SO_2 , 100 μl	-1,600 Hz	10 min.

Table 28

It should be noted that the responses shown in table 28 were the result obtained by presenting sample to a fresh deposit; subsequent sample presentation gave a reduced response as has been described in the text.

The low initial response of these materials is probably due to the absence of intimate gas/solid mixing. The majority of the compounds tested were devised for use as trapping agents in organic elemental microanalysis; in this technique the sample gas is passed through absorption tubes i.e. tubes packed with the absorbing reagent. In this situation the gas is forced into an intimate contact with the

reagent and thus an efficient scrubbing action is obtained. Clearly this degree of intimacy between sample and coating does not exist with coated crystals.

Not only did the low response of the solid coatings present a problem but also the capacity of the coating was problematic.

This was clearly demonstrated when the effective capacity of lead dioxide in static and dynamic systems was studied. It was found that the effective capacity or the critical loading percentage was between 12 and 15% of available material in a static system; this value fell to between 4 and 6% in a dynamic system. Even if the initial response of the lead dioxide coating was high then the restriction on the life i.e. the capacity of the crystal is still severe. It was not possible to extend the life of the crystal by simply increasing the quantity of coating on the crystal as the crystals were already loaded with the maximum quantity of coating that would permit oscillations.

Similar calculations i.e. the determination of the effective capacity cannot be made for the majority of the manganese dioxide crystals for a number of reasons;

- i) most crystals increased their vibrational frequencies therefore the Sauerbrey equation is not applicable:
- ii) with the coatings prepared with the particle fractionation it was not possible to ascertain any build up of nitrogen dioxide as a constant frequency change due to residual nitrogen dioxide (after desorption) was not observed i.e. the frequency changes were complicated by the bulk effect:
- iii) of the manganese dioxide/latex crystals only one crystal, crystal number 12, exhibited any marked tendency to

retain nitrogen dioxide over a longer period. (The other crystals in this series showed retention of nitrogen dioxide over the working day but were generally flushed clean overnight by the continuous carrier gas flow.) As crystal 12 changed its vibrational mode during its life it is not possible to say whether the coating would have absorbed more nitrogen dioxide as a stable state was not reached.

Immediately prior to the frequency jump the frequency of crystal 12 had decreased by a total of 1,300 Hz. This is equivalent to 1.63 μg of nitrogen dioxide retained by the coating. If a similar calculation is made to that used with the lead dioxide/sulphur dioxide system then the 1.63 μg of absorbed nitrogen dioxide had reacted with 1.54 μg of manganese dioxide or 4.8% of the available material on the crystal.

It is thus clear that crystal 12 and probably the other crystals in the manganese dioxide/latex series retain very little nitrogen dioxide on the deposit. This could be as a direct result of the nature of the deposit, i.e. a very thin layer as opposed to a deposit of appreciable thickness in which the nitrogen dioxide would become mechanically trapped prior to chemisorption taking place.

If the rate of the reaction between manganese dioxide and nitrogen dioxide is slow then the initial mechanical trapping becomes an important prelude to chemisorption.

7.5. Suggestions for Further Work

The most obvious question raised by this work is what is the exact nature of the high frequency effect? and could this effect be gainfully employed? perhaps showing a greater mass sensitivity than the Sauerbrey equation.

A study of this effect would be useful even if no special advantage were found, as it would then be possible to predict more closely when the effect would occur and, if necessary, avoid the conditions which may be found to lead to the effect.

With regard to the coatings on the crystal a survey of the polyamine compounds available as g.c. stationary phases for sulphur dioxide determination would be useful. The potential advantages offered by some of these materials are: a higher maximum operating temperature than triethanolamine and therefore, less bleed of material from the crystal surface. The higher operating temperature also leads to the possibility of the inclusion of a heating cycle to aid desorption of the sample gas from the deposit on the crystal; this was not favourable with triethanolamine because of its low maximum operating temperature.

The development of solid coatings could be continued by deliberately saturating the surface of manganese dioxide with nitrogen dioxide and using the resultant material as the substrate, i.e. using the reversible physisorption state of the coating. The capacity could be increased by preparing a sample of manganese dioxide with a very high surface area. This could be obtained by a similar technique used to prepare high pressure liquid chromatography support materials i.e. precipitation of the material from a solution containing a large soluble organic molecule e.g. dextrose. The organic material is included in the precipitate and removed by high temperature ignition of the precipitate, the removal of the organic material leaving a porous solid of high surface area.

REFERENCES

1. Drinker, P.
A.M.A. Arch. Ind. Hyg. 1 (1953) p275.
2. Cholak, J.
Proc. 2nd Natl. Air Pollution Symposium, Pasadena,
Calif. 1952 (1952) p6.
3. Technical Progress Report, Air Quality of Los Angeles
County. Vol. II Los Angeles County Air Pollution
Control District 1961.
4. Lowry, T., Schuman, L. M.
J. Am. Med. Assoc. 162 (1956) p153.
5. Henderson, Y., Haggard, H. W.
Noxious Gases 2nd ed. Reinhold, New York, 1943.
6. Gray, E. Le B.
A.M.A. Arch. Ind. Health 19 (1959) p479
7. "Continuous air monitoring programme in Cincinnati 1962-1963" p189.
Public Health Service, U.S. Department of Health, Education
and Welfare, Cincinnati, Ohio. January 1965.
8. Johnstone, R. T.
Occupational Diseases Saunders, Philadelphia 1942.
9. Kehoe, R. A., Machle, W. F., Kitzmiller, K., Le Blanc, T. J.
J. Ind. Hyg. 14 (1932) p159.

10. Patty, F. A.
Industrial Hygiene and Toxicology Vol. II Interscience,
New York 1962.
11. Sanyal, B., Bhadwar, D. V.
J. Sci. Ind. Res. (India) 18A (1959) p69
12. Aziz, P. M., Godard, H. P.,
Corrosion 15 (1959) p39
13. Vernon, W. H. J.
Trans. Faraday Soc. 31 (1935) p1668
14. Plenderleith, H. J.
The Conservation of Antiquities and Works of Art
p388. Oxford Univ. Press London 1957.
15. West, P. W., Gaeke, G. C.
Anal. Chem. 28 (1956) p1916.
16. Roberts, L. R., McKee, H. L.
J. Air Pollution Control Assoc. 2 (1959) p51.
17. Silverman, L.
Air Conditioning Heating and Ventilation 52 (1955) p88
18. Baker, R. A., Doerr, R. C.
Intern. J. Air Pollution 2 (1959) p142.
19. Acs, L., Barabas, S.
Anal. Chem. 36 (1964) p1825.

20. Barabas, S., Kaminski, J.
Anal. Chem. 35 (1963) p1702.
21. Huitt, H. A., Lodge, J. P. Jr.
Anal. Chem. 36 (1964) p1305.
22. Pate, J. B., Ammons, B. E., Swanson, G. A., Lodge, J. P. Jr.
Anal. Chem. 37 (1965) p942.
23. Scaringelli, F. P., Satzman, B. E., Frey, S. A.
Anal. Chem. 39 (1967) p1709.
24. Jacobs, M. B.
The Chemical Analysis of Air Pollutants
Wiley (Interscience) New York 1960.
25. Jacobs, M. B., Greenburg, L.
Ind. Eng. Chem. 48 (1956) p1916.
26. Thomas, M. D., Ivie, J. O., Fitt, T. C.
Ind. Eng. Chem., Anal Ed. 18 (1946) p383.
27. Thomas, M. D. et al.
Ind. Eng. Chem., Anal. Ed. 15 (1943) p287.
28. Treon, J. F., Crutchfield, W. E.
Ind. Eng. Chem., Anal Ed. 14 (1942) p119.
29. Volmer, W., Frohlich, F. Z.
Anal. Chem. 16 (1944) p414

30. Department of Scientific and Industrial Research.
The Investigation of Atmospheric Pollution 1931 - 1932.
18th Report H.M. Stationary Office, London 1933.
31. Department of Scientific and Industrial Research.
The Investigation of Atmospheric Pollution 1933-1934.
20th Report H.M. Stationary Office, London 1935.
32. Wilsdon, B. H., McConnell, F. J.
J. Soc. Chem. Ind. 53 (1934) p385.
33. Hickey, H. R., Hendrickson, E. R.
J. Air Pollution Control Assoc. 15 (1965) p409.
34. Saltzman, B. E.
Anal. Chem. 26 (1954) p1949.
35. Lyshkow, N. A.,
J. Air Pollution Control Assoc. 15 (1965) p481.
36. Thomas, M. D., Macleod, J. A., Robbins, R. C., Goettelman, R. C.
Eldridge, R. W.
Anal. Chem. 28 (1956) p1810.
37. Patty, F. A., Petty, G. M.
J. Ind. Hyg. Toxicol 25 (1943) p361.
38. Cady, W. G.
Proc. I R.E. 10 (1922) p83.
39. Tillyer, E. D.
U.S. Patent 1,907,613.

40. Lack, F. R., Willard, G. W., Fair, I. E.
B.S.T.J. 13 (1934) p453.
41. Warner, A. W., Stockbridge, C. D.
Vacuum Micro Balance Techniques.
Vol.2 p71 Plenum Press, New York 1962.
42. Stockbridge, C. D.,
Vacuum Micro Balance Techniques.
Vol.5 p147 Plenum Press, New York 1965.
43. Sauerbrey, G.
Physik Verhandl. 8 (1957) p113.
44. Sauerbrey, G.
Z. Physik 155 (1959) p206.
45. Heising, R. A.
Quartz Crystals for Electrical Circuits. Their Design
and Manufacture, p218 Van Nostrand New York 1946.
46. Sauerbrey, G.
Archiv. Electricis. Ubertrag 18 (1964) p617.
47. Sauerbrey, G.
Z. Physik 178 (1964) p457.
48. Behrndt, K. T., Love, R. W.
Vacuum 12 (1962) p1.
49. Lostis, P.
Rev d'Optique 38 (1959) 1 (19).

50. Stockbridge, C. D.
Vacuum Micro Balance Techniques Vol.5 p193.
Plenum Press New York 1966.
51. Wade, W. H., Slutsky, L. J.
Vacuum Micro Balance Techniques Vol.2 p115.
Plenum Press New York 1962.
52. Warner, A. W., Stockbridge, C. D.
Vacuum Micro Balance Techniques Vol.3 p55.
Plenum Press New York 1962.
53. Niedermayer, R., Gladkich, N., and Hillecke, D.
Vacuum Micro Balance Techniques Vol.5 p217.
Plenum Press New York 1966.
54. Eschbach, H. L., Kruidhof, E. W.
Vacuum Micro Balance Techniques Vol.5 p207.
Plenum Press New York 1966.
55. Haller, I., White, P.
Rev. Sci. Inst. 34(1963) p677.
56. Langer, A., Patton, J. T.
Vacuum Micro Balance Techniques Vol.5 p231.
Plenum Press, New York 1966.
57. Hartman, T. E.
J. Vac. Sci. Technol. 2 (1965) p239.
58. Lins S. J., Kukuk, H. S.
Seventh Vacuum Symposium Trans. p333.
Pergamon Press, London, 1960.

59. Riegert, R. P.
Vacuum Micro Balance Techniques Vol.4 p99.
Plenum Press, New York 1964.
60. Behrndt, K. M.
Trans. Sixth Nat. Vac. Symp. (1959) p242.
Pergamon Press, London 1961.
61. Warner, A. W., Stockbridge, C. D.
Vacuum Micro Balance Techniques Vol.2 p93.
Plenum Press New York 1962.
62. Wade, W. H., Slutsky, L. J.
J. Chem. Phys. 40 (1964) p3394.
63. Kahn, G. M.
Rev. Sci. Inst. 43 (1972) p117.
64. Jones, J. L., Mieure, J. P.
Anal. Chem. 41 (1969) p484.
65. Littler, R. L.
U.S. Patent 3,253,219.
66. Wade, W. H., Allen, R. C.
J. Colloid and Interface Science 27 (1968) p722.
67. Shiojiri, M., Hasegawa, Y.
Jap. J. Appl. Phys. 8 (1969) p783.
68. Fischer, W. F., King, W. H. Jr.
Anal. Chem. 39 (1967) p1265.

69. King, W. H. Jr.
Anal. Chem. 36 (1964) p1735.
70. Earp, R. B. W.
Ph.D. Thesis, University of Alabama 1966.
71. Karasek, F. W., Gibbons, K. R.
J. Chromatographic Science 9 (1971) p535.
72. Karasek, F. W., Tierney, J. M.
J. of Chromatog. 89 (1974) p31.
73. Edmonds, T.
Ph.D. Thesis, University of London, 1975.
74. Bonds, J. D.
Ph.D. Thesis, University of Alabama 1969.
75. King, W. H. Jr.
International Symposium on Humidity and Moisture,
Vol. I 1963, Washington DC.
Reinhold Publishing Corporation, New York.
76. King, W. H. Jr.
U.S. Patent 3,266,291.
77. King, W. H. Jr.
U.S. Patent 3,427,864.
78. Williamson, J. A., Janzen, D. W.
Analysis Instrum. 10 (1972) p175.

79. Hartigan, M. J.
Ph.D. Thesis, University of Rhode Island, 1970.
80. Frechette, M. W., Fasching, J. L.
Environmental Sci. and Technol. 7 (1973) p1135.
81. Frechette, M. W., Fashing, J. L., Rosie, D. M.
Anal. Chem. 45 (1973) p1765.
82. Guilbault, G. G., Lopez-Roman, A.
Environmental Letters 2 (1) (1971) p35.
83. Lopez-Roman, A., Guilbault, G. G.
Anal. Lett. 5 (4) (1972) p225.
84. Guilbault, G. G.
Anal. Chim. Acta. 39 (1967) p260.
85. Guilbault, G. G., Scheide, E. P.
Anal. Chem. 44 (1972) p1765.
86. Karmarkar, K. H., Guilbault, G. G.
Anal. Chim. Acta. 75 (1975) p111.
87. Edmonds, T.
Private Communication.
88. Shackelford, W. M., Guilbault, G. G.
Anal. Chim. Acta. 73 (1974) p383.
89. King, W. H. Jr.
U.S. Patent 3,260,104.

90. Feigl, F., Frankel, E.
Ber. dt. chem. Ges. 65 (1932) p545.
91. Pregl, F.
Quantitative Organic Microanalysis.
English Translation, Fyleman, E.
Churchill (London) 1st Ed. 1924.
92. Belcher, R., Ingram, G.
Anal. Chim. Acta. 4 (1950) p118.
93. Belcher, R. Ingram, G.
Anal. Chim. Acta. 4 (1950) p401.
94. Ingram, G.
Mikrochim Acta (1956) p877.
95. Clemser, O.
Ber dt. chem. Ges. 72B (1939) p1879.
96. Dixon, J. P.
Talanta 4 (1960) p221.
97. Swift, H.
Analyst 86 (1961) p621.
98. Salford, H. W., Stragand, G. L.
Anal. Chem. 23 (1951) p520.
99. Belcher, R., Spooner, C. E.
J. Chem. Soc. (1943) p313.

100. Belcher, R.
J. Soc. Chem. Ind. 64 (1945) p111.
101. Ingram, G.
J. Soc. Chem. Ind. 62 (1943) p175.
102. Britton, H. T. S., Robinson, R. A.
J. Chem. Soc. (1930) II p2328.
103. Britton, H. T. S., Robinson, R. A.
J. Chem. Soc. (1933) I p512.
104. Ingram, G.
Anal. Chim. Acta 3 (1949) p137.
105. Heslop, R. B., Robinson, P. L.
Inorganic Chemistry, A Guide to Advanced Study, p652.
Elsevier, Amsterdam, 3rd Ed. 1967.
106. Korbl, J.
Coll. Czechoslav. Chem. Comm. 20 (1955) p948.
107. Korbl, J.
Coll. Czechoslav. Chem. Comm. 20 (1955) p953.
108. Korbl, J., Pribil, R.
Coll. Czechoslav. Chem. Comm. 21 (1956) p322.
109. Parker, A., Richards, S. H.
"Instruments used for the Measurement of Atmospheric
Pollution in Great Britain".
Air Pollution - Proceedings of the U.S. Technical
Conference on Air Pollution.
McGraw Hill, New York (1952).

110. L. Oertling, Ltd.,
Specification of deci-microbalance Model Q01.
111. Olin, J. G., Sem, G. J., Christenson, D. L.
Am. Ind. Hyg. Assoc. 32 (1971) p209.
112. Edmonds, T.
Private Communication.
113. Heising, R. A.
Quartz Crystals for electrical circuits. p205.
114. Brophy, J. J.
Basic Electronics for Scientists. p339.
International Student Edition. McGraw Hill, New York.
115. Hunt, F. V.
Electroacoustics.
The analysis of transduction and its historical back-
ground. p92.
Harvard University Press. J. Wiley, New York 1954.